Neutron-proton pairing correlations in atomic nuclei

Description of pairing coexistence with mean-field methods plus restoration of broken symmetries

Antonio Márquez Romero

Supervisor: Professor Jacek Dobaczewski

A thesis presented for the degree of
Doctor of Philosophy

Department of Physics
University of York
United Kingdom

February 28, 2020

Abstract

The long-standing problem of neutron–proton pairing correlations is revisited by employing the Hartree–Fock–Bogoliubov formalism with neutron–proton mixing in both the particle–hole and particle–particle channels and symmetry-restoration techniques with the Variation After Projection framework. We compare numerical calculations performed within these methods with an exact pairing model based on the SO(8) algebra.

We show that the symmetry-restored paired mean-field states (quasiparticle vacua) properly account for isoscalar versus isovector nuclear pairing properties within this model, whose relevant symmetries are full particle-number, spin, and isospin. Theoretical predictions of the reduced matrix elements of the deuteron transfer, the potential experimental probe to observe neutron-proton condensates in nuclei, are presented.

Prospects to implement a similar approach in a realistic setting are delineated, calculating the matrix elements of a realistic separable interaction in the pairing channel, implementing them in the numerical software HFODD and evaluating them computing the pairing gaps for certain isotopic chains.

Contents

List of Figures

List of Tables

Acknowledgements

- A mis padres, sin su cariño y educación no habría sido posible llegar hasta aquí.
- A Irene, por su incodicional apoyo durante estos tres años y medio. Mila esker!
- To Alessandro, my *unofficial* supervisor.
- To Chris, Ryan, Luke, David, Ben and Matt, thanks for the laughs and the banter!
- A Gustavo, Sonia, Jenn, Suso, Silvia y Juan, por hacerme sentir como en casa.
- To Paolo, thank you for the proofraeding!

This project was supported by the STFC Grants No. ST/M006433/1 and No. ST/P003885/1.

Author's declaration

I declare that this thesis is a presentation of original work and I am the sole author. This work has not previously been presented for an award at this, or any other, University. All sources are acknowledged as References.

The present work lead to the publication of three original articles:

- A. Márquez Romero, J. Dobaczewski, and A. Pastore. "Neutron-Proton Pairing Correlations in a Single l-shell Model." Acta Physica Polonica B 49 (2018): 347.
- A.M. Romero, J. Dobaczewski, and A. Pastore. "Symmetry restoration in the mean-field description of proton-neutron pairing." Physics Letters B 795 177-182 (2019).
- A.M. Romero, J. Dobaczewski, and A. Pastore. "Finite-range separable pairing interaction in Cartesian coordinates." arXiv preprint arXiv:1909.13041 (2019).

Chapter 1

Introduction

The concept of pairing in nuclei was presented for the first time by Bohr, Mottelson and Pines in a seminal paper for nuclear physics [BMP58], as it introduced that short-range two-body correlations are as important as long-range one-body correlations. As depicted in Fig. (1.1), in nuclei with an even number of particles there is a larger energy difference between the ground and first excited states than in nuclei with an odd number of particles, suggesting an additional correlation due to the *evenness* of the nucleus. Based on the similarity of the spectra of nuclei with an even number of particles with the spectra of superconducting metals, they made a connection between the properties of the wavefunction in nuclei and already well-founded theories of superconductivity in condensed matter physics. The theory of superconductivity in metals was introduced by Bardeen, Cooper and Schrieffer (BCS) [BCS57] and met an outstanding success, based upon correlated electron pairs coupled to total spin and momentum zero, referred in the current literature as *Cooper pairs*. Similarly, protons and neutron can form analogous pairs in nuclei. The BCS theory of superconductivity was also implemented in superfluid nuclei for the treatment of like-particle pairing, that is, proton-proton and neutron-neutron pairing. The fundamental ingredient of this theory is the *pairing gap* parameter (usually denoted by Δ) that stipulates the energy necessary to break a pair and therefore excite the nucleus, experimentally found to be around $1 - 2$ MeV. A vanishing value of this quantity will indicate a non superfluid nucleus with no pair correlations, only happening for closed-shell, i.e., magic nuclei. Nevertheless, the remarkable achievement of the BCS theory is counterbalanced by an unavoidable obstacle in its formulation, namely, the proposed wavefunction of the fermionic system is not an eigenfunction of the particle-number operator and, subsequently, it does not have a definite integer number of particles composing the system, but an *average* value, with corresponding fluctuations.

In the mean-field picture, the particle-number symmetry breaking is necessary in order to

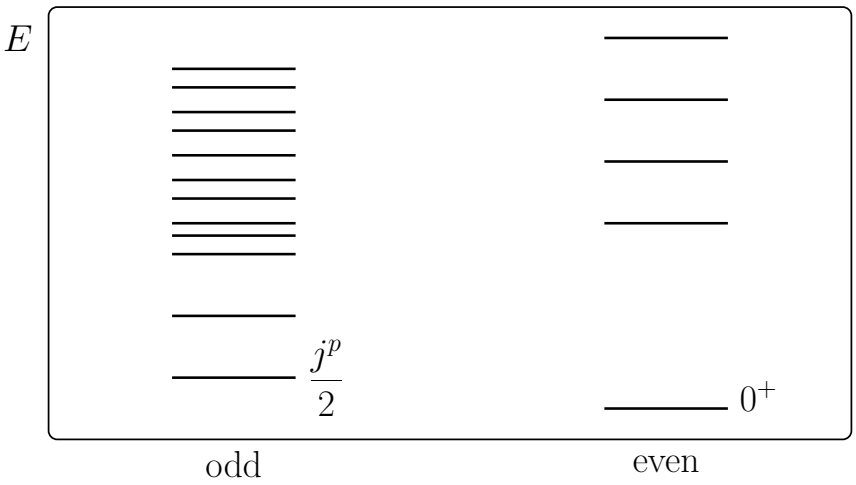

Figure 1.1: Schematic energy spectrum of a nucleus with an odd number of particles (left) and an even number of particles (right). The ground state of an even nucleus is always 0^+. A large difference between the ground and first excited state is seen with regards to the odd spectrum, coming from the breaking of one pair in the otherwise completely pair correlated ground state. For the odd system, whose ground state is in the j-shell with parity p, simple particle-hole excitations are possible at low energy cost.

describe pairing correlations in the nuclear wavefunction. Let us consider a system of particles described by a one-body Hamiltonian with spherical symmetry and no spin-orbit splitting. The different states of the system can be labelled using the quantum numbers of the conserved angular momentum ℓ and projection over the $z-$axis m, the spin and the isospin, with their two different projections. The concept of isospin, with analogous properties to the spin, was introduced in order to treat the two different species building up the nucleus, protons and neutrons, as two different projections of a general particle, the *nucleon*, with isospin $\frac{1}{2}$. Nucleons can move in orbits with different magnetic number m with no preferred direction as they are completely degenerate given the absence of spin-orbit splitting. Therefore, considering a system with $A = 4$ nucleons moving in an $\ell = 2$ shell with total degeneracy $\Omega = 2(2\ell + 1) = 10$ (no isospin degrees of freedom). One of the possible configurations is depicted in Fig. (1.2), which has, in principle, the same ground-state energy as any other configuration of nucleons within the shell. However, we know this is not the case for even nuclei, there is an additional correlation between the nucleons that induces them to form coupled pairs of total angular momentum equal to zero that reduces the ground-state energy of the system. That is, a configuration of the system wherein their nucleons move in time-reversed orbits (orbits with opposite value of angular momentum and spin projection), as in Fig. (1.3), is lower in energy than configurations

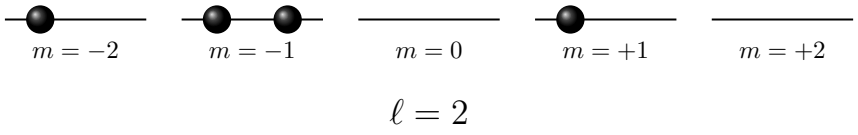

Figure 1.2: An example of one possible configuration of four nucleons moving in a degenerate $\ell = 2$ shell.

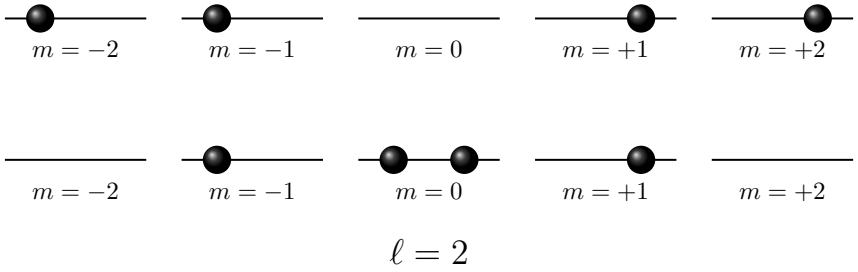

Figure 1.3: Two possible configurations of four nucleons moving in time-reversed orbits within a $\ell = 2$ shell.

where this is not respected, as in Fig. (1.2). The existence of a preferred direction where nucleons move, even in the case of a completely degenerate shell with no spin-orbit splitting, in order to form correlated pairs to reduce the energy of the total system is an indication of the breaking of a symmetry: the particle-number (or gauge) symmetry. The presence of pairing correlations is exposed by means of a collective mode of pair condensates in the nuclear structure, in analogy to the quadrupole degree of freedom, whose effect is observed in the surface deformation of the nucleus and the broken rotational symmetry [Bro73].

The formation of correlated pairs in nuclei is a direct consequence of the attractive short-range part of the nuclear interaction, making the spatial overlap between the two nucleons forming the pair maximal, only counterbalanced by Pauli's exclusion principle. Contrary to the condensed matter case in superconducting metals, where electrons form Cooper pairs due to in-medium vibrational effects, as the single-particle Coulomb interaction is repulsive, nucleons are able to form this kind of pairs in vacuum. Still, the collective vibrations among nucleons give rise to an additional induced pairing in finite nuclei [Bar99; Pas08], however the opposite effect was observed in infinite neutron matter [Cla76; Sch96; She03] as the additional contribution from the collective vibrations reduced the pairing correlations, leading to an open debate and current research far beyond the scope of this project.

In finite nuclei, a measure used to determine empirically the pairing gap for protons and

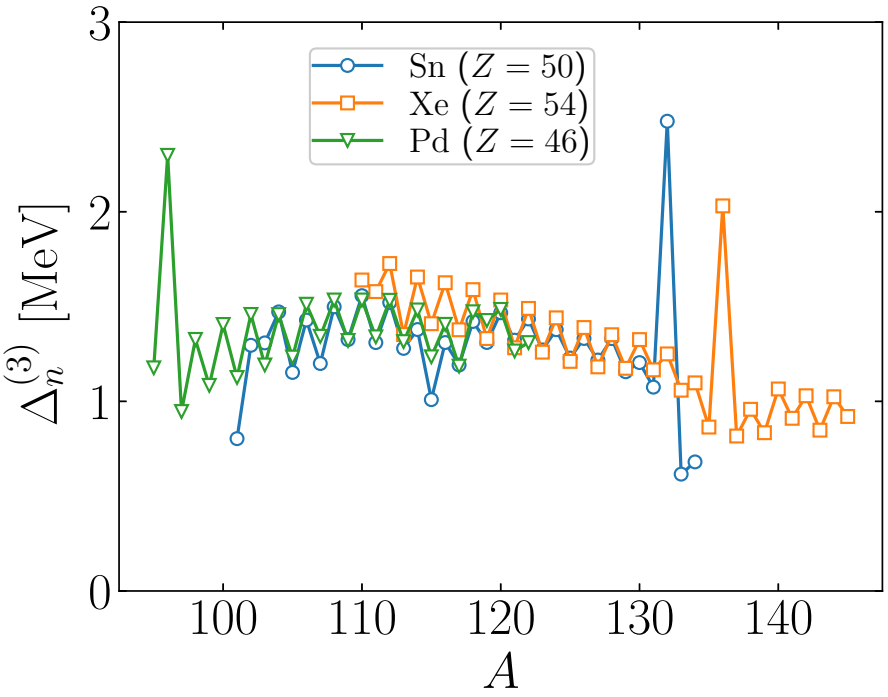

Figure 1.4: Odd-even mass staggering effect observed in the experimental binding energies of the isotopic chains of Tin, Xenon and Palladium, where $A = N + Z$ is the total number of particles. The results were computed using the three-point indicator in Eq. (1.1). The three outliers of the staggering correspond to neutron shell closures. Experimental data was obtained from [Wan17].

neutrons from their binding energies (BE) is given by the *three-point* indicator [SDN98]

$$\begin{aligned} \Delta_n^{(3)} &= \frac{(-1)^N}{2}[BE(N-1) + BE(N+1) - 2BE(N)], \\ \Delta_p^{(3)} &= \frac{(-1)^Z}{2}[BE(Z-1) + BE(Z+1) - 2BE(Z)], \end{aligned} \tag{1.1}$$

where N denotes the number of neutrons and Z the number of protons. Results for different isotopic chains are given in Fig. (1.4).

The gross general trend of the proton and neutron pairing gaps according to the three-point indicator all across the nuclear chart was suggested by Bohr & Mottelson [BM98], roughly following the formula

$$\Delta \sim \frac{12 \text{ MeV}}{A^{1/2}}, \tag{1.2}$$

where $A = N + Z$ is the total number of particles. Theoretical methods describing pairing correlations aim to reproduce the gaps given by the three-point formula, which they are also an

indirect measurement of the *number of pairs*, or the presence of pair condensation, in nuclei.

Early models of nuclear structure, such as the Bethe-Weizsäcker liquid drop model, had pairing correlations included taking the evenness of the nucleus into account. Such a term reads

$$\delta(N,Z) = \begin{cases} +\delta_0 \text{ if } N \text{ even, } Z \text{ even} \\ 0 \text{ if } N+Z \text{ odd} \\ -\delta_0 \text{ if } N \text{ odd, } Z \text{ odd,} \end{cases} \tag{1.3}$$

indicating that a nucleus with an even number of protons and neutrons is more bound than one with an odd number of particles. This effect can be seen, see Fig. (1.4), in the pairing gaps of nuclei and is named the *odd-even mass staggering*: even nuclei are more bound than their correspondent odd neighbours. Therefore we conclude that the odd-even mass staggering is a fingerprint of pairing correlations in nuclei. This effect is present not only in nuclei [Dob01], but also in metal clusters [De 93] and superconducting nanosystems [BRT96]. The origin of such effect is twofold: the spontaneous breaking of spherical symmetry, mainly affecting metal clusters and other macroscopic systems, and the impossibility to form a correlated pair because of the single odd particle, which corresponds to the case of atomic nuclei.

Pairing in nuclear structure was mainly considered between like-particles (proton-proton and neutron-neutron pairing) on the basis that the Fermi surfaces, the last occupied shell-model orbits, of the proton and the neutron were very dissimilar. However, in the region of the nuclear chart where the number of protons is equal to the number of neutrons (the $N = Z$ line), this is no longer true and theoretically proton-neutron pairing needs to also be taken into consideration. The first mention of a pairing correlation between a proton and a neutron was introduced by Goswami and Kisslinger [GK65], introducing the quantity *neutron-proton* gap. They developed a generalised gap equation (explained in Section 3) to find solutions for this quantity, similar in nature to the proton and neutron gaps, in order to study isoscalar[1] pairing correlations in an analogous manner to isovector correlations. This theory was refined by Goodman [Goo72] for neutron-proton (np) pairs that do not necessarily move in time-reversed orbits. Nevertheless, isoscalar np condensates remain elusive [Per04] and, in fact, some phenomenological calculations with the binding energies of even-even and odd-odd nuclei show that *isoscalar condensates do not contribute significantly to the pair correlation energy in* $N = Z$ *nuclei* [FM14] and that *there is no evidence for an isoscalar pair condensate in* $N = Z$ *nuclei* [Mac00], being the fundamental reason why we will not find values of experimental

[1] As protons and neutrons have isospin $\frac{1}{2}$, they can couple in pairs to total isospin 0 (isoscalar pairing) or 1 (isovector pairing).

neutron-proton gaps in the literature. Still, a microscopic calculation in real finite nuclei is very much needed in order to discern the origin of these proton-neutron pairing correlations as theoretical models predict the existence of these condensates. As np pairing only plays a major

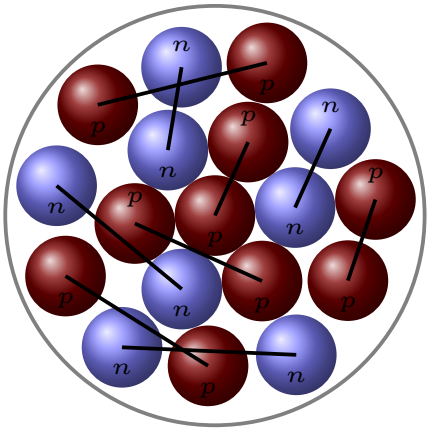

Figure 1.5: Isovector (like-particle) condensate in a nucleus.

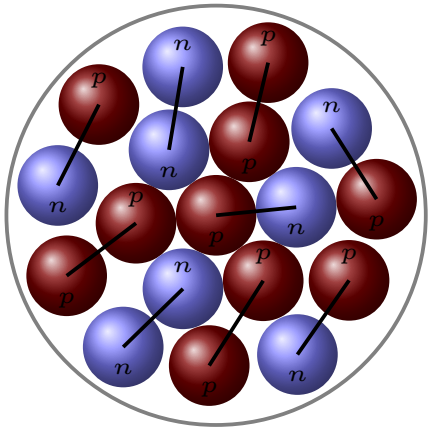

Figure 1.6: Isoscalar-isovector condensate coexistence in a nucleus.

role in $N = Z$ nuclei, it will not be significant in heavy nuclei, as there is a large asymmetry between neutrons and protons resulting from the repulsive Coulomb interaction. The largest $N = Z$ nucleus experimentally measured is ^{100}Sn [Hin12; FGG13]. The study of the $N = Z$ line is very interesting because this line coexists with the proton dripline and it has been argued that np pairing could play a role in the location of the proton dripline [Goo99]. It has also been found that np pairing correlations significantly influence processes such as neutrinoless double β ($0\nu\beta\beta$) decay [Pan96; HE14], Gamow-Teller transitions [Che95] and they could also influence the dynamics of rapid proton capture in stellar nucleosynthesis [Ced11]. Shell model studies show the importance of isoscalar pairing in the nuclear structure of self-conjugate nuclei based on a phenomenological Hamiltonian including a residual interaction between protons and neutrons [Fu16; Qi11; ZV11; Mio19]. However, these shell model works are seldom concerned with the anatomy of the nuclear wavefunction in terms of proton-proton, neutron-neutron and neutron-proton condensates [Van16]. In addition, rather than discussing about isoscalar neutron-proton pair condensates, it is frequent to read in the scientific literature about *spin-aligned* neutron-proton pairs in high-spin states, which are formed due to the rotational force which breaks the standard like-particle correlated pairs and aligns them along the direction of total angular momentum [KSA17]. Consequently, neutron-proton pairing may have a significant effect on the moments of inertia of rotating nuclei, such as ^{80}Zr [Goo01].

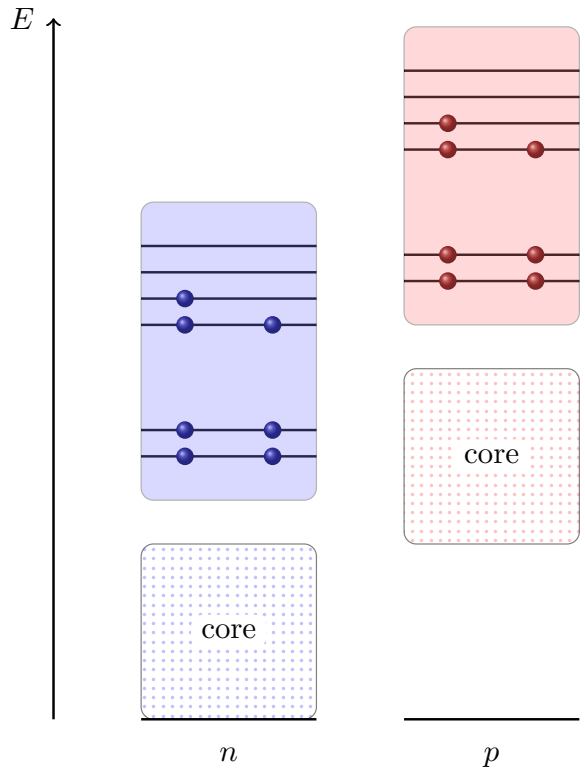

Figure 1.7: Shell model valence space configuration of a $N = Z$ nucleus. While protons and neutrons occupy similar shell-model orbitals, there is a significant difference between their Fermi energies because of the Coulomb interaction.

The major obstacle for the formation of neutron-proton pairs, and like-particle pairs in general, in open-shell nuclei is the spin-orbit interaction. For that reason, while we have stated that neutron-proton pairing plays a major role in $N = Z$ light nuclei below mass $A = 100$, it has been shown theoretically by Gezerlis [GBL11; BG16] that spin-triplet (isoscalar) and spin-singlet (isovector) phases mix in a heavy asymmetric nucleus like $^{132}_{64}$Gd. Moreover, the selective occupation of certain high angular-momentum single-particle orbitals cause the dominance of fully aligned neutron-proton pairs in many nuclei throughout the nuclear chart [Kim18]. This fact encourages the systematic microscopic study of pairing phases across the nuclear chart, only possible nowadays with the tools of density functional theory.

Recently, tentative experimental evidence has been found to support isoscalar and isovector neutron-proton pairing coupling coexistence in the level schemes of ^{96}Cd [Dav19] and ^{92}Pd [Ced11] and the 16^+ isomer of ^{96}Cd [Sin11], which motivates further theoretical work to include the isoscalar pairing correlations in calculations.

Another approach for the description of pairing correlations was introduced by Sandulescu and collaborators [San12; SSJ15; SS13] with the idea of four-body correlations in terms of *quartets*. A quartet is a four-particle object built from two isovector pairs, that is, a proton pair and a neutron pair. The intrinsic mean-field state is then written in terms of quartets and not Cooper isoscalar and isovector pairs. This method has shown a great success to reproduce results from standard shell model calculations with different interactions, for nuclei with the same number of proton and neutrons and also with a neutron excess [Neg18], however it has had limited applications in comparison with the usual mean-field techniques. In summary, there is a lot of interest in the physics of neutron-proton pairing, as its subtle balance with their analogue like-particle pairing influences many aspects in nuclear structure and, so far, while certain features are already well-established, neither a conclusive theoretical model nor experimental rule exist and are generally accepted. In this PhD project, we aim to look at the different pairing couplings from the perspective of the interaction and the nuclear wavefunction, where we give freedom to the formation of any pair condensate with no symmetry restriction or *ad hoc* assumptions. Our approach will be based on the mean-field and density functional theories.

The Thesis is structured as follows: in Section 2 we review existing approaches for the computation of pairing correlations and in particular we study the properties of the $SO(8)$ pairing Hamiltonian, used as a benchmark in our calculations as it allows arbitrary mixing of isoscalar and isovector pairs. In Section 3, a summary of mean-field methods to deal with pairing correlations is given and we provide details of the structure of our approach specifically considering the $SO(8)$ pairing interaction including proton-neutron mixing in the pairing channel, a calculation that has not been done before, and focusing on the isoscalar-isovector pairing coexistence. In Section 4, we assess the problem of restoring the symmetries implicitly broken because of the mean-field approach and in specific in our $SO(8)$ model, where particle-number, spin and isospin symmetries are broken, and what implies for the aforementioned pairing coexistence and several other observables like the deuteron transfer. In Section 5 we present and analyse the results obtained from the myriad of approaches presented in the former sections, coming to the main conclusion from this thesis: pairing coexistence can be observed within a symmetry-unrestricted mean-field method with proper restoration of broken symmetries. In Section 6 we delineate the prospects in order to port the presented methodology for the case of a realistic interaction in the pairing channel. Finally, we present our conclusions in Section 7.

Chapter 2

Interaction models for proton-neutron pairing

Algebraic methods, based on the full exploitation of the symmetries of the system, are very popular and useful since they provide exact solutions to many nuclear Hamiltonians, at the cost of the simplification of the problem and/or reducing the number of degrees of freedom involved. Algebraic models date back to 1958 when Elliott [Ell58b; Ell58a] associated the classification of states from the $SU(3)$ algebra scheme with those resulting of the shell model calculation in the *sd* shell, a breakthrough at the time [Van11]. The success was followed by the introduction of the *Interacting Boson Model* by Arima and Iachello [AI75], which is able to treat nuclear shapes and collective motion within the representations of the $SU(6)$ group. These two methods are the foundation of a myriad of algebraic methods being applied to several aspects of nuclear structure.

Nuclear pairing, and in specific, the coexistence between isoscalar and isovector condensates, can also be studied within these methods and this Section is devoted to them. At the beginning, simple formulas for the energy of different states were drawn from an analysis of the number of pairs broken in the system, referred in the literature as *seniority* models. Later, these models were refined to focus on the structure of the matrix elements of low-dimensional Hamiltonians. While these methods can not provide, at least at present, solutions for the realistic case of finite nuclei with an effective interaction, they are exact nuclear theories that are very interesting to analyse and evaluate their assumptions and symmetries. From a practical point of view, any shell model and mean-field approach could be adjusted to obtain the results from these exact theories, thus becoming an essential benchmark to test new phenomenological theories. The problem of np pairing can thus be described by the classification of states of the $SO(8)$ algebraic model, in a model of non-interacting $\ell-$shells in LS coupling, that is, disregarding

the spin-orbit interaction.

However, as interesting as these algebraic models may be, they are not useful if they are not applicable to realistic scenarios. To that end, after a fruitful analysis of the $SO(8)$ model, we extrapolate the suggested methods using a realistic interaction suitable for our calculations, planned to be implemented in the versatile three-dimensional Cartesian code HFODD [DD97] in order to get results in the foreseeable future.

This Chapter is structured as follows: in Section 2.1 we give a brief introductory review of the seniority model, which was very successful in the description of isovector pairing, and in Section 2.2 we describe the $SO(8)$ algebraic model of isoscalar and isovector pairing, a cornerstone of the present project.

2.1 Seniority model

A rough estimation of the importance and trend of pairing correlations in nuclei can be developed by means of the seniority model [GM96; KLM61]. As the trend will be completely determined by the total number of particles A and the number of pairs formed in the system, it is useful to use the *seniority* s, defined as the number of particles not forming a pair. We consider again a single $\ell-$shell with projection m, going from $-\ell$ to ℓ, with spatial degeneracy $\Omega = 2\ell + 1$ and total degeneracy, counting the spin degrees of freedom, 2Ω. Starting with the definition of pair creation and annihilation operators in the second quantization formalism

$$\hat{P}^+ = \frac{1}{2}\sum_{m\sigma}(-1)^{\ell-m-\frac{1}{2}\sigma}\hat{a}^+_{m\sigma}\hat{a}^+_{-m-\sigma}, \tag{2.1}$$

$$\hat{P}^- = (\hat{P}^+)^+ = \frac{1}{2}\sum_{m\sigma}(-1)^{\ell-m-\frac{1}{2}-\sigma}\hat{a}_{-m-\sigma}\hat{a}_{m\sigma}, \tag{2.2}$$

where $\hat{a}^+, \hat{a}$ are the fermionic single-particle creation and annihilation operators, respectively, defined with their action when applied to a state with zero $|0\rangle$ (the *bare vacuum*) or one $|1\rangle$ particle

$$\hat{a}|0\rangle = 0\ , \qquad \hat{a}^+|0\rangle = |1\rangle, \tag{2.3}$$

$$\hat{a}|1\rangle = |0\rangle, \qquad \hat{a}^+|1\rangle = 0, \tag{2.4}$$

respecting Pauli's exclusion principle, as two or more particles can not occupy the same state. In the definition of the pair creation and annihilation operators we have used the Condon-Shortley phase convention for the time-reversed states. The single-particle operators fulfil the

usual fermionic anticommutation rules

$$[\hat{a}_i, \hat{a}_j^+]_+ = \hat{a}_i\hat{a}_j^+ + \hat{a}_j\hat{a}_i^+ = \delta_{ij} \tag{2.5}$$

$$[\hat{a}_i^+, \hat{a}_j^+]_+ = [\hat{a}_i, \hat{a}_j]_+ = 0, \tag{2.6}$$

where i, j denote different quantum states and δ_{ij} is the Kronecker delta. These anticommutation relations ensure that two particles can not be in the same state. We define a pairing interaction using the pair operators (2.1, 2.2) of the form

$$\hat{V}_{\text{pair}} = -g\hat{P}^+\hat{P}^-, \tag{2.7}$$

where g is a coupling constant. This model forms pairs coupled to total angular momentum zero, in agreement to the experimental evidence. We calculate the spectra given by this interaction, to that purpose we define the following operators

$$\hat{A} = \sum_{m\sigma} \hat{a}_{m\sigma}^+\hat{a}_{m\sigma}, \tag{2.8}$$

$$\hat{P}_0 = \frac{1}{2}(\hat{A} - \Omega). \tag{2.9}$$

The first one can be regarded as the *number* operator, counting the number of particles in the system. We observe that the operators in Eqs. (2.1, 2.2, 2.9) fulfil angular momentum commutation relations

$$[\hat{P}^+, \hat{P}^-] = 2\hat{P}_0, \tag{2.10}$$

$$[\hat{P}_0, \hat{P}^+] = \hat{P}^+, \tag{2.11}$$

$$[\hat{P}_0, \hat{P}^-] = -\hat{P}^-, \tag{2.12}$$

therefore it is possible to find the spectra of the pairing interaction by looking at their Casimir invariants[1], $\hat{P}^2$ and $\hat{P}_0$. Indeed, in the angular momentum formalism, we define ladder operators of the form

$$\begin{aligned} \hat{J}_+ &= \hat{J}_x + i\hat{J}_y, \\ \hat{J}_- &= \hat{J}_x - i\hat{J}_y, \\ [\hat{J}_+, \hat{J}_-] &= 2\hat{J}_z. \end{aligned} \tag{2.13}$$

[1] A Casimir invariant is defined as the operator that commutes with all the generators of the algebra. They are extremely useful as its eigenvalues label the different states of the group representation.

Thus

$$\hat{J}^2 = \hat{J}_x^2 + \hat{J}_y^2 + \hat{J}_z^2 = \frac{1}{2}(\hat{J}_+\hat{J}_- + \hat{J}_-\hat{J}_+) + \hat{J}_z^2 = \hat{J}_+\hat{J}_- + \hat{J}_z^2 - \hat{J}_z. \tag{2.14}$$

Our pair operators follow a similar formula

$$\hat{P}^2 = \hat{P}^+\hat{P}^- + \hat{P}_0^2 - \hat{P}_0. \tag{2.15}$$

The eigenvalues of $\hat{P}^2$, of the form $p(p+1)$, can be determined by looking at the state of maximum projection given by $\hat{P}_0$, with eigenvalue $p = \frac{1}{2}(A - \Omega)$. If we apply the operator $\hat{P}^+$ to this state, the result will be zero, because the shell is completely full. As a consequence, there are no pairs formed in the shell, resulting in a maximal value of the seniority $s = A$ and $p = \frac{1}{2}(s - \Omega)$. Finally, the energy spectrum is obtained as

$$E_{s,A} = \langle s, A|\hat{V}_{\text{pair}}|s, A\rangle = -g\langle s, A|\hat{P}^2 - \hat{P}_0^2 + \hat{P}_0|s, A\rangle = -\frac{g}{4}(A - s)(2\Omega + 2 - A - s). \tag{2.16}$$

This method is sometimes referred in the literature as the *quasispin* formalism [Ker61], because it was completely developed using the commutation relations of the angular momentum (or spin, analogously) operators.

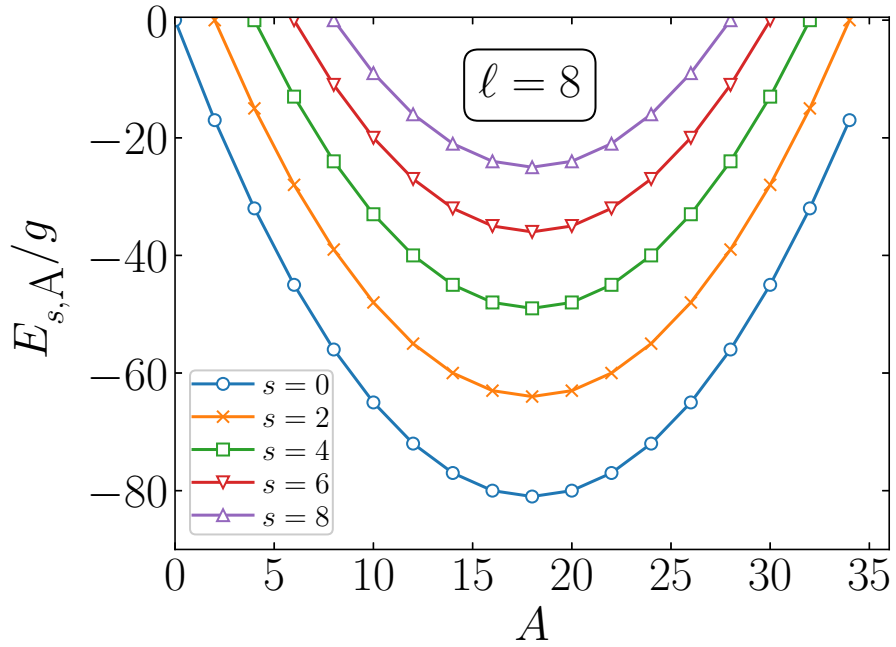

Figure 2.1: Pairing energy in a single $\ell-$shell, given by formula (2.16) for $\ell = 8$ (spatial degeneracy $\Omega = 2\ell + 1 = 17$) and different seniority numbers s. The lowest energy of the system is achieved with $s = 0$, a fully paired system.

We observe from plotting the spectra in Fig. (2.1) that the major contribution from pairing to nuclei is given in the mid-shell configuration, that is, when the shell is half full. When particles are added to the system, they can rearrange in time-reversed states to form correlated pairs and contribute to the total energy. However, when particles are added after the shell is half full, the number of states available decrease due to the Pauli principle and particles are not free to move anywhere, thus making a smaller contribution to the total energy. For a full shell, where all states are occupied, no correlated pairs can be formed and therefore the pairing contribution is zero. For this reason, magic nuclei can be described perfectly by means of a pure single-particle approach, with no need of pairing interaction. Under this line of reasoning, we also conclude that pairing must be a Fermi surface effect, that is, it is only concerned with the last shells, that are not fully occupied yet.

2.2 $SO(8)$ model of proton-neutron pairing

Considering A nucleons moving in one or several degenerate $\ell-$shell orbits subject to a constant interaction between them, the system has a total degeneracy of 4Ω, where $\Omega = \sum_i (2\ell_i + 1)$ is the spatial degeneracy and the factor of 4 comes from the degeneracy of spin and isospin (we do not consider separate protons and neutrons). We assume these nucleons in the system to be paired, coupled to total angular momentum $L = 0$, this channel is experimentally known to give the major contribution to pairing in nuclei [BMS10] and to spin S and isospin T. Because the wavefunction describing the system needs to be antisymmetric, the only possible pairing couplings for $L = 0$ are $(S, T) = (1, 0)$, the isoscalar coupling, and $(S, T) = (0, 1)$, the isovector coupling. The Hamiltonian describing the system is written as [KA06]

$$\hat{H} = -g(1-x)\sum_{\nu} \hat{P}^{+}_{\nu}\hat{P}_{\nu} - g(1+x)\sum_{\mu} \hat{D}^{+}_{\mu}\hat{D}_{\mu}, \tag{2.17}$$

where the isoscalar and isovector operators read

$$\begin{aligned} \hat{P}^{+}_{\nu} &= \sum_{\ell} \sqrt{\frac{2\ell+1}{2}} \left(\hat{a}^{+}_{\ell\frac{1}{2}\frac{1}{2}}\hat{a}^{+}_{\ell\frac{1}{2}\frac{1}{2}}\right)^{L=0,S=0,T=1}_{M=0,S_z=0,T_z=\nu}, \\ \hat{D}^{+}_{\mu} &= \sum_{\ell} \sqrt{\frac{2\ell+1}{2}} \left(\hat{a}^{+}_{\ell\frac{1}{2}\frac{1}{2}}\hat{a}^{+}_{\ell\frac{1}{2}\frac{1}{2}}\right)^{L=0,S=1,T=0}_{M=0,S_z=\mu,T_z=0}. \end{aligned} \tag{2.18}$$

g is the constant pairing strength and x is the mixing parameter controlling the relative competition between isoscalar and isovector pairing. The single-particle operators $\hat{a}^{+}_{\ell\frac{1}{2}\frac{1}{2}}$ create a

particle with angular momentum ℓ, spin $\frac{1}{2}$ and isospin $\frac{1}{2}$. The six different pairs created by these operators are sketched in Fig. (2.2). The Hamiltonian (2.17) has spherical symmetry and it is scalar and isoscalar, that is, invariant under rotations in spin and isospin space. For this reason, the different isoscalar and isovector contributions are sometimes referred to as *spin-triplet* and *spin-singlet* couplings, to avoid the confusion. For $x = -1$, it gives rise to a pure isovector contribution, as only isovector pairs are involved; similarly, for $x = 1$ it is a pure isoscalar interaction and for $x = 0$, they have the same strengths. For any other value of x, there is a contribution from both pairing couplings. The matrix elements of the Hamiltonian (2.17) can be evaluated writing the pair operators involved in terms of the 28 generators of the $SO(8)$ algebra[2], J_{ab}, where $1 \leqslant a < b \leqslant 8$, which fulfil the following algebraic commutation relations [GM96; PH67]

$$\begin{aligned} [J_{pq}, J_{rs}] &= i(\delta_{sp}J_{rq} + \delta_{rq}J_{sp} - \delta_{rp}J_{sq} - \delta_{sq}J_{rp}), \\ J_{pq} &= -J_{qp}, \\ J^{+}_{pq} &= J_{pq}, \end{aligned} \tag{2.19}$$

and whose matrix elements are known [GMY63]. In the same spirit of the quasispin formalism described in the former section, we need a set of physical operators that also generates this algebra. That set consists of the following 28 operators

$$\begin{aligned} &\hat{P}^{+}_{\nu}, \hat{P}_{\nu}, \hat{D}^{+}_{\mu}, \hat{D}_{\mu}, \\ &\hat{S}_{\mu}, \hat{T}_{\nu}, \hat{Q}_0, \hat{E}_{\mu\nu}, \end{aligned} \tag{2.20}$$

where $\hat{P}^{+}_{\nu}, \hat{D}^{+}_{\mu}$ were given in Eqs. (2.18). $\hat{Q}_0, \hat{S}_{\mu}, \hat{T}_{\nu}, \hat{E}_{\mu\nu}$ are one-body operators

$$\begin{aligned} \hat{Q}_0 &= \Omega - \frac{\hat{A}}{2}, \\ \hat{S}_{\mu} &= \left(\hat{a}^{+}_{\frac{1}{2}\frac{1}{2}}\hat{a}_{\frac{1}{2}\frac{1}{2}}\right)^{S=1,T=0}_{S_z=\mu,T_z=0}, \\ \hat{T}_{\nu} &= \left(\hat{a}^{+}_{\frac{1}{2}\frac{1}{2}}\hat{a}_{\frac{1}{2}\frac{1}{2}}\right)^{S=0,T=1}_{S_z=0,T_z=\nu}, \\ \hat{E}_{\mu\nu} &= \left(\hat{a}^{+}_{\frac{1}{2}\frac{1}{2}}\hat{a}_{\frac{1}{2}\frac{1}{2}}\right)^{S=1,T=1}_{S_z=\mu,T_z=\nu}, \end{aligned} \tag{2.21}$$

where ν, μ run over the values -1, 0, 1. We associate $\hat{Q}_0$ to the number operator, as it is related to $\hat{A}$, $\hat{S}_{\mu}$ and $\hat{T}_{\mu}$ to the spin and isospin operators, respectively, holding that $\hat{S}_{-\mu} = \hat{S}^{+}_{\mu}$

[2]In general, a $O(n)$ algebra will have $\frac{1}{2}n(n-1)$ generators.

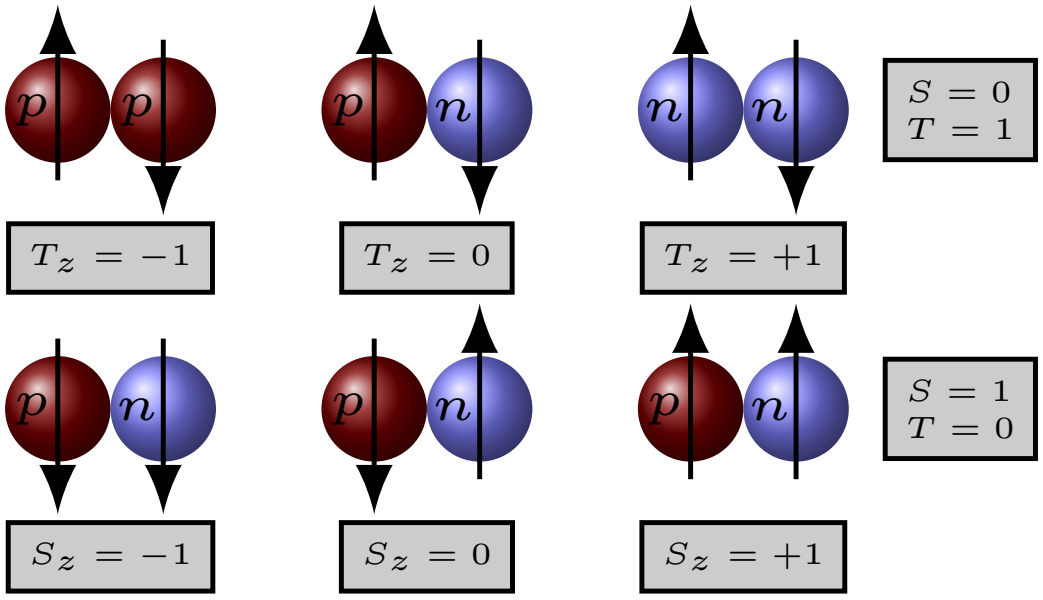

Figure 2.2: The six different pairing couplings constructing the $SO(8)$ Hamiltonian (2.17). The pairs in the top row corresponds to the three different projections of $\hat{P}^+_{T_z}$ and the pairs in the bottom row corresponds to the three different projections of $\hat{D}^+_{S_z}$. The arrows denote the two different projections, up and down, of the spin $\frac{1}{2}$ of protons and neutrons.

and $\hat{T}_{-\nu} = \hat{T}^+_\nu$; and $\hat{E}_{\mu\nu}$ are the spin and charge-exchange operators [FS64], holding that $\hat{E}^+_{\mu\nu} = \hat{E}_{-\mu-\nu}$. As they generate the eight-dimensional algebra, these quasispin operators need to be written in terms of the operators in (2.19). Indeed, they were given in [Pan69] and we summarised them in Table (2.1). Thus, we have an expression for the matrix elements of the pair operators, which are used for the calculation of spectroscopic amplitudes of deuteron and alpha transfers, and consequently of the Hamiltonian, in the so called Gel'fand basis, that is, the vectors of the irreducible representation of the $SO(8)$ algebra [PH67]. Moreover, for specific values of the interaction, namely $x = \pm 1, 0$, the states can be labelled by the representation of the following subalgebras [KA06]

$$\begin{aligned} x = 0 &: SO(8) \supset SO_{ST}(6) \supset SO_S(3) \otimes SO_T(3), \\ x = 1 &: SO(8) \supset [SO_S(5) \supset SO_S(3)] \otimes SO_T(3), \\ x = -1 &: SO(8) \supset [SO_T(5) \supset SO_T(3)] \otimes SO_S(3). \end{aligned} \tag{2.22}$$

In these cases, the energy will follow a formula similar to the one derived *à la* seniority model in the former section using the generators of the $SO(3)$ angular momentum algebra. For details of these formulas and the general matrix elements of the Hamiltonian we refer to Appendix A.

The $SO(8)$ Hamiltonian (2.17) is a *separable interaction*, in the sense that it has the form

$$\hat{V} = \hat{Q}^{+}\hat{Q}, \tag{2.23}$$

with $\hat{Q} = \sum_{ij} q_{ij}\hat{a}_i\hat{a}_j$. That is, the force can be written as a separate bilinear product of a pair of particles and a pair of holes. We will extend this notion of separate coordinates when we port the mean-field plus symmetry restoration methodology to the realistic case of a finite nucleus using a phenomenological effective interaction in coordinate space. We refer to Section 6.1 for details.

$\hat{P}^{+}_{1}$	$\frac{1}{2}\left[i\left(J_{57}+iJ_{67}\right)+\left(J_{58}+iJ_{68}\right)\right]$
$\hat{P}^{+}_{0}$	$\frac{1}{\sqrt{2}}(J_{47}-iJ_{48})$
$\hat{P}^{+}_{-1}$	$\frac{1}{2}[i(J_{57}-iJ_{67})+(J_{58}-iJ_{68})]$
$\hat{D}^{+}_{1}$	$\frac{1}{2}[-(J_{17}+iJ_{27})+i(J_{18}+iJ_{28})]$
$\hat{D}^{+}_{0}$	$\frac{-i}{\sqrt{2}}(J_{37}-iJ_{38})$
$\hat{D}^{+}_{-1}$	$\frac{1}{2}[-(J_{17}-iJ_{27})+i(J_{18}-iJ_{28})]$
$\hat{Q}_{0}$	J_{78}
$\hat{S}_{1}$	$\frac{1}{\sqrt{2}}(J_{13}+iJ_{23})$
$\hat{S}_{0}$	J_{12}
$\hat{S}_{-1}$	$\frac{1}{\sqrt{2}}(J_{13}-iJ_{23})$
$\hat{T}_{1}$	$\frac{1}{\sqrt{2}}(J_{45}+iJ_{46})$

$\hat{T}_{0}$	J_{56}
$\hat{T}_{-1}$	$\frac{1}{\sqrt{2}}(J_{45}-iJ_{46})$
$\hat{E}_{00}$	J_{34}
$\hat{E}_{11}$	$\frac{1}{2}\left[(J_{15}+iJ_{25})+i(J_{16}+iJ_{26})\right]$
$\hat{E}_{-1-1}$	$\frac{1}{2}\left[(J_{15}-iJ_{25})-i(J_{16}-iJ_{26})\right]$
$\hat{E}_{1-1}$	$\frac{1}{2}\left[-(J_{15}+iJ_{25})+i(J_{16}+iJ_{26})\right]$
$\hat{E}_{-11}$	$\frac{1}{2}\left[-(J_{15}-iJ_{25})-i(J_{16}-iJ_{26})\right]$
$\hat{E}_{10}$	$\frac{i}{\sqrt{2}}(J_{14}+iJ_{24})$
$\hat{E}_{-10}$	$-\frac{i}{\sqrt{2}}(J_{14}-iJ_{24})$
$\hat{E}_{01}$	$\frac{-i}{\sqrt{2}}(J_{35}+iJ_{36})$
$\hat{E}_{0-1}$	$\frac{i}{\sqrt{2}}(J_{35}-iJ_{36})$

Table 2.1: Reproduction of Table 1 from [Pan69] of the quasispin operators expressed in terms of the generators of the $SO(8)$ algebra (2.19).

2.2.1 Spectra

Using the algebraic methods described in Section 2.2, exact matrix elements of the pairing Hamiltonian in Eq. (2.17) can be computed and the full solution is obtained by diagonalisation. In particular, we discuss in this Section the physical properties and symmetries of the excitation spectra of the $SO(8)$ Hamiltonian obtained for different values of the spin S and the isospin T. In Fig. (2.3), we plot the ground-state energies for a half-occupied system, for several values of the mixing parameter x. The states are labelled by the spin S in the abscissa and by the isospin T following the classification of states of Table (A.1). We notice the spin vibrational pattern followed by the energies when the interaction is isoscalar dominant ($x > 0$), i.e., panels (d) and

(e). Another interesting feature is the symmetric pattern observed in panel (c) for $x = 0$, where both isoscalar and isovector contributions to the pairing Hamiltonian are equal. For this case, an exchange of the labels $S \leftrightarrow T$ leaves the Hamiltonian invariant and this is reflected in the figure, where states with the same $S + T$ number have the same energy. The $SO(8)$ algebra of the Hamiltonian in this case boils down to the Wigner's $SU(4)$ spin-isospin algebra [Wig37] and, as detailed in Appendix A, it can be exploited to obtain a simple formula for the energies of these ground-states and states with broken pairs (non zero seniority).

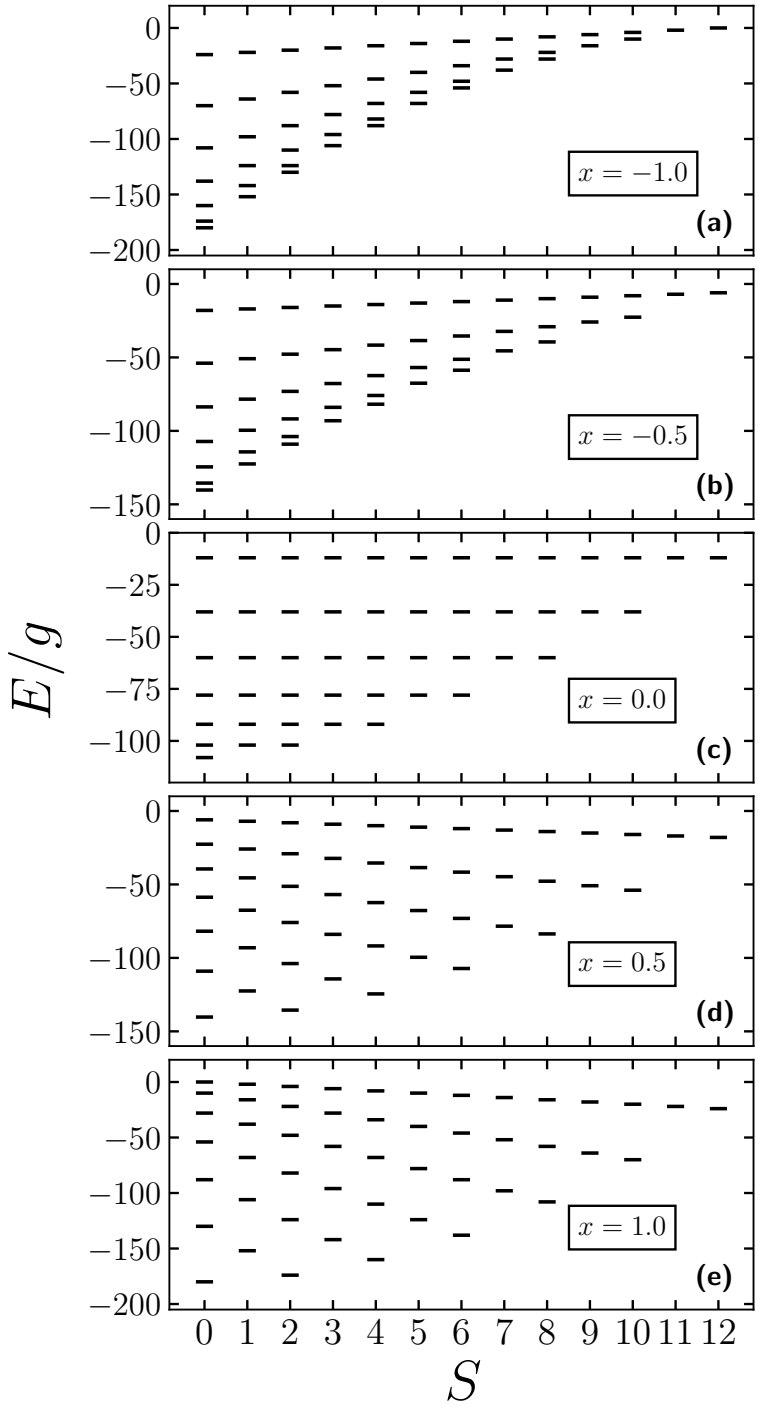

Figure 2.3: Energies, in units of g, of the states labelled with different spin S (abscissa) and isospin T (starting from the bottom with 0 or 1 if S is even or odd, respectively, and increasing in steps of 2, in accordance with the classification of states given in Table (A.1)) for a particle number of $A = 24$ (mid shell configuration) in a system with spatial degeneracy $\Omega = 12$ for $x = -1, 0.5, 0, 0.5, 1$ in the pairing Hamiltonian (2.17) in panels (a)-(e), respectively.

Chapter 3

Self-consistent mean-field methods

When studying properties of nuclei, three main models are predominant within the scientific community: *ab-initio*, *shell-model* and *mean-field* or *density-functional theory* methods. Ab-initio methods rely upon the exact calculation of the solution of a many-body Hamiltonian with an effective nucleon-nucleon interaction. They have proven to be very successful, but their range of application is limited, and heavy nuclei can not be studied within their methods. Among the various ab-initio techniques we can cite the self-consistent Green function methods [DM92; DB04], coupled clusters [KLZ78; Dug14] and quantum Monte Carlo methods [Car15], with a typical accuracy of 1% on the binding energies, which is much worse than the precision of the density-functional theory techniques. Shell-model methods use an active configuration space to build all possible many-body states allowed in the system starting from single-particle states [Tal03; BW88; Cau05]. Although very successful methods too, the size of this configuration space grows exponentially and this mechanism is not suitable for computation of nuclear structure properties in the heavy region. Finally, the self-consistent mean-field methods are focused on the treatment of a general average potential, an interaction, in which all the nucleons move independently from each other, and taking special consideration of the wavefunction of the compound system, the nucleus itself [BHR03]. The energy of the nucleus, when averaged with respect its wavefunction, will be a functional of the density of the nuclear system, even when the potential is not density dependent. The main advantage of these density-functional techniques is that they are the only ones being able to study nuclei all across the nuclear chart, from light to heavy and from stable to exotic regions. The range of application of the three different theories is depicted in Fig. (3.1).

The problem of the coexistence of isoscalar and isovector condensates will be reviewed in this work under these mean-field techniques, working explicitly with nuclear wavefunctions whose structure can be analysed in terms of the different contributions from both kind of

pair condensates. First, we will describe the Hartree-Fock framework, in Section 3.1, dealing

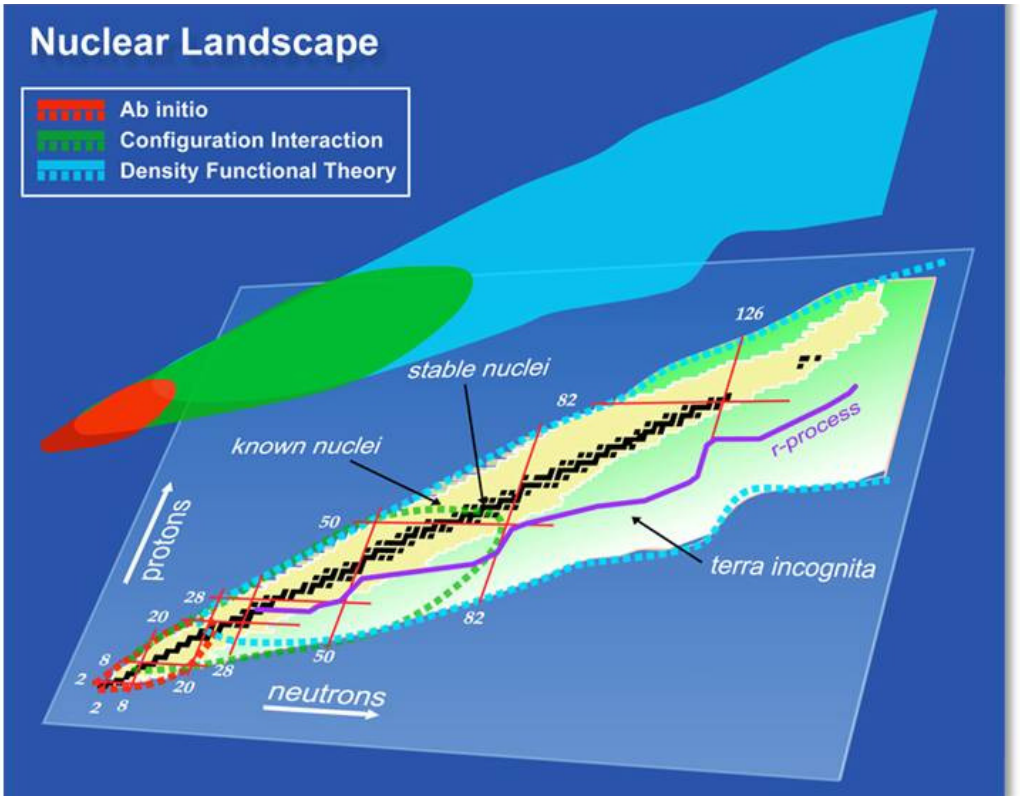

Figure 3.1: Range of application of the three different methods in nuclear structure. Figure taken from [Nam12].

with antisymmetrized product states as ansatzs for the wavefunction of the total system. It will be followed by the Bardeen-Cooper-Schrieffer (BCS) formalism of pairing in Section 3.2, introduced by them to successfully explain superconductivity in metals using the concept of a correlated electron pair (also referred to as Cooper pair) that acts effectively as a boson. The BCS theory was ported to the nuclear field with outstanding success for the description of like-particle (proton-proton and neutron-neutron) pairing using the HF+BCS approach. However, there is a lack of consistency in these approaches as they are not self-consistent, that is, both methods are applied and solved separately and they do not have an influence on each other. A generalisation of this technique to include self-consistenly the long-range particle-hole and the short-range particle-particle pictures is given by the Hartree-Fock-Bogoliubov (HFB) approach, introduced in Section 3.3 which solves for both potentials on the same footing. The HFB method has proven to be very successful in applications over the whole nuclear chart, becoming the cornerstone of nuclear structure calculations within the mean-field or density functional theory. This Chapter will be mostly devoted to describe such framework, involved

in all the results from this project.

3.1 Hartree-Fock picture for a many-body system

It is fair to say that the birth of the mean-field methods comes from atomic and molecular physics, where from the single-particle basis states $|\psi_i(\mathbf{r}_j)\rangle$ of the electrons forming the compound system, a total wavefunction $|\Psi\rangle$ is constructed as the *product state* of all the single-electrons' wavefunctions,

$$|\Psi\rangle \propto \prod_i |\psi_i(\mathbf{r}_j)\rangle, \tag{3.1}$$

called the *Hartree* wavefunction. This wavefunction is not antisymmetric under the exchange of particles, lacking consistency as the system described is fermionic in nature as well. This is solved by introducing the *Slater determinant* and writing the total wavefunction as

$$|\Psi\rangle \propto \det \begin{pmatrix} |\psi_1(\mathbf{r}_1)\rangle & |\psi_2(\mathbf{r}_1)\rangle & \dots & |\psi_A(\mathbf{r}_1)\rangle \\ |\psi_1(\mathbf{r}_2)\rangle & |\psi_2(\mathbf{r}_2)\rangle & \dots & |\psi_A(\mathbf{r}_2)\rangle \\ \vdots & \vdots & \ddots & \vdots \\ |\psi_1(\mathbf{r}_A)\rangle & |\psi_2(\mathbf{r}_A)\rangle & \dots & |\psi_A(\mathbf{r}_A)\rangle \end{pmatrix}, \tag{3.2}$$

which is the usual *Hartree-Fock* (HF) wavefunction, used conventionally in shell-model and mean-field methods, both in atomic and nuclear physics. Using the usual definition of a many-body Hamiltonian in second quantization [RS80]

$$H = \sum_{ij} t_{ij} \hat{a}_i^+ \hat{a}_j + \frac{1}{4} \sum_{ijkl} \overline{v}_{ijkl} \hat{a}_i^+ \hat{a}_j^+ \hat{a}_l \hat{a}_k, \tag{3.3}$$

t are the kinetic energy terms and $\overline{v}$ the antisymmetrised two-body matrix elements, we are able to cast a Hartree-Fock potential h, defined as

$$h|\psi_i\rangle = \epsilon_i |\psi_i\rangle, \tag{3.4}$$

with ϵ_i being the energy of the single-particle state $|\psi_i\rangle$. The HF potential h is written as

$$h = t + \Gamma, \tag{3.5}$$

which is the sum of the kinetic energy and a self-consistent field Γ. The HF potential takes into account correlations given by the long-range part of the nuclear interaction, described by the

field Γ. The Hartree-Fock picture can be described by means of a density-matrix formalism. In the second-quantization framework, the matrix elements of the density ρ are,

$$\rho_{ij} = \langle \Psi | \hat{a}_j^+ \hat{a}_i | \Psi \rangle, \tag{3.6}$$

where $\hat{a}^+, \hat{a}$ are the single-particle creation and annihilation operators, respectively, described in Section 2.1. The matrix elements of the self-consistent field Γ are defined in terms of the density matrix as

$$\Gamma_{ij} = \sum_{kl} \overline{v}_{iljk} \rho_{kl}. \tag{3.7}$$

The Hartree-Fock equations can be compactly casted as

$$[h, \rho] = 0, \tag{3.8}$$

that is, the problem is reduced to an eigenvalue problem to find the basis of states in which both the density ρ and the potential field h are diagonal. In this basis, the density has two fundamental properties

$$\begin{aligned} \rho^2 &= \rho, \\ \operatorname{Tr} \rho &= A. \end{aligned} \tag{3.9}$$

The first relation shows that the density is idempotent and therefore its eigenvalues are either 1 or 0, indicating that a certain level is either filled or empty. As a consequence of this relation, the second holds in any case as the trace is invariant under a change of basis. Sometimes it is convenient to rewrite this problem as a minimisation problem instead of a diagonalisation problem, defining the total energy to be minimised as

$$E_{HF} = \operatorname{Tr}\left(t\rho + \frac{1}{2}\Gamma\rho \right). \tag{3.10}$$

Effects of deformation and collective motion are well described within this methodology. However, it is not a proper picture to describe systems heavily influenced by the short-range part of the nuclear interactions, responsible of pairing correlations.

3.2 BCS framework for treating pairing correlations

The BCS formalism used for treating superconductivity by means of Cooper pairs in metals can be analogously used to treat proton-proton and neutron-neutron pairing in nuclei. The BCS wavefunction reads

$$|\mathrm{BCS}\rangle = \prod_{k>0}(u_k + v_k \hat{a}_k^+ \hat{a}_{\bar{k}}^+)|0\rangle, \tag{3.11}$$

where $|0\rangle$ is the single-particle vacuum, k denotes the single-particle indices and $\bar{k}$ indicates time-reversal. The BCS wavefunction is a superposition of different Slater determinants where there is a probability $|v_k|^2$ that the states with quantum numbers k and $\bar{k}$ are filled and a probability $|u_k|^2$ that those states are empty. These probabilities are treated as variational parameters in order to obtain the optimal wavefunction in (3.11) that gives the energy minimum. Naturally, they must fulfil the condition

$$|v_k|^2 + |u_k|^2 = 1. \tag{3.12}$$

One of the major implications of the BCS formalism is the automatic breaking of the particle-number symmetry by the ansatz wavefunction (3.11). Instead of having a sharp value, we obtain an average value with fluctuations given by

$$A = \langle \mathrm{BCS}|\hat{A}|\mathrm{BCS}\rangle = 2\sum_{k>0} v_k^2, \tag{3.13}$$

$$\Delta A^2 = \langle \mathrm{BCS}|\hat{A}^2|\mathrm{BCS}\rangle - \langle \mathrm{BCS}|\hat{A}|\mathrm{BCS}\rangle^2 = 4\sum_{k} u_k^2 v_k^2. \tag{3.14}$$

As the fluctuations are given by the product of partially filled and empty states v_k, u_k, setting one of these values to zero will force the other to be one according to (3.12) and the BCS wavefunction will collapse to a Slater determinant. Therefore, we conclude that the particle-number breaking is a consequence of the partial filling of the different pair states.

The probability amplitudes are determined by a constrained minimisation of the energy surface E including condition (3.13). It is achieved by means of a Lagrange parameter λ

$$\lambda = \frac{dE}{dA}, \tag{3.15}$$

which is also referred to as the *chemical potential*, adding a contribution of $-\lambda\hat{A}$ to the Hamiltonian. The Lagrange parameter λ is fixed by the average particle condition in Eq. (3.13). Considering a general Hamiltonian of the form (3.3) and the Lagrange multiplier λ, we variate

with respect v_k[1]

$$\frac{d}{dv_k}\langle \mathrm{BCS}|\hat{H} - \lambda\hat{A}|\mathrm{BCS}\rangle, \tag{3.16}$$

to obtain

$$2(\epsilon_k - \lambda)u_k v_k + \Delta_k(v_k^2 - u_k^2) = 0, \tag{3.17}$$

with

$$\Delta_k = \frac{1}{4}\sum_l \bar{v}_{k\bar{k}l\bar{l}} u_l v_l. \tag{3.18}$$

The former quantity Δ is called the *gap parameter* and it gives the strength of the pairing correlations present in the system, as we shall see in the following derivations. From (3.17) and (3.12), we finally obtain

$$v_k^2 = \frac{1}{2}\left(1 - \frac{\epsilon_k - \lambda}{\sqrt{(\epsilon_k - \lambda)^2 + \Delta_k^2}}\right), \quad u_k^2 = \frac{1}{2}\left(1 + \frac{\epsilon_k - \lambda}{\sqrt{(\epsilon_k - \lambda)^2 + \Delta_k^2}}\right), \tag{3.19}$$

that is, the occupation probabilities are a function of the gap parameter Δ. We illustrate the behaviour of these quantities in Fig. (3.2) in a schematic way. For vanishing pairing

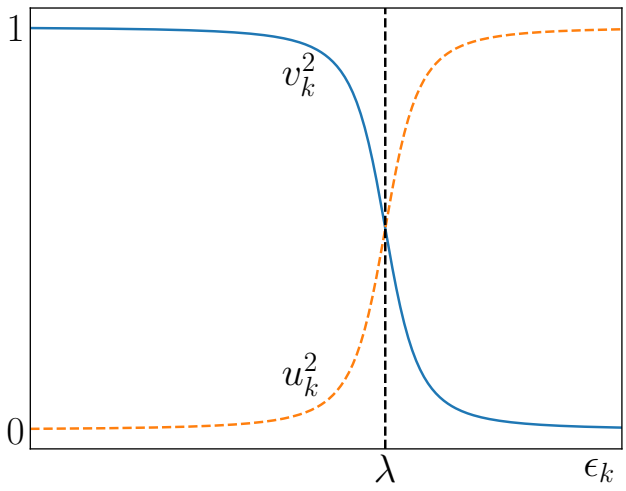

Figure 3.2: Occupation probabilities in the BCS formalism.

[1]Only variation with respect v_k is needed, because of the normalisation condition (3.12).

interactions, that is, for $\Delta = 0$, u_k^2 and v_k^2 collapse to step functions

$$v_k^2 = \begin{cases} 1 & \text{if } \epsilon_k < \lambda, \\ 0 & \text{if } \epsilon_k > \lambda, \end{cases} \qquad u_k^2 = \begin{cases} 0 & \text{if } \epsilon_k < \lambda, \\ 1 & \text{if } \epsilon_k > \lambda, \end{cases} \tag{3.20}$$

and particle-number is again a good quantum number as there is no partial filling of the states, returning to the usual single-particle Hartree-Fock limit. From Equation (3.20), we see that v_k^2 is the probability of the state k to be occupied and u_k^2 the probability of the state k to be empty. Also, as seen in Fig. (3.2), λ acts as a *generalised Fermi energy*, corresponding to the collapsing value of the step functions in the Hartree-Fock limit.

Since the BCS formalism is uniquely determined by the gap parameter Δ, we need a set of equations to solve for this quantity as a function of the two-body interaction matrix elements and the single-particle energies. From (3.18), we have

$$\Delta_k = \frac{1}{8}\sum_l \bar{v}_{k\bar{k}l\bar{l}}\sqrt{1 - \frac{(\epsilon_l - \lambda)^2}{(\epsilon_l - \lambda)^2 + \Delta_l^2}} = \frac{1}{8}\sum_l \bar{v}_{k\bar{k}l\bar{l}}\frac{\Delta_l}{\sqrt{(\epsilon_l - \lambda)^2 + \Delta_l^2}}, \tag{3.21}$$

referred in the literature as the BCS *gap equation*, a nonlinear equation that needs to be solved self-consistently, along with a known expression for the single-particle energies ϵ_k and the Lagrange parameter λ fixed by condition (3.15). In infinite nuclear matter, a system where no finite-size effects are present, there is an equal number of protons and neutrons, it is spin saturated and there is translational invariance, we have a continuum of states. The gap equation in this system is formulated as an integral instead of a sum over all possible states, labelled by the plane-wave momentum $\boldsymbol{k}$. In the nuclear community, a popular calculation of isovector pairing gaps in nuclear matter was given by Gogny and collaborators with the so-called D1 [DG80] and D1S [BGG91] interactions, which we recreate in Fig. (3.3), and many energy density functionals have been fitted in order to reproduce these benchmark results. In Fig. (3.3), we observe that the pairing gap vanishes at low and high densities, and the typical value of 1 MeV is reproduced at the saturation density of nuclear matter $\rho_0 = 0.16$ fm^{-3}, corresponding to $k_F = 1.33$ fm^{-1} as shown by the dotted line. Pairing gaps beyond the densities shown in the figure are thought to be important as well [Bal98].

From the gap equation we confirm again that pairing is a Fermi surface effect, as the states whose energy are near the Fermi energy ($\epsilon_k \sim \lambda$) contribute more to the gap parameter.

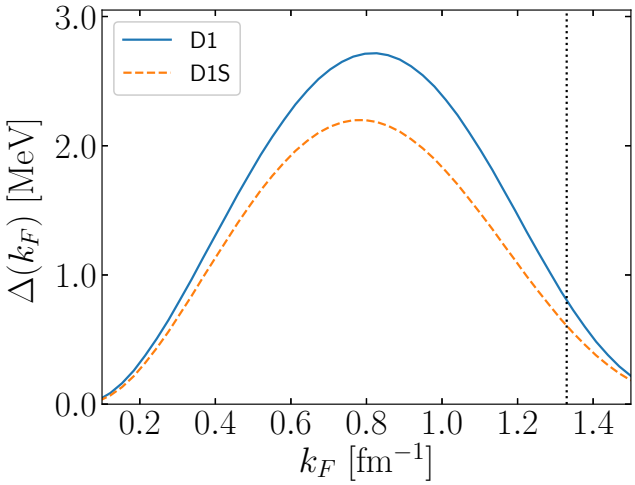

Figure 3.3: Pairing gaps in nuclear matter as a function of the Fermi momentum (which is proportional, according to the free Fermi gas approximation, to $\rho^{1/3}$). Figure extracted from [Kuc89].

3.2.1 Degenerate shell case

If we consider a degenerate system, where all particles sit on single-particle states which have the same energy, the occupation probabilities v_k^2 are the same. Using (3.12) and (3.13) we obtain

$$v^2 = \frac{A}{2\Omega}, \quad u^2 = 1 - \frac{A}{2\Omega}, \tag{3.22}$$

with Ω being the total degeneracy of the system. For this case the pairing gap has a very simple expression, as all the matrix elements $\overline{v}$ in Eq. (3.18) are constant, which we will denote by g, given by

$$\Delta = g\sqrt{\frac{A}{2}\left(\Omega - \frac{A}{2}\right)}, \tag{3.23}$$

and the particle fluctuations are

$$\frac{\Delta A}{A} = \sqrt{\frac{2}{A} - \frac{1}{\Omega}}. \tag{3.24}$$

Thus, for a very large system, with a very large configuration space, the fluctuations tend to zero. For this reason, in the application of the BCS formalism to superconducting metals and generally in condensed-matter physics, which deal with a large number of particles, these fluctuations are not taken into account as they become negligible. In Fig. (3.4), we observe that even with a very simple expression of the pairing gap as in Eq. (3.23), we capture many features when comparing the results to the realistic case, as it follows a bell-shaped curve with

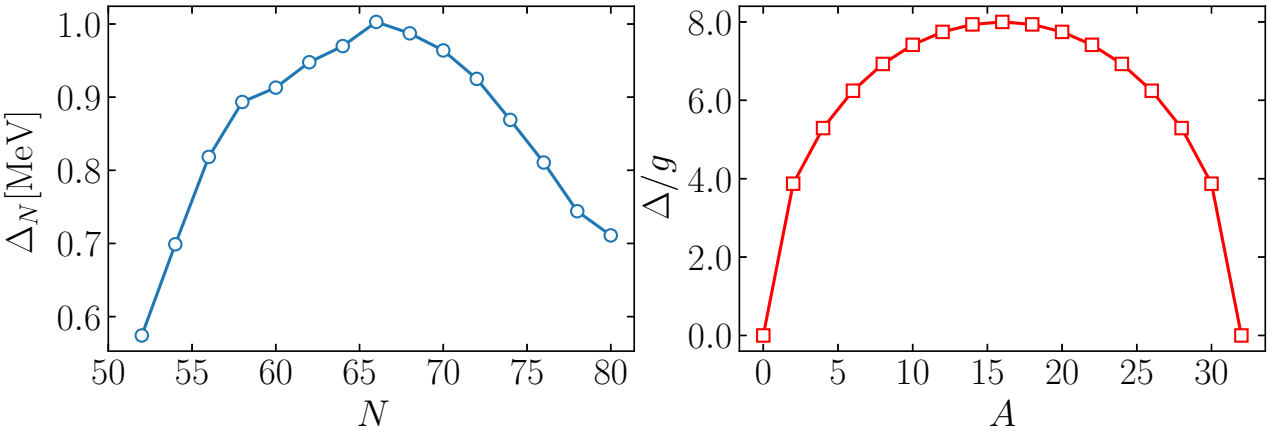

Figure 3.4: Neutron pairing gaps Δ_N as a function of the even number of neutrons N in the open shell for the isotopic chain of Sn (left) using the realistic functional interaction UNEDF0 [Erl12] and pairing gaps in a degenerate shell as in Eq. (3.23) for $\Omega = 16$ (right). We see that they both follow a bell-shaped curve and reach a maximum approximately around the middle of the occupied shell.

maximum centred in the middle of the shell and vanishing values where the shell is empty or full. As the used model is purely schematic, only the qualitative trend is reproduced, and the energy scales are different.

3.2.2 Bogoliubov transformation. Quasiparticle operators.

The former results can be obtained in a more general manner by the introduction of *quasiparticle operators*. In the second quantization formalism, we define a bare *vacuum* state $|0\rangle$ as the one that vanishes after applying a single-particle annihilation operator $\hat{a}$. In the same spirit, we define, for a BCS wavefunction describing a superfluid nucleus

$$\hat{\beta}|\mathrm{BCS}\rangle = 0, \tag{3.25}$$

where $\hat{\beta}$ is a quasiparticle annihilation operator. These new operators are written in terms of the usual single-particle ones using the linear transformation

$$\begin{aligned} \hat{\beta}_k &= u_k \hat{a}_k - v_k \hat{a}_{\bar{k}}^+, \quad \hat{\beta}_k^+ = u_k \hat{a}_k^+ - v_k \hat{a}_{\bar{k}}, \\ \hat{\beta}_{\bar{k}} &= u_k \hat{a}_{\bar{k}} + v_k \hat{a}_k^+, \quad \hat{\beta}_{\bar{k}}^+ = u_k \hat{a}_{\bar{k}}^+ + v_k \hat{a}_k, \end{aligned} \tag{3.26}$$

called *Bogoliubov transformation*. We observe that the application of $\hat{\beta}$ on Eq. (3.11) is zero as required. The Bogoliubov transformation may be rewritten in matrix form as

$$\begin{aligned}\begin{pmatrix}\hat{\beta}^+_k\\ \hat{\beta}_{\bar{k}}\end{pmatrix} &= \begin{pmatrix}u_k & v_k\\ -v_k & u_k\end{pmatrix}\begin{pmatrix}\hat{a}^+_k\\ \hat{a}_{\bar{k}}\end{pmatrix},\\ \begin{pmatrix}\hat{\beta}^+_{\bar{k}}\\ \hat{\beta}_k\end{pmatrix} &= \begin{pmatrix}u_k & -v_k\\ v_k & u_k\end{pmatrix}\begin{pmatrix}\hat{a}^+_{\bar{k}}\\ \hat{a}_k\end{pmatrix}.\end{aligned} \tag{3.27}$$

The transformation is unitary, as the determinant of the transformation matrix is one, ensuring no loss of probability and the existence of the inverse transformation to write the single-particle operators in terms of quasiparticle operators. From this transformation, we observe that the BCS wavefunction is created from these operators and it does not have a good particle-number, as we are mixing explicitly particles $\hat{a}^+$ and holes $\hat{a}$, labelled with the index k.

A simple calculation proves that quasiparticles are fermions,

$$\begin{aligned}[\hat{\beta}_k, \hat{\beta}^+_{k'}]_+ &= [u^*_k\hat{a}_k \pm v^*_k\hat{a}^+_k, u^*_{k'}\hat{a}_{k'} \pm v^*_{k'}\hat{a}^+_{k'}]_+\\ &= u^*_k u_{k'}[\hat{a}_k, \hat{a}^+_{k'}]_+ \pm u^*_k v_{k'}[\hat{a}_k, \hat{a}_{k'}]_+ \pm v^*_k u_{k'}[\hat{a}^+_k, \hat{a}^+_{k'}]_+ + v^*_k v_{k'}[\hat{a}^+_k, \hat{a}_{k'}]_+\\ &= (u^*_k u_{k'} + v^*_k v_{k'})\delta_{kk'} = \delta_{kk'},\end{aligned} \tag{3.28}$$

where we have made use of the anticommutation relations (2.5, 2.6) and the normalisation condition of the quasiparticle amplitudes (3.12). It is a crucial required condition, since we need quasiparticles to fulfil Pauli's exclusion principle.

From the mathematical point of view, the Bogoliubov transformation was introduced in order to diagonalise the matrix elements of the two-body Hamiltonian $\hat{H} - \lambda\hat{A}$. Indeed, if we expand the single-particle operators in terms of the quasiparticle operators we would obtain

$$\hat{H} - \lambda\hat{A} = \hat{H}_{00} + \hat{H}_{11} + \hat{H}_{20} + \hat{H}_{22} + \hat{H}_{31} + \hat{H}_{40}, \tag{3.29}$$

where $\hat{H}_{ij}$ denotes a contribution with i quasiparticle creation and j quasiparticle annihilation operators. An usual approximation is done by neglecting the terms $\hat{H}_{22}$, $\hat{H}_{31}$ and $\hat{H}_{40}$. The BCS equations (3.17) are obtained within this approximation by establishing $\hat{H}_{20} = 0$, i.e., by setting to zero the quasiparticle fluctuations, in a similar fashion to how the Hartree-Fock equations are derived in the single-particle picture. Thus, we observe in Eq. (3.29) that, while the Hamiltonian in the left-hand side has a pair-wise interaction of particles, the Hamiltonian written in the right-hand side only has one quasiparticle terms, that is, it describes a system of non-interacting quasiparticles, which is much easier and convenient to describe, at the cost

of its eigenfunctions not being eigenfunctions of the particle-number operator.

The BCS formalism has proven itself very successful when describing pairing gaps all along the nuclear chart. While it can be applied even for very deformed nuclei[2], the validity of the BCS formalism crucially depends on the fluctuations of the particle-number (3.14), as large values of this quantity is a symptom of many spurious correlations in the wavefunction and values near zero indicate an incorrect use of this wavefunction as particle-number breaking terms are not present. A formal solution to this problem is based upon the *projected BCS* (PBCS) formalism, where by means of projection methods, the particle-number symmetry is restored (see Section 4.3).

The described formalism can be applied for protons and neutrons separately, using pairing gaps Δ_p and Δ_p accordingly, but we have omitted the matrix elements of the neutron-proton interaction. In light nuclei around the $N = Z$ line, this assumption is not correct as stressed before and therefore we need to include proton-neutron pairing into consideration. There is a formalism based on BCS which generalises the results including this isoscalar interaction, see [Bes00], but the most general way to describe pairing correlations will be given by the Hartree-Fock-Bogoliubov approach, explained in the following Section.

3.3 Hartree-Fock-Bogoliubov framework for treating pairing correlations

The BCS formalism treats only short-range correlations between particles and it is independent of the long-range correlations usually described by a Hartree-Fock picture. A general formalism that unifies both approaches is given by the *Hartree-Fock-Bogoliubov* formalism. As the name states, it is similar in structure to Hartree-Fock but including the Bogoliubov transformation for a quasiparticle treatment. The Bogoliubov transformation now reads

$$\begin{aligned} \hat{\beta}_k^+ &= \sum_i v_{ki}\hat{a}_i + u_{ki}\hat{a}_i^+, \\ \hat{\beta}_k &= \sum_i v_{ki}^*\hat{a}_i^+ + u_{ki}^*\hat{a}_i, \end{aligned} \tag{3.30}$$

[2]We note that for nuclei near the dripline or very close to the continuum, the generalised Fermi energy λ vanishes and the BCS approximation is not a suitable framework anymore

where the difference with (3.26) is that this transformation mixes different levels. In matrix form the transformation reads

$$\begin{pmatrix} \hat{\beta}^+ \\ \hat{\beta} \end{pmatrix} = \begin{pmatrix} U^T & V^T \\ V^+ & U^+ \end{pmatrix} \begin{pmatrix} \hat{a}^+ \\ \hat{a} \end{pmatrix}. \tag{3.31}$$

Requesting that the transformation must be unitary, that is

$$\begin{aligned} U^+U + V^+V = 1, \quad UU^+ + V^*V^T = 1, \\ U^TV + V^TU = 0, \quad UV^+ + V^*U^T = 0, \end{aligned} \tag{3.32}$$

we ensure that the inverse transformation from the quasiparticle picture to the single-particle picture exists

$$\begin{pmatrix} \hat{a}^+ \\ \hat{a} \end{pmatrix} = \begin{pmatrix} U^* & V \\ V^* & U \end{pmatrix} \begin{pmatrix} \hat{\beta}^+ \\ \hat{\beta} \end{pmatrix}. \tag{3.33}$$

The wavefunction of the nuclear system, $|\Psi\rangle$, is again represented by a quasiparticle vacuum

$$\hat{\beta}|\Psi\rangle = 0, \tag{3.34}$$

completely determined by the quantities U, V. Similarly to the Hartree-Fock picture, we construct an analogous density matrix formalism where, in addition to the usual single-particle density ρ, an *anomalous* density denoted by κ is introduced to take into account the short-range pairing correlations. The matrix elements of these densities are defined as

$$\rho_{ij} = \langle\Psi|\hat{a}_j^+\hat{a}_i|\Psi\rangle, \tag{3.35}$$

$$\kappa_{ij} = \langle\Psi|\hat{a}_j\hat{a}_i|\Psi\rangle. \tag{3.36}$$

They can be casted again in matrix form, replacing the single-particle operators using the transformation (3.33)

$$\rho = V^*V^T, \quad \kappa = V^*U^T = -UV^+, \tag{3.37}$$

where we have made use of the unitary conditions in (3.32) for the last equality in κ. The normal density matrix ρ is hermitian, as expected, and its matrix elements will be proportional to factors of the form v_iv_j, that is, to occupation probabilities. The matrix elements of the pairing tensor κ are proportional to u_iv_j and contain the information about the pairing structure in the system, because of the u factor. The unitary conditions (3.32) reveal that κ is antihermitian,

therefore

$$\rho^+ = \rho, \quad \kappa^+ = -\kappa, \tag{3.38}$$

which is also physically sensible, as we deal with fermions and under exchange there is a negative phase from antisymmetrization (or, in the mathematical point of view, the annihilation operators a anticommute with each other). Using again the unitary conditions (3.32), two relations between these densities hold

$$\begin{aligned} \rho^2 - \rho &= -\kappa\kappa^+, \\ \rho\kappa &= \kappa\rho^*. \end{aligned} \tag{3.39}$$

We observe that the deviation from the usual single-particle Hartree-Fock picture, corresponding to an idempotent density matrix, $\rho^2 = \rho$, is given by the pairing correlations describe by the pairing tensor κ. We derive a set of equations that solves the quasiparticle vacuum, $|\Psi\rangle$, or, equivalently, the transformation coefficients U, V under the HFB picture. In a similar fashion to the Hartree-Fock picture, where V would be the eigenvector of the density matrix ρ, we realise the vector (U, V) is an eigenvector of the following generalised density matrix

$$\mathcal{R} = \begin{pmatrix} \rho & \kappa \\ -\kappa^* & \mathbb{I} - \rho^* \end{pmatrix}, \tag{3.40}$$

which is hermitian and idempotent. The generalised hamiltonian matrix (namely, the *HFB matrix*) which commutes with the former generalised density is given by

$$\mathcal{H} = \begin{pmatrix} h & \Delta \\ -\Delta^* & -h^* \end{pmatrix}, \tag{3.41}$$

where

$$h_{ij} = \epsilon_{ij} + \sum_{kl} \bar{v}_{ikjl}\rho_{kl} = \epsilon_{ij} + \Gamma_{ij}, \tag{3.42}$$

$$\Delta_{ij} = \frac{1}{2}\sum_{kl} \bar{v}_{ijkl}\kappa_{kl}, \tag{3.43}$$

are the Hartree-Fock and pairing *fields*. Therefore, analogously to Hartree-Fock formalism, we cast the HFB equations in a compact form

$$[\mathcal{H}, \mathcal{R}] = 0, \tag{3.44}$$

yielding the desired HFB equations

$$\begin{pmatrix} h & \Delta \\ -\Delta^* & -h^* \end{pmatrix} \begin{pmatrix} U_q \\ V_q \end{pmatrix} = E_q \begin{pmatrix} U_q \\ V_q \end{pmatrix}. \tag{3.45}$$

We denote the different quasiparticles by q and the eigenvalue E is the quasiparticle energy. It is a double-dimensional matrix, because of the specific shape adopted to allocate the pairing field Δ. It is easy to see that, if (U_q, V_q) is an eigenstate of the HFB equations with eigenvalue E_q, then $(-V_q^*, -U_q^*)$ is also an eigenstate with eigenvalue $-E_q$. That is, we only work with the set of solutions corresponding to either negative or positive quasiparticle energies[3].

The HFB equations need to be solved self-consistently. Starting from an ansatz to the wavefunction (U, V), densities and fields are computed and the HFB supermatrix is diagonalised to obtain the new (U, V). This process is repeated self-consistently until the updated wavefunction is equal to the former one up to a threshold value, that is, the wavefunction has converged. A diagram depicting the process is shown in Fig. (3.5). The total energy of the system described

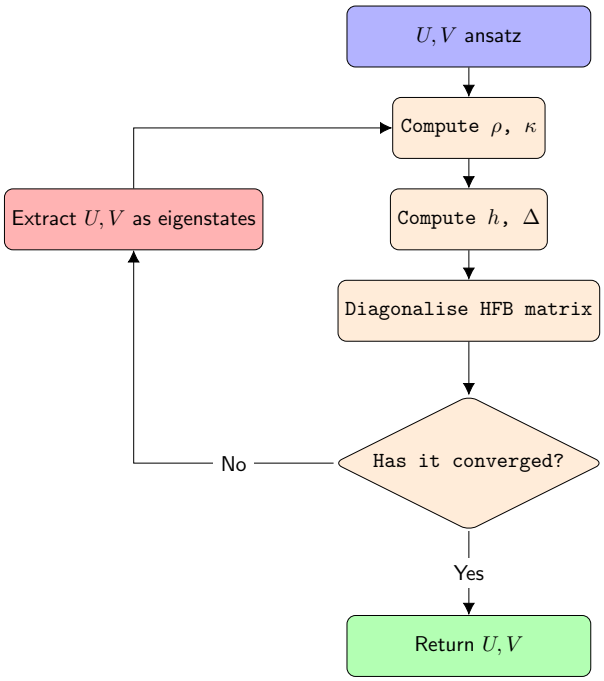

Figure 3.5: Diagram for HFB algorithm.

[3]For $E_q = 0$, the HFB matrix is singular (its determinant is zero) and the only possible solution is the trivial solution $(U_q, V_q) = (0, 0)$.

by this wavefunction will be given by

$$E_{HFB} = \langle\Psi|\hat{H}|\Psi\rangle = \mathrm{Tr}\left(\epsilon\rho + \frac{1}{2}\Gamma\rho - \frac{1}{2}\Delta\kappa^*\right). \tag{3.46}$$

In the limit of vanishing pairing (or Hartree-Fock limit), $\Delta \longrightarrow 0$, the HFB equations reduce to

$$\begin{pmatrix} h & 0 \\ 0 & -h^* \end{pmatrix}\begin{pmatrix} U_q \\ V_q \end{pmatrix} = E_q \begin{pmatrix} U_q \\ V_q \end{pmatrix} \longrightarrow hv_q = E_q v_q, \tag{3.47}$$

where $v_q = U_q$ corresponds now to the usual occupation probabilities in the single-particle picture. It is now clear that the HFB formalism is a generalisation of the single-particle picture to include the pairing correlations by means of an independent potential, which translates, mathematically speaking, to double the dimension of the eigensystem of equations that solves for the wavefunction of the nuclear state. An analogous BCS picture is obtained in this case by using the *canonical basis*, in which the density matrix ρ is diagonal. Because of equation (3.39), if ρ is diagonal, then $\rho^2 - \rho$ is also diagonal, and therefore κ needs to be antidiagonal, given it is skew-symmetric. The matrices then take the form

$$\rho^{(\mathrm{can})} = \begin{pmatrix} v_1^2 & 0 & \cdots & \cdots & \cdots & \cdots & 0 \\ 0 & v_2^2 & \cdots & \cdots & \cdots & \cdots & \vdots \\ \vdots & \cdots & \ddots & \cdots & \cdots & \cdots & \vdots \\ \vdots & \cdots & \cdots & v_n^2 & \cdots & \cdots & \vdots \\ \vdots & \cdots & \cdots & \cdots & v_n^2 & \cdots & \vdots \\ \vdots & \cdots & \cdots & \cdots & \cdots & \ddots & 0 \\ 0 & \cdots & \cdots & \cdots & \cdots & 0 & v_1^2 \end{pmatrix}, \tag{3.48}$$

$$\kappa^{(\mathrm{can})} = \begin{pmatrix} 0 & \cdots & \cdots & \cdots & \cdots & 0 & u_1v_1 \\ \vdots & \ddots & \cdots & \cdots & \cdots & u_2v_2 & 0 \\ \vdots & \cdots & \ddots & \cdots & \iddots & \cdots & \vdots \\ \vdots & \cdots & \cdots & u_nv_n & \cdots & \cdots & \vdots \\ \vdots & \cdots & -u_nv_n & \cdots & \ddots & \cdots & \vdots \\ 0 & \iddots & \cdots & \cdots & \cdots & \ddots & \vdots \\ -u_1v_1 & 0 & \cdots & \cdots & \cdots & \cdots & 0 \end{pmatrix}. \tag{3.49}$$

The double degeneracy imposed by the HFB approach is explicitly observed in the structure of

the former matrices. The occupation probabilities u_k, v_k have a BCS-like expression

$$\begin{aligned} v_k^{2(\mathrm{can})} &= \frac{1}{2}\left(1 - \frac{h_{kk} + h_{\overline{kk}}}{\sqrt{(h_{kk} - h_{\overline{kk}})^2 + 4\Delta_{k\overline{k}}^2}}\right), \\ u_k^{2(\mathrm{can})} &= \frac{1}{2}\left(1 + \frac{h_{kk} + h_{\overline{kk}}}{\sqrt{(h_{kk} - h_{\overline{kk}})^2 + 4\Delta_{k\overline{k}}^2}}\right), \end{aligned} \tag{3.50}$$

where $\overline{k}$ corresponds to the time-reversed state. We observe that for a fully paired system, time-reversal symmetry is conserved and the fields h and Δ are diagonal and antidiagonal, respectively, as the density matrices ρ and κ.

The major obstacle when performing HFB calculations lies in the spontaneous symmetry breaking in the quasiparticle vacuum wavefunction given by the mixing imposed by the Bogoliubov transformation in (3.30). In addition to the breaking particle-number symmetry as in the BCS formalism, angular momentum, spin and isospin symmetries may be broken as well if we mix states of different quantum numbers in transformation (3.30), and they must be constrained at least on average to obtain sensible physical results. It will be imposed by means of Lagrange parameters for each magnitude, modifying the Routhian[4] h in (3.42) as required. A useful algorithm to deal with this vector of Lagrange parameters is reviewed in Section 3.3.3.

The exact model reviewed in Section 2.2 was used extensively to benchmark the results of HFB plus symmetry-restoration method (introduced in Chapter 4), which eventually proved the coexistence of isoscalar and isovector pair condensates [RDP19b]. We derived the antisymmetrized two-body matrix elements of the $SO(8)$ Hamiltonian (2.17) that are used for the computation of the fields (3.42, 3.43) in the HFB calculation, which allowed us to write it in the usual form as in Eq. (3.3). We refer to Appendix H for details.

3.3.1 Thouless state

A conventional and very useful parametrisation of the quasiparticle vacuum $|\Psi\rangle$ was given by Thouless [Tho60]. Formally, it states that a product state $|\Psi_a\rangle$ is related to another, non orthogonal product state $|\Psi_b\rangle$ by

$$|\Psi_a\rangle = \mathcal{N} e^{\sum_{ij} Z_{ij} \hat{\beta}_i^+ \hat{\beta}_j^+} |\Psi_b\rangle. \tag{3.51}$$

[4] In the nuclear physics literature, it is frequent to read about the Routhian, which is a mathematical object analogous to the Hamiltonian, used when constrains are imposed on the system.

$\mathcal{N}$ is a normalisation constant and Z is an antisymmetric matrix (the *Thouless matrix*)

$$Z^T = -Z, \tag{3.52}$$

because of the fermionic nature of the quasiparticle operators, that is, the wavefunction changes sign when we exchange two quasiparticles. Using this theorem with the bare vacuum and expanding the quasiparticle operators in terms of single-particle operators, we thus obtain

$$\begin{aligned}\hat{\beta}_i\hat{\beta}_j &= \sum_{kk'}(v_{ik}\hat{a}_k^+ + u_{ik}\hat{a}_k)(v_{jk'}\hat{a}_{k'}^+ + u_{jk'}\hat{a}_{k'}) \\ &= \sum_{kk'}(v_{ik}v_{jk'}\hat{a}_k^+\hat{a}_{k'}^+ + v_{ik}u_{jk'}\hat{a}_k^+\hat{a}_{k'} + u_{ik}v_{jk'}\hat{a}_k\hat{a}_{k'}^+ + u_{ik}u_{jk'}\hat{a}_k\hat{a}_{k'}).\end{aligned} \tag{3.53}$$

Evaluation of the single-particle operators leads to $\hat{a}|0\rangle = 0$ and $\hat{a}_k\hat{a}_{k'}^+|0\rangle = \delta_{kk'}|0\rangle$. Therefore, the Thouless wavefunction can be written as

$$|\Psi\rangle = \mathcal{N}e^{\sum_{ij} Z_{ij}\hat{a}_i^+\hat{a}_j^+}|0\rangle, \tag{3.54}$$

where it is implied that the coefficients $v_{ik}v_{jk'}$ of the Bogoliubov transformation were absorbed in the renormalised Thouless matrix Z and the factor $\exp\left(\sum_{ij}\sum_k u_{ik}v_{jk}\right)$ in the normalisation constant $\mathcal{N}$. The former expression can be used for a parametrised wavefunction of an even nucleus. It is convenient since, when applying any transformation $\hat{T}$ on $|\Psi\rangle$

$$|\Psi'\rangle = \hat{T}|\Psi\rangle = \hat{T}\sum_k \frac{Z_{ij}^k}{k!}(\hat{a}_i^+\hat{a}_j^+)^k|0\rangle = \sum_k \frac{Z_{ij}'^k}{k!}(\hat{a}_i^+\hat{a}_j^+)^k|0\rangle, \tag{3.55}$$

that is, it is equivalent to transform the pair $\hat{a}^+\hat{a}^+$ accordingly and absorb the terms in the Thouless matrix Z. The transformed wavefunction has then the same functional shape as the original one. We now use the Thouless state for the particular case of the $SO(8)$ Hamiltonian, which is the subject of the present thesis. Using the intrinsic pairs defined in (2.18) and used in this model, we define the Thouless pair $\hat{Z}^+$, for the computation of the Thouless representation of the HFB wavefunction, as

$$\hat{Z}^+ = \sum_{\nu=0,\pm1} p_\nu\hat{P}_\nu^+ + \sum_{\mu=0,\pm1} d_\mu\hat{D}_\mu^+, \tag{3.56}$$

where p_ν, d_μ are the set of six amplitudes stating the importance of each pair. We notice that, since the $SO(8)$ Hamiltonian is invariant under rotations in spin and isospin space, we can reduce the number of parameters needed to describe the mean-field HFB wavefunction.

Indeed, if the system described by this Hamiltonian is independent of the direction of the wavefunction, and only depends on its norm, we could always rotate the pairs that build the wavefunction and align them along a desired direction. Obviously, we would like to exploit this symmetry to simplify the calculations, and to that purpose the desired direction is the $z-$axis in spin and isospin space, where only the respective pair with projection zero will give a nonzero contribution to the wavefunction, while the two others vanish. Thus, the Thouless pair can be effectively reduced to

$$\hat{Z}^+ = p_0 \hat{P}_0^+ + d_0 \hat{D}_0^+. \tag{3.57}$$

The amplitudes can be reparametrised to have a normalised pair

$$\begin{aligned} p_0 &= \sin\left(\frac{1}{2}\alpha\right) e^{-i\varphi}, \\ d_0 &= \cos\left(\frac{1}{2}\alpha\right) e^{i\varphi}, \end{aligned} \tag{3.58}$$

where α is the mixing angle that controls the relative amplitude between isoscalar and isovector pairs and φ the relative phase between the two pair condensates.

3.3.2 Isocranking

The isocranking technique is an extension of the usual mean-field formalism to study the effect of the isospin degree of freedom along isobaric analog states, namely, systems with the same number of particles (baryons) and isospin [SW01a]. This method can be regarded as arbitrary rotations, the usual method of cranking [Ing54; Ing56], in isospin space [SW01b]. This technique allows arbitrary mixing between proton and neutron single-particle states which is what we desire in order to describe the importance of isoscalar pairing correlations [Sat13]. Under this extended method, the Routhian h from the HFB equations (3.45) is transformed as

$$h' = h - \boldsymbol{\lambda} \cdot \boldsymbol{T}, \tag{3.59}$$

where $\boldsymbol{T} = (T_x, T_y, T_z)$ is the isospin vector and $\boldsymbol{\lambda} = (\lambda_x, \lambda_y, \lambda_z)$ is the set of Lagrange parameters that controls the direction and magnitude of the isospin. The third component of the isospin fixes the imbalance between protons and neutrons in the nucleus

$$T_z = \frac{N - Z}{2}, \tag{3.60}$$

and changing the third Lagrange parameter λ_z will then change the number of protons and neutrons in the system, spanning from the $z-$isoaligned $T_z = -T$ state (a pure proton system) to the also $z-$isoaligned $T_z = T$ state (a pure neutron system). For this case, the modulus of λ can be fixed as λ_0 and used as the radius of rotations in isospin space. The first Lagrange parameter λ_x will control the degree of mixing between proton and neutron single particle states, being zero for the aforementioned $z-$isoaligned states. The first component of the isospin gives excitations to different isobaric analog states, that is, different T, with $T_z = 0$, the third component of the isospin gives excitations to different isobaric analog states with $T_z = T$. A schematic representation of these processes is depicted in Fig. (3.6). In practical

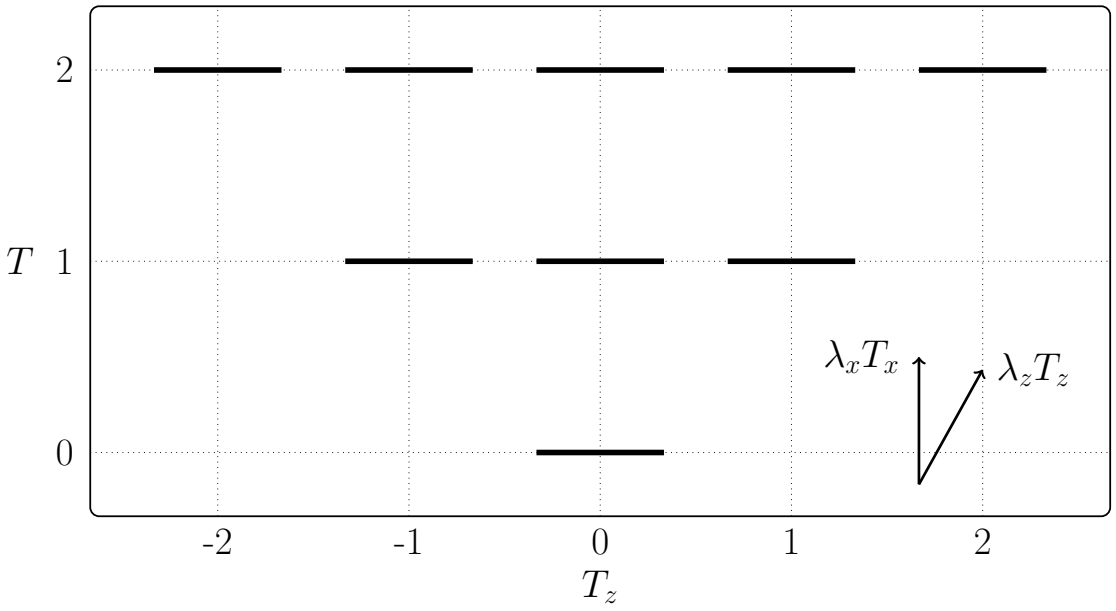

Figure 3.6: Isospin triangle spanned for allowed states of different T and T_z. The term $\lambda_x T_x$ gives rise to a vertical excitation and $\lambda_z T_z$ to a diagonal excitation.

applications with even nuclei, rotations of T_y are neglected since they are redundant when T_x is already under control and they give rise to time-reversal symmetry breaking, which we do not consider since we work in a fully paired system. Therefore it is common to adopt the following parametrisation of the Lagrange parameters λ

$$\lambda = (\lambda_0 \sin\theta, 0, \lambda_0 \cos\theta), \tag{3.61}$$

where θ varies from 0 to π.

3.3.3 Augmented Lagrangian Method

For any HFB calculation, constraints must be implemented to fix average values of certain observables like particle-number or isospin, using Lagrange parameters. A recent method that has become standard to calculate the values of these Lagrange parameters is the *Augmented Lagrangian Method* (ALM) introduced in Ref. [Sta10]. Conventionally, if we constrain the observable $\hat{Q}$ to have a certain value q_0, the Routhian h is modified such as

$$h' = h - \lambda \hat{Q}. \tag{3.62}$$

The Lagrange parameter λ can be obtained by means of a bisection method or other root-solving algorithms. Within the ALM algorithm, it is suggested that the Routhian is modified as

$$h' = h - c_{ALM}[q - q_0(\lambda)]\hat{Q}, \tag{3.63}$$

where c_{ALM} is the update constant, q is the current average value of $\hat{Q}$ and $q_0(\lambda) = q_0 - \lambda/c_{ALM}$. Then, the Lagrange parameter λ is updated in iteration i as

$$\lambda^{i+1} = \lambda^i - c_{ALM}(q - q_0). \tag{3.64}$$

The Augmented Lagrangian Method is easily generalised for several constraints using a vector of independent Lagrange parameters λ. This method has been successfully applied in our HFB implementation to constrain average values of particle-number, the isospin degree of freedom for isocranking, and the spin for polarization.

3.3.4 Gradient method

An alternative solution to the HFB problem that does not rely upon iterative diagonalisation with the convergence relations formerly introduced is based on the gradient method. Under this method, we aim to find the minimum of the energy surface spanned by

$$E_{HFB} = \frac{\langle \Psi | \hat{H} | \Psi \rangle}{\langle \Psi | \Psi \rangle}, \tag{3.65}$$

which will depend on the chosen parameters (3.58) of the wavefunction $|\Psi\rangle$, written using the Thouless expression (3.54). The gradient method is not exclusive for the HFB problem, it is a well known numerical method to find the minimum of a function. It relies upon an update of the parameter domain by a factor proportional to the gradient of the function, that is, its first

derivative, finding the minimum when the gradient is zero up to a threshold value. This gradient can be computed by finite differences of the function, but in the HFB framework, however, we already have an expression for this gradient when we derived the HFB equations, corresponding to the quantity H^{20}. Since in the later sections, we will mostly work on Thouless states, we found this method was easier to manipulate for both the HFB framework with constraints on particle number and going beyond mean-field by applying the symmetry-restoration techniques. An illustrative diagram, using the axial parametrisation of the Thouless pair (3.58), is depicted in Fig. (3.7). A general constrained HFB calculation using the gradient method can be found in [RB11; Egi95].

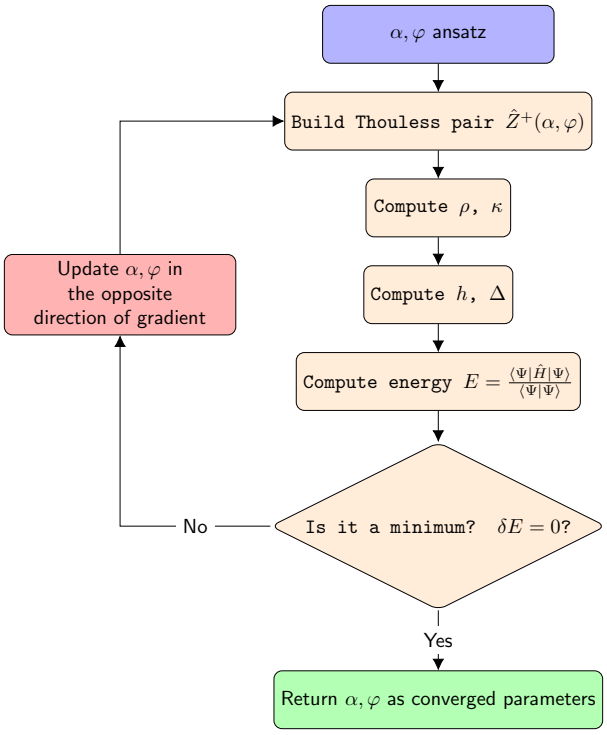

Figure 3.7: Diagram depicting the gradient method using the Thouless axial parametrisation.

3.3.5 Overlap of two quasiparticle states

For many practical purposes, as for example in the computation of transfer matrix elements, where there are different initial and final states, the overlap $\langle\Psi_f|\Psi_i\rangle$ between an initial quasiparticle state $|\Psi_i\rangle$ and a final quasiparticle state $|\Psi_f\rangle$ is needed. For many years, the only

available method to compute this overlap was by means of the Onishi formula [OY66]

$$\langle \Psi_f | \Psi_i \rangle = \pm \sqrt{\det\left(\mathbb{I} - Z_f^* Z_i\right)}. \tag{3.66}$$

The problem with this formula is the undefined sign as a consequence of the square root operation, leaving an overall undefined phase. An alternative computation of the norm overlap, which does not possess this phase problem, was given by Robledo [Rob09]

$$\langle \Psi_f | \Psi_i \rangle = s_N \mathrm{pf} \begin{pmatrix} Z_i & -\mathbb{I} \\ \mathbb{I} & -Z_f^* \end{pmatrix}, \tag{3.67}$$

where s_N is a phase constant that depends on the size of the configuration space and pf stands for the *pfaffian* of a matrix, which fulfils the condition $\mathrm{pf}(A)^2 = \det(A)$, therefore making the connection with the Onishi formula while removing the phase problem. The pfaffian of a matrix can be evaluated upon the Householder decomposition [GRB11].

3.3.6 Convergence of the HFB calculation

In order to obtain the proper mean-field energy after an iterative, self-consistent HFB calculation, we derive an alternative formula for this energy that must agree with the HFB result in Eq. (3.46) up to a very small number, therefore we will not only rely upon the self-consistency of the HFB equations to obtain the solution. Bennaceur [Ben16] suggested an implementation for the scalar constraint on the total number of particles, defining this implementation as the *magic formula*. In the same spirit, in the following subsections, we derive these magic formulas including Lagrange parameters we are interested in to constrain not only the particle-number, but also the first and third components of the isospin.

3.3.6.1 Scalar case: constrain on the particle-number

For the scalar Lagrange parameter λ to fix the total number of particles, the HFB equations read

$$\begin{pmatrix} h - \lambda & \Delta \\ -\Delta^* & -h^* + \lambda \end{pmatrix} \begin{pmatrix} v_i^* \\ u_i^* \end{pmatrix} = E_i \begin{pmatrix} v_i^* \\ u_i^* \end{pmatrix}, \tag{3.68}$$

where i denotes the quantum numbers of the different quasiparticles and we are concerned only with the negative eigenvalues. Taking the first row of the matrix multiplication

$$(h - \lambda) v_i^* + \Delta u_i^* = E_i v_i^*, \tag{3.69}$$

multiplying by v_i

$$(h-\lambda)v_i v_i^* + \Delta u_i^* v_i = E_i v_i v_i^*, \tag{3.70}$$

and summing over all possible quantum numbers in the collective coordinate i, we obtain

$$\sum_i (h\rho_i + \Delta\kappa_i^*) = \sum_i (E_i + \lambda)\rho_i. \tag{3.71}$$

Including the factor $\frac{1}{2}$, in accordance with Eq. (3.46), we finally get for the HFB energy

$$E_{magic} = \frac{1}{2}\sum_i (E_i + \lambda)\rho_i, \tag{3.72}$$

which is a test for convergence of the right physical solution including constrains on the particle-number, thus $|E_{magic} - E_{HFB}| \sim 0$.

3.3.6.2 Third component of the isospin: constrain on protons and neutrons

We denote λ_z as the Lagrange parameter fixing the third component of the isospin. Since the third pauli matrix is

$$\tau_z = \begin{pmatrix} 1 & 0 \\ 0 & -1 \end{pmatrix}, \tag{3.73}$$

then the HFB equations read now

$$\begin{pmatrix} h_{nn}-\lambda-\lambda_z & h_{pn} & \Delta_{nn} & \Delta_{np} \\ h_{pn} & h_{pp}-\lambda+\lambda_z & \Delta_{pn} & \Delta_{pp} \\ -\Delta_{nn}^* & -\Delta_{np}^* & -h_{nn}^*+\lambda+\lambda_z & -h_{pn}^* \\ -\Delta_{pn}^* & -\Delta_{pp}^* & -h_{pn}^* & -h_{pp}^*+\lambda-\lambda_z \end{pmatrix} \begin{pmatrix} v_i^*(n) \\ v_i^*(p) \\ u_i^*(n) \\ u_i^*(p) \end{pmatrix} = E_i \begin{pmatrix} v_i^*(n) \\ v_i^*(p) \\ u_i^*(n) \\ u_i^*(p) \end{pmatrix}, \tag{3.74}$$

where we have made clear the distinction between different isospin projections, neutrons and protons. We take the first two rows in the matrix multiplication

$$\begin{aligned} (h_{nn}-\lambda-\lambda_z)v_i^*(n) + h_{pn}v_i^*(p) + \Delta_{nn}u_i^*(n) + \Delta_{np}u_i^*(p) &= E_i v_i^*(n), \\ (h_{pp}-\lambda+\lambda_z)v_i^*(p) + h_{pn}v_i^*(n) + \Delta_{pn}u_i^*(n) + \Delta_{pp}u_i^*(p) &= E_i v_i^*(p). \end{aligned} \tag{3.75}$$

We multiply these equations by $v_i(n)$ and $v_i(p)$, respectively

$$\begin{aligned} (h_{nn}-\lambda-\lambda_z)v_i^*(n)v_i(n) + h_{pn}v_i^*(p)v_i(n) + \Delta_{nn}u_i^*(n)v_i(n) + \Delta_{np}u_i^*(p)v_i(n) &= E_i v_i^*(n)v_i(n), \\ (h_{pp}-\lambda+\lambda_z)v_i^*(p)v_i(p) + h_{pn}v_i^*(n)v_i(p) + \Delta_{pn}u_i^*(n)v_i(p) + \Delta_{pp}u_i^*(p)v_i(p) &= E_i v_i^*(p)v_i(p), \end{aligned} \tag{3.76}$$

and we have

$$\begin{aligned}(h_{nn}-\lambda-\lambda_z)\rho_i(n)+h_{pn}\rho_i(pn)+\Delta_{nn}\kappa_i^*(n)+\Delta_{np}u_i^*(p)v_i(n)=E_i\rho_i(n),\\(h_{pp}-\lambda+\lambda_z)\rho_i(p)+h_{pn}\rho_i(pn)+\Delta_{pn}u_i^*(n)v_i(p)+\Delta_{pp}\kappa_i^*(p)=E_i\rho_i(p).\end{aligned}\tag{3.77}$$

Taking special attention at the cross terms like $u_i^*(p)v_i(n)$ in the κ matrix. They were in the scalar case as well but here we need to explicitly write them down as we separate protons and neutrons. The density matrix ρ is hermitian and we were able to write $\rho(pn)=v_i^*(p)v_i(n)=v_i^*(n)v_i(p)$. By summing these two equations we have

$$\begin{aligned}h_{pp}\rho_i(p)+h_{nn}\rho_i(n)+2h_{pn}\rho_i(pn)+\Delta_{nn}\kappa_i^*(n)+\Delta_{np}u_i^*(p)v_i(n)+\Delta_{pn}u_i^*(n)v_i(p)+\Delta_{pp}\kappa_i^*(p)\\=E_i[\rho_i(p)+\rho_i(n)]+(\lambda+\lambda_z)\rho_i(n)+(\lambda-\lambda_z)\rho_i(p).\end{aligned}\tag{3.78}$$

Finally, including the factor $\frac{1}{2}$ we obtain

$$E_{magic}=\frac{1}{2}\sum_i\{(E_i+\lambda)[\rho_i(p)+\rho_i(n)]+\lambda_z[\rho_i(n)-\rho_i(p)]\},\tag{3.79}$$

which should be implemented if we are constraining the particle-number and the specific number of protons and neutrons.

3.3.6.3 First component of the isospin: vertical excitations

We denote by λ_x the Lagrange parameter fixing the first component of the isospin. Since the first Pauli matrix is

$$\tau_x=\begin{pmatrix}0&1\\1&0\end{pmatrix},\tag{3.80}$$

then the HFB equations read now

$$\begin{pmatrix}h_{nn}-\lambda-\lambda_z & h_{pn}-\lambda_x & \Delta_{nn} & \Delta_{np}\\ h_{pn}-\lambda_x & h_{pp}-\lambda+\lambda_z & \Delta_{pn} & \Delta_{pp}\\ -\Delta_{nn}^* & -\Delta_{np}^* & -h_{nn}^*+\lambda+\lambda_z & -h_{pn}^*+\lambda_x\\ -\Delta_{pn}^* & -\Delta_{pp}^* & -h_{pn}^*+\lambda_x & -h_{pp}^*+\lambda-\lambda_z\end{pmatrix}\begin{pmatrix}v_i^*(n)\\v_i^*(p)\\u_i^*(n)\\u_i^*(p)\end{pmatrix}=E_i\begin{pmatrix}v_i^*(n)\\v_i^*(p)\\u_i^*(n)\\u_i^*(p)\end{pmatrix}.\tag{3.81}$$

We take the first two rows in the matrix multiplication

$$\begin{aligned}(h_{nn}-\lambda-\lambda_z)v_i^*(n)+(h_{pn}-\lambda_x)v_i^*(p)+\Delta_{nn}u_i^*(n)+\Delta_{np}u_i^*(p)=E_iv_i^*(n),\\(h_{pp}-\lambda+\lambda_z)v_i^*(p)+(h_{pn}-\lambda_x)v_i^*(n)+\Delta_{pn}u_i^*(n)+\Delta_{pp}u_i^*(p)=E_iv_i^*(p).\end{aligned}\tag{3.82}$$

We multiply these equations by $v_i(n)$ and $v_i(p)$, respectively

$$\begin{aligned}(h_{nn} - \lambda - \lambda_z)v_i^*(n)v_i(n) + (h_{pn} - \lambda_x)v_i^*(p)v_i(n) + \Delta_{nn}u_i^*(n)v_i(n) + \Delta_{np}u_i^*(p)v_i(n) = \epsilon_i v_i^*(n)v_i(n),\\ (h_{pp} - \lambda + \lambda_z)v_i^*(p)v_i(p) + (h_{pn} - \lambda_x)v_i^*(n)v_i(p) + \Delta_{pn}u_i^*(n)v_i(p) + \Delta_{pp}u_i^*(p)v_i(p) = \epsilon_i v_i^*(p)v_i(p).\end{aligned} \tag{3.83}$$

So we have the same equations as in the former case but with an additional λ_x multiplying non diagonal elements of the density matrix. The final result is

$$E_{magic} = \frac{1}{2}\sum_i \{(E_i + \lambda)[\rho_i(p) + \rho_i(n)] + \lambda_z[\rho_i(n) - \rho_i(p)] + 2\lambda_x\rho_i(pn)\}. \tag{3.84}$$

This method can be extended as long as required, including other observables as spin polarization, for example. The set of Lagrange parameters $\lambda, \lambda_x, \lambda_z$ in the *magic* formula are the output of the Augmented Lagrangian Method and need to be used accordingly. In Fig. (3.8) we show again a diagram depicting the HFB algorightm with constraints.

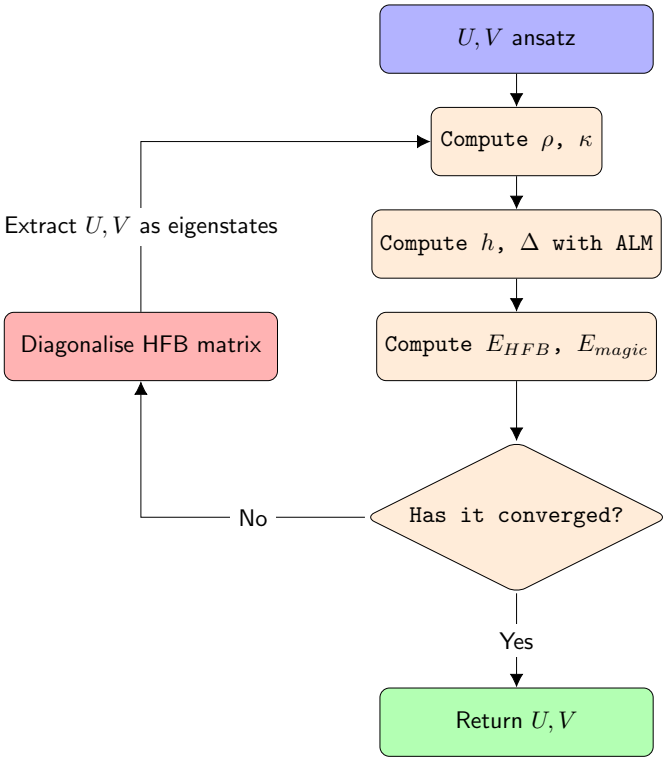

Figure 3.8: HFB algorithm introducing the *magic* formulas (3.72, 3.79, 3.84) using the Augmented Lagrangian Method for an improved convergence.

Chapter 4

Beyond mean-field: restoration of broken symmetries

The concept of symmetry is linked to physics since its conception. The mathematical tools associated with symmetries have shown a tremendous success in describing many physical phenomena, especially in nuclear and particle physics. Namely, *Noether's theorem* states that a symmetry of a system is related to a conserved quantity, which can be used to identify the different configurations of said system. We must exploit the symmetries to get an intrinsic set of coordinates whose total dimension is less than the dimension of the space in which the system is embedded. For example, a system with spherical symmetry in three dimensions is completely described by a number, its radial coordinate, while in general we would need three numbers, therefore reducing the complexity of the problem. Although many symmetries are important in the nuclear Hamiltonian for the description of several observables, the centre of interest in this work will be aimed at the particle-number, angular momentum, spin and isospin symmetries, with devoted sections.

One can define a symmetry transformation $\hat{S}$, satisfying four important conditions

- Given another symmetry transformation $\hat{S}'$, belonging to the same symmetry group, the products $\hat{S}'\hat{S}$ and $\hat{S}\hat{S}'$, which do not necessarily commute, are also symmetry transformations. There is *closure*.
- Given another symmetry transformation $\hat{S}''$, belonging to the same symmetry group, it fulfils $(\hat{S}\hat{S}')\hat{S}'' = \hat{S}(\hat{S}'\hat{S}'')$. There is *associativity*.
- There exists an *identity element* $\hat{\mathbb{I}}$ such that $\hat{S}\hat{\mathbb{I}} = \hat{\mathbb{I}}\hat{S} = \hat{S}$.
- There is an *inverse element* $\hat{S}^{-1}$ such that $\hat{S}\hat{S}^{-1} = \hat{S}^{-1}\hat{S} = \hat{\mathbb{I}}$

A symmetry is thus mathematically associated with the concept of *group*, a set of elements which meet the former criteria. As a consequence, we say that symmetries have a group structure, and the algebraic mathematical methods already developed in the literature can be applied. Conservation of symmetries plays an important role in the structure of new theories in physics, as systems are invariant under certain symmetry transformation by direct observation. Many examples exist in nuclear physics: nuclear matter is translationally invariant and therefore its states are built from plane-waves of continuous linear momentum, magic nuclei are spherical and therefore they can be labelled by states of different angular momentum, and axial nuclei have a rotational symmetry around a specific axis and therefore they can be labelled by the different projections of angular momentum. This Chapter is structured as follows, a brief introduction to the mathematical tools from group theory applied to symmetries is reviewed in the following subsections, giving special emphasis on the angular momentum symmetry, but whose extrapolation to other cases is automatic. Next, we will review under what conditions a symmetry can be broken even when the system itself is symmetric and its consequences, often happening in the mean-field picture. The remaining and main part of the Chapter will be devoted to the technical details of how to properly restore these broken symmetries using projection methods within the mean-field picture and in specific with the HFB framework and the $SO(8)$ Hamiltonian.

4.1 Relevant symmetries in nuclear structure

4.1.1 Angular momentum symmetry

In this Section, we will focus in the rotation symmetry and its relation to the angular momentum, as its mathematical treatment is widely used in many other applications in nuclear and particle physics.

Let us consider that we spatially rotate a wavefunction $\Psi(r,\varphi,\phi)$ an angle θ about the $z-$axis. In terms of the rotation operator $\hat{\mathcal{R}}_z(\theta)$, we have

$$\hat{\mathcal{R}}_z(\theta)\Psi(r,\varphi,\phi) = \Psi(r,\varphi,\phi-\theta). \tag{4.1}$$

By performing a Taylor expansion, we obtain

$$\begin{aligned}\Psi(r,\varphi,\phi-\theta) &= \Psi(r,\varphi,\phi) - \theta\frac{\partial}{\partial\phi}\Psi(r,\varphi,\phi) + \frac{\theta^2}{2}\frac{\partial^2}{\partial\phi^2}\Psi(r,\varphi,\phi) + \cdots \\ &= \sum_{n=0}^{\infty}\frac{1}{n!}\Big(-\theta\frac{\partial}{\partial\phi}\Big)^n\Psi(r,\varphi,\phi),\end{aligned} \tag{4.2}$$

and the rotation operator can be written as

$$\hat{\mathcal{R}}_z(\theta) = e^{-i\theta \hat{J}_z}. \tag{4.3}$$

$\hat{J}_z$ is the well-known angular momentum projection operator on the $z-$axis

$$\hat{J}_z = -i\frac{\partial}{\partial \phi}, \tag{4.4}$$

which is associated with the rotation transformations, also named as the *generator* of these transformations. Expression in Eq. (4.3) is called the *exponential representation* of the symmetry operator, well described in the Lie algebra literature [Wyb74]. A Lie algebra is completely described by the commutation relations fulfilled by the operators involved, in the case of angular momentum $\hat{J}$

$$[\hat{J}_l, \hat{J}_m] = i\sum_{n=1}^{3} \epsilon_{lmn}\hat{J}_n, \tag{4.5}$$

where ϵ_{lmn} is the Levi-Civita tensor. These commutation relations are associated with the structure of the special and unitary algebra of dimension 2, $SU(2)$[1], very important in many-body physics, as it describes particles of spin $\frac{1}{2}$, and whose elements can be represented by unitary matrices of determinant one.

We have now stated that spatial rotations are intimately related to the angular momentum operators. Moreover, because of Noether's theorem, we know that if a system is invariant under rotations, then the angular momentum is conserved. In quantum mechanics, this is of tremendous importance as the different states of the system can be labelled with the eigenvalues of the angular momentum operators $\hat{J}^2$ and one of its components, usually $\hat{J}_z$, labelled as j, m, respectively. In particular

$$\begin{aligned} \hat{J}^2|j,m\rangle &= j(j+1)|j,m\rangle, \\ \hat{J}_z|j,m\rangle &= m|j,m\rangle. \end{aligned} \tag{4.6}$$

$\hat{J}^2$ is also called the *Casimir invariant* of the $SO(3)$ algebra, defined as the operator that commutes with all the generators,

$$[\hat{J}^2, \hat{J}_i] = 0. \tag{4.7}$$

Because $SO(3)$ is a spectrum generating algebra [RW10], that is, its structure generates a set of different states, it is of great importance the introduction of the *ladder operators* $\hat{J}_+, \hat{J}_-$,

[1] Although the group associated with spatial rotations is $SO(3)$, all its elements are in $SU(2)$ but not vice versa and relation (4.5) corresponds only to $SU(2)$

which spans said states generated by the algebra, defined as

$$\begin{aligned}\hat{J}_+ &= \hat{J}_x + i\hat{J}_y,\\ \hat{J}_- &= \hat{J}_x - i\hat{J}_y,\end{aligned} \tag{4.8}$$

which raises or lowers the magnetic quantum number m, respectively,

$$\begin{aligned}\hat{J}_+|j,m\rangle &= \sqrt{(j+m+1)(j-m)}|j,m+1\rangle,\\ \hat{J}_-|j,m\rangle &= \sqrt{(j-m+1)(j+m)}|j,m-1\rangle.\end{aligned} \tag{4.9}$$

It is easily checked that, for the maximum and minimum values of m,

$$\hat{J}_+|j,j\rangle = \hat{J}_-|j,-j\rangle = 0. \tag{4.10}$$

From the definition of the ladder operators, we observe the following equalities

$$\hat{J}^2 = \hat{J}_\pm\hat{J}_\mp + \hat{J}_z^2 \pm \hat{J}_z, \tag{4.11}$$

$$[\hat{J}_+,\hat{J}_-] = -i[\hat{J}_x,\hat{J}_y] + i[\hat{J}_y,\hat{J}_x] = -2i[\hat{J}_x,\hat{J}_y] = 2\hat{J}_z, \tag{4.12}$$

$$[\hat{J}_z,\hat{J}_\pm] = \pm\hat{J}_\pm. \tag{4.13}$$

Spatial rotations are labelled by the *Euler angles* $\Omega = (\alpha,\beta,\gamma)$, and a general expression of these transformations will be given by

$$\hat{R}(\Omega) = \hat{R}(\alpha,\beta,\gamma) = e^{-i\alpha\hat{J}_z}e^{-i\beta\hat{J}_y}e^{-i\gamma\hat{J}_z}. \tag{4.14}$$

The matrix elements between different states with good quantum numbers $|j,m\rangle$ are given by

$$\langle j'm'|\hat{R}(\Omega)|jm\rangle = \delta_{jj'}D^j_{m'm}(\Omega), \tag{4.15}$$

where $D^j_{m'm}(\Omega)$ are the *Wigner D-functions* [VMK88], defining completely the transformation from a state $|j,m\rangle$ to $|j,m\rangle'$ after a rotation of angle Ω. These functions fulfil the following orthogonality relation

$$\int_0^{2\pi}d\alpha\int_0^{\pi}d\beta\sin\beta\int_0^{2\pi}d\gamma D^{J_1}_{M_1M_1'}(\Omega)D^{J_2}_{M_2M_2'}(\Omega) = (-1)^{M_2-M_2'}\frac{8\pi^2}{2J_2+1}\delta_{J_1J_2}\delta_{M_1-M_2}\delta_{M_1'-M_2'}. \tag{4.16}$$

4.1.2 Particle number symmetry

The particle-number symmetry, related to systems having a fixed number of particles, is associated with the unitary group of dimension one, $U(1)$, also known as the *circle group* because it involves the numbers enclosed in a circle on the complex plane. Analogous to the spatial case with the angular momentum operators, symmetry transformations associated to this group can also be defined in terms of *rotations* in the space generated by the variables involved in the transformation (the Euler angles in the case of spatial rotations). The operators of this group acting on a state of definite particle number will just change the phase of said state, while leaving the norm invariant. For this reason, sometimes this space is referred as the *gauge space*, and the only parameter involved is the *gauge angle*.

In the occupation number representation for fermions, we define a single-particle creation $\hat{a}_i^+$ and annihilation $\hat{a}_i$ operator in the state i as with relations (2.5, 2.6), which fulfil the following commutation relations

$$\begin{aligned} [\hat{a}_i, \hat{a}_j^+] &= 2\hat{a}_i\hat{a}_j^+ - \delta_{ij}, \\ [\hat{a}_i^+, \hat{a}_j^+] &= 2\hat{a}_i^+\hat{a}_j^+, \\ [\hat{a}_i, \hat{a}_j] &= 2\hat{a}_i\hat{a}_j. \end{aligned} \tag{4.17}$$

The mathematical structure of the fermionic creation and annihilation operators is referred in the literature as the *Grasmann* algebra. The number operator, defined as

$$\hat{A} = \sum_i \hat{a}_i^+\hat{a}_i, \tag{4.18}$$

is the generator of the $U(1)$ algebra, and therefore the rotation operator in gauge space is given by

$$\hat{R}(\varphi) = e^{-i\varphi\hat{A}}. \tag{4.19}$$

The matrix elements of this operator reads

$$\langle\Psi'|\hat{R}(\varphi)|\Psi\rangle = e^{-i\varphi A}, \tag{4.20}$$

with $A = \langle\Psi'|\hat{A}|\Psi\rangle/\langle\Psi'|\Psi\rangle$, necessarily assuming that the states preserve the particle-number symmetry. The matrix elements fulfil the following orthogonalisation conditions

$$\int_0^{2\pi} d\alpha e^{-i\alpha A} e^{-i\alpha A'} = 2\pi\delta_{AA'}. \tag{4.21}$$

The action of the rotation operator (4.19) over the single-particle operator $\hat{a}^+$ and, subsequently, over the pair $\hat{a}^+\hat{a}^+$, is [BR86]

$$\hat{R}^+(\varphi)\hat{a}^+\hat{R}(\varphi) = e^{i\varphi}\hat{a}^+, \tag{4.22}$$

$$\hat{R}^+(\varphi)\hat{a}^+\hat{a}^+\hat{R}(\varphi) = e^{2i\varphi}\hat{a}^+\hat{a}^+. \tag{4.23}$$

4.1.3 Spin symmetry

Spin is an intrinsic property which makes nucleons align or antialign under an applied magnetic field. The mathematical structure of the spin symmetry operators are the same as those of angular momentum. Protons and neutrons are fermions of spin $\frac{1}{2}$ and thus two different projections (spin up and down). The spin symmetry follows the structure of the $SU(2)$ symmetry group, thus it can be represented by two-dimensional matrices. A convenient representation is given by the Pauli matrices, defined by

$$\sigma_0 = \begin{pmatrix} 1 & 0 \\ 0 & 1 \end{pmatrix}, \ \sigma_1 = \begin{pmatrix} 0 & 1 \\ 1 & 0 \end{pmatrix}, \ \sigma_2 = \begin{pmatrix} 0 & -i \\ i & 0 \end{pmatrix}, \ \sigma_3 = \begin{pmatrix} 1 & 0 \\ 0 & -1 \end{pmatrix}. \tag{4.24}$$

The two-dimensional angular momentum operators are then defined as $J_i = \frac{1}{2}\sigma_i$. Similar formulas derived in Section 4.1.1 hold in this case, where now rotations are done in spin space and not coordinate space.

4.1.4 Isospin symmetry

The substantial difference between protons and neutrons is the charge, protons are positively charged and neutrons are neutral. If we neglect the Coulomb interaction associated to the charge of the protons, the interaction among protons and neutrons is the same as between protons and neutrons themselves[2]. There is experimental evidence of this claim, as mirror nuclei, i.e., nuclei with exchanged numbers of protons and neutrons, have similar binding energy once corrected with the Coulomb interaction, and the same spin and parity. This fact lead us to treat protons and neutrons as specific states of a general particle: the *nucleon*. Introducing the isospin degree of freedom, whose mathematical structure is analogous to the one of the spin, we treat protons and neutrons as different projections (isospin up and isospin down) of a nucleon of isospin $\frac{1}{2}$, as depicted in Fig. (4.1). In this sense, we say that the nuclear Hamiltonian is invariant under rotations in isospin space, that is, under the change of the number of protons and neutrons,

[2]This is not exactly true, as protons and neutrons have different quark constituents, differences in the strong interaction, which lead to the nuclear interaction, are observed [Bac19].

keeping the total number of neutrons invariant. Isospin allows us to treat protons and neutrons self-consistently (that is, protons and neutrons are not independent) and, as we shall see later, it is of great importance to treat the isoscalar pairing correlations. As the mathematical structure

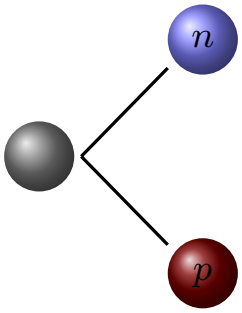

Figure 4.1: Neutron and proton as different states of a nucleon of isospin $t = \frac{1}{2}$.

is completely analogous to the spin case, the same relations regarding the angular momentum symmetry hold for the isospin symmetry.

4.1.5 Spin and isospin signatures

The spin and isospin signature operators are defined as

$$\hat{R}_S = e^{-i\pi \hat{S}_y}, \tag{4.25}$$

$$\hat{R}_T = e^{-i\pi \hat{T}_y}. \tag{4.26}$$

The signature is a discrete symmetry involving a rotation of angle π about the $y-$axis in the respective spin/isospin space. Obviously, if the system is already invariant under any rotation in these spaces, the signature symmetries are already conserved. However, there is in principle no need to conserve spin/isospin symmetries in order to conserve their signatures, just an axial symmetry, that is, the projection onto one axis, needs to be conserved. This result is analogous to the fact that parity, which is related to the space reflection symmetry, is conserved in nuclei even when the linear momentum, related to the translational symmetry of space, is not[3].

The matrix elements of the signature for states with good quantum numbers of spin and isospin can be evaluated by making use of the small Wigner functions

$$\langle SS''_z|\hat{R}_S|SS_z\rangle = \sum_{S'_z} d^S_{S_z S'_z}(\pi)\delta_{S'_z,S''_z} = d^S_{S_z S''_z}(\pi), \tag{4.27}$$

[3]Obviously a finite nucleus will not conserve the linear momentum symmetry as it is localised in space

where $d^J_{MM'}(\beta)$ is related to the usual $D^J_{MM'}(\alpha,\beta,\gamma)$ as [VMK88]

$$D^J_{MM'}(\alpha,\beta,\gamma) = e^{-iM\alpha} d^J_{MM'}(\beta) e^{-iM'\gamma}. \tag{4.28}$$

The resulting Wigner function has a special value with the following phase convention

$$d^J_{MM'}(\pi) = (-1)^{J+M}\delta_{M,-M'} = (-1)^{J-M}\delta_{-M,M'}, \tag{4.29}$$

so

$$\langle SS''_z|\hat{R}_S|SS_z\rangle = \sum_{S'_z} d^S_{S_z S'_z}(\pi)\delta_{S'_z,S''_z} = (-1)^{S+S_z}\delta_{S_z,-S''_z}. \tag{4.30}$$

A similar expression holds for the isospin as well. From the former equation it is possible to obtain the eigenstates and eigenvalues of the signature operator, using the closure relation

$$\hat{R}_S|SS_z\rangle = \sum_{S''_z}(-1)^{S+S_z}\delta_{S_z,-S''_z}|SS''_z\rangle = (-1)^{S+S_z}|S-S_z\rangle. \tag{4.31}$$

The eigenstate of the spin signature operator are those with projection zero $|S0\rangle$ with eigenvalue $(-1)^S$ and for the isospin signature operator $|T0\rangle$ with eigenvalue $(-1)^T$. From the last equation we see that the former transformation involves the spin *flipping* of all the nucleons in the system and, analogously, the exchange of the number of protons and neutrons for the latter. For this reason, the isospin signature symmetry is sometimes referred to as *charge symmetry*. Selection rules can be obtained from the fulfilling of these symmetries as we shall see in Section (4.7).

Isoscalar and isovector pairs in Eq. (3.57) are transformed under the product of signature operators (4.25) as

$$\hat{R}_S\hat{R}_T\left(\hat{a}^+_{\frac{1}{2}\frac{1}{2}}\hat{a}^+_{\frac{1}{2}\frac{1}{2}}\right)^{S=1,T=0}_{S_z=0,T_z=0}\hat{R}^+_T\hat{R}^+_S = d^1_{00}(\pi)d^0_{00}(\pi)\left(\hat{a}^+_{\frac{1}{2}\frac{1}{2}}\hat{a}^+_{\frac{1}{2}\frac{1}{2}}\right)^{S=1,T=0}_{S_z=0,T_z=0} = -\left(\hat{a}^+_{\frac{1}{2}\frac{1}{2}}\hat{a}^+_{\frac{1}{2}\frac{1}{2}}\right)^{S=1,T=0}_{S_z=0,T_z=0}, \tag{4.32}$$

$$\hat{R}_S\hat{R}_T\left(\hat{a}^+_{\frac{1}{2}\frac{1}{2}}\hat{a}^+_{\frac{1}{2}\frac{1}{2}}\right)^{S=0,T=1}_{S_z=0,T_z=0}\hat{R}^+_T\hat{R}^+_S = d^1_{00}(\pi)d^0_{00}(\pi)\left(\hat{a}^+_{\frac{1}{2}\frac{1}{2}}\hat{a}^+_{\frac{1}{2}\frac{1}{2}}\right)^{S=0,T=1}_{S_z=0,T_z=0} = -\left(\hat{a}^+_{\frac{1}{2}\frac{1}{2}}\hat{a}^+_{\frac{1}{2}\frac{1}{2}}\right)^{S=0,T=1}_{S_z=0,T_z=0}, \tag{4.33}$$

therefore, a Thouless state parametrised as in Eq. (3.58) will be transformed under the spin and isospin signature operators as

$$\begin{aligned}\hat{R}_S\hat{Z}^+(\alpha,\varphi)\hat{R}^+_S &= i\hat{Z}^+\left(\alpha,\varphi+\frac{\pi}{2}\right),\\ \hat{R}_T\hat{Z}^+(\alpha,\varphi)\hat{R}^+_T &= i\hat{Z}^+\left(\alpha,\varphi-\frac{\pi}{2}\right).\end{aligned} \tag{4.34}$$

That is, it will render a periodic function of φ with period $\frac{\pi}{2}$, as we shall see in the Results Chapter.

4.1.6 Time-reversal symmetry

The time-reversal symmetry $\hat{\mathcal{K}}$ is an antiunitary transformation[4] which reverses the sign of momentum $\boldsymbol{p}$ and angular momentum m and spin projections σ

$$\hat{\mathcal{K}}|\boldsymbol{p}, m, \sigma\rangle = |-\boldsymbol{p}, -m, -\sigma\rangle. \tag{4.35}$$

Similarly to parity (spatial reflection), the eigenvalues of the time-reversal operator are ± 1, denoting time-odd and time-even states corresponding to systems with odd and even number of particles. Consequently, the ground states of all even nuclei, which we consider in this work, are invariant under time-reversal symmetry and they must be time-even.

Odd nuclei are difficult to describe because of the single nucleon which flips the direction of spin under time-reversal. However, there is a fascinating feature about odd nuclei and odd-particle systems in general. As all their states change sign under time-reversal, but the Hamiltonian is time-reversal invariant, these states come in pairwise degeneracy, called Kramers degenerate states [Mes66; BM98], only removed when a magnetic field is applied, arising spin polarisation [DE05].

Time-reversal symmetry allows us to fix a phase convention for the single-particle operators. The one of *Condon-Shortley* is universally accepted [VMK88], under which

$$\hat{\mathcal{K}}\hat{a}^{+}_{\ell m;\frac{1}{2}\sigma;\frac{1}{2}\tau}\hat{\mathcal{K}}^{+} = (-1)^{\ell-m}(-1)^{\frac{1}{2}-\sigma}\hat{a}^{+}_{\ell -m;\frac{1}{2}-\sigma;\frac{1}{2}\tau}. \tag{4.36}$$

From this convention, it is easy to see that the axial pairs in Eq. (3.57) transform under time-reversal as

$$\hat{\mathcal{K}}\left(\hat{a}^{+}_{\ell\frac{1}{2}\frac{1}{2}}\hat{a}^{+}_{\ell\frac{1}{2}\frac{1}{2}}\right)^{L=0,S=1,T=0}_{M=0,S_z=0,T_z=0}\hat{\mathcal{K}}^{+} = (-1)^{2\ell+1}\left(\hat{a}^{+}_{\ell\frac{1}{2}\frac{1}{2}}\hat{a}^{+}_{\ell\frac{1}{2}\frac{1}{2}}\right)^{L=0,S=1,T=0}_{M=0,S_z=0,T_z=0} = -\left(\hat{a}^{+}_{\ell\frac{1}{2}\frac{1}{2}}\hat{a}^{+}_{\ell\frac{1}{2}\frac{1}{2}}\right)^{L=0,S=1,T=0}_{M=0,S_z=0,T_z=0}, \tag{4.37}$$

$$\hat{\mathcal{K}}\left(\hat{a}^{+}_{\ell\frac{1}{2}\frac{1}{2}}\hat{a}^{+}_{\ell\frac{1}{2}\frac{1}{2}}\right)^{L=0,S=0,T=1}_{M=0,S_z=0,T_z=0}\hat{\mathcal{K}}^{+} = (-1)^{2\ell}\left(\hat{a}^{+}_{\ell\frac{1}{2}\frac{1}{2}}\hat{a}^{+}_{\ell\frac{1}{2}\frac{1}{2}}\right)^{L=0,S=0,T=1}_{M=0,S_z=0,T_z=0} = \left(\hat{a}^{+}_{\ell\frac{1}{2}\frac{1}{2}}\hat{a}^{+}_{\ell\frac{1}{2}\frac{1}{2}}\right)^{L=0,S=0,T=1}_{M=0,S_z=0,T_z=0}, \tag{4.38}$$

[4] An antiunitary transformation A is defined as $A = UK$, where U is unitary and K is the complex conjugation operator. In the case of time-reversal, it is an antiunitary transformation because it changes the sign of the commutation relations.

that is, isoscalar and isovector pairs are time-odd (it changes sign) and time-even (invariant), respectively. A Thouless state parametrised as in Eq. (3.58) will be transformed under time-reversal as

$$\hat{\mathcal{K}}\hat{Z}^{+}(\alpha,\varphi)\hat{\mathcal{K}}^{+} = i\hat{Z}^{+}\left(\alpha,\frac{\pi}{2}-\varphi\right), \tag{4.39}$$

where we had taken into account that the time-reversal operator is antiunitary and subsequently it carries a complex conjugation operation.

From Eq. (4.39) we observe that, for a fully paired system where time-reversal symmetry must be fulfilled, it is necessary that $\varphi = \frac{\pi}{2}$, as we shall see in the Results chapter.

4.2 Breaking of symmetries

In the quantum mechanical picture, the breaking of symmetries is measured with the *fluctuations* of observables. Given an operator $\hat{P}$ of an observable quantity and the wavefunction $|\Psi\rangle$, the fluctuations ΔP^2 on $= \langle\Psi|\hat{P}|\Psi\rangle$ are defined as

$$\Delta P^2 = \langle\Psi|\hat{P}^2|\Psi\rangle - \langle\Psi|\hat{P}|\Psi\rangle^2. \tag{4.40}$$

The origin of these fluctuations is twofold: on one hand, it is certainly possible that the system is not symmetric, and this operator $\hat{P}$ is not invariant under unitary transformations of the relevant symmetry operator $\hat{S}$, that is, the very famous result

$$[\hat{P},\hat{S}] \neq 0. \tag{4.41}$$

On the other hand, if $\hat{P}$ and $\hat{S}$ commute and there are common eigenstates of $\hat{P}$ and $\hat{S}$, a *superposition* of these eigenstates gives rise to fluctuations. It is not only needed that $\hat{P}$ is invariant under symmetry transformations,

$$\hat{P} = \hat{S}^{+}\hat{P}\hat{S}, \tag{4.42}$$

but also the wavefunction $|\Psi\rangle$ itself, for the average value to be invariant,

$$\langle\Psi|\hat{P}|\Psi\rangle = \langle\Psi|\hat{S}^{+}\hat{P}\hat{S}|\Psi\rangle \longrightarrow |\Psi\rangle = \hat{S}|\Psi\rangle. \tag{4.43}$$

For illustrative purposes, let us put the textbook example of the Hamiltonian of a rotor,

$$\hat{H} = a\hat{J}^2 + b\hat{J}_z, \tag{4.44}$$

which is obviously rotationally invariant,

$$[\hat{H}, \hat{J}^2] = [\hat{H}, \hat{J}_z] = 0, \tag{4.45}$$

and has eigenstates $|JM\rangle$. If the system is in a specific eigenstate, then the fluctuations of the energy are

$$\begin{aligned} \Delta E^2 &= \langle JM|\hat{H}^2|JM\rangle - \langle JM|\hat{H}|JM\rangle^2 \\ &= [aJ(J+1) + bM]^2 - [aJ(J+1) + bM]^2 \\ &= 0. \end{aligned} \tag{4.46}$$

The symmetry is not broken as the fluctuations are zero. However, if we take a superposition of these eigenstates

$$|\Psi\rangle = \sum_i c_i |JM_i\rangle, \tag{4.47}$$

then we have

$$\begin{aligned} \Delta E^2 &= \langle \Psi|\hat{H}^2|\Psi\rangle - \langle \Psi|\hat{H}|\Psi\rangle^2 \\ &= a^2J^2(J+1)^2 + b^2 \sum_i c_i^2 M_i^2 + 2abJ(J+1) \sum_i c_i^2 M_i \\ &- a^2J^2(J+1)^2 - b^2 \left(\sum_i c_i M_i \right)^2 - 2abJ(J+1) \sum_i c_i^2 M_i \\ &= b^2 \left[\sum_i c_i^2 M_i^2 - \left(\sum_i c_i M_i \right)^2 \right], \end{aligned} \tag{4.48}$$

which, in general, is not zero. Therefore a wavefunction of the system written as a superposition of eigenstates of the symmetry operator gives rise to fluctuations on certain observables even when these symmetry operators commute with the Hamiltonian. This even affects the symmetry operator itself, as we observe from the last equation, the fluctuations on $\hat{J}_z$ are not zero,

$$\Delta J_z^2 = \left[\sum_i c_i^2 M_i^2 - \left(\sum_i c_i M_i \right)^2 \right]. \tag{4.49}$$

Thus, we conclude that it is not only necessary for the Hamiltonian of the system to be invariant under symmetry transformations, but also the wavefunction describing a given state of the system needs to be symmetry-invariant.

4.3 Projection operators

As we have seen in the former section, the application of the rotation operator on a state results in a final state which is a superposition. If we extract, from this superposition of states, a particular one, we need to make use of projection operators. We give in this section a derivation of the general form of this operators, extracted from Ref. [She19] and [Ham12]. We start from a general definition of the rotation of a state

$$\hat{R}(\omega)|\Psi_j\rangle = \sum_i D_{ij}(\omega)|\Psi_i\rangle. \tag{4.50}$$

We know that the matrix elements $D_{ij}(\omega)$ need to fulfil the orthogonality relation

$$\int d\omega D^*_{i'j'}(\omega)D_{ij}(\omega) = \frac{V}{n}\delta_{ii'}\delta_{jj'}, \tag{4.51}$$

with n being the dimension of the symmetry group and V the volume of the coordinates ω space. If we multiply the first equation by $D^*_{i'j'}(\omega)$ and integrate over the whole space

$$\begin{aligned}\int d\omega D^*_{i'j'}(\omega)\hat{R}(\omega)|\Psi_j\rangle &= \sum_i \int d\omega D^*_{i'j'}(\omega)D_{ij}(\omega)|\Psi_i\rangle \\ &= \frac{V}{n}\sum_i \delta_{ii'}\delta_{jj'}|\Psi_i\rangle \\ &= \frac{V}{n}\delta_{jj'}|\Psi'_i\rangle.\end{aligned} \tag{4.52}$$

Therefore we have for a particular state

$$|\Psi_i\rangle = \frac{n}{V}\int d\omega D^*_{i'j'}(\omega)\hat{R}(\omega)|\Psi_j\rangle. \tag{4.53}$$

We define the projection operator as

$$\hat{P}_{ij} = \frac{n}{V}\int d\omega D^*_{i'j'}(\omega)\hat{R}(\omega), \tag{4.54}$$

which can also be applied to restore symmetries broken implicitly by a state, as this will be a superposition of states with good quantum number, associated with the broken symmetry. For the purposes of this work, we are mostly interested with restoration of particle-number, spin and isospin symmetries and in the following sections we will just be concerned about them, properties of these symmetries are summarised in Table (4.1).

Symmetry	Group	Ω	$\hat{R}(\Omega)$	n	V	$D(\Omega)$
Particle Number ($\hat{A}$)	$U(1)$	φ	$e^{i\varphi\hat{A}}$	1	2π	$e^{i\varphi A}$
Angular momentum ($\hat{L}$)	$SO(3)$	$\{\alpha,\beta,\gamma\}$	$e^{-i\alpha\hat{L}_z}e^{-i\beta\hat{L}_y}e^{-i\gamma\hat{L}_z}$	$2L+1$	$16\pi^2$	$D^L_{L_zL'_z}(\Omega)$
Spin ($\hat{S}$)	$SU(2)$	$\{\alpha_S,\beta_S,\gamma_S\}$	$e^{-i\alpha_S\hat{S}_z}e^{-i\beta_S\hat{S}_y}e^{-i\gamma_S\hat{S}_z}$	$2S+1$	$8\pi^2$	$D^S_{S_zS'_z}(\Omega_S)$
Isospin ($\hat{T}$)	$SU(2)$	$\{\alpha_T,\beta_T,\gamma_T\}$	$e^{-i\alpha_T\hat{T}_z}e^{-i\beta_T\hat{T}_y}e^{-i\gamma_T\hat{T}_z}$	$2T+1$	$8\pi^2$	$D^T_{T_zT'_z}(\Omega_T)$

Table 4.1: Properties of the the most relevant symmetries involved in nuclear structure. It is listed the mathematical group, the domain Ω of the pertinent space, the rotation operator $\hat{R}(\Omega)$ which is the generator of the symmetry transformations, the degeneracy n, the integration volume V of the rotation operator and the matrix elements $D(\Omega)$ of $\hat{R}(\Omega)$ between symmetry-conserving states.

4.4 Average values of observables using a symmetry-restored wavefunction

The application of the projection operators to a symmetry-violating wavefunction $|\Psi\rangle$ yields a state with a good quantum number pertaining to the symmetry in consideration. Let us define a certain general symmetry $\hat{I}$ with good quantum number I, the projected state is

$$|I\rangle = \hat{P}^I|\Psi\rangle. \tag{4.55}$$

We now compute average values of the usual observables like the energy using these projected symmetry-restored states, that is,

$$E = \frac{\langle I|\hat{H}|I\rangle}{\langle I|I\rangle} = \frac{\langle\Psi|\hat{P}^{I^+}\hat{H}\hat{P}^I|\Psi\rangle}{\langle\Psi|\hat{P}^{I^+}\hat{P}^I|\Psi\rangle}. \tag{4.56}$$

If the only source of violation of symmetry is given in the mean-field wavefunction and the Hamiltonian is invariant,

$$[\hat{H},\hat{I}] = 0, \tag{4.57}$$

then the equation for the energy is rewritten as

$$E = \frac{\langle I|\hat{H}|I\rangle}{\langle I|I\rangle} = \frac{\langle\Psi|\hat{P}^{I^+}\hat{H}\hat{P}^I|\Psi\rangle}{\langle\Psi|\hat{P}^{I^+}\hat{P}^I|\Psi\rangle} = \frac{\langle\Psi|\hat{H}\hat{P}^I|\Psi\rangle}{\langle\Psi|\hat{P}^I|\Psi\rangle}, \tag{4.58}$$

where we have made use of the fact that the projectors are idempotent and hermitian[5]. For the case of broken particle-number A, spin S and isospin T symmetries, we define the operators

$$\hat{P}^A = \frac{1}{2\pi}\int_0^{2\pi} d\gamma e^{i\gamma(\hat{A}-A)}, \tag{4.59}$$

$$\hat{P}^S_{MK} = \frac{2S+1}{8\pi^2}\int d\Omega_S D^{S*}_{MK}(\Omega_S)\hat{R}_S(\Omega_S), \tag{4.60}$$

$$\hat{P}^T_{NL} = \frac{2T+1}{8\pi^2}\int d\Omega_T D^{T*}_{NL}(\Omega_T)\hat{R}_T(\Omega_T), \tag{4.61}$$

where M and K are the spin projections on the $z-$axis on the intrinsic and laboratory frame, respectively, and similarly for the isospin. The projected energy reads

$$E = \frac{H_{AST}}{I_{AST}}, \tag{4.62}$$

where

$$H_{AST} = \frac{1}{2\pi}\frac{2S+1}{8\pi^2}\frac{2T+1}{8\pi^2}\int d\varphi d\Omega_S d\Omega_T D^{T*}_{\nu'\nu}(\Omega_T)D^{S*}_{\mu'\mu}(\Omega_S)e^{-iA\varphi}\mathcal{H}(\varphi,\Omega_S,\Omega_T), \tag{4.63}$$

and

$$I_{AST} = \frac{1}{2\pi}\frac{2S+1}{8\pi^2}\frac{2T+1}{8\pi^2}\int d\varphi d\Omega_S d\Omega_T D^{T*}_{\nu'\nu}(\Omega_T)D^{S*}_{\mu'\mu}(\Omega_S)e^{-iA\varphi}\mathcal{I}(\varphi,\Omega_S,\Omega_T). \tag{4.64}$$

$\mathcal{H}$ and $\mathcal{I}$ are the Hamilton and overlap kernels, respectively,

$$\mathcal{H} = \langle\Psi|\hat{H}\hat{R}_A(\varphi)\hat{R}_S(\Omega_S)\hat{R}_T(\Omega_T)|\Psi\rangle = \langle\Psi|\hat{H}|\Psi(\varphi,\Omega_S,\Omega_T)\rangle, \tag{4.65}$$

$$\mathcal{I} = \langle\Psi|\hat{R}_A(\varphi)\hat{R}_S(\Omega_S)\hat{R}_T(\Omega_T)|\Psi\rangle = \langle\Psi|\Psi(\varphi,\Omega_S,\Omega_T)\rangle. \tag{4.66}$$

$|\Psi(\varphi,\Omega_S,\Omega_T)\rangle$ is the rotated mean-field wavefunction. Associating set of parameters Z^0 to the unrotated Thouless state $|\Psi\rangle$ and the generally different set Z^R to the rotated Thouless state $|\Psi(\varphi,\Omega_S,\Omega_T)\rangle$, that is, using (3.54)

$$\begin{aligned} |\Psi\rangle &= \mathcal{N}_0 e^{Z^0\hat{a}^+\hat{a}^+}|0\rangle, \\ |\Psi(\varphi,\Omega_S,\Omega_T)\rangle &= \mathcal{N}_R e^{Z^R(\varphi,\Omega_S,\Omega_T)\hat{a}^+\hat{a}^+}|0\rangle. \end{aligned} \tag{4.67}$$

[5]This is, in general, not true, but it holds for particle-number, spin and isospin restoration with axial symmetry. The general case will be presented in Section 4.8.

It is possible write explicit compact expressions for the Hamilton and overlap kernels

$$\mathcal{H} = \langle\Psi|\Psi(\varphi,\Omega_S,\Omega_T)\rangle \left[\mathrm{Tr}\big(\epsilon\rho^{10}\big) + \frac{1}{2}\,\mathrm{Tr}\big(\Gamma^{10}\rho^{10}\big) - \frac{1}{2}\,\mathrm{Tr}\big(\Delta^{10}\kappa^{01*}\big)\right], \tag{4.68}$$

$$\mathcal{I} = s_N \mathrm{pf}\begin{pmatrix} Z^R & -\mathbb{I} \\ \mathbb{I} & -Z^{0*} \end{pmatrix}. \tag{4.69}$$

The densities and fields are constructed with two different mean-field states on the ket and the bra, defined as *transition* densities and fields. The transition densities read

$$\rho^{10} = -Z^{0^*}(\mathbb{I} - Z^R Z^{0^*})^{-1} Z^R, \tag{4.70}$$

$$\kappa^{10} = Z^{0^*}(\mathbb{I} - Z^R Z^{0^*})^{-1}, \tag{4.71}$$

$$\kappa^{01^*} = (\mathbb{I} - Z^R Z^{0^*})^{-1} Z^R. \tag{4.72}$$

As κ is antisymmetric, two matrix expressions are needed to completely define the pairing tensor between different mean-field states. Apart from the known relation (3.36), κ^{01*} reads

$$\kappa^{01*}_{ij} = \frac{\langle\Psi_1|\hat{a}_i^+\hat{a}_j^+|\Psi_0\rangle}{\langle\Psi_1|\Psi_0\rangle}. \tag{4.73}$$

The transition fields are defined using the transition densities

$$\Gamma^{10}_{ll'} = \sum_{qq'} \bar{v}_{lq'l'q}\rho^{10}_{qq'}, \tag{4.74}$$

$$\Delta^{10}_{ll'} = \frac{1}{2}\sum_{qq'} \bar{v}_{ll'qq'}\kappa^{10}_{qq'}. \tag{4.75}$$

For a derivation of the expression of the transition densities from two generally different Thouless states, we refer to Appendix D. While we have written explicitly the example for the projected energy, the methodology is analogous to any other quantity. For example, for the particle-number observable, written as

$$\hat{A} = \sum_i \hat{a}_i^+\hat{a}_i, \tag{4.76}$$

with i denoting any single-particle state, its kernel is given by the transition density

$$\mathcal{A} = \sum_i \langle\Psi|\Psi(\varphi,\Omega_S,\Omega_T)\rangle\rho^{10}_{ii} = \mathcal{I}\,\mathrm{Tr}\,\rho^{10}, \tag{4.77}$$

so the projected number of particles is

$$A = \frac{\int d\varphi d\Omega_S d\Omega_T D^{T*}_{\nu'\nu}(\Omega_T) D^{S*}_{\mu'\mu}(\Omega_S) e^{-iA\varphi} \mathcal{A}}{\int d\varphi d\Omega_S d\Omega_T D^{T*}_{\nu'\nu}(\Omega_T) D^{S*}_{\mu'\mu}(\Omega_S) e^{-iA\varphi} \mathcal{I}}, \tag{4.78}$$

which has to be the same as the input we give in the complex exponential within the integrand. For the particle number fluctuations, its formula is

$$\sigma_A^2 = \langle\Psi|\hat{A}^2|\Psi\rangle - \langle\Psi|\hat{A}|\Psi\rangle^2 = -2\,\mathrm{Tr}\big(\rho^2 - \rho\big), \tag{4.79}$$

therefore, the particle-number fluctuations kernel is

$$\sigma_{\mathcal{A}}^2 = -2\mathcal{I}\,\mathrm{Tr}\Big(\rho^{10^2} - \rho^{10}\Big), \tag{4.80}$$

and its projected value is

$$\sigma_A^2 = \frac{\int d\varphi d\Omega_S d\Omega_T D^{T*}_{\nu'\nu}(\Omega_T) D^{S*}_{\mu'\mu}(\Omega_S) e^{-iA\varphi} \sigma_{\mathcal{A}}^2}{\int d\varphi d\Omega_S d\Omega_T D^{T*}_{\nu'\nu}(\Omega_T) D^{S*}_{\mu'\mu}(\Omega_S) e^{-iA\varphi} \mathcal{I}}, \tag{4.81}$$

and, obviously, this quantity has to be zero. Alternatively, it is possible to derive an expression for the projected isospin. The one-body isospin operator is

$$\hat{T} = \sum_{ab} t_{ab} \hat{a}_a^+ \hat{a}_b, \tag{4.82}$$

where t_{ab} is the compact expression of the three Pauli matrices, i.e.,

$$t_{ab} = \begin{pmatrix} 1 & 1-i \\ 1+i & -1 \end{pmatrix}. \tag{4.83}$$

Making use again of the definition of the transition density we have

$$\mathcal{T} = \mathcal{I}\left(\sum_{ab} t_{ab} \rho^{10}_{ba}\right), \tag{4.84}$$

and therefore the projected isospin will be

$$T = \frac{\int d\varphi d\Omega_S d\Omega_T D^{T*}_{\nu'\nu}(\Omega_T) D^{S*}_{\mu'\mu}(\Omega_S) e^{-iA\varphi} \mathcal{T}}{\int d\varphi d\Omega_S d\Omega_T D^{T*}_{\nu'\nu}(\Omega_T) D^{S*}_{\mu'\mu}(\Omega_S) e^{-iA\varphi} \mathcal{I}}, \tag{4.85}$$

where it has to be the same value as given in the input of the Wigner $D-$function. These examples become a benchmark for a proper numerical implementation of the symmetry restoration techniques.

4.4.1 Reduction to the axial case

In many cases, the system has an axial symmetry which becomes useful to exploit when projecting onto states of good spin and isospin. From a general wavefunction $|\Psi\rangle$, we get an isospin-projected state by the application of the projection operator $\hat{P}^T_{T'_zT_z}$ as

$$|T, T'_z, T_z\rangle = \hat{P}^T_{T'_zT_z}|\Psi\rangle = \frac{2T+1}{8\pi^2}\int d\Omega D^{T*}_{T'_zT_z}(\Omega)\hat{R}(\Omega)|\Psi\rangle, \tag{4.86}$$

where Ω is the set of three Euler angles (α, β, γ) and $d\Omega = \sin\beta d\alpha d\beta d\gamma$. We expand the integral to obtain

$$|T, T'_z, T_z\rangle = \frac{2T+1}{8\pi^2}\int_0^{2\pi} d\alpha \int_0^{2\pi} d\gamma \int_0^{\pi} d\beta \sin\beta D^{T*}_{T'_zT_z}(\alpha, \beta, \gamma)\hat{R}(\alpha, \beta, \gamma)|\phi\rangle. \tag{4.87}$$

The definitions of the Wigner D-function and the rotation operator are

$$D^{T*}_{T'_zT_z}(\alpha, \beta, \gamma) = e^{iT'_z\alpha}d^T_{T'_zT_z}(\beta)e^{iT_z\gamma}, \tag{4.88}$$

$$\hat{R}(\alpha, \beta, \gamma) = e^{-i\alpha\hat{T}_z}e^{-i\beta\hat{T}_y}e^{-i\gamma\hat{T}_z}. \tag{4.89}$$

If the state $|\Psi\rangle$ has an axial symmetry around the T_z-axis, then it is an eigenstate of the $\hat{T}_z$ operator. Therefore

$$e^{-i\gamma\hat{T}_z}|\Psi\rangle = e^{-i\gamma T_{z_0}}|\Psi\rangle. \tag{4.90}$$

Using this fact and the former definitions of Wigner function and rotation operator, we find the overlap $I = \langle\Psi|T, T'_z, T_z\rangle$ to be

$$I = \frac{2T+1}{8\pi^2}\int_0^{2\pi} d\alpha \int_0^{2\pi} d\gamma \int_0^{\pi} d\beta \sin\beta e^{i(T'_z-T_{z_0})\alpha}d^T_{T'_zT_z}(\beta)e^{i(T_z-T_{z_0})\gamma}\mathcal{I}(\beta), \tag{4.91}$$

where $\mathcal{I}(\beta) = \langle\Psi|e^{-i\beta\hat{T}_y}|\Psi\rangle$ is the overlap kernel. We now focus on the integral over α (or γ),

$$\int_0^{2\pi} d\alpha e^{i(T'_z-T_{z_0})\alpha}, \tag{4.92}$$

and define $n = T'_z - T_{z_0}$, which is an integer quantity. If $n = 0$, i.e., $T'_z = T_{z_0}$, we have

$$\int_0^{2\pi} d\alpha = 2\pi. \tag{4.93}$$

If $n \neq 0$, then we get

$$\int_0^{2\pi} d\alpha e^{in\alpha} = \frac{e^{in\alpha}}{in}\bigg|_0^{2\pi} = \frac{e^{2\pi ni} - 1}{in} = 0. \tag{4.94}$$

In summary, the integral over α (and, similarly, the integral over γ) can be expressed as

$$\int_0^{2\pi} d\alpha e^{i(T'_z - T_{z_0})\alpha} = 2\pi\delta_{T'_z,T_{z_0}}. \tag{4.95}$$

The final expression will be

$$I = \frac{2T+1}{2}\delta_{T'_z,T_{z_0}}\delta_{T_z,T_{z_0}}\int_0^{\pi} d\beta \sin(\beta) d^T_{T'_z T_z}\mathcal{I}(\beta). \tag{4.96}$$

A similar derivation can be applied to the Hamiltonian matrix elements $H = \langle\Psi|\hat{H}|T, T'_z, T_z\rangle$ to obtain

$$H = \frac{2T+1}{2}\delta_{T'_z,T_{z_0}}\delta_{T_z,T_{z_0}}\int_0^{\pi} d\beta \sin(\beta) d^T_{T'_z T_z}\mathcal{H}(\beta), \tag{4.97}$$

where $\mathcal{H}(\beta) = \langle\Psi|\hat{H}e^{-i\beta\hat{T}_y}|\Psi\rangle$. The procedure is analogous for the spin projection.

The computation of the energy in the case of axial symmetry is simpler, as the quantities (4.65, 4.66) reduce to

$$H = \frac{1}{2\pi}\frac{2S+1}{2}\frac{2T+1}{2}\int d\varphi d\beta_S d\beta_T \sin(\beta_S)\sin(\beta_T) d^T_{00}(\beta_T) d^S_{00}(\beta_S) e^{-iA\varphi}\mathcal{H}(\varphi,\beta_S,\beta_T), \tag{4.98}$$

$$I = \frac{1}{2\pi}\frac{2S+1}{2}\frac{2T+1}{2}\int d\varphi d\beta_S d\beta_T \sin(\beta_S)\sin(\beta_T) d^T_{00}(\beta_T) d^S_{00}(\beta_S) e^{-iA\varphi}\mathcal{I}(\varphi,\beta_S,\beta_T). \tag{4.99}$$

The integration is easily performed numerically using a Gauss-Chebyshev quadrature for the gauge space and a Gauss-Legendre quadrature for the spin and isospin spaces [Pre92]. We emphasise here again the huge importance of the proper exploitation of the symmetries of the system, as we have reduced a seven-dimensional integration calculation to just a three-dimensional one, not only saving computational time, but eventually making this sort of calculations feasible.

4.5 Variation after projection versus projection after variation

When restoring the symmetries broken by the mixing in the Bogoliubov transformation, two different approaches exist for the implementation. Either the projectors (4.59) are applied to the optimal HFB wavefunction giving the minimum of the energy (3.46), a technique called *projection after variation* (PAV)

$$\delta \frac{\langle \Psi | \hat{H} | \Psi \rangle}{\langle \Psi | \Psi \rangle} \bigg|_{|\Psi_{\rm PAV}\rangle} = 0 \longrightarrow E^{\rm PAV}_{\rm AST} = \frac{\langle \Psi_{\rm PAV} | \hat{H} | AST \rangle}{\langle \Psi_{\rm PAV} | AST \rangle}, \tag{4.100}$$

or the energy is computed with respect to the symmetry-restored state $|AST\rangle$ and then finding its minimum, a technique called *variation after projection* (VAP)

$$\delta \frac{\langle \Psi | \hat{H} | AST \rangle}{\langle \Psi | AST \rangle} \bigg|_{|\Psi_{\rm VAP}\rangle} = 0 \longrightarrow E^{\rm VAP}_{\rm AST} = \frac{\langle \Psi_{\rm VAP} | \hat{H} | AST \rangle}{\langle \Psi_{\rm VAP} | AST \rangle}. \tag{4.101}$$

The former implies only one application of the projectors at the minimum of the mean-field energy. The latter will imply the application of the projectors at every iteration of our minimisation procedure, such as the gradient method depicted in Fig. (3.7), and consequently it takes a lot of computational effort. However, any mean-field formalism relies upon the variational principle, which states that the choosing of an ansatz closer to the exact state will result on a closer upper bound to the exact energy. Obviously, a symmetry-restored mean-field wavefunction is a much better ansatz than a symmetry-breaking mean-field one, as we shall see in Section 5, when the system fulfils these symmetries.

4.6 General rotation of the Thouless state in spin and isospin space

To restore the broken symmetries, we have observed that we need to integrate over the whole volume using kernels that are computed using a rotated wavefunction in the respective space. In this Section, we derive expressions for these rotated wavefunctions in terms of the six intrinsic pairs building up the mean-field wavefunction: isoscalar and isovector pairs, with three different

projections. Using the Thouless parametrisation, the wavefunction of our system is

$$|\Psi\rangle = \mathcal{N} \exp\left(\sum_{ij} Z_{ij} \hat{a}_i^+ \hat{a}_j^+\right) |0\rangle. \tag{4.102}$$

The initial Thouless matrix is defined as

$$Z^0(i,j) = \frac{1}{2}\left(\sum_{\mu} C^{00}_{lm_i;lm_j} C^{1\mu}_{\frac{1}{2}\sigma_i;\frac{1}{2}\sigma_j} C^{00}_{\frac{1}{2}\tau_i;\frac{1}{2}\tau_j} Z^{10}_{\mu 0} + \sum_{\nu} C^{00}_{lm_i;lm_j} C^{00}_{\frac{1}{2}\sigma_i;\frac{1}{2}\sigma_j} C^{1\nu}_{\frac{1}{2}\tau_i;\frac{1}{2}\tau_j} Z^{01}_{0\nu}\right), \tag{4.103}$$

with $C^{\mathcal{C}\gamma}_{a\alpha;b\beta}$ being the Clebsch-Gordan coefficients needed for the coupling of the pairs and $Z^{ST}_{\mu\nu}$ will be our set of six general parameters modelling the strength of each pair. In order to perform a general rotation of the parameters in spin and isospin space, we define $\hat{R}(\Omega_S)$ as the rotation operator in spin space, being Ω_S the set of three Euler angles $(\alpha_S, \beta_S, \gamma_S)$. Similarly, we define $\hat{R}(\Omega_T)$ as the rotation operator in isospin space.

For a pair coupled to $T = 0$ and $S = 1$ (isoscalar pair), we have

$$\hat{R}(\Omega_S)\hat{R}(\Omega_T) \sum_{\mu} Z^{10}_{\mu 0} \left(\hat{a}^+_{\frac{1}{2}\frac{1}{2}} \hat{a}^+_{\frac{1}{2}\frac{1}{2}}\right)^{S=1,T=0}_{S_z=\mu,T_z=0} \hat{R}(\Omega_T)^+ \hat{R}(\Omega_S)^+. \tag{4.104}$$

Since this pair is coupled to total isospin zero, the parameters will be invariant under rotations in this space, therefore we are left with

$$\hat{R}(\Omega_S) \sum_{\mu} Z^{10}_{\mu 0} \left(\hat{a}^+_{\frac{1}{2}\frac{1}{2}} \hat{a}^+_{\frac{1}{2}\frac{1}{2}}\right)^{S=1,T=0}_{S_z=\mu,T_z=0} \hat{R}(\Omega_S)^+. \tag{4.105}$$

The rotation of the coupled pair will be given by the following transformation

$$\begin{aligned} &\hat{R}(\Omega_S) \sum_{\mu} Z^{10}_{\mu 0} \left(\sum_{\sigma_1\sigma_2\tau_1\tau_2} C^{1\mu}_{\frac{1}{2}\sigma_1\frac{1}{2}\sigma_2} C^{00}_{\frac{1}{2}\tau_1\frac{1}{2}\tau_2} \hat{a}^+_{\sigma_1\tau_1} \hat{a}^+_{\sigma_2\tau_2}\right) \hat{R}(\Omega_S)^+ = \\ &= \sum_{\mu\sigma'_1\sigma'_2\tau_1\tau_2} Z^{10}_{\mu 0} C^{00}_{\frac{1}{2}\tau_1\frac{1}{2}\tau_2} \left(\sum_{\sigma_1\sigma_2} C^{1\mu}_{\frac{1}{2}\sigma_1\frac{1}{2}\sigma_2} D^{\frac{1}{2}*}_{\sigma'_1\sigma_1}(\Omega_S) D^{\frac{1}{2}*}_{\sigma'_2\sigma_2}(\Omega_S)\right) \hat{a}^+_{\sigma'_1\tau_1} \hat{a}^+_{\sigma'_2\tau_2}. \end{aligned} \tag{4.106}$$

Using now the coupling of the Wigner D-functions [BR86]

$$\sum_{N\sigma_1\sigma_2} C^{1\mu}_{\frac{1}{2}\sigma_1\frac{1}{2}\sigma_2} D^{\frac{1}{2}*}_{\sigma'_1\sigma_1}(\Omega_S) D^{\frac{1}{2}*}_{\sigma'_2\sigma_2}(\Omega_S) = \sum_{N} C^{1N}_{\frac{1}{2}\sigma'_1\frac{1}{2}\sigma'_2} D^{1*}_{N\mu}(\Omega_S), \tag{4.107}$$

where the Clebsch-Gordan coefficients are real, we get

$$\begin{aligned}\hat{R}(\Omega_S)\sum_{\mu} Z^{10}_{\mu 0}\left(\hat{a}^{+}_{\frac{1}{2}\frac{1}{2}}\hat{a}^{+}_{\frac{1}{2}\frac{1}{2}}\right)^{S=1,T=0}_{S_z=\mu,T_z=0}\hat{R}(\Omega_S)^{+} = \\ = \sum_{\mu\sigma_1'\sigma_2'\tau_1\tau_2} Z^{10}_{\mu 0} C^{00}_{\frac{1}{2}\tau_1\frac{1}{2}\tau_2} C^{1N}_{\frac{1}{2}\sigma_1'\frac{1}{2}\sigma_2'} D^{1*}_{N\mu}(\Omega_S)\hat{a}^{+}_{\sigma_1'\tau_1}\hat{a}^{+}_{\sigma_2'\tau_2}.\end{aligned} \tag{4.108}$$

Defining the *rotated parameters* as

$$Z^{10}_{N0}(\Omega_S) = \sum_{\mu} D^{1*}_{N\mu}(\Omega_S) Z^{10}_{\mu 0}, \tag{4.109}$$

we obtain a general compact expression for the spin and isospin rotated isoscalar pair

$$\begin{aligned}\hat{R}(\Omega_S)\sum_{\mu} Z^{10}_{\mu 0}\left(\hat{a}^{+}_{\frac{1}{2}\frac{1}{2}}\hat{a}^{+}_{\frac{1}{2}\frac{1}{2}}\right)^{S=1,T=0}_{S_z=\mu,T_z=0}\hat{R}(\Omega_S)^{+} = \\ = \sum_{N\sigma_1'\sigma_2'\tau_1\tau_2} C^{00}_{\frac{1}{2}\tau_1\frac{1}{2}\tau_2} C^{1N}_{\frac{1}{2}\sigma_1'\frac{1}{2}\sigma_2'} Z^{10}_{N0}(\Omega_S)\hat{a}^{+}_{\sigma_1'\tau_1}\hat{a}^{+}_{\sigma_2'\tau_2}.\end{aligned} \tag{4.110}$$

We have introduced an additional sum over N, the projection of the total spin along the laboratory frame, for completeness. An analogous formula holds for the pair coupled to $T = 1$ and $S = 0$ (isovector pair)

$$\begin{aligned}\hat{R}(\Omega_T)\sum_{\nu} Z^{01}_{0\nu}\left(\hat{a}^{+}_{\frac{1}{2}\frac{1}{2}}\hat{a}^{+}_{\frac{1}{2}\frac{1}{2}}\right)^{S=0,T=1}_{S_z=0,T_z=\nu}\hat{R}(\Omega_T)^{+} = \\ = \sum_{M\sigma_1\sigma_2\tau_1'\tau_2'} C^{00}_{\frac{1}{2}\sigma_1\frac{1}{2}\sigma_2} C^{1M}_{\frac{1}{2}\tau_1'\frac{1}{2}\tau_2'} Z^{01}_{0M}(\Omega_T)\hat{a}^{+}_{\sigma_1\tau_1'}\hat{a}^{+}_{\sigma_2\tau_2'},\end{aligned} \tag{4.111}$$

where in this case the rotated parameters are

$$Z^{01}_{0M}(\Omega_T) = \sum_{\nu} D^{1*}_{M\nu}(\Omega_T) Z^{01}_{0\nu}. \tag{4.112}$$

Expressions (4.110) and (4.111) for the rotated isoscalar and isovector pairs have the same structure as the unrotated ones, where now the parameters $Z^{ST}_{\mu\nu}$ depend on the angle Ω_S and Ω_T, respectively.

In the axial case, we only work with two kinds of pairs: Z^{10}_{00} and Z^{01}_{00}, corresponding to isoscalar and isovector pairs with projection zero. The rest of them will be set to zero, since they are not needed as only variations in the magnitude of these pairs, not their directions in spin and isospin space, will yield different results. In this case, equations (4.110) and (4.111)

reduce to

$$\begin{aligned}\hat{R}(\Omega_S) Z^{10}_{00} \left(\hat{a}^+_{\frac{1}{2}\frac{1}{2}} \hat{a}^+_{\frac{1}{2}\frac{1}{2}}\right)^{S=1,T=0}_{S_z=0,T_z=0} \hat{R}(\Omega_S)^+ = \\ = \sum_{N\sigma'_1\sigma'_2\tau_1\tau_2} C^{00}_{\frac{1}{2}\tau_1\frac{1}{2}\tau_2} C^{1N}_{\frac{1}{2}\sigma'_1\frac{1}{2}\sigma'_2} Z^{10}_{N0}(\Omega_S) \hat{a}^+_{\sigma'_1\tau_1} \hat{a}^+_{\sigma'_2\tau_2},\end{aligned} \tag{4.113}$$

with

$$Z^{10}_{N0}(\Omega_S) = D^{1*}_{N0}(\Omega_S) Z^{10}_{00}, \tag{4.114}$$

and

$$\begin{aligned}\hat{R}(\Omega_T) \sum_\nu Z^{01}_{0\nu} \left(\hat{a}^+_{\frac{1}{2}\frac{1}{2}} \hat{a}^+_{\frac{1}{2}\frac{1}{2}}\right)^{S=0,T=1}_{S_z=0,T_z=\nu} \hat{R}(\Omega_T)^+ = \\ = \sum_{M\sigma_1\sigma_2\tau'_1\tau'_2} C^{00}_{\frac{1}{2}\sigma_1\frac{1}{2}\sigma_2} C^{1M}_{\frac{1}{2}\tau'_1\frac{1}{2}\tau'_2} Z^{01}_{0M}(\Omega_T) \hat{a}^+_{\sigma_1\tau'_1} \hat{a}^+_{\sigma_2\tau'_2},\end{aligned} \tag{4.115}$$

with

$$Z^{01}_{0M}(\Omega_T) = D^{1*}_{M0}(\Omega_T) Z^{01}_{00}. \tag{4.116}$$

We notice that, even when we have fixed the projections μ, ν, there is still a sum over N, M corresponding to the projections of spin and isospin in the laboratory frame when constructing the rotated wavefunction. Finally, we define the rotated Z matrix

$$\begin{aligned}Z^R(i,j) = \frac{1}{2}\Bigg[\sum_N C^{00}_{\ell m_i;\ell m_j} C^{00}_{\frac{1}{2}\tau_i;\frac{1}{2}\tau_j} C^{1N}_{\frac{1}{2}\sigma_i;\frac{1}{2}\sigma_j} Z^{10}_{N0}(\varphi,\Omega_S) + \\ + \sum_M C^{00}_{\ell m_i;\ell m_j} C^{00}_{\frac{1}{2}\sigma_i;\frac{1}{2}\sigma_j} C^{1M}_{\frac{1}{2}\tau_i;\frac{1}{2}\tau_j} Z^{01}_{0M}(\varphi,\Omega_T)\Bigg],\end{aligned} \tag{4.117}$$

with $Z^{10}_{N0}(\varphi,\Omega_S)$ and $Z^{01}_{0M}(\varphi,\Omega_T)$ being

$$Z^{01}_{0M}(\varphi,\Omega_T) = e^{2i\varphi} D^{1*}_{M0}(\Omega_T) Z^{01(0)}_{00}, \tag{4.118}$$

$$Z^{10}_{N0}(\varphi,\Omega_S) = e^{2i\varphi} D^{1*}_{N0}(\Omega_S) Z^{10(0)}_{00}, \tag{4.119}$$

which will be used alongside the unrotated Z matrix (4.103) for the definition of the mean-field quasiparticle wavefunction.

4.6.1 Axial symmetry test with isovector pairs

For the general computation of the projected energy, we define our integrated hamiltonian and overlap kernels with Eqs. (4.98, 4.99). We have made use of the axial symmetry because all the intrinsic states can be built from axial pairs (the isovector Z^{01}_{00} and the isoscalar Z^{10}_{00}). In order to make sure that this implementation is correct, we test it by doing the following: first, we choose some values for the pairs Z^{01}_{00} and Z^{10}_{00} and calculate the projected energy using Eqs. (4.98, 4.99). Secondly, we rotate only the isovector pair using the Wigner D-functions as

$$\begin{aligned} Z^{01}_{0-1}(\Omega_T) &= D^{1*}_{-10}(\Omega_T) Z^{01}_{00}, \\ Z^{01}_{00}(\Omega_T) &= D^{1*}_{00}(\Omega_T) Z^{01}_{00}, \\ Z^{01}_{01}(\Omega_T) &= D^{1*}_{10}(\Omega_T) Z^{01}_{00}, \end{aligned} \tag{4.120}$$

where the set of Euler angles in isospin space Ω_T is arbitrary. These results come from the general formula of the rotation of the pairs

$$Z^{01}_{0M}(\Omega_T) = \sum_{\nu} D^{1*}_{M\nu}(\Omega_T) Z^{01}_{0\nu}, \tag{4.121}$$

where only Z^{01}_{00} is nonzero. Lastly, with these new isovector pairs with three projections (not axial anymore) we compute the projected energy using a full integration in isospin space as

$$E_{AST} = \frac{H_{AST}}{I_{AST}}, \tag{4.122}$$

with

$$H_{AST} = \frac{1}{2\pi} \frac{2S+1}{2} \frac{2T+1}{8\pi^2} \int d\varphi d\beta_S d\Omega_T \sin(\beta_S) d^S_{\mu\mu}(\beta_S) D^{T*}_{\nu'\nu}(\Omega_T) e^{-iA\varphi} \mathcal{H}(\varphi, \beta_S, \Omega_T), \tag{4.123}$$

$$I_{AST} = \frac{1}{2\pi} \frac{2S+1}{2} \frac{2T+1}{8\pi^2} \int d\varphi d\beta_S d\Omega_T \sin(\beta_S) d^S_{\mu\mu}(\beta_S) D^{T*}_{\nu'\nu}(\Omega_T) e^{-iA\varphi} \mathcal{I}(\varphi, \beta_S, \Omega_T). \tag{4.124}$$

Both energies, computed with axial and non-axial pairs, must be the same. Equivalently, the same condition holds for rotations of the isoscalar pair. If they are not, the system does not possess an axial symmetry.

4.7 Signature analysis of the Thouless pairs

Applying the signature operators to the isovector pairs (only the isospin signature will have an effect, as these pairs are scalar in spin space) we obtain the following *rotated* parameters

$$Z^{01}_{0M}(\pi) = \sum_{\nu} d^{1}_{M\nu}(\pi) Z^{01}_{0\nu}, \tag{4.125}$$

or, in matrix form

$$\begin{aligned} \begin{pmatrix} Z^{01}_{0-1}(\pi) \\ Z^{01}_{00}(\pi) \\ Z^{01}_{01}(\pi) \end{pmatrix} &= \begin{pmatrix} d^{1}_{-1-1}(\pi) & d^{1}_{-10}(\pi) & d^{1}_{-11}(\pi) \\ d^{1}_{0-1}(\pi) & d^{1}_{00}(\pi) & d^{1}_{01}(\pi) \\ d^{1}_{1-1}(\pi) & d^{1}_{10}(\pi) & d^{1}_{11}(\pi) \end{pmatrix} \begin{pmatrix} Z^{01}_{0-1} \\ Z^{01}_{00} \\ Z^{01}_{01} \end{pmatrix} \\ &= \begin{pmatrix} 0 & 0 & 1 \\ 0 & -1 & 0 \\ 1 & 0 & 0 \end{pmatrix} \begin{pmatrix} Z^{01}_{0-1} \\ Z^{01}_{00} \\ Z^{01}_{01} \end{pmatrix}. \end{aligned} \tag{4.126}$$

We observe that

- Axial Thouless pairs (with isospin projection zero) always have a definite signature of -1.
- The superposition of Thouless pairs with projection ± 1 has a definite signature of $+1$, that is
$$Z^{01}_{0-1}(\pi) + Z^{01}_{01}(\pi) = Z^{01}_{01} + Z^{01}_{0-1}. \tag{4.127}$$
- In general, an arbitrary combination of the Thouless pairs will not have a definite signature.

We also calculate the exact eigenstates $|TT_zSS_z\rangle$ of the product of both signatures, corresponding as demonstrated before to the case where $T_z = S_z = 0$,

$$\hat{R}_T(\pi)\hat{R}_S(\pi)|T0S0\rangle = (-1)^{S+T}|T0S0\rangle. \tag{4.128}$$

In Table (4.2) we gather all the information obtained from the application of the signature operators in spin and isospin space on the exact states and the axial and non-axial Thouless pairs.

Now that we have the expressions of the tranformed Thouless pairs under signature, we apply the signature operator to particle-number projected (PNP) states $|A\rangle$. Indeed, these

Operator	Exact	Sig	Thouless (axial)	Sig	Thouless (non axial)	Sig
$\hat{R}_T$	$\|T0\rangle$	$(-1)^T$	Z_{00}^{01}	-1	$Z_{01}^{01} + Z_{0-1}^{01}$	1
$\hat{R}_S$	$\|S0\rangle$	$(-1)^S$	Z_{00}^{10}	-1	$Z_{10}^{10} + Z_{-10}^{10}$	1
$\hat{R}_T\hat{R}_S$	$\|T0S0\rangle$	$(-1)^{S+T}$	Z_{00}^{01}, Z_{00}^{10}	-1	$Z_{10}^{10} + Z_{-10}^{10}$ $Z_{01}^{01} + Z_{0-1}^{01}$	1

Table 4.2: Exact and Thouless pairs (axial and non axial, only nonzero parameters composing the different pairs) eigenstates of the signature operator in spin, isospin and both spaces. Next to the column of the states is the corresponding eigenvalue referred to as the signature (Sig).

states are defined as

$$|A\rangle = \hat{P}^A|\Psi\rangle = \frac{1}{2\pi}\int_0^{2\pi} d\varphi e^{i\varphi(\hat{A}-A)}|\Psi\rangle, \tag{4.129}$$

where $\hat{A}$ is the particle number operator and we remember that the Thouless state is given by $|\Psi\rangle = e^{\hat{Z}}|0\rangle$ with $\hat{Z}$ our Thouless matrix composed by the pairs. These PNP states are then

$$|A\rangle = \frac{\hat{Z}^{A/2}}{(A/2)!}|0\rangle. \tag{4.130}$$

Applying now the general product of signatures in spin and isospin space on this state is equivalent to transform the Thouless pair $\hat{Z}^{A/2}$, therefore

$$\hat{R}_T(\pi)\hat{R}_S(\pi)\hat{Z}^{A/2}\hat{R}_T^+(\pi)\hat{R}_S^+(\pi) = (-1)^{A/2}\hat{Z}^{A/2}. \tag{4.131}$$

In the case of axial pairs, thus we see that the particle-number projected states are good signature states with value $(-1)^{A/2}$.

4.7.1 Selection rules for the projected states

The Thouless state $|\Psi\rangle$ is a superposition of states of good particle number, spin and isospin $|AST\rangle$ but we do not know which of these states are part of the generalised product state. We check this, for a given Thouless state, performing the full projection and then computing the overlap between this exact state and the Thouless state, $\langle\Psi|AST\rangle$. If this overlap is zero, it means that it is not possible to extract an exact state with given particle number, spin and isospin because it is not part of the Thouless state.

From the analysis in the former section of the Thouless states, we come to the following

selection rule for the projected states $|AST\rangle$

$$(-1)^{S+T} = (-1)^{A/2}. \tag{4.132}$$

Therefore, if $S+T$ is an *even* number, then the number of pairs $A/2$ must be *even*. Secondly, if $S+T$ is an *odd* number, then there is an *odd* number of pairs.

This selection rule must be fulfilled, as the Hamiltonian is invariant under the product of signatures and the axial Thouless states are eigenstates of these operators, as shown in the last Section.

4.8 Projection methods for different initial and final states

So far, we have applied projection methods for restoration of broken symmetries for the computation of several observables in cases where the operator related to the observable commutes with the symmetry operator and we project onto the same good state on the ket and the bra. There are cases where we would like to have different initial and final states, as it happens for example in any particle-transfer reaction, or where the observable is not invariant under transformations from the symmetry operator. As it happens when we include Coulomb potential in the Hamiltonian, for example, it will no longer be invariant under isospin transformations. Under such cases, a transformation rule for an arbitrary spherical tensor of rank λ and projection μ [Dob09] needs to be applied

$$\hat{P}^{I_f}_{K_f M_f} \hat{T}_{\lambda\mu} \hat{P}^{I_i}_{M_i K_i} = C^{I_f M_f}_{I_i M_i \lambda\mu} \sum_{M\mu'} (-1)^{2\mu'} C^{I_f K_f}_{I_i M \lambda\mu'} \hat{T}_{\lambda\mu'} \hat{P}^{I_i}_{M K_i}. \tag{4.133}$$

Applying this transformation will cast a familiar equation of similar structure to the diagonal case. For illustrative purposes, we apply this method to the deuteron and alpha transfer case. This is of special interest as it is a potential experimental microscopic probe of the presence of proton-neutron condensates in nuclei.

4.8.1 Symmetry-restored deuteron transfer matrix elements

We define the deuteron transfer matrix element as the addition of an isoscalar pair into the system

$$P_d = \langle A+2, S+1, T | \hat{D}^{+}_{\mu} | A, S, T \rangle. \tag{4.134}$$

The reaction is sketched in Fig. (4.2).

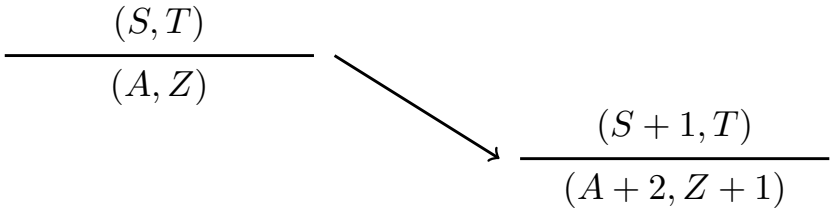

Figure 4.2: Schematic representation of a general deuteron addition transfer. A proton-neutron pair coupled to total spin one and isospin zero is transferred to the system.

We realise that the pair $\hat{D}^+_\mu$ in (4.134) can be written as the tensor product of a tensor of rank 1 in spin space and a tensor of rank 0 in isospin space

$$\left(\hat{a}_{\frac{1}{2}\frac{1}{2}}\hat{a}_{\frac{1}{2}\frac{1}{2}}\right)^{S=1,T=0}_{S_z=\mu,T_z=0} = \left(\hat{a}_{\frac{1}{2}}\hat{a}_{\frac{1}{2}}\right)^{S=1}_{S_z=\mu} \otimes \left(\hat{a}_{\frac{1}{2}}\hat{a}_{\frac{1}{2}}\right)^{T=0}_{T_z=0}, \tag{4.135}$$

therefore the projection operators in spin and isospin spaces are applied separately. For the case of isospin, the result is

$$\begin{aligned}\hat{P}^T_{00}\left(\hat{a}_{\frac{1}{2}}\hat{a}_{\frac{1}{2}}\right)^{T=0}_{T_z=0}\hat{P}^T_{00} &= C^{T0}_{T000}\sum_{M\mu'}(-1)^{2\mu'}C^{T0}_{TM0\mu'}\left(\hat{a}_{\frac{1}{2}}\hat{a}_{\frac{1}{2}}\right)^{T=0}_{T_z=0}\hat{P}^T_{M0} \\ &= \left(\hat{a}_{\frac{1}{2}}\hat{a}_{\frac{1}{2}}\right)^{T=0}_{T_z=0}\hat{P}^T_{00},\end{aligned} \tag{4.136}$$

that is, there is no change with respect to the diagonal case, as expected, since the deuteron is a scalar in isospin space and therefore invariant under isorotations. For spin case, we obtain

$$\hat{P}^{S+1}_{00}\left(\hat{a}_{\frac{1}{2}}\hat{a}_{\frac{1}{2}}\right)^{S=1}_{S_z=\mu}\hat{P}^S_{00} = C^{S+1,0}_{S01\mu}\sum_M(-1)^{-2M}C^{S+1,0}_{SM1-M}\left(\hat{a}_{\frac{1}{2}}\hat{a}_{\frac{1}{2}}\right)^{S=1}_{S_z=-M}\hat{P}^S_{M0}, \tag{4.137}$$

thus

$$\hat{P}^T_{00}\hat{P}^{S+1}_{00}\left(\hat{a}_{\frac{1}{2}\frac{1}{2}}\hat{a}_{\frac{1}{2}\frac{1}{2}}\right)^{S=1,T=0}_{S_z=\mu,T_z=0}\hat{P}^S_{00}\hat{P}^T_{00} = C^{S+1,0}_{S01\mu}\sum_M(-1)^{-2M}C^{S+1,0}_{SM1-M}\left(\hat{a}_{\frac{1}{2}\frac{1}{2}}\hat{a}_{\frac{1}{2}\frac{1}{2}}\right)^{S=1,T=0}_{S_z=-M,T_z=0}\hat{P}^S_{M0}\hat{P}^T_{00}. \tag{4.138}$$

Now we need to compute non-diagonal matrix elements between different particle-number projected states

$$\langle A+2|\hat{a}^+\hat{a}^+|A\rangle = \langle\Psi_L|\hat{P}^{A+2}\hat{a}^+\hat{a}^+\hat{P}^A|\Psi_R\rangle. \tag{4.139}$$

$|\Psi_L\rangle$ and $|\Psi_R\rangle$ are the Left and Right optimal quasiparticle states obtained after a HFB cal-

culation. Now we have to prove how $\hat{P}^A$ and $\hat{a}^+\hat{a}^+$ commutes. We know that the projection operator is related to the rotation operator in gauge space as

$$\hat{P}^A \longrightarrow e^{i\varphi(\hat{A}-A)}, \tag{4.140}$$

and we work with two general fermion annihilation operators $\hat{a}_i, \hat{a}_j$, where i, j denote the single-particle states. The problem can be reduced to see how $\hat{A}$ and $\hat{a}_i\hat{a}_j$ commute. Using the anticommutation relations (2.5, 2.6) we see that

$$\hat{A}\hat{a}_i\hat{a}_j = \sum_l \hat{a}_l^+\hat{a}_l\hat{a}_i\hat{a}_j = \sum_l(\delta_{li}\hat{a}_j\hat{a}_l - \delta_{lj}\hat{a}_i\hat{a}_l + \hat{a}_i\hat{a}_j\hat{a}_l^+\hat{a}_l) = -2\hat{a}_i\hat{a}_j + \hat{a}_i\hat{a}_j\hat{A}, \tag{4.141}$$

and thus

$$\hat{A}\hat{a}_i\hat{a}_j = \hat{a}_i\hat{a}_j(\hat{A}-2). \tag{4.142}$$

We realise that the following relation is also true

$$\hat{A}^k\hat{a}_i\hat{a}_j = \hat{a}_i\hat{a}_j(\hat{A}-2)^k. \tag{4.143}$$

Finally, the particle-number exponential and the pair removal operator commute as

$$e^{i\varphi(\hat{A}-A)}\left(\hat{a}_{\frac{1}{2}\frac{1}{2}}\hat{a}_{\frac{1}{2}\frac{1}{2}}\right) = \left(\hat{a}_{\frac{1}{2}\frac{1}{2}}\hat{a}_{\frac{1}{2}\frac{1}{2}}\right)e^{i\varphi(\hat{A}-A-2)}, \tag{4.144}$$

or, equivalently

$$\hat{P}^A\left(\hat{a}_{\frac{1}{2}\frac{1}{2}}\hat{a}_{\frac{1}{2}\frac{1}{2}}\right) = \left(\hat{a}_{\frac{1}{2}\frac{1}{2}}\hat{a}_{\frac{1}{2}\frac{1}{2}}\right)\hat{P}^{A+2}. \tag{4.145}$$

As we are interested in a pair addition instead of a pair removal, the following relation is fulfilled instead

$$\hat{P}^{A+2}\left(\hat{a}^+_{\frac{1}{2}\frac{1}{2}}\hat{a}^+_{\frac{1}{2}\frac{1}{2}}\right) = \left(\hat{a}^+_{\frac{1}{2}\frac{1}{2}}\hat{a}^+_{\frac{1}{2}\frac{1}{2}}\right)\hat{P}^A. \tag{4.146}$$

Finally, Eq. (4.139) is reduced to

$$\langle\Psi|\hat{P}^A\left(\hat{a}_{\frac{1}{2}\frac{1}{2}}\hat{a}_{\frac{1}{2}\frac{1}{2}}\right)\hat{P}^{A+2}|\Psi\rangle = \langle\Psi|\left(\hat{a}_{\frac{1}{2}\frac{1}{2}}\hat{a}_{\frac{1}{2}\frac{1}{2}}\right)\left(\hat{P}^{A+2}\right)^2|\Psi\rangle = \langle\Psi|\left(\hat{a}_{\frac{1}{2}\frac{1}{2}}\hat{a}_{\frac{1}{2}\frac{1}{2}}\right)\hat{P}^{A+2}|\Psi\rangle, \tag{4.147}$$

where we have made use of the fact that $\hat{P}^A$ is an idempotent projector. Now we have everything to construct our deuteron transfer matrix element from Eq. (4.134)[6], combining equations we

[6]Note that Eq. (4.134) is not a probability, as its computation involves setting up a specific reaction.

obtain

$$P_d = C^{S+1,0}_{S01\mu}\sum_M(-1)^{-2M}C^{S+1,0}_{SM1-M}\langle\Psi_f|\hat{D}^+_{-M}\hat{P}^A\hat{P}^S_{M0}\hat{P}^T_{00}|\Psi_i\rangle, \tag{4.148}$$

and evaluating the former expression we come up to

$$\begin{aligned}P_d = &\frac{(2S+1)(2T+1)}{8\pi}C^{S+1,0}_{S01\mu}\sum_M(-1)^{-2M}C^{S+1,0}_{SM1-M}\sum_{\ell m\sigma_1\sigma_2\tau}C^{1-M}_{\frac{1}{2}\sigma_1\frac{1}{2}\sigma_2}\frac{(-1)^{\ell-m+\frac{1}{2}+\tau}}{\sqrt{2(2\ell+1)}}\\ &\times\int_0^{2\pi}d\varphi e^{-i\varphi A}\int_0^{\pi}d\beta_T\sin(\beta_T)\int_0^{\pi}d\beta_S\sin(\beta_S)d^S_{M0}(\beta_S)\mathcal{I}(\varphi,\beta_T,\beta_S)\kappa^{01*}_{kk'}(\varphi,\beta_T,\beta_S),\end{aligned} \tag{4.149}$$

with

$$\kappa^{01*}_{kk'}(\varphi,\beta_T,\beta_S) = \frac{\langle\Psi^L_{A+2,S+1,T}|\hat{a}^+_k\hat{a}^+_{k'}|\Psi^R_{A,S,T}(\varphi,\beta_T,\beta_S)\rangle}{\mathcal{I}(\varphi,\beta_T,\beta_S)}, \tag{4.150}$$

where

$$k \equiv \left\{l, m, \frac{1}{2}, \sigma_2, \frac{1}{2}, \tau\right\}, \tag{4.151}$$

$$k' \equiv \left\{l, -m, \frac{1}{2}, \sigma_1, \frac{1}{2}, -\tau\right\}. \tag{4.152}$$

$\mathcal{I}(\varphi,\beta_T,\beta_S) = \langle\Psi^L_{A+2,S+1,T}|\Psi^R_{A,S,T}(\varphi,\beta_T,\beta_S)\rangle$ is the overlap kernel between the rotated Thouless state with A,S,T quantum numbers and the unrotated Thouless state with $A+2,S+1,T$ quantum numbers.

To guarantee that the deuteron transfer matrix element is properly normalised, we need to rescale P_d as

$$P_d \to \frac{P_d}{\sqrt{I_{A+2,S=1,T=0}I_{A,S=0,T=0}}}, \tag{4.153}$$

where I_{AST} is the norm of the projected state $|AST\rangle$

$$\begin{aligned}I_{AST} = &\frac{1}{2\pi}\frac{2S+1}{2}\frac{2T+1}{2}\int_0^{2\pi}d\varphi e^{-iA\varphi}\int_0^{\pi}d\beta_S\sin(\beta_S)d^S_{00}(\beta_S)\int_0^{\pi}d\beta_T\sin(\beta_T)d^T_{00}(\beta_T)\\ &\times\langle\Psi^L_{AST}|\Psi^R_{AST}(\varphi,\beta_S,\beta_T)\rangle.\end{aligned} \tag{4.154}$$

We realise that combining expressions in Eqs. (4.134) and (4.149) is a specific application of the formula

$$\langle I_fM_fK_f|\hat{T}_{\lambda\mu}|I_iM_iK_i\rangle = C^{I_fM_f}_{I_iM_i\lambda\mu}\sum_{M\mu'}(-1)^{2\mu'}C^{I_fK_f}_{I_iM\lambda\mu'}\langle\Psi_f|\hat{T}_{\lambda\mu'}\hat{P}^{I_i}_{MK_i}|\Psi_i\rangle, \tag{4.155}$$

thus, we go further and compute the reduced matrix elements of the general tensor $\hat{T}_{\lambda\mu}$, which

will be independent of the orientation μ (in our case, the projection S_z). Using the Wigner-Eckhart theorem

$$\langle I_f M_f K_f|\hat{T}_{\lambda\mu}|I_i M_i K_i\rangle = (-1)^{2\lambda} C^{I_f M_f}_{I_i M_i \lambda\mu} \frac{\langle I_f K_f||\hat{T}_\lambda||I_i K_i\rangle}{\sqrt{2I_f+1}}, \tag{4.156}$$

where the phases $(-1)^{2\mu'}$ and $(-1)^{2\lambda}$ are equal to one as we deal with integer ranks. Combining equations we obtain

$$\langle I_f K_f||\hat{T}_\lambda||I_i K_i\rangle = \sqrt{2I_f+1}\sum_{M\mu'} C^{I_f K_f}_{I_i M \lambda\mu'} \langle\Psi_f|\hat{T}_{\lambda\mu'}\hat{P}^{I_i}_{MK_i}|\Psi_i\rangle, \tag{4.157}$$

which is exactly equation (4.155) apart from a factor $\sqrt{2I_f+1}/C^{I_f M_f}_{I_i M_i \lambda\mu}$. Therefore the reduced deuteron transfer matrix elements are evaluated as

$$\langle A+2, S+1, T||\hat{D}^+||A, S, T\rangle = \frac{\sqrt{2I_f+1}}{C^{I_f M_f}_{I_i M_i \lambda\mu}} P_d = \frac{\sqrt{2S+3}}{C^{S+1,0}_{S01\mu}} P_d, \tag{4.158}$$

to obtain the final expression

$$\langle A{+}2, S{+}1, T||\hat{D}^+||A, S, T\rangle = \sqrt{2S+3}\sum_M (-1)^{-2M} C^{S+1,0}_{SM1-M} \langle\Psi_f|\hat{D}^+_{-M}\hat{P}^A\hat{P}^S_{M0}\hat{P}^T_{00}|\Psi_i\rangle. \tag{4.159}$$

These reduced matrix elements are used in the evaluation of the probability of a pair transfer reaction, which we do not consider here.

4.8.2 Symmetry-restored alpha transfer matrix elements

We define the alpha transfer as

$$P_\alpha = \langle A+4ST|\hat{T}^+_\alpha|AST\rangle = \langle\Psi_L|\hat{P}^{A+4}\hat{P}^S\hat{P}^T\hat{T}^+_\alpha\hat{P}^A\hat{P}^S\hat{P}^T|\Psi_R\rangle, \tag{4.160}$$

where

$$\hat{T}^+_\alpha = (\hat{P}^+\hat{P}^+)^{00} + (\hat{D}^+\hat{D}^+)^{00}. \tag{4.161}$$

Since $\hat{T}^+_\alpha$ is a spherical tensor of rank zero, the alpha transfer is equal to

$$\langle A+4ST|\hat{T}^+_\alpha|AST\rangle = \langle\Psi_L|\hat{T}^+_\alpha\hat{P}^A\hat{P}^S\hat{P}^T|\Psi_R\rangle. \tag{4.162}$$

We proceed to evaluate the former expression. For the product of isoscalar pairs, we have

$$\begin{aligned}\langle\Psi_L|(\hat{D}^+\hat{D}^+)^{00}\hat{P}^A\hat{P}^S\hat{P}^T|\Psi_R\rangle &= \sum_{\mu\mu'} C^{00}_{1\mu1\mu'}\langle\Psi_L|\hat{D}^+_\mu\hat{D}^+_{\mu'}\hat{P}^A\hat{P}^S\hat{P}^T|\Psi_R\rangle \\ &= \sum_{ijkl\mu\mu'} C^{00}_{1\mu1\mu'}C^{00}_{lm_ilm_j}C^{00}_{\frac{1}{2}\tau_i\frac{1}{2}\tau_j}C^{1\mu}_{\frac{1}{2}\sigma_i\frac{1}{2}\sigma_j} \\ &\times C^{00}_{lm_klm_l}C^{00}_{\frac{1}{2}\tau_k\frac{1}{2}\tau_l}C^{1\mu}_{\frac{1}{2}\sigma_k\frac{1}{2}\sigma_l} \\ &\times \langle\Psi_L|\hat{a}^+_i\hat{a}^+_j\hat{a}^+_k\hat{a}^+_l\hat{P}^A\hat{P}^S\hat{P}^T|\Psi_R\rangle.\end{aligned} \tag{4.163}$$

The i label stands for the orbital angular momentum and projection, spin and isospin of the single-particle. Making use of the definition of the projectors

$$\begin{aligned}\langle\Psi_L|(\hat{D}^+\hat{D}^+)^{00}\hat{P}^A\hat{P}^S\hat{P}^T|\Psi_R\rangle &= \sum_{ijkl\mu\mu'} C^{00}_{1\mu1\mu'}C^{00}_{lm_ilm_j}C^{00}_{\frac{1}{2}\tau_i\frac{1}{2}\tau_j}C^{1\mu}_{\frac{1}{2}\sigma_i\frac{1}{2}\sigma_j} \\ &\times C^{00}_{lm_klm_l}C^{00}_{\frac{1}{2}\tau_k\frac{1}{2}\tau_l}C^{1\mu}_{\frac{1}{2}\sigma_k\frac{1}{2}\sigma_l}\frac{1}{2\pi}\frac{2S+1}{2}\frac{2T+1}{2} \\ &\times \int_0^{2\pi} d\varphi d\varphi e^{-i\varphi A}\int_0^{\pi} d\beta_T \sin(\beta_T) d^T_{00}(\beta_T) \\ &\times \int_0^{\pi} d\beta_S \sin(\beta_S) d^S_{00}(\beta_S)\langle\Psi_L|\hat{a}^+_i\hat{a}^+_j\hat{a}^+_k\hat{a}^+_l|\Psi_R(\varphi,\beta_T,\beta_S)\rangle.\end{aligned} \tag{4.164}$$

The evaluation of the matrix elements of the product of four single-particle operators can be easily done by means of Wick's theorem, the general result being

$$\langle\Psi|\hat{a}^+_i\hat{a}^+_j\hat{a}^+_k\hat{a}^+_l|\Psi\rangle = \kappa^*_{ij}\kappa^*_{kl} + \kappa^*_{il}\kappa^*_{jk} - \kappa^*_{ik}\kappa^*_{jl}. \tag{4.165}$$

Thus, defining the following quantity

$$\mathcal{K}^{0R}_{ijkl} = \kappa^{*0R}_{ij}\kappa^{*0R}_{kl} + \kappa^{*0R}_{il}\kappa^{*0R}_{jk} - \kappa^{*0R}_{ik}\kappa^{*0R}_{jl}, \tag{4.166}$$

we finally have

$$\begin{aligned}\langle\Psi_L|(\hat{D}^+\hat{D}^+)^{00}\hat{P}^A\hat{P}^S\hat{P}^T|\Psi_R\rangle &= \sum_{ijkl\mu\mu'} C^{00}_{1\mu1\mu'}C^{00}_{lm_ilm_j}C^{00}_{\frac{1}{2}\tau_i\frac{1}{2}\tau_j}C^{1\mu}_{\frac{1}{2}\sigma_i\frac{1}{2}\sigma_j} \\ &\times C^{00}_{lm_klm_l}C^{00}_{\frac{1}{2}\tau_k\frac{1}{2}\tau_l}C^{1\mu'}_{\frac{1}{2}\sigma_k\frac{1}{2}\sigma_l}\frac{1}{2\pi}\frac{2S+1}{2}\frac{2T+1}{2} \\ &\times \int_0^{2\pi} d\varphi d\varphi e^{-i\varphi A}\int_0^{\pi} d\beta_T \sin(\beta_T) d^T_{00}(\beta_T) \\ &\times \int_0^{\pi} d\beta_S \sin(\beta_S) d^S_{00}(\beta_S)\mathcal{I}^{0R}\mathcal{K}^{0R}_{ijkl}.\end{aligned} \tag{4.167}$$

The contribution from the isovector pairs is analogous

$$\begin{aligned}\langle\Psi_L|(\hat{P}^+\hat{P}^+)^{00}\hat{P}^A\hat{P}^S\hat{P}^T|\Psi_R\rangle = &\sum_{ijkl\nu\nu'} C^{00}_{1\nu1\nu'}C^{00}_{lm_ilm_j}C^{00}_{\frac{1}{2}\sigma_i\frac{1}{2}\sigma_j}C^{1\nu}_{\frac{1}{2}\tau_i\frac{1}{2}\tau_j}\\ &\times C^{00}_{lm_klm_l}C^{00}_{\frac{1}{2}\sigma_k\frac{1}{2}\sigma_l}C^{1\nu'}_{\frac{1}{2}\tau_k\frac{1}{2}\tau_l}\frac{1}{2\pi}\frac{2S+1}{2}\frac{2T+1}{2}\\ &\times\int_0^{2\pi}d\varphi d\varphi e^{-i\varphi A}\int_0^{\pi}d\beta_T\sin(\beta_T)d^T_{00}(\beta_T)\\ &\times\int_0^{\pi}d\beta_S\sin(\beta_S)d^S_{00}(\beta_S)\mathcal{I}^{0R}\mathcal{K}^{0R}_{ijkl},\end{aligned} \tag{4.168}$$

and the alpha particle transfer matrix element is

$$P_\alpha = \langle\Psi_L|(\hat{D}^+\hat{D}^+)^{00}\hat{P}^A\hat{P}^S\hat{P}^T|\Psi_R\rangle + \langle\Psi_L|(\hat{P}^+\hat{P}^+)^{00}\hat{P}^A\hat{P}^S\hat{P}^T|\Psi_R\rangle. \tag{4.169}$$

We observe at light of these calculations that the simplistic $SO(8)$ model is a powerful tool that allows us to compute exactly deuteron and alpha particle transfers. These results may be used in the future to inspect the origins of pairing, if it comes from the coupling of pairs or quarters. We refer to Section 5.4 for more details about this aspect.

Chapter 5

Results

In this Chapter, we present and comment results for the different theoretical tools reviewed in the former Chapters with the goal of the pairing coexistence description, as it is our main motivation from the beginning. The exact solution given by the $SO(8)$ algebraic model Hamiltonian described in Section 2 will be used as a benchmark.

We start with results from a mean-field HFB calculation, where symmetries are spontaneously broken in the intrinsic state, and continue with symmetry restoration techniques using the VAP framework, which this Chapter is really focused on. We finish the Chapter with a comment on the implementation of the realistic separable interaction reviewed in Section 6.1.

5.1 HFB results

When using the $SO(8)$ pure pairing Hamiltonian, as it does not include any single-particle interaction that splits the levels, a HFB calculation is reduced to the BCS picture, generalised now for the case where protons and neutrons are mixed in the transformation (3.30) [Bes00]. Firstly, as mentioned in Section 3.3, the single-particle density ρ and pairing tensor κ will have a diagonal and antidiagonal structure, respectively, as in Eqs. (3.48, 3.49), because the solutions are in the canonical basis. Secondly, we notice in the implementation of the matrices needed for the HFB algorithm that the Hamiltonian (2.17) has spherical symmetry, as the pairs are coupled to total angular momentum $L = 0$. Thus, both the densities and the fields matrices will render a periodic block structure of identical 4×4 matrices, corresponding to the spin and

isospin degrees of freedom considered in the model,

$$h = \begin{pmatrix} \mathcal{H} & 0 & \cdots & 0 \\ 0 & \mathcal{H} & \cdots & 0 \\ \vdots & \vdots & \ddots & \vdots \\ 0 & 0 & \cdots & \mathcal{H} \end{pmatrix}, \quad \Delta = \begin{pmatrix} 0 & \cdots & 0 & \mathcal{D} \\ \vdots & \ddots & -\mathcal{D} & 0 \\ 0 & \iddots & \ddots & \vdots \\ -\mathcal{D} & 0 & \cdots & 0 \end{pmatrix}, \tag{5.1}$$

where there is a phase factor of the form $(-1)^{\ell-m}$ in the structure of the Δ matrix as a consequence of time-reversal invariance. Thus, for the purposes of diagonalisation and evaluation of the field matrices, only the computation of the 4×4 matrices $\mathcal{H}$ and $\mathcal{D}$ is necessary.

Analytical results for this *generalised BCS* treatment have been obtained in [Bes00] and are summarised in Table (5.1). In the HFB picture, while working self-consistently with the single-particle and pairing fields, it is possible to separate contributions to the total energy coming from the mean field and from the pairing field as

$$E_{HF} = \frac{1}{2}\,\mathrm{Tr}(h\rho), \tag{5.2}$$

$$E_{\mathrm{pair}} = -\frac{1}{2}\,\mathrm{Tr}(\Delta\kappa^*). \tag{5.3}$$

Notice that, compared to the standard form given in Eq. (3.46), in the $SO(8)$ model Hamiltonian we do not consider any one-body kinetic energy contribution as previously stated.

		Isovector	Isoscalar
Isovector	Δ_1	$\frac{1}{2}g(1-x)\Omega\sqrt{1-\eta^2}$	0
Isoscalar	Δ_0	0	$\frac{1}{\sqrt{2}}g(1+x)\Omega\sqrt{1-\eta^2}$
Quasiparticle energy	E_{qs}	$\frac{1}{2}g(1-x)\Omega$	$\frac{1}{2}g(1+x)\Omega$
Single-particle energy	ϵ	$-\eta E_{qs}$	$-\eta E_{qs}$
HFB energy	E_{pair}	$-\frac{1}{2}g(1-x)\Omega^2(1-\eta^2)$	$\frac{1}{2}g(1+x)\Omega(1-\eta^2)$

Table 5.1: Isovector (first row) and isoscalar (second row) gaps and quasiparticle (third row), single-particle, or eigenvalues of the HF field (fourth row), and total HFB (fifth row) energies analytical expressions from [Bes00], where $\eta = \frac{Z}{\Omega} - 1$. The first column shows results when the isovector interaction in the pairing Hamiltonian is dominant ($x < 0$) and the second column shows results when the isoscalar interaction is dominant ($x > 0$).

The results from the generalised BCS formalism were an important benchmark to test our implementation of the HFB method including isospin mixing in the Bogoliubov transformation,

which was completely successful with differences of the order of machine precision. Our HFB calculations were run with just the usual constraint on the average value of particle number A, using a Lagrange multiplier with ALM and average values of spin and isospin equal to zero, for which the corresponding Lagrange parameters are zero as well. In Fig. (5.1) we plot the trend followed by the pairing energy as a function of the mixing parameter x as in the fourth row of Table (5.1). The energy is symmetric under the exchange $x \longrightarrow -x$, which is obvious

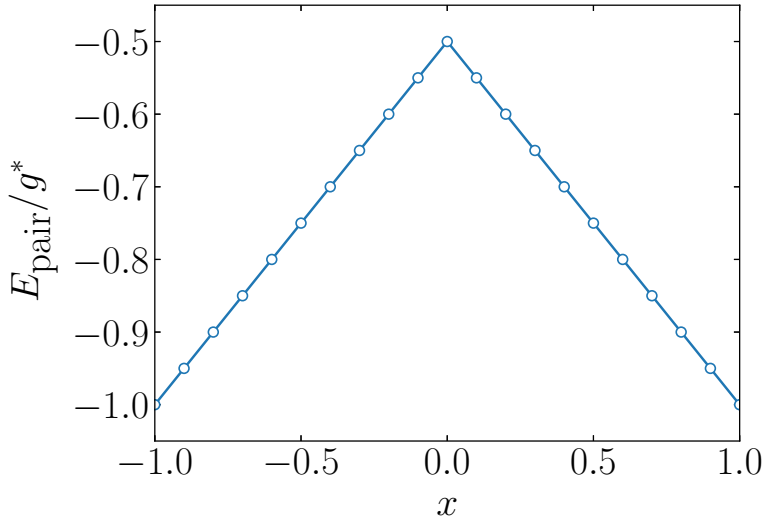

Figure 5.1: Pairing energy E_{pair} as a function of the mixing parameter x according to the analytical formula in Table (5.1), where $g^* = g\Omega^2(1-\eta^2)$. The trend of the pairing energy is dictated by $(1 \pm x)$ terms.

from the fact that it is computed for a system with equal values of spin and isospin and the pairing Hamiltonian (2.17) is again symmetric under that exchange when we exchange the spin S and isospin T numbers as well. It is seen that the trend is completely dictated by the terms $(1 \pm x)$, suggesting that the contributions from the isoscalar and isovector pairs, that is, the terms $\langle\Psi|\hat{D}^+\hat{D}^+|\Psi\rangle$ and $\langle\Psi|\hat{P}^+\hat{P}^+|\Psi\rangle$, where $|\Psi\rangle$ is the optimal quasiparticle vacuum, are mere constants for all possible interactions. In Fig. (5.2) we plot the same pairing energy now as a function of the number of particles occupying the shells, for different values of the interaction parameter x and for a system with total degeneracy of $4\Omega = 48$. We see that it follows a symmetric parabola centred at the middle of the shell, where the contribution to the pairing energy is peaked, for any value of x, recalling the symmetry under $x \longrightarrow -x$ exchange. This parabolic symmetric behaviour is a consequence of the total number of correlated pairs that is found in such a system, which is a combination of the particles allocated and the possible states that they could occupy, referred as holes. As the sum of particles and holes is constant, an

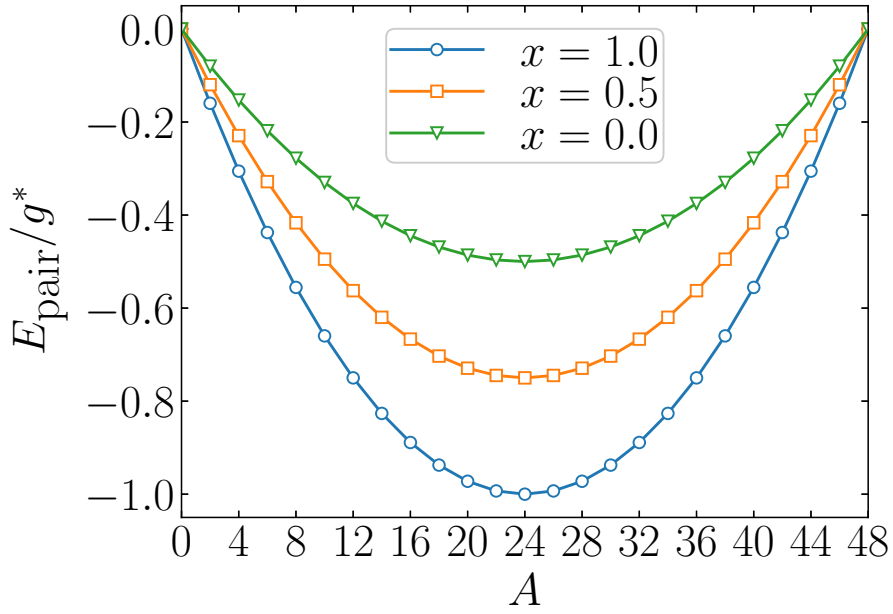

Figure 5.2: Pairing energy E_{pair} as a function of the number of particles A according to the analytical formula in Table (5.1), where $g^* = g\Omega^2$. It is observed that the trend follows a bell-shaped curve, reaching the maximum contribution to the energy in the half-occupied shell ($A = 24$), where pairing correlations are expected to contribute most.

exchange of these results in the same contribution to the pairing energy, therefore displaying this symmetry around the half-occupied shell. We notice again from Table (5.1) that the quasiparticle energies E_{qs} and subsequently the single-particle energies, that is, the eigenvalues of the HF field h, do not depend on the number of particles in the shells but only on the total size of the configuration space, related to Ω. It is a consequence of the complete degeneracy of the shells, as no one-body terms are included in the Hamiltonian (2.17), and its only contribution is coming from the pairing interaction, which is a constant of strength g. Thus, the HF field h is a diagonal matrix whose entries are all ϵ. Obviously, the parabolic symmetry in Fig. (5.2) is manifested only when all the states in the shells are degenerate, thus the probability of a particle occupying any state is constant, that is, there is no preferred configuration of particles which gives a lower energy.

After we have guaranteed that all the results and features of the HFB method were properly benchmarked, we compare them to the generalised BCS model and the exact results provided by the $SO(8)$ model, namely, the lowest eigenvalues of the pairing Hamiltonian (2.17) in Fig. (5.3). It is observed that the total HFB and generalised BCS formalisms reproduce trends of the exact results, with the HFB results being closer, as it does not neglect the HF field h, which is responsible for the shift towards the exact results. However, for this simplistic case of a single-ℓ

shell, they are not similar to these exact results predicted by the $SO(8)$ model.

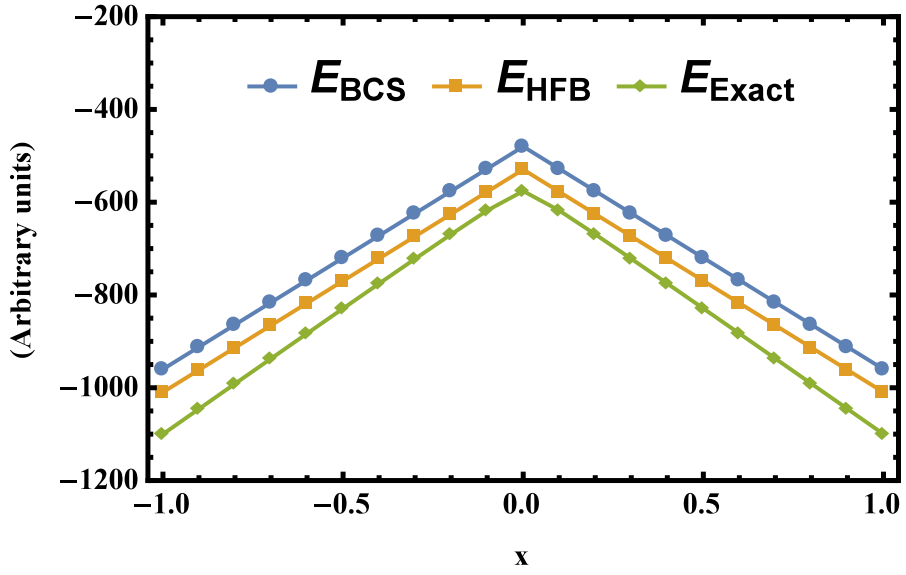

Figure 5.3: Pairing energy E_{BCS}, computed using formula (5.3), total HFB energy E_{HFB}, computed using formula (3.46) and the exact energy result, in arbitrary units, as a function of the mixing parameter x of the pairing Hamiltonian (2.17) for a single-ℓ shell with $\ell = 12$ and $A = 24$ particles and spin and isospin $S = T = 0$. We observe how the mean-field results are not close to the exact values. Figure extracted from [MDP17].

5.1.1 Pairing gaps

The main goal in this project is the description of coexistence between isoscalar and isovector pairing couplings. Pairing gaps are very interesting quantities to analyse, as they provide indirect measurements of the presence of isoscalar and isovector pairs. In Fig. (5.4), the pairing gaps resulting from the HFB calculations are plotted as functions of the interaction parameter x, following the expressions given in the first two rows of Table (5.1), and they were computed in our implementation using the following formulas

$$\Delta_q = -g(1-x)\sum_w u_{qw}v_{qw}, \tag{5.4}$$

$$\Delta_0 = -\frac{g(1+x)}{\sqrt{2}}\sum_w (u_{pw}v_{nw} + u_{nv}v_{pv}), \tag{5.5}$$

where q stands for protons p and neutrons n and w runs for all quasiparticle eigenstates U, V of the diagonalised HFB supermatrix as in (3.45). As we do not make any difference between

protons and neutrons at the moment, the isovector pairing gaps are equal, $\Delta_n = \Delta_p = \Delta_1$. These formulas were extracted from [Bes00].

In Fig. (5.4) we observe that, for a specific number of particles, the gaps follow a linear trend given by $\pm x$, indicating that coexistence is not allowed in this model by means of just a mean-field HFB method, and suddenly they drop to zero when the dominant interaction in the pairing Hamiltonian changes from isoscalar to isovector. Only around $x = 0$, where both interactions are similar in strength in the Hamiltonian, both pairing couplings can coexist. The difference in the values of the isoscalar and isovector gaps comes from the different definitions used in [Bes00], where a factor of $\sqrt{2}$ is inserted in the isoscalar gap in Eq. (5.4). Apart from this factor, the gaps are symmetrical under the exchange $x \longrightarrow -x$, as expected to be since the average values of the spin and isospin of the system are zero, indicating a similar behaviour for the isoscalar and isovector couplings. To summarise, this sharp phase transition in the pairing gaps resulting from a HFB calculation does not correspond to the physical picture we should expect from the pair condensation behaviour.

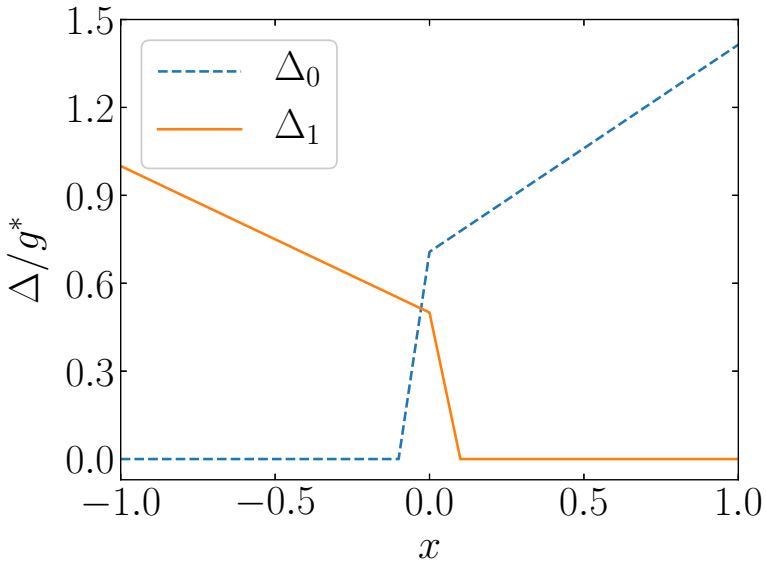

Figure 5.4: Isoscalar and isovector pairing gaps Δ as a function of the mixing parameter x according to the analytical formulas in Table (5.1), where $g^* = g\Omega\sqrt{1-\eta^2}$. They are an indirect measure of the presence of isoscalar and isovector pairs in the system.

We therefore conclude that the HFB approximation is an unsatisfactory approximation to the description of the states of the pairing Hamiltonian and the problem of pairing coexistence in general.

5.1.2 Isocranking and number of pairs

The HFB results from the last Section were performed imposing only a constraint on the average number of particles using ALM. After we tested our HFB implementation of the $SO(8)$ pairing Hamiltonian with analytical results given in [Bes00], our aim is to implement the isocranking technology to control the isospin degree of freedom. The Routhian is changed as in Eq. (3.59) and we fix the Lagrange parameters constraining average values of the first and third component of the isospin as in Eq. (3.61). We perform isorotations in the $T_x - T_z$ plane in isospace by changing θ from 0 to π, being then able to study the entire multiplet of isobaric analog states [MDP17]. The radius λ_0 was obtained fixing the proton and neutron average numbers, giving a $z-$isoaligned state of $\langle \hat{T}_z \rangle|_{\theta=0}= 15$. Results from this calculation are shown in Fig. (5.5). We see that the average values of these components of the isospin are parallel to the $\boldsymbol{\lambda}$ isovector, as it was concluded from [Sat13], because the Hamiltonian (2.17) does not include any isospin breaking term. The proton-neutron mixing is effectively implemented within this method for all values of the isocranking angle $0 < \theta < \pi$, being a pure neutron or proton state for $\theta = 0, \pi$, respectively, and becoming fully mixed for $\theta = \frac{\pi}{2}$, as seen in the trend of $\langle \hat{T}_x \rangle$ in Fig. (5.5). These results are in complete agreements with those shown in [She14]. We are also interested

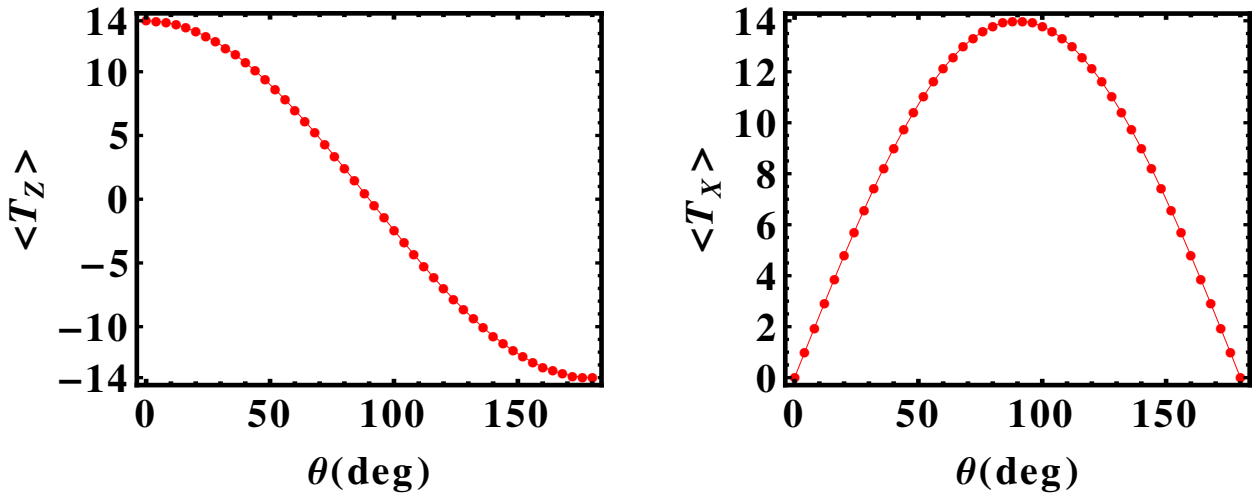

Figure 5.5: Average values of the first and third components of the isospin, in units of the Planck constant $\hbar$. We see that they follow the same trend as the chosen Lagrange parametrisation in (3.61). Figure extracted from [MDP17].

in the behaviour of the pairs when the average projection of the isospin T_z is different from zero, that is, there is an imbalance between protons and neutrons. The number of pairs can be investigated using the pair operators $\hat{P}^+$ and $\hat{D}^+$ [Dob97; ELV96] from the pairing model

Hamiltonian, computing the quantities $\langle\Psi|\hat{P}^{+}\hat{P}|\Psi\rangle$ and $\langle\Psi|\hat{D}^{+}\hat{D}|\Psi\rangle$ and normalising them to unity. Expressions for the matrix elements of two-body operators were derived in general terms of the density ρ and pairing tensor κ in Appendix B, resulting for this case of degenerate $\ell-$shells in a combination of elements from κ. As we see in Fig. (5.6), where we plot these measures, the HFB plus ALM method allows coexistence for an extended region around $x = 0$ on the isoscalar side. It also follows a smooth curve rapidly, but not sharply, converging to constant values, contrary to the results shown in Fig. (5.4), being the isovector pairs more present in the isoscalar region. On the isovector side of the plot, no difference is shown with respect to the $T_z = 0$ case. The asymmetric behaviour of pairs is due to the nonzero value of the average value of $\hat{T}_z$, and increases with larger values of this quantity. Neither the isoscalar nor the isovector pairs go to zero when x approaches the value of full isoscalar or isovector contribution in the pairing Hamiltonian because of the chosen normalisation of the pairs. Making a direct comparison of the gaps in Fig. (5.6) with the pairs in Fig. (5.4), we conclude that the ratio from both measures yields a $(1 \pm x)$ factor.

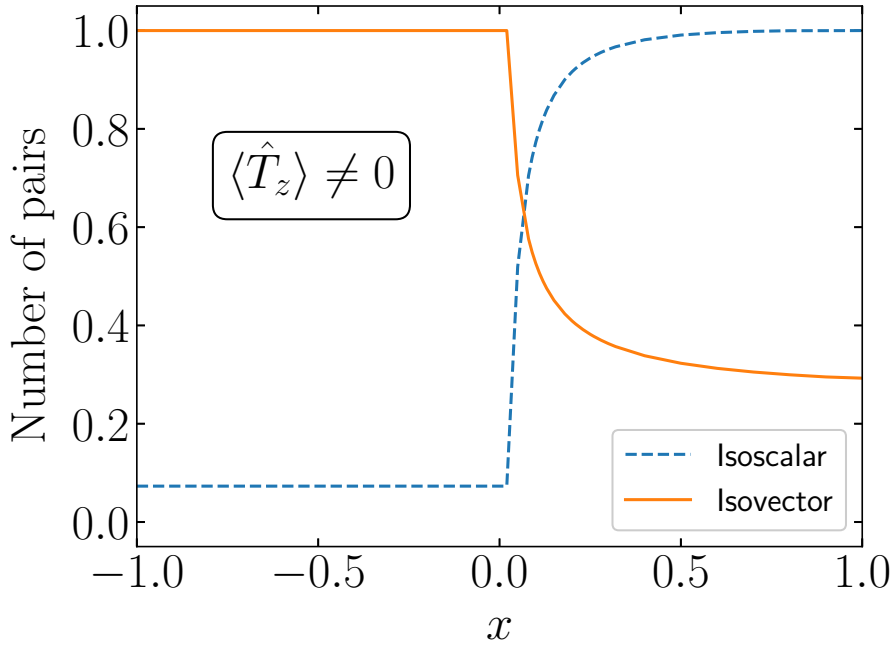

Figure 5.6: Number of pairs computed using a HFB calculation plus a constraint on the third component of the isospin $\hat{T}_z$ to have a proton-neutron imbalance in the system. Isovector pairs have more presence in the isoscalar region of the interaction $x > 0$, not suddenly dropping to zero in a sharp phase transition.

While the results including constraints on the isospin in the HFB picture improve considerably, coexistence between isoscalar and isovector pairs is still not shown for all possible values

of the mixing parameter x. For this reason, we need to go beyond mean-field and remove the fluctuations caused by using a quasiparticle vacuum which mixes different states, by means of symmetry restoration with projection methods.

5.2 Symmetry restoration

In this Section, we will discuss the results obtained after we restore the symmetries broken by the intrinsic HFB state. We have seen in Section 4.5 that two methods can be implemented to restore these symmetries, namely, VAP and PAV, concluding that the former will always yield better results, being closer upper bounds to the energies of the exact state. In the following, we will only be concerned about VAP calculations and results, making a comment on Section 5.3 about the accuracy of the PAV method.

5.2.1 Energy manifold

Because of the symmetry considerations given in Section 2.2 and exploited in Section 4.4.1, we will only work with *axial* Thouless states parametrised by expressions (3.58). The parametrisation is compact, that is, $(\alpha, \varphi) \in [0, \pi]$, then it is possible to plot the whole energy manifold in this domain region, the average of the $SO(8)$ pairing Hamiltonian (2.17) with respect to the projected states $|AST\rangle$ as a function of these parameters and find its minimum using, in this case, the gradient method. We evaluate the quantity

$$\frac{\langle \Psi | \hat{H} | AST \rangle}{\langle \Psi | AST \rangle}, \tag{5.6}$$

for all α, φ considered. The minimum of this energy manifold is then found, as sketched in Eq. (4.101).

We show these results in Fig. (5.7), where we also compare the VAP results with the results obtained from the mean-field HFB method, without symmetry restoration, for several values of the mixing parameter x spanning from -1 to 1.

Firstly, we notice the periodicity of the energy manifold with respect to the parameter φ with period $\frac{\pi}{2}$. This is a fingerprint of the invariance of the pairing Hamiltonian (2.17) with respect to the spin and isospin signatures. Indeed, as the intrinsic Thouless state does not break these symmetries, the energies will be periodic as a consequence of the transformation relation of the Thouless pairs as in Eq. (4.34).

Secondly, we notice that, disregarding the periodicity of the energies, the position of the

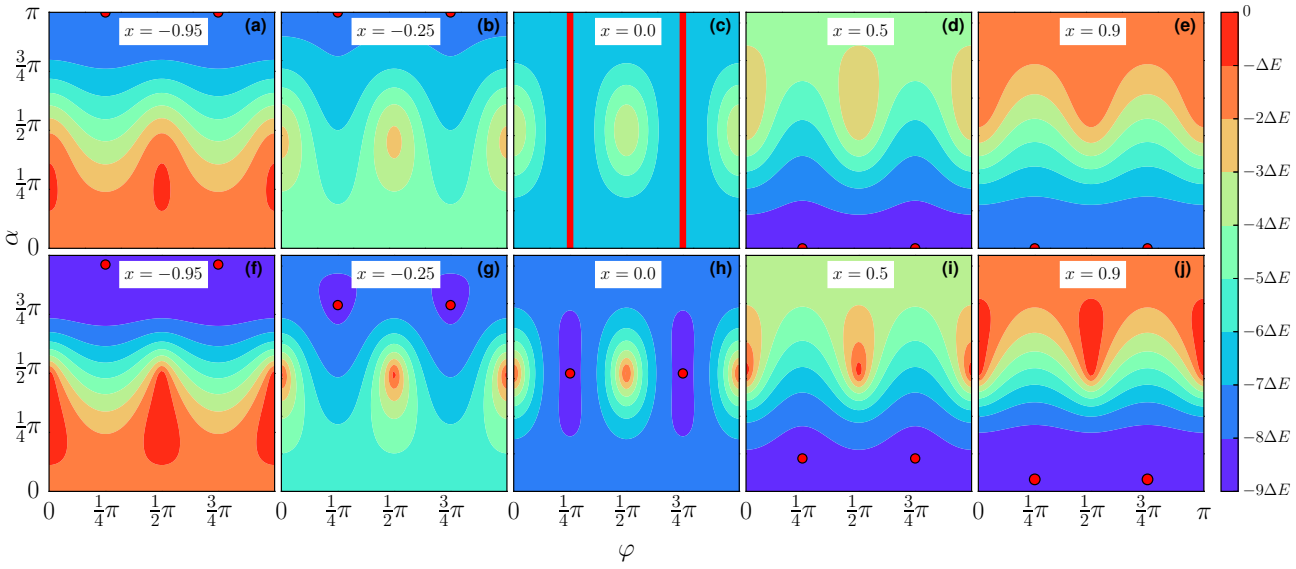

Figure 5.7: Energy surface as a function of α (relative amplitude) and φ (relative phase) from Eqs. (3.58) for different values of x computed using the HFB method (upper panels) and VAP method (lower panels) for a system with $A = 24$ particles and spin and isospin $S = T = 0$ and spatial degeneracy $\Omega = 12$ (total degeneracy being 4Ω). From left to right panel, the colour bands correspond to steps of $\Delta E = 20, 15, 13, 17$ and 20, respectively. The minima of the different surfaces are plotted within by red dots (bands). All results are in units of g. Figure taken from [RDP19b].

minima is always at $\varphi = \frac{\pi}{4}$. This is the fingerprint of time-reversal symmetry, as expected since the system is fully paired and the pairing Hamiltonian is time-reversal invariant. It is a consequence of the transformation of the Thouless pair under time reversal, as in Eq. (4.39), where it is easily seen that it will be invariant for $\varphi = \frac{\pi}{4}$.

Again, these energy manifolds are symmetric with respect to the exchange $x \longrightarrow -x$, transforming the parameter $\alpha \longrightarrow \alpha + \pi$, as they were computed for a system with the number of particles $A = 24$ and spin and isospin $S = T = 0$.

Let's focus on the position of the minima with respect to the angle α, shown in the plot by red dots and bands. We see that for the HFB calculations (top row panels), there are only two possible cases for the position of these minima: either we have $\alpha = \pi$ when $x < 0$ in panels (a) and (b), or $\alpha = 0$ when $x > 0$ in panels (d) and (e), with a sharp transition at $x = 0$ in panel (c), where any value of α is possible. According to Eqs. (3.58), for $\alpha = 0$ we get $p_0 = 0$ and $d_0 = 1$, thus a pure condensation of isoscalar pairs is present in the system, and for $\alpha = \pi$, we get $p_0 = 1$ and $d_0 = 0$, thus a pure condensation of isovector pairs is present in the system. That is, under the HFB mechanism, only isoscalar or isovector condensation is allowed in the system and coexistence between these two pairing couplings is not possible apart from a very

small region around $x = 0$, where it could mix as it pleases. These results are in agreement with the HFB results we found in Section 5.1.1.

However, for the VAP results (bottom row panels), projecting onto states of good particle-number, spin and isospin, the picture changes completely. Now the position of the minima with respect to the mixing angle α varies smoothly for different values of x, decreasing from π to 0 as x increases meaning that isovector pairing gains more importance but coexistence is shown for all values of x, as physically expected from this model. Specifically, for $x = 0$, shown in panel (h), the minimum at $\alpha = \frac{\pi}{2}$ indicates an equal presence of isoscalar and isovector pairs in the system according to the parametrisation in Eq. (3.58), as predicted from the $SO(8)$ pairing Hamiltonian since the isoscalar and isovector contributions are equal in strength. In view of these results, we conclude that the existence of a proton-neutron condensate in the self-consistent mean-field picture relies upon the full mixing and proper restoration of the broken symmetries in the intrinsic HFB quasiparticle vacuum state, which is the norm in mean-field calculations.

5.2.2 Energy, accuracy, pairing coexistence and deuteron transfer

We generalise the results obtained in the former section for all values of particle-number, spin and isospin, in order to analyse the behaviour of the coexistence between isoscalar and isovector pairs. We have in mind the powerful versatility of the $SO(8)$ model and the mean-field description, which allows us to compute important observables such as the deuteron transfer. All these results are summarised in Fig. (5.8), where we plot the ground-state energies resulting from the minimization of the energy manifold built using Eq. (5.6) and the exact energies corresponding to the lowest eigenvalue of the pairing Hamiltonian in panels (a) and (b) and their relative differences are plotted in panels (c) and (d).

The isoscalar norm of the Thouless pairs, that is, the quantity $|d_0|^2$ from the parametrisation used in (3.58), where obviously the isovector norm will be given by $|p_0|^2 = 1 - |d_0|^2$, is plotted in panels (e) and (f), and the deuteron transfer matrix elements, as calculated in Eqs. (4.159) and (A.13), is plotted in panels (g) and (h). The different plots in the grid correspond to several values of particle-number and isospin in a system with spatial degeneracy $\Omega = 12$, being the total degeneracy $4\Omega = 48$. The results were computed using the VAP symmetry restoration method, denoted by symbols, and where applicable they are compared to the exact results, denoted by solid lines. As the pair norm in the Thouless state is not an observable, the exact model can not calculate it, and we rely upon the match of the rest of observables as the assurance of the correctness for these results.

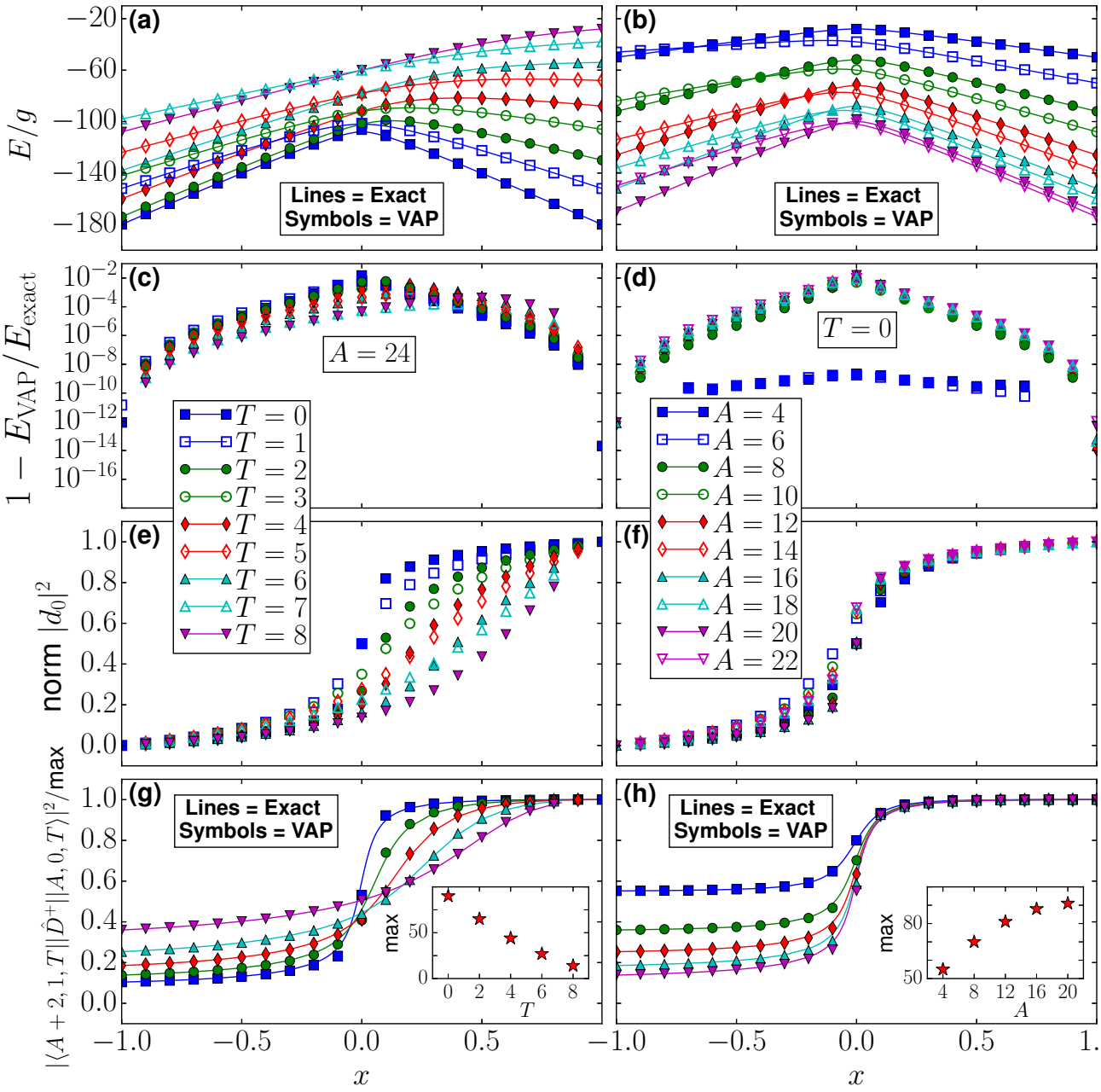

Figure 5.8: Energies, in units of g (First row), relative errors in comparison to the exact results shown in logarithmic scale (second row), norm of the isoscalar Thouless pair from Eq. (3.58) (third row), and deuteron transfer matrix elements (fourth row) computed using VAP method, for different values of isospin (left column) and particle-number (right column). Figure taken from [RDP19b].

Because of the total degeneracy of the shells, the panels in Fig. (5.8) are symmetrical with respect to the exchange of particles and holes, thus results are only shown up to mid-shell occupation. The panels are also symmetrical under the exchange of spin and isospin quantum

numbers, transforming the mixing parameter as $x \longrightarrow -x$ and the mixing angle in Eq. (3.58) as $\alpha \longrightarrow \alpha + \pi$. Therefore, all the information varying particle-number, spin and isospin is contained in the figure, exploiting the symmetries of the system.

We observe that there is a remarkable accuracy for the energy computed using the VAP method (E_{VAP} in the figures) and the exact ones in panels (a) and (b). We recall that this kind of precision was not met at all by the results from the HFB method shown in Fig. (5.3).

In fact, only by plotting the relative differences between the VAP energies E_{VAP} and the exact ones we are able to notice the disagreement, with maximum errors of around 2% for $x \sim 0$, as shown in panels (c) and (d). When x heads towards ± 1, that is, towards a pure isovector or isoscalar interaction, the differences decrease significantly to the point of just noise around the machine precision. The trend followed by these differences is indicative of missing correlations in the wavefunction and this aspect will be discussed in more detail in Section 5.4.

We see in panels (e) and (f) that there is always pairing coexistence for all values of particle-number, spin and isospin, but the isoscalar norm starts to decrease when increasing the isospin of the system, as expected, since we know it starts fading off when there is a large proton-neutron difference. Still, it does not vanish as quickly as we may have previously thought, although we can not extrapolate these conclusions to the case of finite real nuclei as important ingredients such as the spin-orbit interaction are not taken into account in the $SO(8)$ model.

The deuteron transfer, the potential link between theory and experiment for the microscopic description of proton-neutron condensates, is reproduced remarkably well within the VAP method, as we see in the comparison with the exact results in panels (g) and (h), where the results are normalised to one by dividing with respect to the maximum amplitude value obtained, which is plotted as well in the correspondent inset figure. As expected, this maximum amplitude decreases and increases for larger values of the isospin and particle-number, respectively. It is interesting to notice, in panel (h), how they all converge to one in the isoscalar region ($x > 0$), while you can distinguish different amplitudes in the isovector region ($x < 0$) as a result of the different spin in the initial and final states. In addition, we observe that at $x = -1$, when the contribution in the pairing Hamiltonian is purely isovector, while the deuteron transfer is very small, it is not actually zero. The system allows a deuteron to be added even when it is only composed of isovector pairs.

At last, we also notice that the selection rules provided by the signature analysis of the Thouless pairs in Section 4.7.1 hold, as the total spin in the left column panels is $S = 0$ for the full symbols and $S = 1$ for the empty symbols, in order to make $S + T$ even, as the number of pairs in a system with number of particles $A = 24$ is even. A similar convention is used in the right column panels, where now we fix $T = 0$ and we vary A. If we do not take these

considerations into account, the numerical implementation of this method will fail to find a solution, as it does not exist, as discussed in Section 4.7.1.

5.2.3 Pairing gaps

While we have evaluated the coexistence between isoscalar and isovector pairs using the norms parametrised by Eqs. (3.58), it could also be measured using the pairing gaps, which are quantities that can be measured experimentally. The isovector Δ_1 (proton Δ_p and neutron Δ_n, being equal in strength) and isoscalar Δ_0 pairing gaps can be directly extracted from the pairing field matrix. Denoting them by $\Delta_{\sigma,\tau;\sigma',\tau'}$, the expressions for the isovector and isoscalar gaps are

$$\begin{aligned}
\Delta_p &= \frac{1}{2}\sum_{\sigma=\pm\frac{1}{2}} (-1)^{1+2\sigma}\Delta_{\sigma,-\frac{1}{2};-\sigma,-\frac{1}{2}}, \\
\Delta_n &= \frac{1}{2}\sum_{\sigma=\pm\frac{1}{2}} (-1)^{1+2\sigma}\Delta_{\sigma,\frac{1}{2};-\sigma,\frac{1}{2}}, \\
\Delta_0 &= \frac{1}{2}\sum_{\tau=\pm\frac{1}{2}} (-1)^{1+2\tau}\Delta_{\frac{1}{2},\tau;\frac{1}{2},-\tau}.
\end{aligned} \tag{5.7}$$

The phase factor $(-1)^{1+2\sigma}$ is necessary to take into consideration that the pairing field is anti-symmetric under exchange of spin indices (and, equivalently, for the isospin indices). Observing Fig. (5.9), we come to the same conclusions as in the former section. The isoscalar and isovector gaps computed using the HFB method follow a straight line given by the interaction terms $(1 \pm x)$ and abruptly jumping at $x = 0$, meaning that coexistence between the two pairing couplings is not possible, only a pure isovector or isoscalar condensates builds up the nucleus. On the contrary, the isoscalar and isovector gaps computed with the VAP method follow a smooth trend that coexists for all different interactions and matches with the HFB results when $x = \pm 1$. In Fig. (5.10), the isoscalar and isovector gaps are plotted for different values of the total isospin T of the system, observing that the isoscalar gap starts to decrease when the isospin is larger, in agreement with panel (e) of Fig. (5.8), in the isoscalar region, $x > 0$, where we clearly distinguish three different lines.

5.3 Projection after variation

So far, we have only plotted results obtained from the variation after projection approach to go beyond-mean-field and restore the broken symmetries. As mentioned in Section 4.5, this is

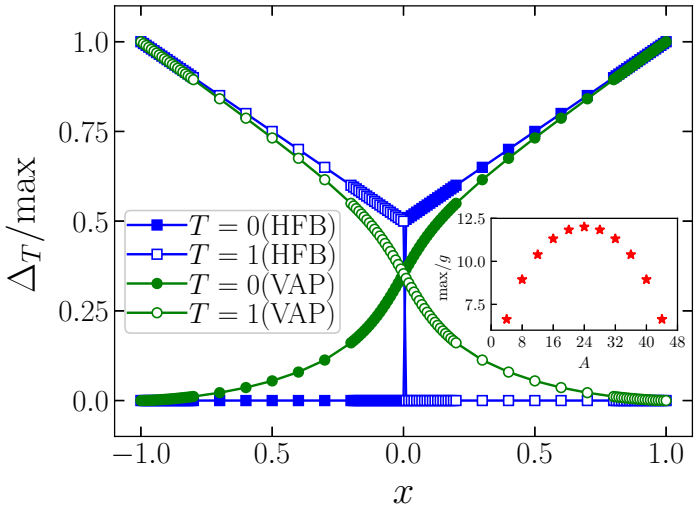

Figure 5.9: Isoscalar Δ_0 (full symbols) and isovector Δ_1 (open symbols) pairing gaps, rescaled by $\Delta_0(x = 1)$, computed using a mean-field HFB (squares) and a VAP (circles) calculation for a system with $A = 24$ particles (half-occupied shell) with spin and isospin equal to zero. Isoscalar (isovector) gaps suddenly drops to zero at $x = 0$ when the interaction is isovector (isoscalar) stronger for the HFB method, while the pairing gaps computed for the VAP method follow a smooth curve, showing coexistence for all x.

the method that will yield the best results, but due to the numerical intensive evaluations of the integrals of projectors (4.59), it is not the most used method to go beyond-mean-field. In this Section, we make a brief comment about the accuracy and validity of the PAV approach to the problem of pairing coexistence and the exact solution of the $SO(8)$ Hamiltonian.

We recall that PAV only applies the projectors in Eq. (4.59) at one point only, namely the minimum computed using a mean-field HFB method. Therefore the position of the minimum in the energy manifold spanned by parameters (3.58) will not be changed by the application of the projectors to this point, in opposition to the VAP mechanism, where it is applied for every point considered before reaching the minimum. Consequently, as well as the HFB method, PAV fails to reproduce the coexistence between isoscalar and isovector pairing couplings.

The improvement of the PAV method with respect to the HFB method over the results is reflected in the magnitude of the observables computed with the projected wavefunction at the HFB minimum. In Fig. (5.11), we plot the energies as a function of the mixing parameter x of the pairing Hamiltonian (2.17) for the three different methods that we have discussed so far. We see that, while PAV does a better job in getting closer to the exact results, it fails to reproduce the smooth curve at $x \sim 0$ and shows the sharp peak also present in the HFB result. From this perspective, the HFB and PAV methods only differ in a constant shift of the absolute

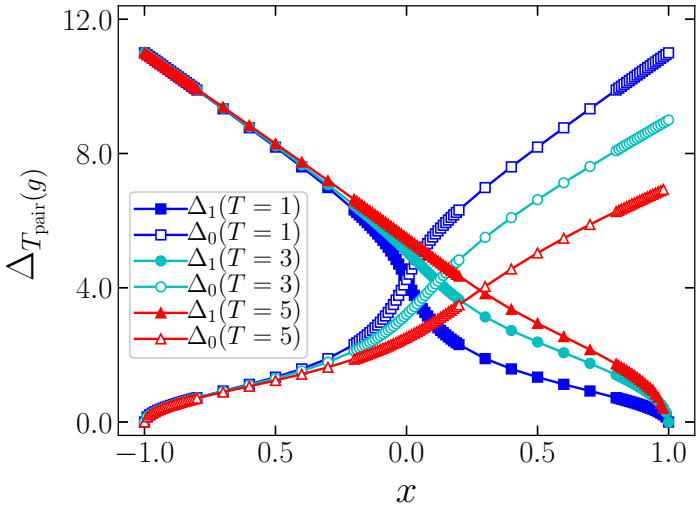

Figure 5.10: Isoscalar Δ_0 (full symbols) and isovector Δ_1 (open symbols) pairing gaps, computed using the VAP method, for a system with $A = 24$ particles, spin $S = 1$ and isospin $T = 1$ (squares), $T = 3$ (circles) and $T = 5$ (triangles). As the isospin increases, the point where $\Delta_0 = \Delta_1$ is shifted towards the isoscalar side, and Δ_0 gets weaker.

values, as the trend followed by the results is identical. However, at the limits of pure isoscalar or isovector pairing, that is, at around $x = \pm 1$, the PAV method is successful in describing the ground-state energy of the exact states.

There is another underlying problem with PAV calculations. It was said already that a mean-field calculation of the many-body wavefunction of the system will result on a pure condensation of isoscalar or isovector pairs, with a sharp transition from one to another if the interaction has a slightly stronger isovector contribution than isoscalar, around $x = 0$. Due to this feature, it is not possible to apply the PAV method for the restoration of broken symmetries in the cases where $S, T \neq 0$ for all values x of the interaction.

Physically, the interpretation is simple: if the wavefunction is written as a condensation of isovector pairs of spin zero, the only possible total spin coupling of the system has to be zero. It is not possible to project to a state of total spin one because it is not part of the intrinsic wavefunction.

Mathematically, we prove it using the form of the Thouless parametrised wavefunction and the projectors: if the wavefunction is composed of a condensation of isovector pairs, the only nonvanishing parameter of the wavefunction is $Z^{ST} = Z^{01}$. Since $S = 0$, this wavefunction will be invariant under rotations in spin space and therefore the overlap kernel will be

$$I = \frac{2S+1}{2} \int_0^\pi \sin\beta d^S_{00}(\beta)\mathcal{I}(\beta)d\beta, \tag{5.8}$$

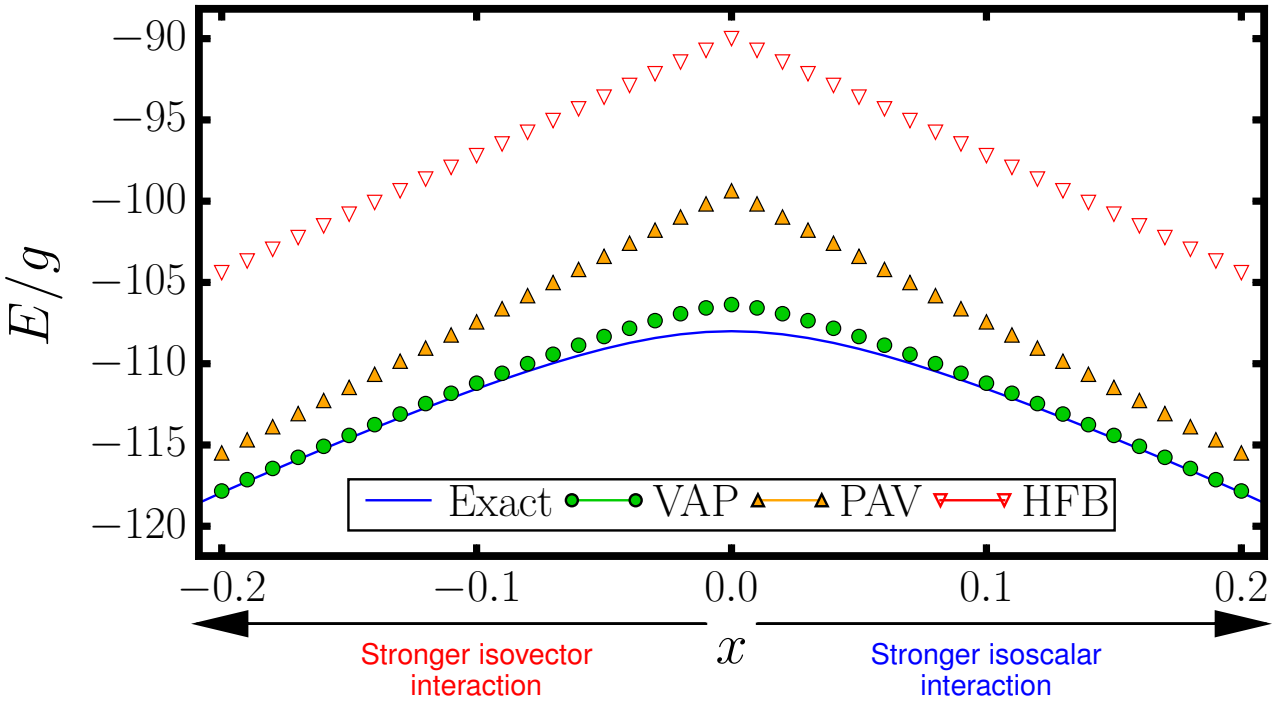

Figure 5.11: Energy as a function of the mixing parameter x for a system with $A = 24$ particles, $S = T = 0$ and spatial degeneracy $\Omega = 12$.

where now $\mathcal{I}(\beta) = \mathcal{I}(0) = 1$. Consequently

$$I = \frac{2S+1}{2} \int_0^\pi \sin\beta d^S_{00}(\beta) d\beta = (2S+1)\delta_{S0}, \tag{5.9}$$

and given that I is the overlap of the mean-field wavefunction and the projected state, this result proves that the HFB wavefunction only has a $S = 0$ component and therefore it is not possible to project to a state with $S = 1$. An analogous logic applies for the isospin as well.

We conclude from these arguments that PAV is not suitable for the restoration of broken symmetries in systems with an odd number of pairs (where, because of the signature symmetries, the system is forced to have $S + T$ equal to an odd number, cf Section 4.7.1). Specifically, the spin symmetry can not be restored in these systems, if $S \neq 0$, for $x < 0$, where the state is a condensate of isovector pairs according to the HFB description. Similarly, the isospin symmetry can not be restored in these systems, if $T \neq 0$, for $x > 0$, where the state is a condensate of isoscalar pairs according to the HFB description. The same argument applies for all particle-numbers in order to describe states with total $S + T > 0$.

5.4 Analogy between the pairing and quartetting pictures

When we look carefully at panel (d) of Fig. (5.8), we observe there are two cases for which the VAP results correspond exactly to the results obtained from the diagonalisation of the $SO(8)$ Hamiltonian. Indeed, for $A = 4$ and $A = 6$, the relative differences show little fluctuations around machine precision, indicating that the projected states used in the numerical implementation of the VAP framework exactly corresponds to the eigenstates $|AST\rangle$ of the $SO(8)$ Hamiltonian (2.17).

The reason behind this absolute agreement relies upon the structure of the exact states as combinations of the pairs considered in the Thouless state. An exact state with four particles coupled to total spin and isospin zero (that is, an alpha particle) necessarily needs to be built up as a linear combination of a quadruple, being two coupled isovector pairs; and a quartet, two coupled isoscalar pairs,

$$|A = 4, S = T = 0\rangle = \left[a(\hat{P}^+\hat{P}^+)^{(00)} + b(\hat{D}^+\hat{D}^+)^{(00)}\right]|0\rangle. \tag{5.10}$$

A sketch of this nuclear system is depicted in Fig. (5.12). An exact state with six particles

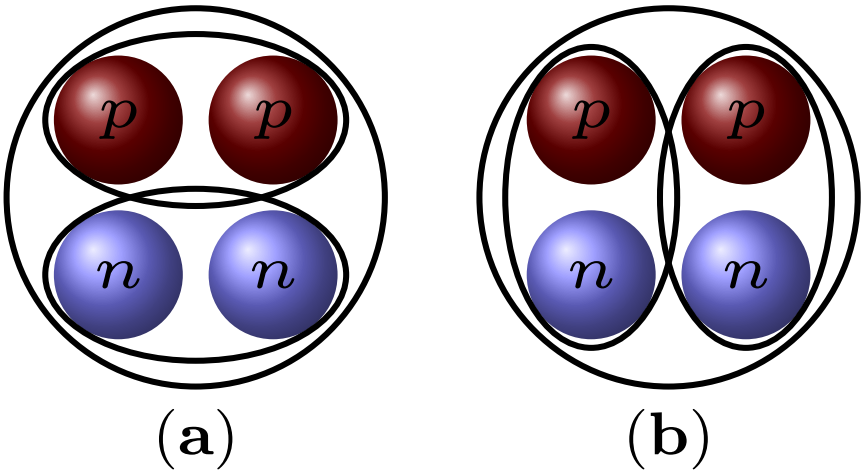

Figure 5.12: Quartet (a) and quadruple (b) structures, coupled to form an α-particle state with $S = T = 0$.

coupled to total spin one and isospin zero necessarily needs to be built up from the former alpha particle state, adding an isoscalar pair on top. No other combination is possible, as long

as these nuclear systems are fully paired,

$$|A = 6, S = 1, T = 0\rangle = \hat{D}^{+}|A = 4, S = T = 0\rangle. \tag{5.11}$$

As these states are built from isoscalar and isovector pairs only, they can be represented exactly by means of a projected Thouless state. Indeed, a particle-number projected Thouless state is written as

$$|A\rangle = \frac{(\hat{Z}^{+})^{A/2}}{(A/2)!}|0\rangle. \tag{5.12}$$

For $A = 4$, the square of the Thouless pair $\hat{Z}^{+}$ needs to be evaluated, which involves a combination of five different terms, namely $(\hat{P}^{+}\hat{P}^{+})^{(00)}$, $(\hat{D}^{+}\hat{D}^{+})^{(00)}$, $(\hat{P}^{+}\hat{D}^{+})^{(11)}$, $(\hat{P}^{+}\hat{P}^{+})^{(02)}$ and $(\hat{D}^{+}\hat{D}^{+})^{(20)}$, where the superscripts (ST) denotes coupling to total spin S and isospin T. Thus, a spin and isospin symmetry restoration by projection methods will yield a projected wavefunction where only the two first terms are involved, removing the last three and this corresponds to the structure of the exact state as in Eq. (5.10).

We see that by means of symmetry restoration with projection methods, we obtain under certain circumstances the exact wavefunction. For $A > 6$, as we see from the trend in the differences in panel (d) of Fig. (5.8), the VAP method does not obtain the exact wavefunction, though it is successful in taking into account the main components of the wavefunction being given by the two scalar-isoscalar quartets [RDP19b].

As it is seen in Appendix G, we make the analogy between the exact and projected states writing them explicitly in terms of isoscalar and isovector pairs that are used in the $SO(8)$ model for $A = 4$ and $A = 6$ particles. It would an interesting and educational exercise to extrapolate this analogy to exact $A > 6$ states and identify the missing ingredients in the wavefunction, that is, apart from the isoscalar and isovector pairs, what particle correlations need to be taken into account.

5.5 Partial projections

The remarkable accuracy of the energy and deuteron transfer results from the VAP method in comparison to the exact results of the $SO(8)$ model, which lead us to conclude the importance of VAP for the description of pairing coexistence, was due to the restoration of all relevant symmetries in the system in consideration: particle number, spin and isospin. A calculation of this sort implies the evaluation of the projection integrals 4.59 for every point of the energy parametrised by the isoscalar and isovector pairs we minimize, thus it is very intensive in terms

of computational time.

This Section is devoted to an examination of the quantitative importance of each and every one of the broken symmetries that are restored using this method. Since there are three of them, six possible combinations of projections need to be considered, without taking into account the full restoration considered in the last sections

- Particle-number projection (PNP).
- Spin projection (AMP).
- Isospin projection (ISOP).
- Particle-number plus spin projection (PNPAMP).
- Particle-number plus isospin projection (PNPISOP).
- Spin plus isospin projection (AMPISOP).

The energy surfaces of Fig. (5.7) are reproduced for PNP and AMPISOP in Figs. (5.13, 5.15), respectively. The energy, its differences with respect to the exact results, the isoscalar pair norms and deuteron transfer matrix elements that were shown in Fig. (5.8) are reproduced for PNP and AMPISOP in Figs. (5.14, 5.16), respectively.

We observe that coexistence is not seen by restoration of particle-number symmetry only (and similarly for spin or isospin symmetries restoration only, that is, for AMP and ISOP), as shown by the position of the minima on the bottom row panels in Fig. (5.13), which do not differ from the HFB results in the top row panels, and the step-like functions displayed in panels (e) and (f) of Fig. (5.14). We conclude that particle-number symmetry restoration, even when employing the VAP method, is not accountable for the presence of coexistence in the system, and it merely shifts the results obtained from the HFB method.

In Fig. (5.14) we observe how, when not implementing the projection onto states of good isospin, all energies are collapsing to the same values in panel (a), while they are different in panel (b) as we are restoring the particle-number symmetry.

The trend shown in the relative differences in panels (c) and (d) is lost, now observing random fluctuations around 2%, the largest error shown when restoring all the symmetries.

Lastly, it is important to notice the role played by the coexistence of isoscalar and isovector pairs in the deuteron transfer. As we do not observe it using only particle-number symmetry restoration, the deuteron transfer behaves in a similar fashion to the isoscalar norms, as depicted

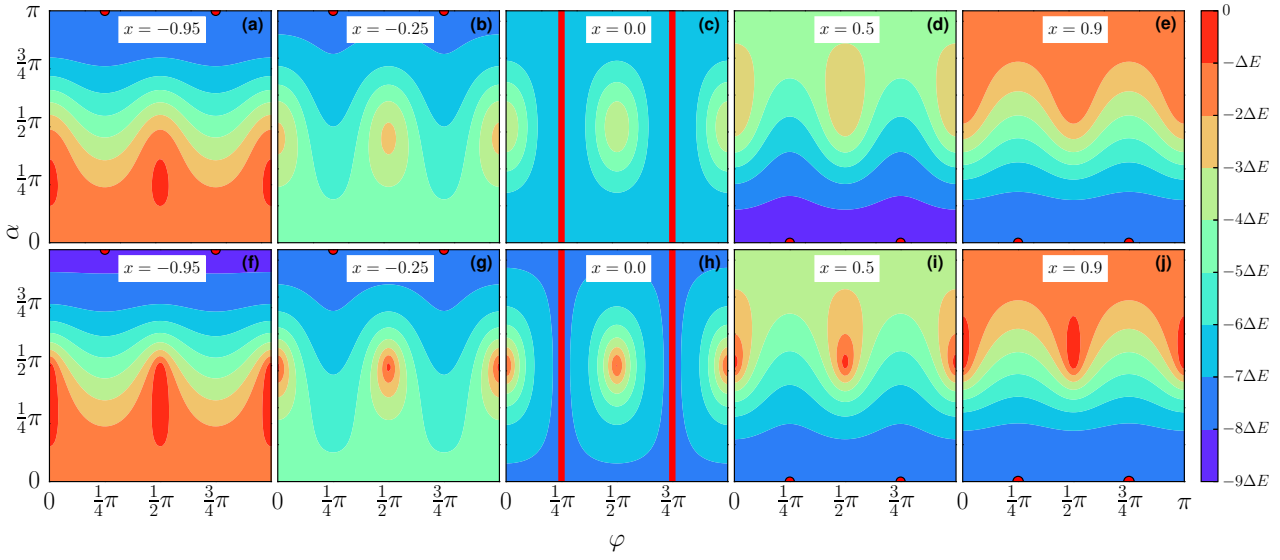

Figure 5.13: Energy surface as a function of α (relative amplitude) and φ (relative phase) for different values of x computed using the HFB method (upper panels) and VAP method with PNP only (lower panels). Coexistence between isoscalar and isovector pairing couplings is not shown, as the minima of the VAP energy surfaces are identical to those of the HFB energy surfaces.

in panels (g) and (h). A promising indication of the deuteron transfer observable as a measure of pair coexistence in nuclei.

If, on top of the particle-number symmetry restoration, we restore the spin (isospin) symmetry, coexistence is only seen for stronger isovector (isoscalar) contribution in the Hamiltonian, suddenly jumping onto the HFB results when the stronger contribution is isoscalar (isovector). In other words, coexistence between isoscalar and isovector pairing couplings is not shown for all possible interactions.

We come to the conclusion that the restoration of angular momentum (spin) and isospin is crucial for the observation of coexistence of np and like-particle pairing, as the position of the minima of the energy surfaces for the AMPISOP method in Fig. (5.15) is almost identical to the full restoration of broken symmetries, for all values of x modelling the isoscalar-isovector competition in the Hamiltonian.

In Fig. (5.16), we observe that, while accuracy with the exact results is lost because of lack of particle-number symmetry restoration, especially in the right column panels, where results are shown for different values of the particle-number of the system, the trend followed by the AMPISOP results is identical to that of the exact results, and the accuracy improves heading towards half-occupation of the variational space, where pairing correlations are strongest. The

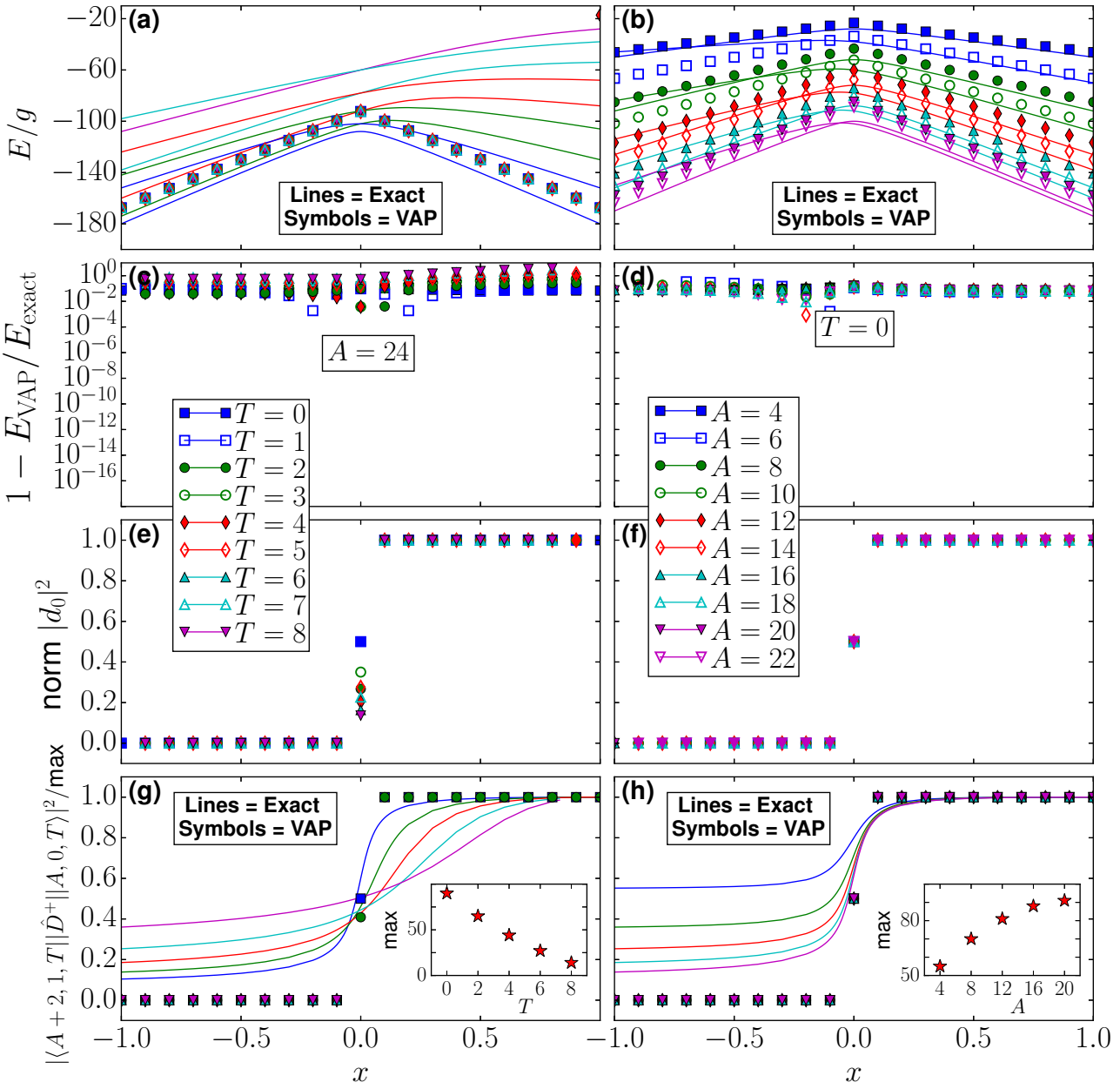

Figure 5.14: Energies in units of g (First row), relative errors (second row), norm of the isoscalar pair (third row), and deuteron transfer matrix elements (fourth row). The results were computed using the VAP method with PNP only, for different values of isospin (left column) and particle-number (right column). Coexistence between isoscalar and isovector pairing couplings is not shown. As the isospin symmetry restoration is not implemented, all the results in the left column are on top of each other.

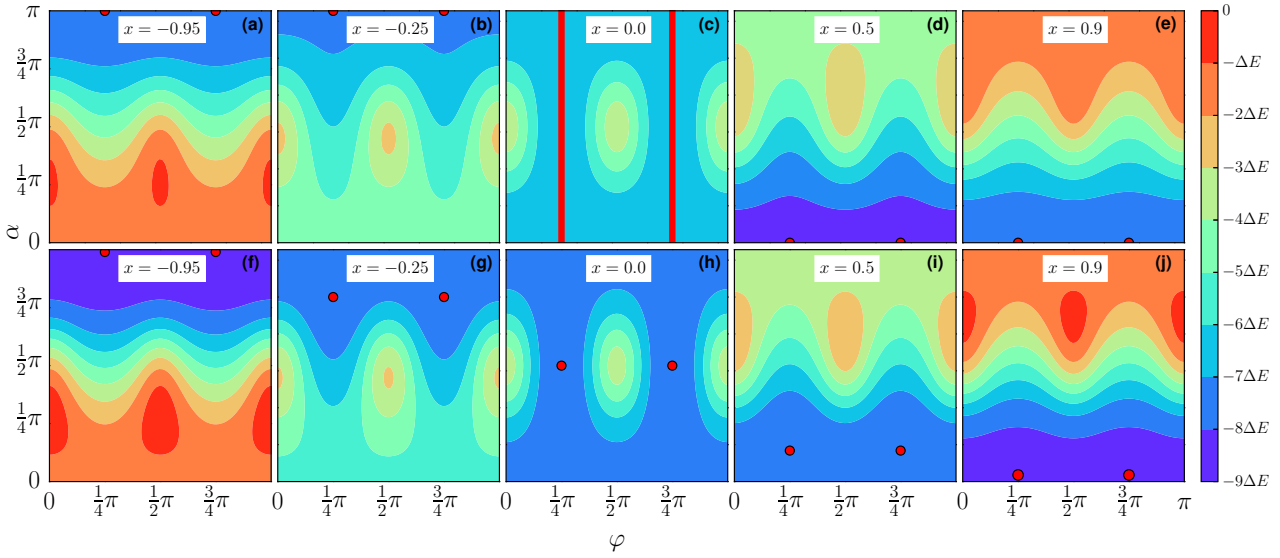

Figure 5.15: Energy surface as a function of α (relative amplitude) and φ (relative phase) for different values of x computed using the HFB method (upper panels) and VAP method with AMPISOP (lower panels). Coexistence between isoscalar and isovector pairing couplings is shown with proper values of mixing.

position of the minima in the bottom row panels of Fig. (5.15) and the plots of the isoscalar norms in panels (c) and (d) show that coexistence is present in all cases, but it is affected for low particle-number systems where restoration of this symmetry becomes important. Moreover, the AMPISOP values for the deuteron transfer matrix elements in panels (g) and (h) of Fig. (5.16) agree as well on the trend in comparison with the exact results, behaviour that was not shown in any other combination of partial restoration of broken symmetries, demonstrating once again the delicate sensitivity of the pairing coexistence under non-zero fluctuations of angular momentum and isospin and consequently the huge importance of the proper restoration of these symmetries. We observe again in panel (h) the poor accuracy of AMPISOP for low particle-number systems.

From the analysis of the partial projection figures we draw the following conclusions: first, the restoration of spin or isospin symmetries on top of particle-number symmetry restoration is needed to see the coexistence between isoscalar and isovector pairs. Second, the restoration of spin and isospin symmetries gives the best results overall, apart from the restoration of all the symmetries present on the system, while particle-number symmetry restoration is inconspicuous for the purposes of pairing coexistence.

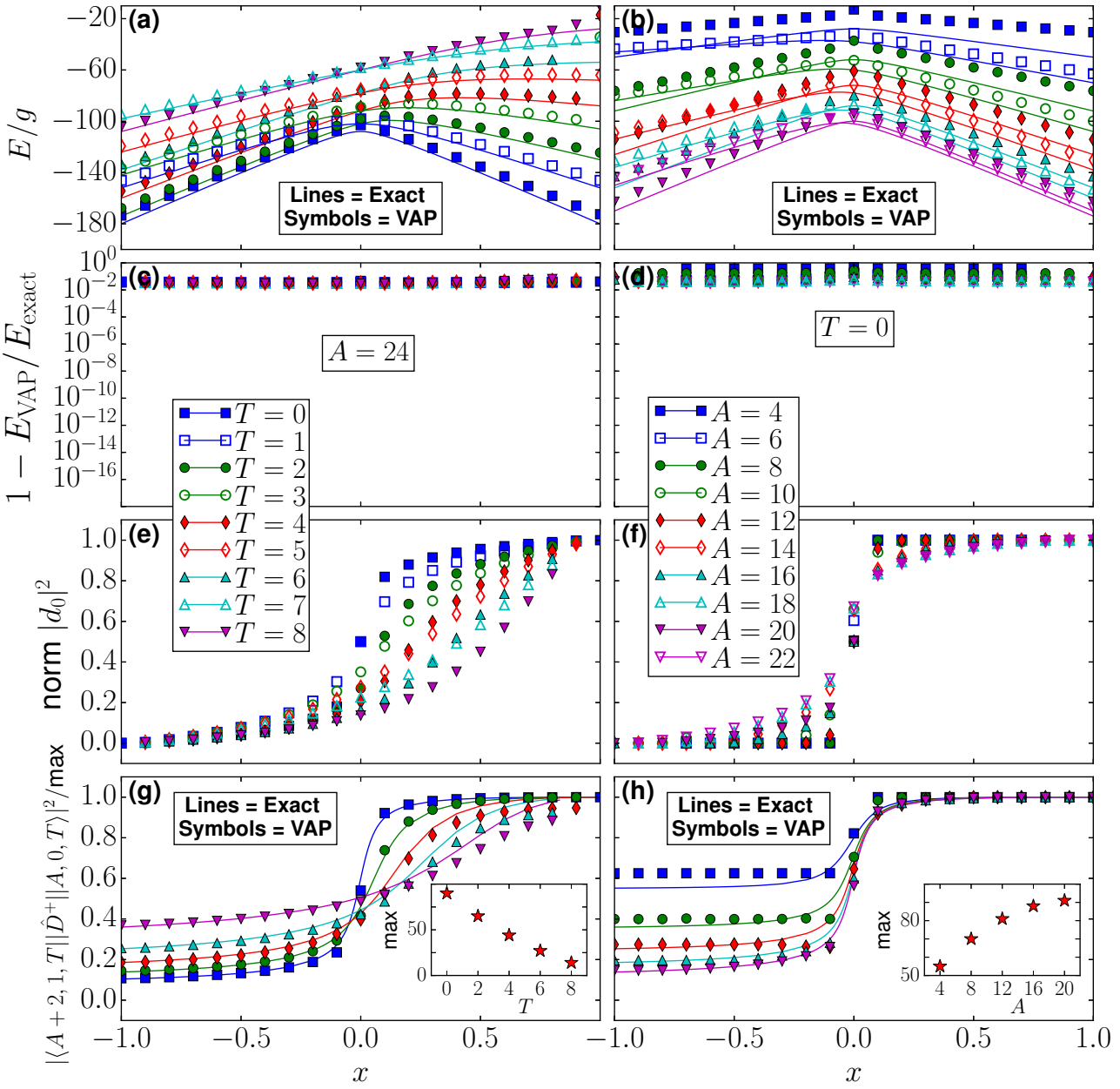

Figure 5.16: Energies in units of g (First row), relative errors (second row), norm of the isoscalar pair (third row), and deuteron transfer matrix elements (fourth row). The results were computed using the VAP method with AMPISOP only, for different values of isospin (left column) and particle-number (right column). Coexistence between isoscalar and isovector pairing couplings is shown properly. Consequently, the deuteron transfer matrix elements are very close to the exact results.

Chapter 6

Pairing coexistence in finite nuclei

The algebraic $SO(8)$ model of exact solutions of the pairing Hamiltonian (2.17) was studied thoroughly in this work, obtaining not only ground-state energies particle transfer results for different values of particle-number, spin and isospin. We could advance in this direction and study a myriad of features on top of this model, as for example including the Coulomb interaction or adding a spin-orbit splitting term and analyse the behaviour of pairing coexistence under those cases. We could also compute the matrix elements of more observables such as the Gamow-Teller operator and study the influence of np pairing on β decay transitions [Eng99].

However, we have opted for a more pragmatic endeavour, namely, the description of pairing coexistence in finite nuclei. To that end, we introduce in this Chapter the necessary tools in order to address this problem incorporating the symmetry-restoration machinery developed in the former chapters.

The most important object to take into account is the choice of the interaction modelling the nuclei. A natural problem in nuclear physics is the multiple variety of functionals that were fitted to describe certain properties of certain nuclei, and thus no general parametrisation is found to work all across the nuclear chart.

After the decision of a suitable interaction, we make a determination to implement it in an already written and benchmarked nuclear physics software well-known for its versatility: the code HFODD [Sch17], which is able to solve the Hartree-Fock-Bogoliubov equations using a deformed Cartesian harmonic oscillator basis.

This Chapter is organised as follows: first, we introduce the realistic interactions we will use in the particle-hole (ph) and particle-particle (pp) channels, putting special emphasis on the latter as we focus on the modelling of pairing coexistence. Next, we review the necessary tools in order to program this interaction for practical purposes in the code HFODD. Lastly, we show promising results obtained by these means and compare them to those obtained from

usual pairing interactions and experimentally measured.

6.1 Realistic separable interaction in the pairing channel

In the non-relativistic nuclear physics literature, two main interactions are used for the fitting of properties of nuclei: the zero-range Skyrme interaction [Sky56; Sky58] and the finite-range Gogny interaction [DG80].

We would like to extend the idea of separability, as introduced in the function form of the interaction (2.23) and used in the $SO(8)$ Hamiltonian (2.17) for a realistic interaction able to model the case of a finite nucleus. The ideal goal is to have matrix elements of such an interaction that can be separated as a product of different terms, making its numerical implementation easier in terms of computational time. Starting from the central direct terms of the Gogny interaction

$$\hat{V}(\boldsymbol{r},\boldsymbol{r}') = (W + B\hat{P}_\sigma - H\hat{P}_\tau - M\hat{P}_\sigma\hat{P}_\tau)e^{-(\boldsymbol{r}-\boldsymbol{r}')^2/\mu^2}, \tag{6.1}$$

with the *Wigner* (W), *Bartlett* (B), *Heisenberg* (H) and *Majorana* (M) as coupling constants parametrising the interaction. $\hat{P}^\sigma$ and $\hat{P}^\tau$ are the spin and isospin exchange operators, respectively. In order to compute mean-field potentials out of this interaction, we need to calculate integrals of the form

$$\int d\boldsymbol{r}d\boldsymbol{r}'\hat{V}(\boldsymbol{r},\boldsymbol{r}'), \tag{6.2}$$

whose implementation is computationally intensive, as there are crossed terms in the exponent of (6.1), making the integral *non separable* as a product.

In 2009, Tian and collaborators [TMR09] introduced such a separable interaction in the isovector pairing ${}^1S_0$ channel, being able to reproduce pairing gaps in nuclear matter given by the Gogny interaction. The interaction has the form

$$\hat{V}(\boldsymbol{r}_1,\boldsymbol{r}_2,\boldsymbol{r}_1',\boldsymbol{r}_2') = -\frac{G}{2}\delta(\boldsymbol{R}-\boldsymbol{R}')P(r)P(r')(1-\hat{P}^\sigma), \tag{6.3}$$

where $\boldsymbol{r} = \boldsymbol{r}_2 - \boldsymbol{r}_1$ and $\boldsymbol{R} = \frac{\boldsymbol{r}_1+\boldsymbol{r}_2}{2}$ are the relative and center of mass coordinates, respectively. The form factor has a Gaussian shape of the relative coordinates

$$P(r) = \frac{1}{(4\pi a^2)^{3/2}}e^{-\frac{r^2}{4a^2}}, \tag{6.4}$$

with a being the range of the interaction. We observe immediately that interaction (6.3) has a

separable functional form as the two form factors for the four particles involved are written as a product of separate terms, analogous to (2.23). The operator $\hat{P}^\sigma$ is the spin exchange operator between a pair of particles, therefore, for a pair coupled to total spin S, which can only be zero (singlet state) or one (triplet state), this operator has the following eigenvalues

$$\langle S|\hat{P}^\sigma|S\rangle = \begin{cases} +1, & \text{if } S=1 \\ -1, & \text{if } S=0 \end{cases}. \tag{6.5}$$

Thus, the expression $\frac{1}{2}(1-\hat{P}^\sigma)$ will project the wavefunction onto the ${}^1S_0$ channel, as done in this interaction, and $\frac{1}{2}(1+\hat{P}^\sigma)$ onto the ${}^3P_1$ channel, associated with isoscalar pairing.

6.1.1 Realistic separable interaction in Cartesian coordinates

We implement the former interaction in the code HFODD [Sch17], which has a three-dimensional Cartesian coordinates harmonic oscillator basis implementation. To that end, we devote this section to derive the matrix elements of the separable interaction (6.3) in these (x, y, z) coordinates.

Since we know that the form factor is a Gaussian that depends only on the norm, and using that the radius of a sphere is

$$r^2 = x^2 + y^2 + z^2, \tag{6.6}$$

the form factor can be written as a product in each Cartesian direction,

$$P(r) = P(x)P(y)P(z), \tag{6.7}$$

where we used

$$P(x) = \frac{1}{\sqrt{4\pi a^2}} e^{-\frac{x^2}{4a^2}}. \tag{6.8}$$

Using the properties of the Delta function, we also know that

$$\delta(\boldsymbol{R}-\boldsymbol{R'}) = \delta(X-X')\delta(Y-Y')\delta(Z-Z'), \tag{6.9}$$

with

$$X = \frac{x_1+x_2}{2}. \tag{6.10}$$

Therefore, the analogous form of the interaction in three-dimensional Cartesian coordinates is

$$\begin{aligned}\hat{V}(\boldsymbol{r_1},\boldsymbol{r_2};\boldsymbol{r'_1},\boldsymbol{r'_2}) = &-\delta(X-X')\delta(Y-Y')\delta(Z-Z')P(x)P(y)P(z)P(x')P(y')P(z') \\ &\times [W + B\hat{P}^\sigma - H\hat{P}^\tau - M\hat{P}^\sigma\hat{P}^\tau],\end{aligned} \tag{6.11}$$

where $\boldsymbol{r_i} = (x_i, y_i, z_i)$, $x = x_1 - x_2$ and $X = \frac{1}{2}(x_1 + x_2)$, with analogous expressions for Y and Z. Our definition of the Gaussian form factor is

$$P(x) = \frac{1}{\sqrt{\pi}a} e^{-\frac{x^2}{a^2}}, \tag{6.12}$$

with a being the range of the interaction. We have written a general spin-isospin dependence using the W, B, H, M coupling constants but, since the Gaussian form factor is symmetric in space coordinates, only W and B are independent.

The single-particle harmonic oscillator basis in which we evaluate this interaction, in the $^1S_0$ channel, is

$$|n_1 n_2, S=0\rangle = \phi_{n_1}(x_1, b)\phi_{n_2}(x_2, b)|S=0\rangle, \tag{6.13}$$

with

$$\phi_n(x, b) = b^{1/2}(\sqrt{\pi}2^n n!)^{-1/2} H_n(bx) e^{-b^2x^2/2}, \tag{6.14}$$

where $H_n(x)$ are the Hermite polynomials [AS48], n is the quantum number labelling the harmonic oscillator states and b is the harmonic oscillator constant. We use the following definition [DD97]

$$H_n^{(0)}(x) = (\sqrt{\pi}2^n n!)^{-1/2} H_n(x), \tag{6.15}$$

to cast the harmonic oscillator wavefunction in a simpler form

$$\phi_n(x, b) = b^{1/2} H_n^{(0)}(bx) e^{-b^2x^2/2}. \tag{6.16}$$

The separable pairing matrix elements in this basis will then have the following structure

$$\langle n'_1 n'_2, S=0|V|n_1 n_2, S=0\rangle = -I_x I_y I_z (W - B), \tag{6.17}$$

with

$$I_x(n_1 n_2; n'_1 n'_2) = \int dx_1 dx_2 dx'_1 dx'_2 \delta(X - X') P(x)P(x')\phi_{n_1}(x_1, b)\phi_{n_2}(x_2, b)\phi_{n'_1}(x'_1, b)\phi_{n'_2}(x'_2, b), \tag{6.18}$$

and similarly for I_y and I_z. For the evaluation of this expression we need to transform to the

center of mass coordinates, using the Moshinsky coefficients [Mos59], given by

$$\phi_{n_1}(x_1,b)\phi_{n_2}(x_2,b) = \sum_{nN} M^{nN}_{n_1n_2}\phi_n(\tilde{x},b)\phi_N(\tilde{X},b), \tag{6.19}$$

with $\tilde{x} = \frac{1}{\sqrt{2}}(x_1 - x_2) = \frac{x}{\sqrt{2}}$ and $\tilde{X} = \frac{1}{\sqrt{2}}(x_1 + x_2) = \sqrt{2}X$. The original derivation of these coefficients just involved spherical coordinates, the expression for Cartesian coordinates was published in [Dob09], and we refer to Appendix C for its elegant derivation.

The matrix elements involve the product of three analogous quantities like (6.18). We transform the integral in that expression to the center of mass coordinates (the Jacobian of the transformation is one)

$$\begin{aligned} I_x(n_1n_2;n_1'n_2') = &\sum_{n,n',N,N'} M^{nN}_{n_1n_2}M^{n'N'}_{n_1'n_2'} \\ &\times \int dxdx'dXdX'\delta(X-X')P(x)P(x')\phi_n(\tilde{x},b)\phi_{n'}(\tilde{x}',b)\phi_N(\tilde{X},b)\phi_{N'}(\tilde{X}',b). \end{aligned} \tag{6.20}$$

We integrate over the coordinates X, X' using the δ function,

$$\begin{aligned} &\int dXdX'\delta(X-X')\phi_N(\tilde{X},b)\phi_{N'}(\tilde{X}',b) = \\ &\int dX\phi_N(\tilde{X},b)\phi_{N'}(\tilde{X},b) = \\ &\frac{b}{\sqrt{2}}\int d\tilde{X}H^{(0)}_N(b\tilde{X})H^{(0)}_{N'}(b\tilde{X})e^{-b^2\tilde{X}^2}, \end{aligned} \tag{6.21}$$

making the change $t = b\tilde{X}$ we observe immediately that the integral is the normalisation condition of the Hermite polynomials $H^{(0)}_n(x)$

$$\frac{1}{\sqrt{2}}\int dtH^{(0)}_N(t)H^{(0)}_{N'}(t)e^{-t^2} = \frac{\delta_{NN'}}{\sqrt{2}}. \tag{6.22}$$

Inserting this result, we get

$$I_x(n_1n_2;n_1'n_2') = \frac{1}{\sqrt{2}}\sum_{n,n',N} M^{nN}_{n_1n_2}M^{n'N}_{n_1'n_2'}\int dxdx'P(x)P(x')\phi_n(\tilde{x},b)\phi_{n'}(\tilde{x}',b), \tag{6.23}$$

which can be written in terms of

$$I_x(n_1n_2;n_1'n_2') = \frac{1}{\sqrt{2}}\sum_{n,n',N} M^{nN}_{n_1n_2}M^{n'N}_{n_1'n_2'}W(n)W(n'), \tag{6.24}$$

with

$$W(n) = \int dx P(x)\phi_n(\tilde{x}, b). \tag{6.25}$$

Expanding the harmonic oscillator wavefunction, the integral can be expressed as

$$\begin{aligned} W(n) &= \frac{b^{1/2}}{\sqrt{\pi a^2}} \int dx e^{-x^2/a^2} H_n^{(0)}(b\tilde{x}) e^{-\frac{b^2\tilde{x}^2}{2}} \\ &= \frac{b^{1/2}}{\sqrt{\pi a^2}} \int dx e^{-x^2/a^2} H_n^{(0)}(bx/\sqrt{2}) e^{-\frac{b^2x^2}{4}}, \end{aligned} \tag{6.26}$$

and making the change $t = bx/\sqrt{2}$, we get

$$W_x(n) = \frac{\sqrt{2}}{\sqrt{\pi b a^2}} \int dt e^{-2t^2/(ba)^2} H_n^{(0)}(t) e^{-\frac{t^2}{2}}. \tag{6.27}$$

Using the following identity [GR14]

$$\int_{-\infty}^{+\infty} du H_{2m}^{(0)}(\alpha u) e^{-u^2} = \pi^{1/4} \frac{\sqrt{(2m)!}}{m!} \left(\frac{\alpha^2 - 1}{2}\right)^m, \tag{6.28}$$

we obtain for the final result

$$W(n) = \frac{2\pi^{-1/4}\sqrt{b}}{\sqrt{a^2b^2 + 4}} \frac{\sqrt{n!}}{(n/2)!} \left(\frac{a^2b^2 - 4}{2a^2b^2 + 8}\right)^{n/2}. \tag{6.29}$$

We observe that the sum over n, n' in Eq. (6.23) can be reduced making use of the fact that the Moshinsky coefficients will be zero unless $n = n_1 + n_2 - N$ and $n' = n_1' + n_2' - N$. It is convenient to rewrite the final expression of the matrix elements as

$$I_x(n_1 n_2; n_1' n_2') = \frac{1}{\sqrt{2}} \sum_{N=0}^{n_1+n_2} G(N, n_1, n_2) G(N, n_1', n_2'), \tag{6.30}$$

defining the auxiliary functions

$$G(N, n_1, n_2) = M_{n_1 n_2}^{n_1+n_2-N, N} W(n_1 + n_2 - N). \tag{6.31}$$

A similar derivation of these matrix elements in Cartesian space coordinates was already given in [Nik10], but we found several errors and missing factors in the final expressions. A general and compact formalism to obtain local separable terms from an expansion in an interaction is found in [Rob10]. An alternative approach can be followed to obtain the same results, we refer to Appendix I for details.

6.1.2 Spin-isospin decomposition of the separable force

It is necessary to implement the separable interaction in the different spin-isospin channels V_{ST} to model the isoscalar or isovector pairing, starting from the general expression

$$\hat{V}(r) = P(r)(W + B\hat{P}_\sigma - H\hat{P}_\tau - M\hat{P}_\sigma\hat{P}_\tau), \tag{6.32}$$

where $P(r)$ is the Gaussian form factor (6.12) and the exchange operators are written as

$$\hat{P}_\sigma = \frac{1}{2} + \frac{1}{2}\sum_{\mu=x,y,z} \sigma_\mu^{(1)}\sigma_\mu^{(2)}, \tag{6.33}$$

$$\hat{P}_\tau = \frac{1}{2} + \frac{1}{2}\sum_{k=1,2,3} \tau_k^{(1)}\tau_k^{(2)}, \tag{6.34}$$

fulfilling that $\hat{P}_\sigma^2 = \hat{P}_\tau^2 = 1$. An antisymmetrized expression of the former force is written as

$$\hat{V}_{\text{ant}} = \hat{V}(1 - \hat{P}_\sigma\hat{P}_\tau\hat{P}_M) = \hat{V}_{\text{dir}} + \hat{V}_{\text{exc}}. \tag{6.35}$$

P_M being the spatial exchange operator and where we denoted by $\hat{V}_{\text{dir}}$ and $\hat{V}_{\text{exc}}$ the direct and exchange terms of the interaction, respectively.

Inserting the exchange operators definitions in the expression of the force we get, for the direct term

$$\begin{aligned}\hat{V}_{\text{dir}}(r) = P(r)\Bigg[W + B\left(\frac{1}{2} + \frac{1}{2}\sum_{\mu=x,y,z}\sigma_\mu^{(1)}\sigma_\mu^{(2)}\right) - H\left(\frac{1}{2} + \frac{1}{2}\sum_{k=1,2,3}\tau_k^{(1)}\tau_k^{(2)}\right) \\ - M\left(\frac{1}{2} + \frac{1}{2}\sum_{\mu=x,y,z}\sigma_\mu^{(1)}\sigma_\mu^{(2)}\right)\left(\frac{1}{2} + \frac{1}{2}\sum_{k=1,2,3}\tau_k^{(1)}\tau_k^{(2)}\right)\Bigg].\end{aligned} \tag{6.36}$$

Thus, in order to write the former expression in the compact form of

$$\hat{V}_{\text{dir}} = P(r)\sum_{\mu k} V_{ST}^D \sigma_\mu^{(1)}\sigma_\mu^{(2)}\tau_k^{(1)}\tau_k^{(2)}. \tag{6.37}$$

We have to set the following relations

$$V_{00}^{D} = W + \frac{1}{2}B - \frac{1}{2}H - \frac{1}{4}M \tag{6.38}$$

$$V_{01}^{D} = -\frac{1}{2}H - \frac{1}{2}M \tag{6.39}$$

$$V_{10}^{D} = \frac{1}{2}B - \frac{1}{2}M \tag{6.40}$$

$$V_{11}^{D} = -\frac{1}{4}M. \tag{6.41}$$

Analogously, for the exchange term, we have

$$\begin{aligned}\hat{V}_{\text{exc}} = P(r)\Bigg[&W\left(\frac{1}{2}+\frac{1}{2}\sum_{\mu=x,y,z}\sigma_{\mu}^{(1)}\sigma_{\mu}^{(2)}\right)\left(\frac{1}{2}+\frac{1}{2}\sum_{k=1,2,3}\tau_{k}^{(1)}\tau_{k}^{(2)}\right)P_M \\ &+B\left(\frac{1}{2}+\frac{1}{2}\sum_{\mu=x,y,z}\sigma_{\mu}^{(1)}\sigma_{\mu}^{(2)}\right)^2\left(\frac{1}{2}+\frac{1}{2}\sum_{k=1,2,3}\tau_{k}^{(1)}\tau_{k}^{(2)}\right)P_M \\ &-H\left(\frac{1}{2}+\frac{1}{2}\sum_{\mu=x,y,z}\sigma_{\mu}^{(1)}\sigma_{\mu}^{(2)}\right)\left(\frac{1}{2}+\frac{1}{2}\sum_{k=1,2,3}\tau_{k}^{(1)}\tau_{k}^{(2)}\right)^2P_M \\ &-M\left(\frac{1}{2}+\frac{1}{2}\sum_{\mu=x,y,z}\sigma_{\mu}^{(1)}\sigma_{\mu}^{(2)}\right)^2\left(\frac{1}{2}+\frac{1}{2}\sum_{k=1,2,3}\tau_{k}^{(1)}\tau_{k}^{(2)}\right)^2P_M\Bigg],\end{aligned} \tag{6.42}$$

and again, rewriting it in a compact form like

$$V_{\text{exc}} = P(r)\sum_{\mu k} V_{ST}^{E}\hat{P}_M\sigma_{\mu}^{(1)}\sigma_{\mu}^{(2)}\tau_{k}^{(1)}\tau_{k}^{(2)}, \tag{6.43}$$

we get

$$V_{00}^{E} = -\frac{W}{4} - \frac{1}{2}B + \frac{1}{2}H + M \tag{6.44}$$

$$V_{01}^{E} = -\frac{1}{4}W - \frac{1}{2}B \tag{6.45}$$

$$V_{10}^{E} = \frac{1}{4}W + \frac{1}{2}H \tag{6.46}$$

$$V_{11}^{E} = -\frac{1}{4}W. \tag{6.47}$$

For the pairing channel, we need the following compact form

$$\hat{V} = P(r)\sum_{\mu k} V_{ST}^{P}\tilde{\sigma}_{\mu}^{L}\tilde{\sigma}_{\mu}^{R}\tilde{\tau}_{k}^{L}\tilde{\tau}_{k}^{R}, \tag{6.48}$$

with L and R denoting the left (bra) and the right (ket) states, respectively, and where the new Pauli matrices read

$$\tilde{\sigma}_0 = \begin{pmatrix} 0 & -1 \\ 1 & 0 \end{pmatrix}, \ \tilde{\sigma}_1 = \begin{pmatrix} -1 & 0 \\ 0 & 1 \end{pmatrix}, \ \tilde{\sigma}_2 = \begin{pmatrix} -i & 0 \\ 0 & -i \end{pmatrix}, \ \tilde{\sigma}_3 = \begin{pmatrix} 0 & 1 \\ 1 & 0 \end{pmatrix}, \tag{6.49}$$

The spin and isospin identity and exchange operators in the particle-particle representation have a different form [Per04]

$$\hat{I}^{\sigma} = \frac{1}{2}\tilde{\sigma}_0^L\tilde{\sigma}_0^R + \frac{1}{2}\sum_{\mu=x,y,z}\tilde{\sigma}_\mu^L\tilde{\sigma}_\mu^R, \tag{6.50}$$

$$\hat{P}^{\sigma} = -\frac{1}{2}\tilde{\sigma}_0^L\tilde{\sigma}_0^R + \frac{1}{2}\sum_{\mu=x,y,z}\tilde{\sigma}_\mu^L\tilde{\sigma}_\mu^R, \tag{6.51}$$

$$\hat{I}^{\tau} = \frac{1}{2}\tilde{\tau}_0^L\tilde{\tau}_0^R + \frac{1}{2}\sum_{k=x,y,z}\tilde{\tau}_k^L\tilde{\tau}_k^R, \tag{6.52}$$

$$\hat{P}^{\tau} = -\frac{1}{2}\tilde{\tau}_0^L\tilde{\tau}_0^R + \frac{1}{2}\sum_{\mu=x,y,z}\tilde{\tau}_k^L\tilde{\tau}_k^R. \tag{6.53}$$

We get then

$$\begin{aligned}\hat{V} = P(r)\Bigg[&W\left(\frac{1}{2}\tilde{\sigma}_0^L\tilde{\sigma}_0^R + \frac{1}{2}\sum_{\mu=x,y,z}\tilde{\sigma}_\mu^L\tilde{\sigma}_\mu^R\right)\left(\frac{1}{2}\tilde{\tau}_0^L\tilde{\tau}_0^R + \frac{1}{2}\sum_{k=x,y,z}\tilde{\tau}_k^L\tilde{\tau}_k^R\right)\\
&+ B\left(-\frac{1}{2}\tilde{\sigma}_0^L\tilde{\sigma}_0^R + \frac{1}{2}\sum_{\mu=x,y,z}\tilde{\sigma}_\mu^L\tilde{\sigma}_\mu^R\right)\left(\frac{1}{2}\tilde{\tau}_0^L\tilde{\tau}_0^R + \frac{1}{2}\sum_{k=x,y,z}\tilde{\tau}_k^L\tilde{\tau}_k^R\right)\\
&- H\left(\frac{1}{2}\tilde{\sigma}_0^L\tilde{\sigma}_0^R + \frac{1}{2}\sum_{\mu=x,y,z}\tilde{\sigma}_\mu^L\tilde{\sigma}_\mu^R\right)\left(-\frac{1}{2}\tilde{\tau}_0^L\tilde{\tau}_0^R + \frac{1}{2}\sum_{k=x,y,z}\tilde{\tau}_k^L\tilde{\tau}_k^R\right)\\
&- M\left(-\frac{1}{2}\tilde{\sigma}_0^L\tilde{\sigma}_0^R + \frac{1}{2}\sum_{\mu=x,y,z}\tilde{\sigma}_\mu^L\tilde{\sigma}_\mu^R\right)\left(-\frac{1}{2}\tilde{\tau}_0^L\tilde{\tau}_0^R + \frac{1}{2}\sum_{k=x,y,z}\tilde{\tau}_k^L\tilde{\tau}_k^R\right)\Bigg],\end{aligned} \tag{6.54}$$

and making the comparison with Eq. (6.48), we finally get

$$\begin{aligned}V_{00}^P &= \frac{1}{4}\left(W - B + H - M\right),\\
V_{01}^P &= \frac{1}{4}(W - B - H + M),\\
V_{10}^P &= \frac{1}{4}(W + B + H + M),\\
V_{11}^P &= \frac{1}{4}(W + B - H - M).\end{aligned} \tag{6.55}$$

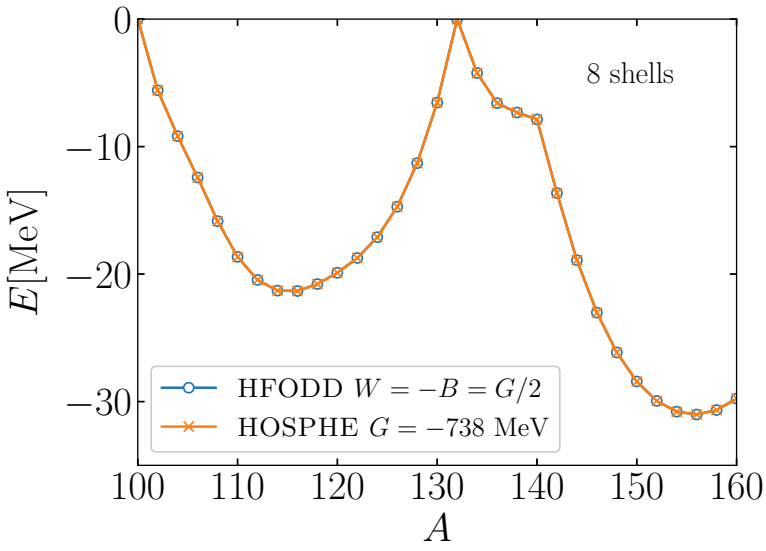

Figure 6.1: Energies computed using the 3D Cartesian code HFODD and the spherical code HOSPHE for the chain of Sn isotopes, evaluated on a basis consisting on eight harmonic oscillator shells whose frequency was chosen to be $\hbar\omega = \frac{1.2\times 41 \text{ MeV}}{A^{1/3}}$ with $A = 132$.

That is, we have rewritten the coupling constants W, B, H, M of the interaction in Eq. (6.1) in order to obtain the direct (D), exchange (E) and pairing (P) contributions to the total energy in the four different channels given by the coupling of the pair of particles to total spin and isospin [Sch17].

6.2 Implementation of the realistic separable interaction

As mentioned before, we will implement the VAP technology using realistic interactions and shell structure settings in the 3D Cartesian coordinates harmonic oscillator basis code HFODD. We implemented the separable generators reviewed in Section 6.1 in the pp channel and tested them against the results obtained from the spherical basis code HOSPHE [Car10], evaluating the ground-state energies of the chain of tin isotopes, as shown in Fig. (6.1), with a very successful agreement up to the order of keV. The number of shells in the harmonic oscillator basis was chosen to be eight in order to make calculations faster. After the implementation was succesful, we made sure that the results stood correctly for any number of shells. In both programs, the Skyrme functional SLy4 [Cha97] in the ph channel was implemented and benchmarked.

After we have made sure that the implementation is correct, we evaluate pairing gaps using this interaction. We compare these results with those obtained using a conventional

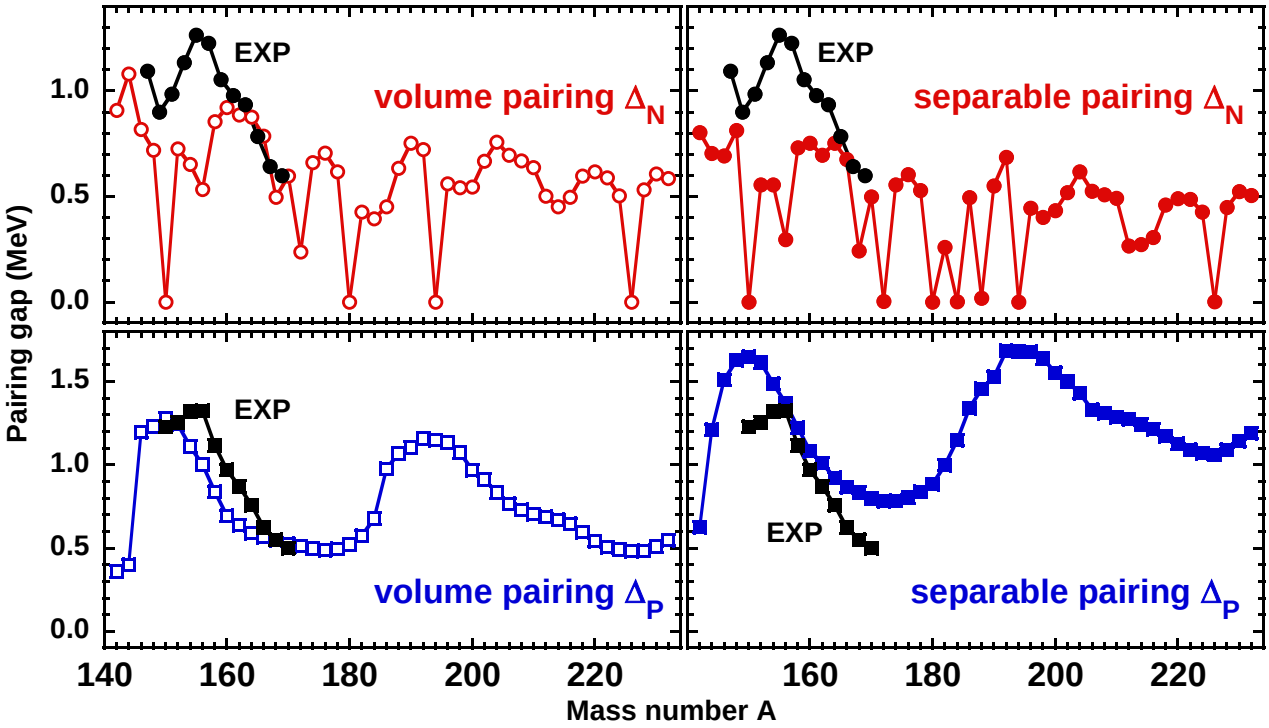

Figure 6.2: Neutron Δ_N and proton Δ_P pairing gaps for the isotopic chain of Erbium computed using a separable (6.32) and a volume (6.56) interaction in the right and left panels, respectively. Experimental results are also shown using the three-point indicator (1.1). Figure taken from [RDP19a].

density dependent delta interaction (DDDI) for protons and neutrons in the pairing channel, also referred to as the volume pairing interaction [DNS03; BHM67; Cha76], whose functional form is

$$\hat{V}(\boldsymbol{r},\boldsymbol{r}') = V_0 \left\{ 1 - \left[\frac{\rho(\boldsymbol{r})}{\rho_0} \right]^{\alpha} \right\} \delta(\boldsymbol{r}-\boldsymbol{r}'), \tag{6.56}$$

where V_0, α are the parameters defining the interaction and ρ_0 is the saturation density.

In Fig. (6.2), we plot the gaps of the chain of Erbium isotopes for 14 shells using the separable and volume pairing interactions, and we compare them to experimental results of neutron and proton gaps based on the binding energies according to the three-point indicator formula (1.1) for consistency. For the separable pairing, we fit the values of $W = -B = 300$ MeV that best reproduce the experimental proton and neutron gaps of ^{170}Er. Similarly, for the zero-range volume pairing, a value of $V_0 = -195$ MeV fm and $\alpha = 1$ was chosen to this purpose, used for the interaction in protons and neutrons, making it charge-symmetric. Also, the usual cut-off of 60 MeV was chosen in order to avoid divergences in the integrals with this zero-range interaction.

We observe that the separable pairing tends to give a weaker pairing for neutrons and a stronger for protons than the volume pairing. It is interesting to note that in some nuclei the separable interaction leads to a vanishing neutron gap, whereas the volume interaction may still give a non-zero value of $\Delta_N \approx 0.5$ MeV. Since Erbium nuclei are deformed (apart from the semi-magic isotopes), we checked that the values of the quadrupole moment, obtained for both interactions, are the same.

Chapter 7

Conclusions and perspectives

Neutron-proton pairing has recently gained abundant attention due to the evidence of such a paired phase in ^{92}Pd [Ced11]. While envisioned more than half a century ago, coexistence between this pairing coupling and the usual isovector like-particle coupling is still under discussion in the scientific community and no definitive conclusions can be drawn, as it is quite elusive both in experimental measures and in theoretical predictions.

In this PhD project, we have shown that by means of a symmetry-unrestricted self-consistent mean-field formalism with restoration of broken symmetries using the variation after projection approach, based on the minimisation of the energy after all symmetries are restored, we were able to reproduce exact solutions of an algebraic $SO(8)$ model based on degenerate $\ell-$shells, while observing the elusive isoscalar and isovector pairing coexistence as well. This is the first time that such a coexistence is described within self-consistent mean-field techniques.

The observed outstanding results open the possibility of new studies within self-consistent mean-field methods to examine the role of neutron-proton pairing in the structure of nuclei near the proton dripline. Realistic density functional theory calculations with a proper effective interaction (including spin-orbit, of course, as it makes pairing correlations weaker because of the breaking of the degeneracy of the shells) and shell structure settings are required.

A potential experimental probe with direct links to theoretical estimates is the deuteron transfer. We suggest that a profound study of this observable in nuclei along the proton dripline and in heavy nuclei, where the neutron-proton paired phase is predicted to vanish, will be extremely valuable and be a conclusive argument to the role and existence of this pairing coupling. So far, the deuteron transfer are hard to measure experimentally, due to its diluted neutron-proton pair composition in the nucleus, in opposition to, for example, alpha particles, which are known to form clusters in certain nuclei.

The major obstacle in the implementation of this sophisticated approach is the burden in

computational resources. A fully fledged realistic VAP calculation is not feasible yet in a reasonable time frame and every problem needs to be examined carefully, exploiting the symmetries of the system or making good approximations in order to accelerate the computation. The Madrid group studies a possible implementation using a restricted variational space [RER05; Rod05].

Restoration of angular momentum (spin) and isospin becomes more important than particle-number symmetry restoration when describing pairing coexistence, especially in systems known to have strong pairing correlations (mid-shell systems). Consequently, a straightforward projected BCS approach is not suitable to describe this desired coexistence, and focus should be placed on angular momentum (orbital and spin) and isospin symmetry unrestricted methods.

The main perspectives from this project would be to continue by implementing the idea within a realistic mean-field calculation and energy density functionals, proven to be very successful and versatile in all regions of the nuclear chart. Running such a calculation would be extremely enlightening and a crucial key to solve one of the main puzzles in nuclear structure physics. Important quantities can be extracted as results from these calculations, e.g., nuclear pairing gaps. On top of that, a quasiparticle random phase approximation (QRPA) or Generator Coordinate Method (GCM) may be implemented, with inputs given by the mean-field density function theory calculation, with wide applications such as to obtain accurate nuclear matrix elements for extracting the neutrino mass [AEE08] or the Pygmy Dipole Resonance [Paa05], where in the latter a good isoscalar-isovector coexistence as a function of the isospin is fundamental.

A realistic, self-consistent mean-field with VAP implementation is currently ongoing in the nuclear structure code HFODD, with separable generators for the interaction already achieved. Care should be placed not only on the mixing of protons and neutrons in the Bogoliubov transformation for the HFB calculation, but also in the Coulomb term of the potential Hamiltonian.

Appendix A

Exact solutions of the $SO(8)$ model

A.1 Ground-state energies

In order to compute the energies given by the pairing $SO(8)$ Hamiltonian (2.17) for all possible values of the mixing parameter x, we need an expression of its matrix elements in a given basis. Pang [Pan69] computed explicitly these matrix elements for the seniority zero case, that is, for the case of no unpaired nucleons, in the Gelfand basis (or $SU(4)$ basis) $|n, A, S, T\rangle$, where n is the representation label, A is the total number of nucleons, S is the total spin and T is the total isospin. They read

$$
\begin{aligned}
H_{nn} = & -\frac{g(1-x)}{2}\left\{\frac{(\Omega+n+\lambda+6)(\Omega-n-\lambda)}{8(n+2)(n+3)}\right. \\
& \times\left[\frac{(S+1)(n+S+T+4)(n+S-T+3)+S(n-S+T+3)(n-S-T+2)}{2S+1}\right] \\
& +\frac{(\Omega-n+\lambda+2)(\Omega+n-\lambda+4)}{8(n+1)(n+2)} \\
& \left.\times\left[\frac{(S+1)(n-S+T+1)(n-S-T)+S(n+S-T+1)(n+S+T+2)}{2S+1}\right]\right\} \\
& -\frac{g(1+x)}{2}\left\{\frac{(\Omega+n+\lambda+6)(\Omega-n-\lambda)}{8(n+2)(n+3)}\right. \\
& \times\left[\frac{(T+1)(n+S+T+4)(n-S+T+3)+T(n-T+S+3)(n-S-T+2)}{2T+1}\right] \\
& +\frac{(\Omega-n+\lambda+2)(\Omega+n-\lambda+4)}{8(n+1)(n+2)} \\
& \left.\times\left[\frac{(T+1)(n-T+S+1)(n-S-T)+T(n+T-S+1)(n+S+T+2)}{2T+1}\right]\right\},
\end{aligned}
\tag{A.1}
$$

A	n	(S,T)
2	1	(10)(01)
4	0	(00)
	2	(02)(11)(20) (00)
6	1	(10)(01)
	3	(03)(12)(21)(30) (01)(10)
8	0	(00)
	2	(02)(11)(20) (00)
	4	(04)(13)(22)(31)(40) (02)(11)(20) (00)

Table A.1: Classification of states for a system with $A = 2, 4, 6, 8$ particles.

$$H_{n+2,n} = -\frac{gx}{8(n+3)}\left[\frac{(\Omega+n+\lambda+6)(\Omega+n-\lambda+6)(\Omega-n+\lambda)(\Omega-n-\lambda)}{(n+2)\boldsymbol{(n+4)}},\right.$$
$$\left.\times\,(n+S+T+4)(n+S-T+3)(n-S+T+3)(n-S-T+2)\right]^{1/2}, \tag{A.2}$$

and $H_{n-2,n} = H_{n,n-2}$. g is the strength of the interaction and x is the mixing parameter; $\Omega = \sum_\ell (2\ell+1)$ is the number of spatial states and $\lambda = \Omega - A$. Of course, H has to be hermitian and it is tridiagonal because a pair creation (annihilation) operator can only connect a given state with itself or to a state plus (minus) a pair. The size of this matrix is $K = 1 + \frac{A}{4} - \frac{S+T}{2}$.

In equation (A.2), the factor $(n+4)$ in the denominator is not found in the original derivation [Pan69] because of a typo, as reported in [Eng97]. Equation (A.2) gives the proper expression for the non-diagonal matrix elements of the pairing Hamiltonian. The quantum numbers n, A, S, T defining our basis follow a specific classification that is different for an even and an odd number of pairs $\mathcal{N} = \frac{A}{2}$. From Table (A.1) we find the following pattern:

- For odd $\mathcal{N}$, the representation label n is odd, starting from $S+T$ and ending in $\mathcal{N}$.

- For even $\mathcal{N}$, the representation label n is even, starting from $S+T$ and ending in $\mathcal{N}$.
- The number $\mathcal{K}=S+T$ can not be bigger than $\mathcal{N}$, and it is odd for odd $\mathcal{N}$ and even for even $\mathcal{N}$. This conclusion was also drawn after an analysis of the signature symmetry of the states in Section (4.7).

Therefore, the exact ground-state energy of a system of A particles with total spin S and isospin T is obtained as the lowest eigenvalue of the Hamiltonian matrix (A.3)

$$\hat{H}=\begin{pmatrix} H_{\mathcal{K}\mathcal{K}} & H_{\mathcal{K}+2\mathcal{K}} & 0 & 0 & \dots & 0 \\ H_{\mathcal{K}+2\mathcal{K}} & H_{\mathcal{K}+2\mathcal{K}+2} & H_{\mathcal{K}+4\mathcal{K}+2} & 0 & \dots & 0 \\ 0 & H_{\mathcal{K}+4\mathcal{K}+2} & H_{\mathcal{K}+4\mathcal{K}+4} & H_{\mathcal{K}+6\mathcal{K}+4} & \dots & 0 \\ 0 & 0 & H_{\mathcal{K}+6\mathcal{K}+4} & H_{\mathcal{K}+6\mathcal{K}+6} & \dots & 0 \\ \vdots & \vdots & \vdots & \vdots & \ddots & \vdots \\ 0 & 0 & 0 & 0 & H_{\mathcal{N}\mathcal{N}-2} & H_{\mathcal{N}\mathcal{N}} \end{pmatrix}. \tag{A.3}$$

For $x=\pm 1,0$, the general $SO(8)$ symmetry of the Hamiltonian reduces to a $SO(5)$ and $SU(4)$ symmetry, respectively, and in those cases there are explicit formulas for the computation of the ground-state energy of the system [Eng97; KA06]

- For $x=-1$ (pure isovector case):

$$E=-\frac{g}{4}[2\mathcal{N}(4\Omega+6-2\mathcal{N})-4T(T+1)]. \tag{A.4}$$

- For $x=1$ (pure isoscalar case):

$$E=-\frac{g}{4}[2\mathcal{N}(4\Omega+6-2\mathcal{N})-4S(S+1)]. \tag{A.5}$$

- For $x=0$ (equal isoscalar-isovector interaction case):

$$E=-\frac{g}{2}[2\mathcal{N}(\Omega+3)-\mathcal{N}^2-n(n+4)]. \tag{A.6}$$

These formulas become extraordinary benchmarks for the energy matrix (A.3) and, in fact, they were essential for finding the typo in the non-diagonal matrix elements of the pairing Hamiltonian (A.2).

A.2 Deuteron transfer

As part of the ingredients for the computation of the matrix elements of the pairing Hamiltonian in [Pan69], the first step was to compute the matrix elements of the pair creation and annihilation operators composing it. The deuteron transfer is an observable entirely related to these quantities, as it is described as the spectroscopic amplitude of a scalar-isoscalar pair from an initial state $|A, S, T\rangle$ to a final state $|A+2, S+1, T\rangle$. We focus explicitly in the case of a deuteron addition

$$\langle A+2, S+1, T|\hat{D}^{+}_{\mu}|A, S, T\rangle. \tag{A.7}$$

Owing to the symmetry of the system, we choose the spin projection to be zero. The matrix elements of this pair operator, in the Gelfand basis of states $|n, A, S, T\rangle$, are then written as

$$\langle n', A+2, S', T'|\hat{D}^{+}_{0}|n, A, S, T\rangle = C^{S'0}_{S010}C^{T'0}_{T000}F(\Omega;\lambda,\lambda-1;n',n)\left\langle \begin{matrix}[nn0]\\ ST\end{matrix};\begin{matrix}[110]\\ 10\end{matrix}\middle\| \begin{matrix}[n'n'0]\\ S'T'\end{matrix}\right\rangle, \tag{A.8}$$

where the C quantities are Clebsch-Gordan coefficients. The $F-$factors, in this case, read

$$\begin{aligned} F(\Omega;\lambda+1,\lambda;n-1,n) &= \frac{1}{2}\sqrt{\frac{n(\Omega-n+\lambda+2)(\Omega+n-\lambda+4)}{n+2}},\\ F(\Omega;\lambda+1,\lambda;n+1,n) &= \frac{1}{2}\sqrt{\frac{(n+4)(\Omega+n+\lambda+6)(\Omega-n-\lambda)}{n+2}}, \end{aligned} \tag{A.9}$$

and the Wigner supermultiplets [HP69]

$$\begin{aligned} \left\langle \begin{matrix}[nn0]\\ S-1T\end{matrix};\begin{matrix}[110]\\ 10\end{matrix}\middle\| \begin{matrix}[n+1n+10]\\ ST\end{matrix}\right\rangle &= \sqrt{\frac{S(n+S+T+3)(n+S-T+2)}{2(n+1)(n+2)(2S+1)}},\\ \left\langle \begin{matrix}[nn0]\\ S-1T\end{matrix};\begin{matrix}[110]\\ 10\end{matrix}\middle\| \begin{matrix}[n-1n-10]\\ ST\end{matrix}\right\rangle &= -\sqrt{\frac{S(n-S-T+1)(n-S+T+2)}{2(n+2)(n+3)(2S+1)}}. \end{aligned} \tag{A.10}$$

Our goal is to compute this quantity in the basis $|AST\rangle$, corresponding to the ground state of a system with A particles, spin S and isospin T. These states were the eigenvectors of the Hamiltonian matrix (A.3), written in the Gelfand basis as well. Therefore, we apply this transformation

$$|AST\rangle = \sum_i c_i|n_i AST\rangle, \tag{A.11}$$

where c_i are the components of the eigenvector of the Hamiltonian matrix (A.3) corresponding

to the ground-state energy. Therefore, our desired quantity is written as

$$\langle A+2, S+1, T|\hat{D}_0^+|AST\rangle = \sum_{ij} c_i^* c_j \langle n_i, A+2, S+1, T'|\hat{D}_0^+|n_j, A, S, T\rangle, \tag{A.12}$$

with c_i being the coefficients of the eigenvector corresponding to the state on the left and c_j corresponding to the state on the right. Applying the Wigner-Eckhart theorem, the final result for the deuteron transfer is

$$\langle A+2, S+1, T||\hat{D}^+||AST\rangle = \frac{\sqrt{2S+3}}{C^{S+1,0}_{S010}}\langle A+2, S+1, T|\hat{D}_0^+|AST\rangle. \tag{A.13}$$

Analogous expressions can be worked out for the pair operator $\hat{P}^+$ and the pair removals matrix elements can be obtained from these by hermitian conjugation, for the case of deuteron removal.

A.3 Alpha transfer

The $SO(8)$ model is also suitable for the computation of matrix elements of an alpha particle transfer, whose operator is defined as

$$\begin{aligned}\hat{T}^+_\alpha &= (\hat{P}^+\hat{P}^+)^{00} + (\hat{D}^+\hat{D}^+)^{00} \\ &= \frac{1}{\sqrt{3}}\left[\sum_\nu (-1)^{1-\nu}\hat{P}^+_\nu \hat{P}^+_{-\nu} + \sum_\mu (-1)^{1-\mu}\hat{D}^+_\mu \hat{D}^+_{-\mu}\right].\end{aligned} \tag{A.14}$$

For its evaluation, we need the matrix elements of the pair creation operators, which were given in [Pan69]. We write them explicitly

$$\hat{D}_0^+|n\lambda ST\rangle = \sum_{n'S'T'} C^{S'0}_{S010} C^{T'0}_{T000} F(\Omega, \lambda, \lambda-1, n, n') \left\langle \begin{matrix}[nn0] \\ ST\end{matrix}; \begin{matrix}[110] \\ 10\end{matrix} \middle|\middle| \begin{matrix}[n'n'0] \\ S'T'\end{matrix} \right\rangle |n'\lambda-1 S'T'\rangle, \tag{A.15}$$

where λ is related to the particle number A as $\lambda = \Omega - A$, C are the Clebsch-Gordan coefficients and expressions for the $F-$factors and the Wigner supermultiplets can be found in [HP69].

Therefore,

$$\begin{aligned}\langle n''\lambda - 2ST|\hat{D}_0^+\hat{D}_0^+|n\lambda ST\rangle = &\sum_{n'S'T'} C^{S'0}_{S010}C^{T'0}_{T000}C^{S0}_{S'010}C^{T0}_{T'000} \\ &\times F(\Omega,\lambda,\lambda-1,n,n')F(\Omega,\lambda-1,\lambda-2,n',n'') \\ &\times \left\langle \begin{matrix}[nn0]\\ ST\end{matrix}; \begin{matrix}[110]\\ 10\end{matrix}\middle\| \begin{matrix}[n'n'0]\\ S'T'\end{matrix}\right\rangle \left\langle \begin{matrix}[n'n'0]\\ S'T'\end{matrix}; \begin{matrix}[110]\\ 10\end{matrix}\middle\| \begin{matrix}[n''n''0]\\ ST\end{matrix}\right\rangle,\end{aligned} \tag{A.16}$$

reduced to,

$$\begin{aligned}\langle n''\lambda - 2ST|\hat{D}_0^+\hat{D}_0^+|n\lambda ST\rangle = &\sum_{n'S'} C^{S'0}_{S010}C^{S0}_{S'010} \\ &\times F(\Omega,\lambda,\lambda-1,n,n')F(\Omega,\lambda-1,\lambda-2,n',n'') \\ &\times \left\langle \begin{matrix}[nn0]\\ ST\end{matrix}; \begin{matrix}[110]\\ 10\end{matrix}\middle\| \begin{matrix}[n'n'0]\\ S'T\end{matrix}\right\rangle \left\langle \begin{matrix}[n'n'0]\\ S'T\end{matrix}; \begin{matrix}[110]\\ 10\end{matrix}\middle\| \begin{matrix}[n''n''0]\\ ST\end{matrix}\right\rangle.\end{aligned} \tag{A.17}$$

More generally we have

$$\begin{aligned}\langle n''\lambda - 2ST|\hat{D}_\mu^+\hat{D}_{-\mu}^+|n\lambda ST\rangle = &\sum_{n'S'} C^{S'-\mu}_{S01-\mu}C^{S0}_{S'-\mu1\mu} \\ &\times F(\Omega,\lambda,\lambda-1,n,n')F(\Omega,\lambda-1,\lambda-2,n',n'') \\ &\times \left\langle \begin{matrix}[nn0]\\ ST\end{matrix}; \begin{matrix}[110]\\ 10\end{matrix}\middle\| \begin{matrix}[n'n'0]\\ S'T\end{matrix}\right\rangle \left\langle \begin{matrix}[n'n'0]\\ S'T\end{matrix}; \begin{matrix}[110]\\ 10\end{matrix}\middle\| \begin{matrix}[n''n''0]\\ ST\end{matrix}\right\rangle.\end{aligned} \tag{A.18}$$

For the isovector pair operators, the result is analogous

$$\begin{aligned}\langle n''\lambda - 2ST|\hat{P}_\nu^+\hat{P}_{-\nu}^+|n\lambda ST\rangle = &\sum_{n'T'} C^{T'-\nu}_{T01-\nu}C^{T0}_{T'-\nu1\nu} \\ &\times F(\Omega,\lambda,\lambda-1,n,n')F(\Omega,\lambda-1,\lambda-2,n',n'') \\ &\times \left\langle \begin{matrix}[nn0]\\ ST\end{matrix}; \begin{matrix}[110]\\ 01\end{matrix}\middle\| \begin{matrix}[n'n'0]\\ ST'\end{matrix}\right\rangle \left\langle \begin{matrix}[n'n'0]\\ ST'\end{matrix}; \begin{matrix}[110]\\ 01\end{matrix}\middle\| \begin{matrix}[n''n''0]\\ ST\end{matrix}\right\rangle.\end{aligned} \tag{A.19}$$

The matrix elements of the alpha particle transfer are written in the Gelfand basis. We need to transform them to the physical basis by the transformation

$$\langle A+4ST|\hat{T}_\alpha^+|AST\rangle = \sum_{ij} c_i^* c_j \langle n'A+4ST|\hat{T}_\alpha^+|nAST\rangle, \tag{A.20}$$

where c_i^* and c_j are the elements of the eigenvector of the Hamiltonian of the $SO(8)$ interaction.

Appendix B

Matrix elements of one and two-body operators

B.1 Wick's theorem

The mechanism needed for the computation of matrix elements of any operator relies upon Wick's theorem. We refer to the extensive literature about the theoretical aspects of this well-known theorem and the purpose of this appendix only concerns its practical implementation. We will follow closely the derivation given in [Suh07].

Given two fermion creation or annihilation operators, $\hat{A}$ and $\hat{B}$, we define a contraction, or contracted pair, as

$$\overbrace{\hat{A}\hat{B}} = \langle\Psi|\hat{A}\hat{B}|\Psi\rangle, \tag{B.1}$$

where $|\Psi\rangle$ is the vacuum with respect to the fermion operators $\hat{A}, \hat{B}$, e.g., the bare vacuum $|0\rangle$ for the case of the single particle operators $\hat{a}, \hat{a}^\dagger$. If we now define $\hat{A}_i$ as a fermion creation operator and $\hat{B}_j$ as a fermion annihilation operator, the four possible contractions are

$$\overbrace{\hat{B}_j\hat{A}_i} = \delta_{ij} \quad , \quad \overbrace{\hat{A}_i\hat{B}_j} = \overbrace{\hat{A}_i\hat{A}_j} = \overbrace{\hat{B}_i\hat{B}_j} = 0. \tag{B.2}$$

Wick's theorem establishes that the vacuum expectation value of any product of n fermion creation and annihilation operators is given by

$$\langle\Psi|A_1A_2\dots A_n|\Psi\rangle = \sum_i^N (-1)^r \times \underbrace{A_1A_2\dots A_n}_{\substack{i\text{-th combination of} \\ \text{all contracted pairs}}} , \tag{B.3}$$

where r is the number of contraction line crossings and i runs over all the possible combinations of all contracted pairs in the ordered product, whose total number is

$$N = \frac{n!}{(n/2)!2^{\frac{n}{2}}}. \tag{B.4}$$

For the sake of clarity, we will give here two examples of the application of the former formula for the normal density and pairing tensor matrix elements and the following subsections we will use Wick's theorem again for the computation of matrix elements of one- and two-body operators.

The normal density matrix elements are given by

$$\rho_{ll'} = \langle\Psi|\hat{a}^+_{l'}\hat{a}_l|\Psi\rangle, \tag{B.5}$$

where $|\Psi\rangle$ is now the HFB vacuum and $\hat{a}^+$, $\hat{a}$ are the single-particle creation and annihilation operators, respectively. The state $|\Psi\rangle$ is the vacuum defined by the quasiparticle operator $\hat{\beta}$, therefore, for a proper application of Wick's theorem, we need to transform the single-particle operators to quasiparticle operators, given by formula (3.30). The matrix elements of the density then become

$$\rho_{ll'} = \sum_{kk'}\langle\Psi|(u^*_{l'k'}\hat{\beta}^+_{k'} + v_{l'k'}\hat{\beta}_k)(u_{lk}\hat{\beta}_{k'} + v^*_{lk}\hat{\beta}^+_k)|\Psi\rangle, \tag{B.6}$$

owing to formula (B.2), the only non-vanishing contraction is given by $\hat{\beta}\hat{\beta}^+$, reducing the former expression to

$$\rho_{ll'} = \sum_{kk'} v_{l'k'}v^*_{lk}\hat{\beta}_{k'}\hat{\beta}^\dagger_k = \sum_{kk'} v_{l'k'}v^*_{lk}\delta_{kk'} = \sum_k v^*_{lk}v_{l'k} = V^*V^T. \tag{B.7}$$

This is the usual matrix expression of the normal density. For the pairing tensor we have

$$\kappa_{ll'} = \langle\Psi|\hat{a}_{l'}\hat{a}_l|\Psi\rangle, \tag{B.8}$$

therefore, in a similar fashion

$$\kappa_{ll'} = \sum_{kk'} u_{l'k'}v^*_{lk}\hat{\beta}_{k'}\hat{\beta}^+_k = \sum_{kk'} u_{l'k'}v^*_{lk}\delta_{kk'} = \sum_k v^*_{lk}u_{l'k} = V^*U^T, \tag{B.9}$$

which is again the usual matrix expression of the pairing tensor.

B.2 One-body operators

Any one-body operator $\hat{O}$ can be written in the basis of the single-particle operators as

$$\hat{O} = \sum_{\alpha\beta} O_{\alpha\beta} \hat{a}^+_\beta \hat{a}_\alpha, \tag{B.10}$$

where $O_{\alpha\beta} = \langle\alpha|\hat{O}|\beta\rangle$ are its matrix elements in the single-particle basis spanned by $|\alpha\rangle, |\beta\rangle$. Its expectation value in the quasiparticle HFB vacuum $|\Psi\rangle$ will be

$$\langle\Psi|\hat{O}|\Psi\rangle = \sum_{\alpha\beta} O_{\alpha\beta} \langle\Psi|\hat{a}^+_\beta \hat{a}_\alpha|\Psi\rangle = \sum_{\alpha\beta} O_{\alpha\beta}\rho_{\alpha\beta}, \tag{B.11}$$

that is, the quasiparticle vacuum expectation value of any one-body operator will be completely defined by the density matrix. For example, the particle-number operator is defined by

$$\hat{A} = \sum_{ij} \delta_{ij} \hat{a}^+_j \hat{a}_i, \tag{B.12}$$

so its expectation value in the HFB framework will be

$$A = \langle\Psi|\hat{A}|\Psi\rangle = \sum_{ij} \delta_{ij}\rho_{ij} = \sum_i \rho_{ii} = \mathrm{Tr}\,\rho. \tag{B.13}$$

The isospin operator is defined by

$$\hat{T} = \sum_{lk} t_{lk} \hat{a}^+_k \hat{a}_l, \tag{B.14}$$

where $t_{lk} = \frac{1}{2}\tau_{lk}$ with τ_{lk} being the Pauli vector in the usual representation (4.83). Therefore

$$T = \langle\Psi|\hat{T}|\Psi\rangle = \sum_{ij} t_{lk}\rho_{lk} = \frac{1}{2}(\rho_{11} - \rho_{22} + 2\rho_{12}), \tag{B.15}$$

where we have made use of the symmetry of the density matrix.

B.2.1 One-body operators squared and fluctuations

When the quasiparticle vacuum state $|\Psi\rangle$ is not an eigenstate of the operator $\hat{O}$, there will be fluctuations around the expectation value $\langle\Psi|\hat{O}|\Psi\rangle$. These fluctuations, which we shall denote

ΔO can be computed using the formula

$$\Delta O^2 = \langle\Psi|\hat{O}^2|\Psi\rangle - \langle\Psi|\hat{O}|\Psi\rangle^2. \tag{B.16}$$

If $\hat{O}$ is a one-body operator, its squared is given by

$$\hat{O}^2 = \hat{O}\cdot\hat{O} = \sum_{ij} O_{ij}\hat{a}_j^+\hat{a}_i \sum_{lk} O_{lk}\hat{a}_k^+\hat{a}_l = \sum_{ijlk} O_{ij}O_{lk}\hat{a}_j^+\hat{a}_i\hat{a}_k^+\hat{a}_l. \tag{B.17}$$

Evaluating this squared one-body operator over the quasiparticle vacuum and performing the transformation from the single-particle basis to the quasiparticle basis, we obtain

$$\begin{aligned} O^2 = \sum_{ijlk} O_{ij}O_{lk} \sum_{k_1k_2k_3k_4} \langle\Psi|(u^*_{jk_1}\hat{\beta}^+_{k_1} + v_{jk_1}\hat{\beta}_{k_1}) \\ \times (u_{ik_2}\hat{\beta}_{k_2} + v^*_{ik_2}\hat{\beta}^+_{k_2}) \\ \times (u^*_{kk_3}\hat{\beta}^+_{k_3} + v_{kk_3}\hat{\beta}_{k_3}) \\ \times (u_{lk_4}\hat{\beta}_{k_4} + v^*_{lk_4}\hat{\beta}^+_{k_4})|\Psi\rangle. \end{aligned} \tag{B.18}$$

The only non-zero expectation values are

$$\begin{aligned} O^2 = \sum_{ijlk} O_{ij}O_{lk} \sum_{k_1k_2k_3k_4} v_{jk_1}u_{ik_2}u^*_{kk_3}v^*_{lk_4}\langle\Psi|\hat{\beta}_{k_1}\hat{\beta}_{k_2}\hat{+}^+_{k_3}\hat{\beta}^+_{k_4}|\Psi\rangle + \\ + v_{jk_1}v^*_{ik_2}v_{kk_3}v^*_{lk_4}\langle\Psi|\hat{\beta}_{k_1}\hat{\beta}^+_{k_2}\hat{\beta}_{k_3}\hat{\beta}^+_{k_4}|\Psi\rangle, \end{aligned} \tag{B.19}$$

and we evaluate them using Wick's theorem

$$\langle\Psi|\hat{\beta}_{k_1}\hat{\beta}^+_{k_2}\hat{\beta}_{k_3}\hat{\beta}^+_{k_4}|\Psi\rangle = (-1)^0\overbrace{\hat{\beta}_{k_1}\hat{\beta}^+_{k_2}}\overbrace{\hat{\beta}_{k_3}\hat{\beta}^+_{k_4}} = \delta_{k_1k_2}\delta_{k_3k_4}, \tag{B.20}$$

$$\begin{aligned} \langle\Psi|\hat{\beta}_{k_1}\hat{\beta}_{k_2}\hat{\beta}^+_{k_3}\hat{\beta}^+_{k_4}|\Psi\rangle &= (-1)^0\overbrace{\hat{\beta}_{k_1}\hat{\beta}_{k_2}\hat{\beta}^+_{k_3}\hat{\beta}^+_{k_4}} + (-1)^1\overbrace{\hat{\beta}_{k_1}\hat{\beta}_{k_2}\hat{\beta}^+_{k_3}}\hat{\beta}^\dagger_{k_4} \\ &= \delta_{k_1k_4}\delta_{k_2k_3} - \delta_{k_1k_3}\delta_{k_2k_4}. \end{aligned} \tag{B.21}$$

The sum is then reduced to

$$O^2 = \sum_{ijlk} O_{ij}O_{lk} \sum_{ab} (v_{ja}u_{ib}u^*_{kb}v^*_{la} - v_{ja}u_{ib}u^*_{ka}v^*_{lb} + v_{ja}v^*_{ia}v_{kb}v^*_{lb}). \tag{B.22}$$

Using now definitions (B.7), (B.9) and

$$\delta_{ll'} - \rho_{ll'} = \sum_k u_{lk} u^*_{l'k}, \tag{B.23}$$

the addends in (B.22) are reduced to

$$\sum_{ab} v_{ja} v^*_{ia} v_{kb} v^*_{lb} = \rho_{ij}\rho_{lk}, \tag{B.24}$$

$$\sum_{ab} v_{ja} u_{ib} u^*_{kb} v^*_{la} = \rho_{lj}(\delta_{ki} - \rho_{ki}), \tag{B.25}$$

$$\sum_{ab} v_{ja} u_{ib} u^*_{ka} v^*_{lb} = \kappa_{li}\kappa^*_{jk}. \tag{B.26}$$

Finally, the one-body operator squared takes the form

$$O^2 = \langle\Psi|\hat{O}^2|\Psi\rangle = \sum_{ijlk} O_{ij}O_{lk}(\rho_{ij}\rho_{lk} + \rho_{lj}(\delta_{ki} - \rho_{ki}) - \kappa_{li}\kappa^*_{jk}). \tag{B.27}$$

Now we evaluate the fluctuations, using (B.16)

$$\begin{aligned} \Delta O^2 &= \sum_{ijlk} O_{ij}O_{lk}(\rho_{ij}\rho_{lk} + \rho_{lj}(\delta_{ki} - \rho_{ki}) - \kappa_{li}\kappa^*_{jk}) - \sum_{ijlk} O_{ij}O_{lk}\rho_{ij}\rho_{lk} \\ &= \sum_{ijlk} O_{ij}O_{lk}(\rho_{lj}(\delta_{ki} - \rho_{ki}) - \kappa_{li}\kappa^*_{jk}). \end{aligned} \tag{B.28}$$

Let us work with the specific example of the particle-number operator $\hat{N}$. Its fluctuations will then be

$$\Delta A^2 = \sum_{ijlk} \delta_{ij}\delta_{lk}(\rho_{lj}(\delta_{ki} - \rho_{ki}) - \kappa_{li}\kappa^*_{jk}) = \sum_{ij}(\rho_{ji}(\delta_{ij} - \rho_{ji}) - \kappa_{ji}\kappa^*_{ij}), \tag{B.29}$$

reduced to a compact expression knowing that $\rho^2 - \rho = -\kappa\kappa^+ = \kappa\kappa^*$

$$\Delta A^2 = 2\,\mathrm{Tr}\big(\rho - \rho^2\big) = -2\,\mathrm{Tr}\big(\kappa\kappa^+\big). \tag{B.30}$$

B.3 Two-body operators

Any two-body operator $\hat{O}$, as for example the particle-particle or pairing interaction, can be written in the basis of single-particle operators as

$$\hat{O} = \frac{1}{4}\sum_{ijlk} \overline{O}_{ijlk}\hat{a}_i^+\hat{a}_j^+\hat{a}_k\hat{a}_l, \tag{B.31}$$

with $\overline{O}_{ijlk} = O_{ijlk} - O_{ijkl}$ being the anti-symmetrized matrix elements. We evaluate this operator over the HFB vacuum $|\Psi\rangle$ and perform the transformation from the single-particle basis to the quasiparticle basis

$$\begin{aligned} O = \langle\Psi|\hat{O}|\Psi\rangle = \sum_{ijlk}\overline{O}_{ijlk} \sum_{k_1k_2k_3k_4} & \langle\Psi|(u^*_{ik_1}\hat{\beta}^+_{k_1} + v_{ik_1}\hat{\beta}_{k_1}) \\ & \times (u^*_{jk_2}\hat{\beta}^+_{k_2} + v^*_{jk_2}\hat{\beta}_{k_2}) \\ & \times (u_{kk_3}\hat{\beta}_{k_3} + v^*_{kk_3}\hat{\beta}^+_{k_3}) \\ & \times (u_{lk_4}\hat{\beta}_{k_4} + v'^*_{lk_4}\hat{\beta}^+_{k_4})|\Psi\rangle, \end{aligned} \tag{B.32}$$

$$\begin{aligned} O = \sum_{ijlk}\overline{O}_{ijlk} \sum_{k_1k_2k_3k_4} & v_{ik_1}u^*_{jk_2}u_{kk_3}v^*_{lk_4}\langle\Psi|\hat{\beta}_{k_1}\hat{\beta}^+_{k_2}\hat{\beta}_{k_3}\hat{\beta}^+_{k_4}|\Psi\rangle + \\ & + v_{ik_1}v_{jk_2}v^*_{kk_3}v^*_{lk_4}\langle\Psi|\hat{\beta}_{k_1}\hat{\beta}_{k_2}\hat{\beta}^+_{k_3}\hat{\beta}^+_{k_4}|\Psi\rangle. \end{aligned} \tag{B.33}$$

Using the contractions (B.20), (B.21), we find

$$O = \sum_{ijlk}\overline{O}_{ijlk}\sum_{ab}(v_{ia}u^*_{ja}u_{kb}v^*_{lb} + v_{ia}v_{jb}v^*_{kb}v^*_{la} - v_{ia}v_{jb}v^*_{ka}v^*_{lb}), \tag{B.34}$$

and, finally, with expressions (B.24), (B.26), we reduce the two-body operator expectation value to a compact form

$$O = \sum_{ijlk}\overline{O}_{ijlk}(\rho_{li}\rho_{kj} - \rho_{ki}\rho_{lj} + \kappa_{lk}\kappa^*_{ij}) = \sum_{ijlk}\overline{O}_{ijlk}(\overline{\rho_{li}\rho_{kj}} + \kappa_{lk}\kappa^*_{ij}). \tag{B.35}$$

Appendix C

Moshinsky coefficients for the one-dimensional harmonic oscillator

For the evaluation of matrix elements of the interaction in the harmonic oscillator basis, sometimes it is convenient to perform a transformation from the individual particle coordinates frame, spanned by the states $|n_1 n_2\rangle$, where n_i denotes the wavefunction of particle i; to the relative n and center-of-mass N coordinates, spanned by $|nN\rangle$. That is

$$|nN\rangle = \sum_{n_1 n_2} M^{nN}_{n_1 n_2} |n_1 n_2\rangle, \tag{C.1}$$

where the brackets $M^{nN}_{n_1 n_2} = \langle n_1 n_2 | nN \rangle$ are called the Moshinsky coefficients and uniquely describe such transformation. In the coordinate-space frame, such a transformation reads

$$x = \frac{1}{\sqrt{2}}(x_1 - x_2), \qquad X = \frac{1}{\sqrt{2}}(x_1 - x_2). \tag{C.2}$$

In the second-quantization frame, then we have [Dob09]

$$\hat{a}_{\mathrm{rel}} = \frac{1}{\sqrt{2}}(\hat{a}_1 - \hat{a}_2), \qquad \hat{a}_{\mathrm{CM}} = \frac{1}{\sqrt{2}}(\hat{a}_1 + \hat{a}_2). \tag{C.3}$$

A one-dimensional harmonic oscillator state with quantum number n is written as

$$|n\rangle = \frac{(\hat{a}^+)^n}{\sqrt{n!}}|0\rangle, \tag{C.4}$$

with $|0\rangle$ being the particle vacuum. Thus, the brackets can be written as

$$\langle n_1 n_2 | nN \rangle = (n_1! n_2! n! N!)^{-\frac{1}{2}} \langle 0 | (\hat{a}_1)^{n_1} (\hat{a}_2)^{n_2} (\hat{a}^+_{\text{rel}})^n (\hat{a}^+_{\text{CM}})^N | 0 \rangle. \tag{C.5}$$

Using (C.3) and the binomial expansion, we obtain

$$(\hat{a}^+_{\text{rel}})^n = \frac{(\hat{a}^+_1 - \hat{a}^+_2)^n}{2^{n/2}} = \frac{1}{2^{n/2}} \sum_{k=0}^{n} \binom{n}{k} (-1)^{n-k} (\hat{a}^+_1)^k (\hat{a}^+_2)^{n-k}, \tag{C.6}$$

$$(\hat{a}^+_{\text{CM}})^N = \frac{(\hat{a}^+_1 + \hat{a}^+_2)^N}{2^{N/2}} = \frac{1}{2^{N/2}} \sum_{k'=0}^{N} \binom{N}{k'} (\hat{a}^+_1)^{k'} (\hat{a}^+_2)^{N-k'}. \tag{C.7}$$

Therefore, (C.5) becomes

$$\begin{aligned} \langle n_1 n_2 | nN \rangle = (n_1! n_2! n! N!)^{-\frac{1}{2}} \frac{1}{2^{\frac{n+N}{2}}} \sum_{k'=0}^{N} \sum_{k=0}^{n} (-1)^{n-k} \binom{N}{k'} \binom{n}{k} \\ \times \langle 0 | (\hat{a}_1)^{n_1} (\hat{a}_2)^{n_2} (\hat{a}^+_1)^k (\hat{a}^+_2)^{n-k} (\hat{a}^+_1)^{k'} (\hat{a}^+_2)^{N-k'} | 0 \rangle. \end{aligned} \tag{C.8}$$

Using now the commutators for the harmonic oscillator operators

$$[\hat{a}, \hat{a}^+] = 1, \qquad [\hat{a}, \hat{a}] = [\hat{a}^+, \hat{a}^+] = 0, \tag{C.9}$$

we reorder the operators in the bracket in (C.8)

$$\langle 0 | (\hat{a}_1)^{n_1} (\hat{a}^+_1)^k (\hat{a}^+_1)^{k'} (\hat{a}_2)^{n_2} (\hat{a}^+_2)^{n-k} (\hat{a}^+_2)^{N-k'} | 0 \rangle. \tag{C.10}$$

It is obvious that this bracket will be different from zero only if the following selection rules are fulfilled

$$n_1 + n_2 = n + N, \tag{C.11}$$

$$n_1 = k + k'. \tag{C.12}$$

We see that, starting from the left in (C.10), $n_1 - k$ annihilation operators will be compensated with $(\hat{a}^+_1)^k$, and then $n_1 - k - k'$ annihilation operators will be compensated with $(\hat{a}^+_1)^{k'}$. Applying this logic everywhere in the bracket and the following identity, valid for the harmonic oscillator operators

$$[\hat{a}^n, \hat{a}] = n \hat{a}^{n-1}, \tag{C.13}$$

the bracket can be computed as

$$\begin{aligned}\langle 0|(\hat{a}_1)^{n_1}(\hat{a}_1^+)^k(\hat{a}_1^+)^{k'}(\hat{a}_2)^{n_2}(\hat{a}_2^+)^{n-k}(\hat{a}_2^+)^{N-k'}|0\rangle &= \delta_{n_1+n_2,n+N}\delta_{n_1,k+k'} \\ &\times \frac{n_1!}{(n_1-k)!}\frac{(n_1-k)!}{(n_1-k-k')!}\frac{n_2!}{(n_2-n+k)!}\frac{(n_2-n+k)!}{(n_2-n+k-N+k')!}.\end{aligned} \tag{C.14}$$

Finally, (C.5) is written as

$$\begin{aligned}\langle n_1 n_2|nN\rangle &= (n_1!n_2!n!N!)^{-\frac{1}{2}}\frac{1}{2^{\frac{n+N}{2}}}\sum_{k'=0}^{N}\sum_{k=0}^{n}(-1)^{n-k}\binom{N}{k'}\binom{n}{k}\delta_{n_1+n_2,n+N}\delta_{n_1,k+k'} \\ &\times \frac{n_1!}{(n_1-k-k')!}\frac{n_2!}{(n_2-n+k-N+k')!}.\end{aligned} \tag{C.15}$$

We choose to reduce one of the two sums using the second Kronecker delta, if we reduce the first one, then the final expression for the Moshinsky brackets is

$$\langle n_1 n_2|nN\rangle = \frac{\sqrt{n_1!n_2!n!N!}}{2^{\frac{n+N}{2}}}\delta_{n_1+n_2,n+N}\sum_{k=0}^{n}\frac{(-1)^{n-k}}{k!(n-k)!(n_1-k)!(N-n_1+k)!}, \tag{C.16}$$

which is exactly the expression given in [Nik10]. Beware that, because of the factorials in the denominator, we must change the lower and upper limits of the sum, a, b, to $a = \max(0, n_1 - N)$, $b = \max(n, n_1)$. If we decide to reduced the second sum, then the Moshinsky brackets are

$$\langle n_1 n_2|nN\rangle = \frac{\sqrt{n_1!n_2!n!N!}}{2^{\frac{n+N}{2}}}\delta_{n_1+n_2,n+N}\sum_{k=0}^{N}\frac{(-1)^{n-n_1+k}}{k!(N-k)!(n_1-k)!(n-n_1+k)!}, \tag{C.17}$$

which is exactly the expression given in [Dob09]. Again, because of the factorials in the denominator, we must change the lower and upper limits of the sum, a, b, to $a = \max(0, n_1 - n)$, $b = \min(N, n_1)$.

Appendix D

Derivation of the transition densities expressed by the Thouless matrices

We start with the transition pairing tensor

$$\kappa^{10}_{\mu\nu} = \frac{\langle\Psi_1|\hat{a}_\nu\hat{a}_\mu|\Psi_0\rangle}{\langle\Psi_1|\Psi_0\rangle}. \tag{D.1}$$

If a Thouless state $|\Psi_0\rangle$ can be written as

$$|\Psi_0\rangle = \exp\left(\sum_{ij} Z^0_{ij}\hat{a}^+_i\hat{a}^+_j\right)|0\rangle, \tag{D.2}$$

then the transition pairing tensor is

$$\begin{aligned}\langle\Psi_1|\Psi_0\rangle\kappa^{10}_{\mu\nu} &= \langle 0|\exp\left(\sum_{ij} Z^{1*}_{ij}\hat{a}_j\hat{a}_i\right)\hat{a}_\nu\hat{a}_\mu|\Psi_0\rangle = \frac{\partial}{\partial Z^{1*}_{\mu\nu}}\langle 0|\exp\left(\sum_{ij} Z^{1*}_{ij}\hat{a}_j\hat{a}_i\right)|\Psi_0\rangle \\ &= \frac{\partial}{\partial Z^{1*}_{\mu\nu}}\langle\Psi_1|\Psi_0\rangle = \frac{\partial}{\partial Z^{1*}_{\mu\nu}}\sqrt{\det(\mathbb{I} - Z^{1*}Z^0)}.\end{aligned} \tag{D.3}$$

$\langle\Psi_1|\Psi_0\rangle$ is the overlap and we have made use of the Onishi formula (3.66). Now we make use of the Jacobi formula for the derivative of the determinant of a matrix

$$\frac{d}{dt}\det A(t) = \mathrm{Tr}\left(C^T(A)\frac{dA(t)}{dt}\right), \tag{D.4}$$

where $C(A)$ is the cofactor of the matrix A. This is related again to the determinant as

$$A \cdot C^T(A) = \det(A)\mathbb{I}, \tag{D.5}$$

therefore

$$\frac{d}{dt}\det A(t) = \det(A)\,\mathrm{Tr}\left(A^{-1}\frac{dA(t)}{dt}\right). \tag{D.6}$$

Applying these relations to our case we obtain

$$\langle\Psi_1|\Psi_0\rangle\kappa^{10}_{\mu\nu} = -\frac{\det(\mathbb{I}-Z^{1*}Z^0)}{2\sqrt{\det(\mathbb{I}-Z^{1*}Z^0)}}\,\mathrm{Tr}\left((\mathbb{I}-Z^{1*}Z^0)^{-1}\frac{\partial(Z^{1*}Z^0)}{\partial Z^{1*}_{\mu\nu}}\right), \tag{D.7}$$

thus

$$\kappa^{10}_{\mu\nu} = -\frac{1}{2}\,\mathrm{Tr}\left((\mathbb{I}-Z^{1*}Z^0)^{-1}\frac{\partial(Z^{1*}Z^0)}{\partial Z^{1*}_{\mu\nu}}\right). \tag{D.8}$$

Now, we use the following identities

$$\begin{aligned}(\mathbb{I}-Z^{1*}Z^0)^{-1}_{ij} &= (\delta_{ij}-\sum_k Z^{1*}_{ik}Z^0_{kj})^{-1},\\ \left(\frac{\partial(Z^{1*}Z^0)}{\partial Z^{1*}_{\mu\nu}}\right)_{ij} &= Z^0_{\nu j}\delta_{i\mu} - Z^0_{\mu j}\delta_{i\nu},\end{aligned} \tag{D.9}$$

where we have made use, in the second identity, the derivative of a second order antisymmetric tensor $A_{\mu\nu}$

$$\frac{dA_{\mu\nu}}{dA_{ij}} = \delta_{\mu i}\delta_{\nu j} - \delta_{\mu j}\delta_{\nu i}. \tag{D.10}$$

Therefore, we have

$$\begin{aligned}\left((\mathbb{I}-Z^{1*}Z^0)^{-1}\frac{\partial(Z^{1*}Z^0)}{\partial Z^{1*}_{\mu\nu}}\right)_{ij} &= \sum_k (\mathbb{I}-Z^{1*}Z^0)^{-1}_{ik}\left(\frac{\partial(Z^{1*}Z^0)}{\partial Z^{1*}_{\mu\nu}}\right)_{kj}\\ &= \sum_k\left((\delta_{ik}-\sum_{k'}Z^{1*}_{ik'}Z^0_{k'k})^{-1}(Z^0_{\nu j}\delta_{k\mu}-Z^0_{\mu j}\delta_{k\nu})\right)\\ &= \left((\delta_{i\mu}-\sum_{k'}Z^{1*}_{ik'}Z^0_{k'\mu})^{-1}Z^0_{\nu i} - (\delta_{i\nu}-\sum_{k'}Z^{1*}_{ik'}Z^0_{k'\nu})^{-1}Z^0_{\mu j}\right).\end{aligned} \tag{D.11}$$

Applying the *trace* operation on both sides

$$\mathrm{Tr}(A) = \sum_i A_{ii}, \tag{D.12}$$

we obtain

$$\begin{aligned}\mathrm{Tr}\left((\mathbb{I}-Z^{1*}Z^{0})^{-1}\frac{\partial(Z^{1*}Z^{0})}{\partial Z^{1*}_{\mu\nu}}\right) &= \sum_i(\delta_{i\mu}-\sum_{k'}Z^{1*}_{ik'}Z^{0}_{k'\mu})^{-1}Z^{0}_{\nu i}-\sum_i(\delta_{i\nu}-\sum_{k'}Z^{1*}_{ik'}Z^{0}_{k'\nu})^{-1}Z^{0}_{\mu i}\\ &= \sum_i(\mathbb{I}-Z^{1*}Z^{0})^{-1}_{i\mu}Z^{0}_{\nu i}-\sum_i(\mathbb{I}-Z^{1*}Z^{0})^{-1}_{i\nu}Z^{0}_{\mu i}\\ &= \left(Z^{0}(\mathbb{I}-Z^{1*}Z^{0})^{-1}\right)_{\nu\mu}-\left(Z^{0}(\mathbb{I}-Z^{1*}Z^{0})^{-1}\right)_{\mu\nu}.\end{aligned} \tag{D.13}$$

Comparing this expression with Eq. (D.8) we obtain

$$\kappa^{10}_{\mu\nu}=\frac{1}{2}\left[\left(Z^{0}(\mathbb{I}-Z^{1*}Z^{0})^{-1}\right)_{\mu\nu}-\left(Z^{0}(\mathbb{I}-Z^{1*}Z^{0})^{-1}\right)_{\nu\mu}\right], \tag{D.14}$$

and this expression is the definition of a skew-symmetric matrix, ie, $A=\frac{1}{2}(A-A^{T})$, therefore

$$\kappa^{10}=Z^{0}(\mathbb{I}-Z^{1*}Z^{0})^{-1}. \tag{D.15}$$

For κ^{01*}, a similar derivation holds, using the derivative with respect $Z_{\mu\nu}$ instead of $Z^{*}_{\mu\nu}$, to obtain

$$\kappa^{01*}=(\mathbb{I}-Z^{1*}Z^{0})^{-1}Z^{1*}. \tag{D.16}$$

For the transition density matrix ρ^{10}, we first write the Bogoliubov transformation

$$\beta_k=\sum_l U^{*}_{lk}\hat{a}_l+V^{*}_{lk}\hat{a}^{+}_l, \tag{D.17}$$

and we define a new quasiparticle annihilation operator as

$$\hat{\tilde{\beta}}_k=\sum_{k'}U^{*-1}_{k'k}\hat{\beta}_{k'}. \tag{D.18}$$

Since $\hat{\beta}$ annihilates the quasiparticle vacuum, $\hat{\tilde{\beta}}$ does as well. Explicitly

$$\hat{\tilde{\beta}}_k=\sum_{k'l}U^{*-1}_{k'k}U^{*}_{lk'}\hat{a}_l+U^{*-1}_{k'k}V^{*}_{lk'}\hat{a}^{+}_l=\hat{a}_k+\sum_l Z_{lk}\hat{a}^{+}_l, \tag{D.19}$$

and, analogously

$$\hat{\tilde{\beta}}^{+}_k=\hat{a}^{+}_k+\sum_l Z^{*}_{lk}\hat{a}_l. \tag{D.20}$$

Using the fact that $\langle\Psi_1|\hat{\tilde{\beta}}^+_\nu = 0$ we write

$$\langle\Psi_1|\hat{a}^+_\nu\hat{a}_\mu + \sum_l Z^{1*}_{l\nu}\hat{a}_l\hat{a}_\mu|\Psi_0\rangle = 0, \tag{D.21}$$

thus

$$\langle\Psi_1|\hat{a}^+_\nu\hat{a}_\mu|\Psi_0\rangle = -\sum_l Z^{1*}_{l\nu}\langle\Psi_1|\hat{a}_l\hat{a}_\mu|\Psi_0\rangle = -\sum_l Z^{1*}_{l\nu}\langle\Psi_1|\Psi_0\rangle\kappa^{10}_{\mu l}. \tag{D.22}$$

Finally, the transition density matrix is obtained using the transition pairing tensor

$$\rho^{10}_{\mu\nu} = \frac{\langle\Psi_1|\hat{a}^+_\nu\hat{a}_\mu|\Psi_0\rangle}{\langle\Psi_1|\Psi_0\rangle} = -\sum_l \kappa^{10}_{\mu l}Z^{1*}_{l\nu} = -Z^0(\mathbb{I} - Z^{1*}Z^0)^{-1}Z^{1*}. \tag{D.23}$$

Appendix E

Sum rules for the projected states

As the symmetry-violating HFB state is a superposition of states with good particle, spin and isospin numbers, the so called projected states $|AST\rangle$

$$|\Psi\rangle = \sum_{AST} |AST\rangle. \tag{E.1}$$

We obtain, for a properly normalized HFB quasiparticle vacuum,

$$\langle\Psi|\Psi\rangle = 1 = \sum_{AST}\langle\Psi|AST\rangle = \sum_{AST}\langle\Psi|\hat{P}^A\hat{P}^S\hat{P}^T|\Psi\rangle = \sum_{AST} I_{AST}, \tag{E.2}$$

that is, the sum of the projected norms has to be unity, as physically expected since there is no loss in probability. The former equation not only becomes a benchmark for the correct implementation of the symmetry-restoration techniques, but it is also a useful mechanism to see which states contribute more to the quasiparticle vacuum. The projected energies also follow a sum rule. The HFB energy can be rewritten as

$$E_{HFB} = \langle\Psi|\hat{H}|\Psi\rangle = \sum_{AST}\langle\Psi|\hat{H}|AST\rangle = \sum_{AST} I_{AST}E_{AST}, \tag{E.3}$$

where

$$E_{AST} = \frac{\langle\Psi|\hat{H}|\Psi\rangle}{\langle\Psi|AST\rangle}. \tag{E.4}$$

The numerical accuracy of the symmetry-restoration implementation can be tested using Eqs. (E.2, E.3) [Dob07].

E.1 Non-diagonal sum rule

An analogous sum-rule formula for the case of non-diagonal matrix elements, that is, with generally different ket and bra states, can be implemented. We will use again the deuteron transfer as an example to write a non-diagonal sum rule. The HFB state $|\Psi\rangle$ is a superposition of the projected states $|AST\rangle$, the deuteron transfer, associated with the pair addition operator $\hat{D}_0^+$, needs to fulfil

$$\sum_{ASTA'S'T'} \langle AST|D_0^+|A'S'T'\rangle = \langle \Psi_L|D_0^+|\Psi_R\rangle. \tag{E.5}$$

D_0^+ is

$$D_0^+ = \sum_\ell \sqrt{\frac{2\ell+1}{2}} \left(\hat{a}^+_{\ell\frac{1}{2}\frac{1}{2}}\hat{a}^+_{\ell\frac{1}{2}\frac{1}{2}}\right)^{L=0,S=1,T=0}_{L_z=0,S_z=0,T_z=0}. \tag{E.6}$$

The rhs of (E.5) is written in the uncoupled (single-particle) basis as

$$\langle\Psi|D_0^+|\Psi'\rangle = \sum_{\ell m_i m_j \sigma_i\sigma_j\tau_i\tau_j} C^{00}_{\ell m_i \ell m_j} C^{10}_{\frac{1}{2}\sigma_i\frac{1}{2}\sigma_j} C^{00}_{\frac{1}{2}\tau_i\frac{1}{2}\tau_j} \langle\Psi_L|\hat{a}^+_{\ell m_i\frac{1}{2}\sigma_i\frac{1}{2}\tau_i}\hat{a}^+_{\ell m_j\frac{1}{2}\sigma_j\frac{1}{2}\tau_j}|\Psi_R\rangle. \tag{E.7}$$

For the lhs, the projected states can be written as $|AST\rangle = \hat{P}^A\hat{P}^S_{00}\hat{P}^T_{00}|\Psi\rangle$. Using the transformation rule (4.133) again, we obtain for the sum rule

$$\sum_{ASTA'S'T'} \delta_{TT'}\delta_{A',A-2} C^{S0}_{S'010} \sum_{M\mu'} (-1)^{2\mu'} C^{S0}_{S'M1\mu'} \langle\Psi_L|D^+_{\mu'}\hat{P}^{A'}\hat{P}^{S'}_{M0}\hat{P}^{T'}_{00}|\Psi_R\rangle = \langle\Psi_L|\hat{D}_0^+|\Psi_R\rangle, \tag{E.8}$$

reduced to

$$\sum_{ASTS'} C^{S0}_{S'010} \sum_{M=\pm1,0} C^{S0}_{S'M1-M} \langle\Psi_L|D^+_{-M}\hat{P}^{A-2}\hat{P}^{S'}_{M0}\hat{P}^T_{00}|\Psi_R\rangle = \langle\Psi_L|D_0^+|\Psi_R\rangle. \tag{E.9}$$

Writing down the integrals from the projectors we obtain

$$\begin{aligned}
&\sum_{ASTS'} C^{S0}_{S'010} \sum_{M=\pm1,0} C^{S0}_{S'M1-M} \frac{1}{2\pi}\frac{(2T+1)}{2}\frac{(2S'+1)}{4\pi} \\
&\times \int_0^{2\pi} d\varphi e^{-i\varphi(A-2)} \int_0^\pi d\beta_T \sin(\beta_T) d^T_{00}(\beta_T) \int_0^{2\pi} d\alpha_{S'} e^{iM\alpha_{S'}} \int_0^\pi d\beta_{S'} \sin(\beta_{S'}) d^{S'}_{M0}(\beta_{S'}) \\
&\times \langle\Psi_L|D^+_{-M}\hat{R}(\varphi)\hat{R}(\beta_T)\hat{R}(\alpha_{S'})\hat{R}(\beta_{S'})|\Psi_R\rangle = \langle\Psi_L|\hat{D}_0^+|\Psi_R\rangle,
\end{aligned} \tag{E.10}$$

and the dependence on $\alpha_{S'}$ is removed using the fact that the operator $\hat{R}(\alpha_{S'}) = \exp\left(-i\alpha_{S'}\hat{S'}_z\right)$ commutes with the coupled creation pair as

$$e^{i\alpha_{S'}(\hat{S'}_z - M)}\hat{D}^+_{-M} = \hat{D}^+_{-M}e^{-i\alpha_{S'}\hat{S'}_z}, \tag{E.11}$$

and, since $|\Psi\rangle$ is an axial state with projection zero

$$e^{i\alpha_{S'}\hat{S'}_z}|\Psi\rangle = e^{i\alpha_{S'}S'_z}|\Psi\rangle = |\Psi\rangle, \tag{E.12}$$

the integral in $\alpha_{S'}$ is

$$\int_0^{2\pi} d\alpha_{S'} = 2\pi. \tag{E.13}$$

The non-diagonal sum rule is reduced then to

$$\sum_{ASTS'} C^{S0}_{S'010} \sum_{M=\pm1,0} C^{S0}_{S'M1-M} \frac{1}{2\pi} \frac{(2T+1)}{2} \frac{(2S'+1)}{2} \int_0^{2\pi} d\varphi e^{-i\varphi(A-2)} \int_0^{\pi} d\beta_T \sin(\beta_T) d^T_{00}(\beta_T)$$
$$\times \int_0^{\pi} d\beta_{S'} \sin(\beta_{S'}) d^{S'}_{M0}(\beta_{S'}) \langle \Psi_L | D^+_{-M} | \Psi_R(\varphi, \beta_T, \beta_S) \rangle = \langle \Psi_L | D^+_0 | \Psi_R \rangle. \tag{E.14}$$

The deuteron transfer is just, from formula (E.14), a term in the non-diagonal sum rule,

$$\langle AST | \hat{D}^+_0 | A-2S'T \rangle = \frac{1}{\sqrt{I_{AST} I_{A-2S'T}}} C^{S0}_{S'010} \sum_{M=\pm1,0} C^{S0}_{S'M1-M} \frac{1}{2\pi} \frac{(2T+1)}{2} \frac{(2S'+1)}{2}$$
$$\times \int_0^{2\pi} d\varphi e^{-i\varphi(A-2)} \int_0^{\pi} d\beta_T \sin(\beta_T) d^T_{00}(\beta_T) \int_0^{\pi} d\beta_{S'} \sin(\beta_{S'}) d^{S'}_{M0}(\beta_{S'}) \langle \Psi_L | D^+_{-M} | \Psi_R(\varphi, \beta_T, \beta'_S) \rangle, \tag{E.15}$$

properly rescaled by the norms of the projected states $|AST\rangle$. With the non-diagonal pairing tensor

$$\kappa^{01*}_{ij} = \frac{\langle \Psi_L | \hat{a}^+_i a^+_j | \Psi_R \rangle}{\langle \Psi_L | \Psi_R \rangle}. \tag{E.16}$$

We rewrite the quantities

$$\begin{aligned} \langle \Psi | \hat{D}^+_0 | \Psi' \rangle &= \sum_{\ell m_i m_j \sigma_i \sigma_j \tau_i \tau_j} \sqrt{\frac{2\ell+1}{2}} C^{00}_{\ell m_i \ell m_j} C^{10}_{\frac{1}{2}\sigma_i \frac{1}{2}\sigma_j} C^{00}_{\frac{1}{2}\tau_i \frac{1}{2}\tau_j} \langle \Psi | \hat{a}^+_{\ell m_i \frac{1}{2}\sigma_i \frac{1}{2}\tau_i} \hat{a}^+_{\ell m_j \frac{1}{2}\sigma_j \frac{1}{2}\tau_j} | \Psi' \rangle = \\ &= \sum_{\ell m_i m_j \sigma_i \sigma_j \tau_i \tau_j} \sqrt{\frac{2\ell+1}{2}} C^{00}_{\ell m_i \ell m_j} C^{10}_{\frac{1}{2}\sigma_i \frac{1}{2}\sigma_j} C^{00}_{\frac{1}{2}\tau_i \frac{1}{2}\tau_j} \langle \Psi_L | \Psi_R \rangle \kappa^{01*}_{ij}, \end{aligned} \tag{E.17}$$

where $i = \{\ell, m_i; \frac{1}{2}, \sigma_i, ; \frac{1}{2}, \tau_i\}$, $j = \{\ell, m_j; \frac{1}{2}, \sigma_j, ; \frac{1}{2}, \tau_j\}$ and "0" stands for $|\Psi_L\rangle$ and "1" for $|\Psi_R\rangle$ in the superscripts of the pairing tensor. Analogously,

$$\begin{aligned}\langle\Psi_L|D^+_{-M}|\Psi_R(\varphi,\beta_T,\beta_S)\rangle &= \sum_{\substack{\ell m_i m_j\\ \sigma_i\sigma_j\tau_i\tau_j}} \sqrt{\frac{2\ell+1}{2}} C^{00}_{\ell m_i \ell m_j} C^{1-M}_{\frac{1}{2}\sigma_i\frac{1}{2}\sigma_j} C^{00}_{\frac{1}{2}\tau_i\frac{1}{2}\tau_j} \langle\Psi_L|\hat{a}^+_{\ell m_i\frac{1}{2}\sigma_i\frac{1}{2}\tau_i}\hat{a}^+_{\ell m_j\frac{1}{2}\sigma_j\frac{1}{2}\tau_j}|\Psi_R(\varphi,\beta_T,\beta_S)\rangle \\ &= \sum_{\substack{\ell m_i m_j\\ \sigma_i\sigma_j\tau_i\tau_j}} \sqrt{\frac{2\ell+1}{2}} C^{00}_{\ell m_i \ell m_j} C^{1-M}_{\frac{1}{2}\sigma_i\frac{1}{2}\sigma_j} C^{00}_{\frac{1}{2}\tau_i\frac{1}{2}\tau_j} \langle\Psi_L|\Psi_R(\varphi,\beta_T,\beta_S)\rangle\kappa^{01*}_{ij}(\varphi,\beta_T,\beta_S).\end{aligned} \tag{E.18}$$

Another strong benchmark to test the deuteron transfer formula is to use full projection in spin space, ie, from formula (E.15)

$$\begin{aligned}\langle AST|D^+_0|A-2S'T\rangle &= \frac{1}{\sqrt{I_{AST}I_{A-2S'T}}} C^{S0}_{S'010} \sum_{M=\pm1,0} C^{S0}_{S'M1-M} \frac{1}{2\pi}\frac{(2T+1)}{2}\frac{(2S'+1)}{8\pi^2} \\ &\times \int_0^{2\pi} d\varphi e^{-i\varphi(N-2)} \int_0^{\pi} d\beta_T \sin(\beta_T) d^T_{00}(\beta_T) \int d\Omega_{S'} D^{S'*}_{M0}(\Omega_{S'}) \langle\Psi_L|D^+_{-M}|\Psi_R(\varphi,\beta_T,\Omega_{S'})\rangle,\end{aligned} \tag{E.19}$$

with $\Omega_{S'} = (\alpha_{S'}, \beta_{S'}, \gamma_{S'})$. The results must be the same.

E.2 Non-diagonal sum rule for the projected norms

As we have mentioned, the mean-field state $|\Psi\rangle$ is a superposition of the projected states. For the case of two different mean-field states $|\Psi_R\rangle$, $|\Psi_L\rangle$, we have

$$|\Psi_R\rangle = \sum_{AST} |AST\rangle_R, \tag{E.20}$$

$$|\Psi_L\rangle = \sum_{AST} |AST\rangle_L. \tag{E.21}$$

Making emphasis that the projected states $|AST\rangle$ building up the different mean-field wavefunctions are not the same. Therefore, the non-diagonal sum rule for the projected norms is

$$\langle\Psi_L|\Psi_R\rangle = \sum_{AST}\langle\Psi_L|AST\rangle_R = \sum_{AST}\langle\Psi_L|\hat{P}^A\hat{P}^S\hat{P}^T|\Psi_R\rangle, \tag{E.22}$$

where the mean-field overlap norm $\langle\Psi_L|\Psi_R\rangle$ is evaluated using the pfaffian formula (3.67).

Appendix F

Matrix elements of the angular momentum operator in $\ell-$scheme

The matrix elements of the angular-momentum operator in the single-particle basis are needed to evaluate its expectation value over the quasiparticle vacuum to benchmark the spherical symmetry of the system.

To evaluate the matrix elements of $\hat{L}$, $l_{mm'}$. We use the fact that

$$\begin{aligned} \hat{L}_x &= \frac{1}{2}(\hat{L}^+ + \hat{L}^-), \\ \hat{L}_y &= \frac{1}{2i}(\hat{L}^+ - \hat{L}^-), \\ \hat{L}_z \left|\ell m\right\rangle &= m \left|\ell m\right\rangle, \end{aligned} \tag{F.1}$$

where

$$\hat{L}^\pm \left|\ell m\right\rangle = \sqrt{\ell(\ell+1) - m(m\pm 1)} \left|\ell m \pm 1\right\rangle. \tag{F.2}$$

The matrix elements $l_{mm'} = \langle \ell m' | \hat{L} | \ell m \rangle$ can now be evaluated

$$\begin{aligned} l_{mm'} = m\delta_{mm'} &+ \frac{1}{2}(1-i)\sqrt{\ell(\ell+1) - m(m+1)}\delta_{m+1,m'} \\ &+ \frac{1}{2}(1+i)\sqrt{\ell(\ell+1) - m(m-1)}\delta_{m-1,m'}, \end{aligned} \tag{F.3}$$

in the form of a tridiagonal matrix.

Appendix G

Analytical expressions of the deuteron transfer for the $A = 2, 4$ particles (holes) cases

The powerful tools of algebraic models are used in this Appendix to derive the deuteron transfer from an initial $|A = 2, S = 1, T = 0\rangle$ state to a $|A = 4, S = 0, T = 0\rangle$ state by means of only the commutations relations of the generators of the $SO(8)$ algebra. The general case was already reviewed in Appendix A.

The deuteron addition transfer is defined as

$$P_d = \langle A = 4, S = 0, T = 0|\hat{D}_0^+|A = 2, S = 1, T = 0\rangle. \tag{G.1}$$

We observe that there is only one way to build up the state $|A = 2, S = 1, T = 0\rangle$ from the isoscalar and isovector pairs considered in the $SO(8)$ model

$$|A = 2, S = 1, T = 0\rangle = \hat{D}_0^+|0\rangle, \tag{G.2}$$

and two possible ways to build up the state $|A = 4, S = 0, T = 0\rangle$, from the coupling of two isoscalar pairs or coupling of two isovector pairs

$$|A = 4, S = 0, T = 0\rangle = \left[\alpha \left(\hat{P}^+\hat{P}^+\right)^{S=0T=0} + \beta \left(\hat{D}^+\hat{D}^+\right)^{S=0T=0}\right]|0\rangle. \tag{G.3}$$

The pair operators $\hat{P}^+, \hat{D}^+, \hat{P}, \hat{D}$ are quasispin operators which can be written as a linear combination of the generators of the $SO(8)$ algebra, as seen in Table (2.1). Their commutators

are going to be equal to a linear combination of the rest of the generators of the algebra, in general being a scalar (spin or isospin equal to zero), vector (spin or isospin equal to one) or tensor (spin or isospin equal to two).

The different commutators between the pair operators are then

$$\begin{aligned}
[\hat{P}_{\mu'}, \hat{P}^+_{\mu}] =& \hat{Q}_0\delta_{\mu 0}\delta_{\mu' 0} - \hat{T}_-\delta_{\mu 0}\delta_{\mu' 1} - \hat{T}_+\delta_{\mu 0}\delta_{\mu' -1} - \hat{T}_+\delta_{\mu 1}\delta_{\mu' 0} \\
&+ (\hat{Q}_0 - \hat{T}_0)\delta_{\mu 1}\delta_{\mu' 1} + (\hat{Q}_0 + \hat{T}_0)\delta_{\mu -1}\delta_{\mu' -1} - \hat{T}_-\delta_{\mu -1}\delta_{\mu' 0}, \\
[\hat{D}_{\mu'}, \hat{D}^+_{\mu}] =& \hat{Q}_0\delta_{\mu 0}\delta_{\mu' 0} - \hat{S}_-\delta_{\mu 0}\delta_{\mu' 1} - \hat{S}_+\delta_{\mu 0}\delta_{\mu' -1} - \hat{S}_+\delta_{\mu 1}\delta_{\mu' 0} \\
&+ (\hat{Q}_0 - \hat{S}_0)\delta_{\mu 1}\delta_{\mu' 1} + (\hat{Q}_0 + \hat{S}_0)\delta_{\mu -1}\delta_{\mu' -1} - \hat{S}_-\delta_{\mu -1}\delta_{\mu' 0},
\end{aligned} \tag{G.4}$$

$$\begin{aligned}
[\hat{P}_{\mu'}, \hat{D}^+_{\mu}] =& - \hat{E}_{00}\delta_{\mu 0}\delta_{\mu' 0} + \hat{E}_{0-1}\delta_{\mu 0}\delta_{\mu' 1} - \hat{E}_{01}\delta_{\mu 0}\delta_{\mu' -1} \\
&+ \hat{E}_{10}\delta_{\mu 1}\delta_{\mu' 0} - \hat{E}_{1-1}\delta_{\mu 1}\delta_{\mu' 1} + \hat{E}_{11}\delta_{\mu 1}\delta_{\mu' -1} \\
&- \hat{E}_{-10}\delta_{\mu -1}\delta_{\mu' 0} + \hat{E}_{-1-1}\delta_{\mu -1}\delta_{\mu' 1} - \hat{E}_{-11}\delta_{\mu -1}\delta_{\mu' -1}, \\
[\hat{D}_{\mu'}, \hat{P}^+_{\mu}] =& - \hat{E}_{00}\delta_{\mu 0}\delta_{\mu' 0} + \hat{E}_{-10}\delta_{\mu 0}\delta_{\mu' 1} - \hat{E}_{10}\delta_{\mu 0}\delta_{\mu' -1} \\
&+ \hat{E}_{01}\delta_{\mu 1}\delta_{\mu' 0} - \hat{E}_{-11}\delta_{\mu 1}\delta_{\mu' 1} + \hat{E}_{11}\delta_{\mu 1}\delta_{\mu' -1} \\
&- \hat{E}_{0-1}\delta_{\mu -1}\delta_{\mu' 0} + \hat{E}_{-1-1}\delta_{\mu -1}\delta_{\mu' 1} - \hat{E}_{1-1}\delta_{\mu -1}\delta_{\mu' -1}.
\end{aligned} \tag{G.5}$$

We apply the Hamiltonian (2.17) to the state (G.3), and for that we will need the following identities

$$\begin{aligned}
\hat{\hat{H}}\hat{P}^+_{\mu_1}\hat{P}^+_{\mu_2} &= \hat{P}^+_{\mu_1}\hat{P}^+_{\mu_2}\hat{\hat{H}} + \hat{P}^+_{\mu_1}[\hat{\hat{H}}, \hat{P}^+_{\mu_2}] + [\hat{\hat{H}}, \hat{P}^+_{\mu_1}]\hat{P}^+_{\mu_2}, \\
\hat{\hat{H}}\hat{D}^+_{\nu_1}\hat{D}^+_{\nu_2} &= \hat{D}^+_{\nu_1}\hat{D}^+_{\nu_2}\hat{H} + \hat{D}^+_{\nu_1}[\hat{H}, \hat{D}^+_{\nu_2}] + [\hat{H}, \hat{D}^+_{\nu_1}]\hat{D}^+_{\nu_2}.
\end{aligned} \tag{G.6}$$

Thus

$$\begin{aligned}
\hat{\hat{H}}|A=4, S=0, T=0\rangle = \Bigg[\alpha \sum_{\mu_1\mu_2} C^{00}_{1\mu_1 1\mu_2}\Big(\hat{P}^+_{\mu_1}[\hat{H}, \hat{P}^+_{\mu_2}] + [\hat{H}, \hat{P}^+_{\mu_1}]\hat{P}^+_{\mu_2}\Big) + \\
+ \beta \sum_{\nu_1\nu_2} C^{00}_{1\nu_1 1\nu_2}\Big(\hat{D}^+_{\nu_1}[\hat{H}, \hat{D}^+_{\nu_2}] + [\hat{H}, \hat{D}^+_{\nu_1}]\hat{D}^+_{\nu_2}\Big)\Bigg]|0\rangle,
\end{aligned} \tag{G.7}$$

with

$$\begin{aligned}
[\hat{H}, \hat{P}^+_{\mu'}] &= -(1-x)\sum_{\mu}\hat{P}^+_{\mu}[\hat{P}_{\mu}, \hat{P}^+_{\mu'}] - (1+x)\sum_{\nu}\hat{D}^+_{\nu}[\hat{D}_{\nu}, \hat{P}^+_{\mu'}], \\
[\hat{H}, \hat{D}^+_{\nu'}] &= -(1-x)\sum_{\mu}\hat{P}^+_{\mu}[\hat{P}_{\mu}, \hat{D}^+_{\nu'}] - (1+x)\sum_{\nu}\hat{D}^+_{\nu}[\hat{D}_{\nu}, \hat{D}^+_{\nu'}].
\end{aligned} \tag{G.8}$$

It can be shown by direct application on the vacuum that the following commutators obey

$$\begin{aligned}
[\hat{P}_\mu, \hat{P}^+_{\mu'}]|0\rangle &= \Omega\delta_{\mu\mu'}(\delta_{\mu 1} + \delta_{\mu 0} + \delta_{\mu -1})|0\rangle, \\
[\hat{D}_\nu, \hat{D}^+_{\nu'}]|0\rangle &= \Omega\delta_{\nu\nu'}(\delta_{\nu 1} + \delta_{\nu 0} + \delta_{\nu -1})|0\rangle, \\
[\hat{D}_\nu, \hat{P}^+_{\mu}]|0\rangle &= [\hat{P}_\mu, \hat{D}^+_{\nu}]|0\rangle = 0,
\end{aligned} \tag{G.9}$$

therefore

$$\begin{aligned}
[\hat{H}, \hat{P}^+_{\mu_2}]|0\rangle &= -(1-x)(\delta_{\mu_2 1} + \delta_{\mu_2 0} + \delta_{\mu_2 -1})\Omega\hat{P}^+_{\mu_2}|0\rangle, \\
[\hat{H}, \hat{D}^+_{\nu_2}]|0\rangle &= -(1+x)(\delta_{\nu_2 1} + \delta_{\nu_2 0} + \delta_{\nu_2 -1})\Omega\hat{D}^+_{\nu_2}|0\rangle.
\end{aligned} \tag{G.10}$$

We now evaluate the term $[\hat{H}, \hat{P}^+_{\mu_1}]\hat{P}^+_{\mu_2}$

$$\begin{aligned}
[\hat{H}, \hat{P}^+_{\mu_1}]\hat{P}^+_{\mu_2} &= -(1-x)\sum_\mu \hat{P}^+_\mu[\hat{P}_\mu, \hat{P}^+_{\mu_1}]\hat{P}^+_{\mu_2} - (1+x)\sum_\nu \hat{D}^+_\nu[\hat{D}_\nu, \hat{P}^+_{\mu_1}]\hat{P}^+_{\mu_2} \\
&= -(1-x)\sum_\mu \hat{P}^+_\mu\Big(\hat{Q}_0\hat{P}^+_{\mu_2}\delta_{\mu_1 0}\delta_{\mu 0} - \hat{T}_-\hat{P}^+_{\mu_2}\delta_{\mu_1 0}\delta_{\mu 1} - \hat{T}_+\hat{P}^+_{\mu_2}\delta_{\mu_1 0}\delta_{\mu -1} - \hat{T}_+\hat{P}^+_{\mu_2}\delta_{\mu_1 1}\delta_{\mu 0} \\
&\quad + (\hat{Q}_0 - \hat{T}_0)\hat{P}^+_{\mu_2}\delta_{\mu_1 1}\delta_{\mu 1} + (\hat{Q}_0 + \hat{T}_0)\hat{P}^+_{\mu_2}\delta_{\mu_1 -1}\delta_{\mu -1} - \hat{T}_-\hat{P}^+_{\mu_2}\delta_{\mu_1 -1}\delta_{\mu 0}\Big) \\
&\quad - (1+x)\sum_\nu \hat{D}^+_\nu\Big(- \hat{E}_{00}\hat{P}^+_{\mu_2}\delta_{\mu_1 0}\delta_{\nu 0} + \hat{E}_{-10}\hat{P}^+_{\mu_2}\delta_{\mu_1 0}\delta_{\nu 1} - \hat{E}_{10}\hat{P}^+_{\mu_2}\delta_{\mu_1 0}\delta_{\nu -1} \\
&\quad + \hat{E}_{01}\hat{P}^+_{\mu_2}\delta_{\mu_1 1}\delta_{\nu 0} - \hat{E}_{-11}\hat{P}^+_{\mu_2}\delta_{\mu_1 1}\delta_{\nu 1} + \hat{E}_{11}\hat{P}^+_{\mu_2}\delta_{\mu_1 1}\delta_{\nu -1} \\
&\quad - \hat{E}_{0-1}\hat{P}^+_{\mu_2}\delta_{\mu_1 -1}\delta_{\nu 0} + \hat{E}_{-1-1}\hat{P}^+_{\mu_2}\delta_{\mu_1 -1}\delta_{\nu 1} - \hat{E}_{1-1}\hat{P}^+_{\mu_2}\delta_{\mu_1 -1}\delta_{\nu -1}\Big),
\end{aligned} \tag{G.11}$$

where we need to make use of the commutation relations of $\hat{P}^+$ with the rest of the generators

of the $SO(8)$ algebra, tabulated in Table (G.1), becoming

$$
\begin{aligned}
[\hat{H},\hat{P}^+_{\mu_1}]\hat{P}^+_{\mu_2} = &-(1-x)\sum_{\mu}\hat{P}^+_{\mu}\Big[(\hat{P}^+_{\mu_2}\hat{Q}_0-\hat{P}^+_{\mu_2})\delta_{\mu_10}\delta_{\mu 0}-(\hat{P}^+_{\mu_2}\hat{T}_-+\hat{P}^+_{\mu_2-1})\delta_{\mu_10}\delta_{\mu 1}\\
&-(\hat{P}^+_{\mu_2}\hat{T}_++\hat{P}^+_{\mu_2+1})\delta_{\mu_10}\delta_{\mu -1}-(\hat{P}^+_{\mu_2}\hat{T}_++\hat{P}^+_{\mu_2+1})\delta_{\mu_11}\delta_{\mu 0}+\hat{P}^+_{\mu_2}(\hat{Q}_0-\hat{T}_0-\mu_2-1)\delta_{\mu_11}\delta_{\mu 1}\\
&+\hat{P}^+_{\mu_2}(\hat{Q}_0+\hat{T}_0+\mu_2-1)\delta_{\mu_1-1}\delta_{\mu -1}-(\hat{P}^+_{\mu_2}\hat{T}_-+\hat{P}^+_{\mu_2-1})\delta_{\mu_1-1}\delta_{\mu 0}\Big]\\
&-(1+x)\sum_{\nu}\hat{D}^+_{\nu}\Big[-(\hat{P}^+_{\mu_2}\hat{E}_{00}+\hat{D}^+_{\mu_2}\delta_{\mu_20})\delta_{\mu_10}\delta_{\nu 0}+(\hat{P}^+_{\mu_2}\hat{E}_{-10}+\hat{D}^+_{\mu_2-1}\delta_{\mu_20})\delta_{\mu_10}\delta_{\nu 1}\\
&-(\hat{P}^+_{\mu_2}\hat{E}_{10}-\hat{D}^+_{\mu_2+1}\delta_{\mu_20})\delta_{\mu_10}\delta_{\nu -1}+(\hat{P}^+_{\mu_2}\hat{E}_{01}+\hat{D}^+_{\mu_2+1}\delta_{\mu_2-1})\delta_{\mu_11}\delta_{\nu 0}\\
&-(\hat{P}^+_{\mu_2}\hat{E}_{-11}+\hat{D}^+_{\mu_2}\delta_{\mu_2-1})\delta_{\mu_11}\delta_{\nu 1}+(\hat{P}^+_{\mu_2}\hat{E}_{11}-\hat{D}^+_{-\mu_2}\delta_{\mu_2-1})\delta_{\mu_11}\delta_{\nu -1}\\
&-(\hat{P}^+_{\mu_2}\hat{E}_{0-1}-\hat{D}^+_{\mu_2-1}\delta_{\mu_21})\delta_{\mu_1-1}\delta_{\nu 0}+(\hat{P}^+_{\mu_2}\hat{E}_{-1-1}-\hat{D}^+_{-\mu_2}\delta_{\mu_21})\delta_{\mu_1-1}\delta_{\nu 1}\\
&-(\hat{P}^+_{\mu_2}\hat{E}_{1-1}+\hat{D}^+_{\mu_2}\delta_{\mu_21})\delta_{\mu_1-1}\delta_{\nu -1}\Big).
\end{aligned}
\tag{G.12}
$$

We reduce the former expression knowing that it is applied to the bare vacuum $|0\rangle$

$$
\begin{aligned}
[\hat{H},\hat{P}^+_{\mu_1}]\hat{P}^+_{\mu_2}|0\rangle = &\Big\{-(1-x)\sum_{\mu}\hat{P}^+_{\mu}\Big[(\hat{P}^+_{\mu_2}\hat{Q}_0-\hat{P}^+_{\mu_2})\delta_{\mu_10}\delta_{\mu 0}-\hat{P}^+_{\mu_2-1}\delta_{\mu_10}\delta_{\mu 1}-\hat{P}^+_{\mu_2+1}\delta_{\mu_10}\delta_{\mu -1}\\
&-\hat{P}^+_{\mu_2+1}\delta_{\mu_11}\delta_{\mu 0}+\hat{P}^+_{\mu_2}(\hat{Q}_0-\mu_2-1)\delta_{\mu_11}\delta_{\mu 1}+\hat{P}^+_{\mu_2}(\hat{Q}_0+\mu_2-1)\delta_{\mu_1-1}\delta_{\mu -1}-\hat{P}^+_{\mu_2-1}\delta_{\mu_1-1}\delta_{\mu 0}\Big]\\
&-(1+x)\sum_{\nu}\hat{D}^+_{\nu}\Big(-\hat{D}^+_{\mu_2}\delta_{\mu_20}\delta_{\mu_10}\delta_{\nu 0}+\hat{D}^+_{\mu_2-1}\delta_{\mu_20}\delta_{\mu_10}\delta_{\nu 1}+\hat{D}^+_{\mu_2+1}\delta_{\mu_20}\delta_{\mu_10}\delta_{\nu -1}\\
&+\hat{D}^+_{\mu_2+1}\delta_{\mu_2-1}\delta_{\mu_11}\delta_{\nu 0}-\hat{D}^+_{\mu_2}\delta_{\mu_2-1}\delta_{\mu_11}\delta_{\nu 1}-\hat{D}^+_{-\mu_2}\delta_{\mu_2-1}\delta_{\mu_11}\delta_{\nu -1}\\
&+\hat{D}^+_{\mu_2-1}\delta_{\mu_21}\delta_{\mu_1-1}\delta_{\nu 0}-\hat{D}^+_{-\mu_2}\delta_{\mu_21}\delta_{\mu_1-1}\delta_{\nu 1}-\hat{D}^+_{\mu_2}\delta_{\mu_21}\delta_{\mu_1-1}\delta_{\nu -1}\Big)\Big\}|0\rangle,
\end{aligned}
\tag{G.13}
$$

finally obtaining the expression

$$
\begin{aligned}
[\hat{H},\hat{P}^+_{\mu_1}]\hat{P}^+_{\mu_2}|0\rangle = \Big\{ &-(1-x)\Big[\hat{P}^+_0(\hat{P}^+_{\mu_2}\hat{Q}_0-\hat{P}^+_{\mu_2})\delta_{\mu_1 0}-\hat{P}^+_1\hat{P}^+_{\mu_2-1}\delta_{\mu_1 0}-\hat{P}^+_{-1}\hat{P}^+_{\mu_2+1}\delta_{\mu_1 0}\\
&-\hat{P}^+_0\hat{P}^+_{\mu_2+1}\delta_{\mu_1 1}+\hat{P}^+_1\hat{P}^+_{\mu_2}(\hat{Q}_0-\mu_2-1)\delta_{\mu_1 1}+\hat{P}^+_{-1}\hat{P}^+_{\mu_2}(\hat{Q}_0+\mu_2-1)\delta_{\mu_1-1}-\hat{P}^+_0\hat{P}^+_{\mu_2-1}\delta_{\mu_1-1}\Big]\\
&-(1+x)\Big(-\hat{D}^+_0\hat{D}^+_{\mu_2}\delta_{\mu_2 0}\delta_{\mu_1 0}+\hat{D}^+_1\hat{D}^+_{\mu_2-1}\delta_{\mu_2 0}\delta_{\mu_1 0}+\hat{D}^+_{-1}\hat{D}^+_{\mu_2+1}\delta_{\mu_2 0}\delta_{\mu_1 0}+\hat{D}^+_0\hat{D}^+_{\mu_2+1}\delta_{\mu_2-1}\delta_{\mu_1 1}\\
&-\hat{D}^+_1\hat{D}^+_{\mu_2}\delta_{\mu_2-1}\delta_{\mu_1 1}-\hat{D}^+_{-1}\hat{D}^+_{-\mu_2}\delta_{\mu_2-1}\delta_{\mu_1 1}+\hat{D}^+_0\hat{D}^+_{\mu_2-1}\delta_{\mu_2 1}\delta_{\mu_1-1}-\hat{D}^+_1\hat{D}^+_{-\mu_2}\delta_{\mu_2 1}\delta_{\mu_1-1}\\
&-\hat{D}^+_{-1}\hat{D}^+_{\mu_2}\delta_{\mu_2 1}\delta_{\mu_1-1}\Big)\Big\}|0\rangle.
\end{aligned}
\tag{G.14}
$$

In a similar fashion, for the evaluation of the term $[\hat{H},\hat{D}^+_{\nu_1}]\hat{D}^+_{\nu_2}$ we obtain

$$
\begin{aligned}
[\hat{H},\hat{D}^+_{\nu_1}]\hat{D}^+_{\nu_2}|0\rangle = \Big\{ &-(1-x)\Big(-\hat{P}^+_0\hat{P}^+_{\nu_2}\delta_{\nu_2 0}\delta_{\nu_1 0}+\hat{P}^+_1\hat{P}^+_{\nu_2-1}\delta_{\nu_2 0}\delta_{\nu_1 0}+\hat{P}^+_{-1}\hat{P}^+_{\nu_2+1}\delta_{\nu_2 0}\delta_{\nu_1 0}+\hat{P}^+_0\hat{P}^+_{\nu_2+1}\delta_{\nu_2-1}\delta_{\nu_1 1}\\
&-\hat{P}^+_1\hat{P}^+_{\nu_2}\delta_{\nu_2-1}\delta_{\nu_1 1}-\hat{P}^+_{-1}\hat{P}^+_{-\nu_2}\delta_{\nu_2-1}\delta_{\nu_1 1}+\hat{P}^+_0\hat{P}^+_{\nu_2-1}\delta_{\nu_2 1}\delta_{\nu_1-1}-\hat{P}^+_1\hat{P}^+_{-\nu_2}\delta_{\nu_2 1}\delta_{\nu_1-1}\\
&-\hat{P}^+_{-1}\hat{P}^+_{\nu_2}\delta_{\nu_2 1}\delta_{\nu_1-1}\Big)\\
&-(1+x)\Big[\hat{D}^+_0(\hat{D}^+_{\nu_2}\hat{Q}_0-\hat{D}_{\nu_2})\delta_{\nu_1 0}-\hat{D}^+_1\hat{D}^+_{\nu_2-1}\delta_{\nu_1 0}-\hat{D}^+_{-1}\hat{D}^+_{\nu_2+1}\delta_{\nu_1 0}-\hat{D}^+_0\hat{D}^+_{\nu_2+1}\delta_{\nu_1 1}\\
&+\hat{D}^+_1\hat{D}^+_{\nu_2}(\hat{Q}_0-\nu_2-1)\delta_{\nu_1 1}+\hat{D}^+_{-1}\hat{D}^+_{\nu_2}(\hat{Q}_0+\nu_2-1)\delta_{\nu_1-1}-\hat{D}^+_0\hat{D}^+_{\nu_2-1}\delta_{\nu_1-1}\Big]\Big\}|0\rangle.
\end{aligned}
\tag{G.15}
$$

We have now all the necessary terms for writing the final expression

$$
\begin{aligned}
\hat{H}|A=4,S=0,T=0\rangle = \Big\{ &\frac{\alpha}{\sqrt{3}}\Big(-\hat{P}^+_0[\hat{H},\hat{P}^+_0]-[\hat{H},\hat{P}^+_0]\hat{P}^+_0+\hat{P}^+_1[\hat{H},\hat{P}^+_{-1}]+[\hat{H},\hat{P}^+_1]\hat{P}^+_{-1}\\
&+\hat{P}^+_{-1}[\hat{H},\hat{P}^+_1]+[\hat{H},\hat{P}^+_{-1}]\hat{P}^+_1\Big)\\
&+\frac{\beta}{\sqrt{3}}\Big(-\hat{D}^+_0[\hat{H},\hat{D}^+_0]-[\hat{H},\hat{D}^+_0]\hat{D}^+_0+\hat{D}^+_1[\hat{H},\hat{D}^+_{-1}]+[\hat{H},\hat{D}^+_1]\hat{D}^+_{-1}\\
&+\hat{D}^+_{-1}[\hat{H},\hat{D}^+_1]+[\hat{H},\hat{D}^+_{-1}]\hat{D}^+_1\Big)\Big\}|0\rangle,
\end{aligned}
\tag{G.16}
$$

explicitly

$$
\begin{aligned}
-\hat{P}_0^+[\hat{H},\hat{P}_0^+]-[\hat{H},\hat{P}_0^+]\hat{P}_0^+ &= (1-x)\Omega\hat{P}_0^+\hat{P}_0^+ + (1-x)\Big[(\Omega-1)\hat{P}_0^+\hat{P}_0^+ - \hat{P}_1^+\hat{P}_{-1}^+ - \hat{P}_{-1}^+\hat{P}_1^+\Big] \\
&\quad + (1+x)(-\hat{D}_0^+\hat{D}_0^+ + \hat{D}_1^+\hat{D}_{-1}^+ + \hat{D}_{-1}^+\hat{D}_1^+), \\
\hat{P}_1^+[\hat{H},\hat{P}_{-1}^+]+[\hat{H},\hat{P}_1^+]\hat{P}_{-1}^+ &= -(1-x)\Omega\hat{P}_1^+\hat{P}_{-1}^+ - (1-x)(-\hat{P}_0^+\hat{P}_0^+ + \Omega\hat{P}_1^+\hat{P}_{-1}^+) \\
&\quad - (1+x)(\hat{D}_0^+\hat{D}_0^+ - \hat{D}_1^+\hat{D}_{-1}^+ - \hat{D}_{-1}^+\hat{D}_1^+), \\
\hat{P}_{-1}^+[\hat{H},\hat{P}_1^+]+[\hat{H},\hat{P}_{-1}^+]\hat{P}_1^+ &= -(1-x)\Omega\hat{P}_{-1}^+\hat{P}_1^+ - (1-x)(-\hat{P}_0^+\hat{P}_0^+ + \Omega\hat{P}_{-1}^+\hat{P}_1^+) \\
&\quad - (1+x)(\hat{D}_0^+\hat{D}_0^+ - \hat{D}_1^+\hat{D}_{-1}^+ - \hat{D}_{-1}^+\hat{D}_1^+),
\end{aligned}
\tag{G.17}
$$

$$
\begin{aligned}
-\hat{D}_0^+[\hat{H},\hat{D}_0^+]-[\hat{H},\hat{D}_0^+]\hat{D}_0^+ &= (1+x)\Omega\hat{D}_0^+\hat{D}_0^+ + (1-x)(-\hat{P}_0^+\hat{P}_0^+ + \hat{P}_1^+\hat{P}_{-1}^+ + \hat{P}_{-1}^+\hat{P}_1^+) \\
&\quad + (1+x)\Big[(\Omega-1)\hat{D}_0^+\hat{D}_0^+ - \hat{D}_1^+\hat{D}_{-1}^+ - \hat{D}_{-1}^+\hat{D}_1^+\Big], \\
\hat{D}_1^+[\hat{H},\hat{D}_{-1}^+]+[\hat{H},\hat{D}_1^+]\hat{D}_{-1}^+ &= -(1+x)\Omega\hat{D}_1^+\hat{D}_{-1}^+ - (1-x)(\hat{P}_0^+\hat{P}_0^+ - \hat{P}_1^+\hat{P}_{-1}^+ - \hat{P}_{-1}^+\hat{P}_1^+) \\
&\quad - (1+x)(\Omega\hat{D}_1^+\hat{D}_{-1}^+ - \hat{D}_0^+\hat{D}_0^+), \\
\hat{D}_{-1}^+[\hat{H},\hat{D}_1^+]+[\hat{H},\hat{D}_{-1}^+]\hat{D}_1^+ &= -(1+x)\Omega\hat{D}_{-1}^+\hat{D}_1^+ - (1-x)(\hat{P}_0^+\hat{P}_0^+ - \hat{P}_1^+\hat{P}_{-1}^+ - \hat{P}_{-1}^+\hat{P}_1^+) \\
&\quad - (1+x)(\Omega\hat{D}_{-1}^+\hat{D}_1^+ - \hat{D}_0^+\hat{D}_0^+).
\end{aligned}
\tag{G.18}
$$

Therefore, collecting all the terms

$$
\begin{aligned}
\hat{H}|A=4,S=0,T=0\rangle &= \frac{1}{\sqrt{3}}\Big\{ -\Big[2\alpha(1-x)\Omega+\alpha(1-x)-3\beta(1-x)\Big]\Big[-\hat{P}_0^+\hat{P}_0^+ + \hat{P}_1^+\hat{P}_{-1}^+ + \hat{P}_{-1}^+\hat{P}_1^+\Big] \\
&\quad - \Big[2\beta(1+x)\Omega+\beta(1+x)-3\alpha(1+x)\Big]\Big[-\hat{D}_0^+\hat{D}_0^+ + \hat{D}_1^+\hat{D}_{-1}^+ + \hat{D}_{-1}^+\hat{D}_1^+\Big]\Big\}|0\rangle \\
&= \hat{E}_{A=4,S=0,T=0}\left[\alpha\left(\hat{P}_{\mu_1}^+\hat{P}_{\mu_2}^+\right)^{S=0T=0} + \beta\left(\hat{D}_{\nu_1}^+\hat{D}_{\nu_2}^+\right)^{S=0T=0}\right]|0\rangle,
\end{aligned}
\tag{G.19}
$$

sets up an eigenvalue problem for the complex amplitudes α and β

$$
\begin{pmatrix} -2(1-x)\Omega-(1-x) & 3(1-x) \\ 3(1+x) & -2(1+x)\Omega-(1+x) \end{pmatrix}\begin{pmatrix}\alpha\\ \beta\end{pmatrix} = \hat{E}_{A=4,S=0,T=0}\begin{pmatrix}\alpha\\ \beta\end{pmatrix}. \tag{G.20}
$$

The deuteron transfer is computed as

$$
P_d = \langle 0|(\alpha^*(PP)^{00} + \beta^*(DD)^{00})\hat{D}_0^+\hat{D}_0^+|0\rangle, \tag{G.21}
$$

thus

$$\begin{aligned} P_d = \frac{\alpha^*}{\sqrt{3}}\Big(&- \langle 0|\hat{P}_0\hat{P}_0\hat{D}_0^+\hat{D}_0^+|0\rangle + \langle 0|\hat{P}_1\hat{P}_{-1}\hat{D}_0^+\hat{D}_0^+|0\rangle + \langle 0|\hat{P}_{-1}\hat{P}_1\hat{D}_0^+\hat{D}_0^+|0\rangle\Big) \\ + \frac{\beta^*}{\sqrt{3}}\Big(&- \langle 0|\hat{D}_0\hat{D}_0\hat{D}_0^+\hat{D}_0^+|0\rangle + \langle 0|\hat{D}_1\hat{D}_{-1}\hat{D}_0^+\hat{D}_0^+|0\rangle + \langle 0|\hat{D}_{-1}\hat{D}_1\hat{D}_0^+\hat{D}_0^+|0\rangle\Big), \end{aligned} \tag{G.22}$$

and, computing the terms explicitly

$$\begin{aligned} \langle 0|\hat{P}_0\hat{P}_0\hat{D}_0^+\hat{D}_0^+|0\rangle &= -\Omega, \\ \langle 0|\hat{P}_1\hat{P}_{-1}\hat{D}_0^+\hat{D}_0^+|0\rangle &= \Omega, \\ \langle 0|\hat{P}_{-1}\hat{P}_1\hat{D}_0^+\hat{D}_0^+|0\rangle &= \Omega, \\ \langle 0|\hat{D}_0\hat{D}_0\hat{D}_0^+\hat{D}_0^+|0\rangle &= \Omega(2\Omega-1), \\ \langle 0|\hat{D}_1\hat{D}_{-1}\hat{D}_0^+\hat{D}_0^+|0\rangle &= -\Omega, \\ \langle 0|\hat{D}_{-1}\hat{D}_1\hat{D}_0^+\hat{D}_0^+|0\rangle &= -\Omega, \end{aligned} \tag{G.23}$$

we end up with

$$P_d = \langle A=4,S=0,T=0|\hat{D}_0^+|A=2,S=1,T=0\rangle = \sqrt{3}\Omega\alpha^* - \frac{2\Omega^2+\Omega}{\sqrt{3}}\beta^*. \tag{G.24}$$

We have to make sure that the ket and the bra are properly normalized. To that end, we compute the norm c_{210} of the right state $|A=2,S=1,T=0\rangle$

$$c_{210} = \langle A=2,S=1,T=0|A=2,S=1,T=0\rangle = \langle 0|\hat{D}_0\hat{D}_0^+|0\rangle = \Omega\langle 0|0\rangle = \Omega, \tag{G.25}$$

and the norm c_{400} of left state $|A=4,S=0,T=0\rangle$

$$\langle A=4,S=0,T=0|A=4,S=0,T=0\rangle = \langle 0|[\alpha^*(PP)^{00} + \beta^*(DD)^{00}][\alpha(\hat{P}^+\hat{P}^+)^{00} + \beta(\hat{D}^+\hat{D}^+)^{00}]|0\rangle, \tag{G.26}$$

writing explicitly

$$\begin{aligned} \langle 0|(PP)^{00}(\hat{P}^+\hat{P}^+)^{00}|0\rangle &= \Omega(2\Omega+1), \\ \langle 0|(PP)^{00}(\hat{D}^+\hat{D}^+)^{00}|0\rangle &= -3\Omega, \\ \langle 0|(DD)^{00}(\hat{D}^+\hat{D}^+)^{00}|0\rangle &= \Omega(2\Omega+1), \\ \langle 0|(DD)^{00}(\hat{P}^+\hat{P}^+)^{00}|0\rangle &= -3\Omega, \end{aligned} \tag{G.27}$$

we obtain

$$c_{400} = \langle A=4, S=0, T=0 | A=4, S=0, T=0 \rangle = \Omega \Big[\left(|\alpha|^2 + |\beta|^2 \right) (2\Omega + 1) - 3\alpha^* \beta - 3\alpha \beta^* \Big]. \tag{G.28}$$

Finally, the properly normalized deuteron transfer is obtained as

$$\hat{P}_d = \frac{\langle A=4, S=0, T=0 | \hat{D}_0^+ | A=2, S=1, T=0 \rangle}{\sqrt{c_{210} c_{400}}}. \tag{G.29}$$

A \ B	$\hat{P}^+_\mu$	$\hat{D}^+_\nu$
$\hat{Q}_0$	$-\hat{P}^+_\mu$	$-\hat{D}^+_\nu$
$\hat{T}_0$	$\mu \hat{P}^+_\mu$	0
$\hat{T}_+$	$\hat{P}^+_{\mu+1}$	0
$\hat{T}_-$	$\hat{P}^+_{\mu-1}$	0
$\hat{S}_0$	0	$\nu \hat{D}^+_\nu$
$\hat{S}_+$	0	$\hat{D}^+_{\nu+1}$
$\hat{S}_-$	0	$\hat{D}^+_{\nu-1}$
$\hat{E}_{00}$	$\hat{D}^+_\mu \delta_{\mu 0}$	$\hat{P}^+_\nu \delta_{\nu 0}$
$\hat{E}_{-10}$	$\hat{D}^+_{\mu-1} \delta_{\mu 0}$	$-\hat{P}^+_{-\nu-1} \delta_{\nu 1}$
$\hat{E}_{10}$	$-\hat{D}^+_{\mu+1} \delta_{\mu 0}$	$\hat{P}^+_{\nu+1} \delta_{\nu -1}$
$\hat{E}_{0-1}$	$-\hat{D}^+_{\mu-1} \delta_{\mu 1}$	$\hat{P}^+_{\nu-1} \delta_{\nu 0}$
$\hat{E}_{01}$	$\hat{D}^+_{\mu+1} \delta_{\mu -1}$	$-\hat{P}^+_{\nu+1} \delta_{\nu 0}$
$\hat{E}_{-1-1}$	$-\hat{D}^+_{-\mu} \delta_{\mu 1}$	$-\hat{P}^+_{-\nu} \delta_{\nu 1}$
$\hat{E}_{1-1}$	$\hat{D}^+_\mu \delta_{\mu 1}$	$\hat{P}^+_\nu \delta_{\nu -1}$
$\hat{E}_{-11}$	$\hat{D}^+_\mu \delta_{\mu -1}$	$\hat{P}^+_\nu \delta_{\nu 1}$
$\hat{E}_{11}$	$-\hat{D}^+_{-\mu} \delta_{\mu -1}$	$-\hat{P}^+_{-\nu} \delta_{\nu -1}$

Table G.1: Evaluation of commutators $[A, B]$ of the $SO(8)$ algebra.

G.1 Analytical computation of the projected norms

For the $A = 2$ and $A = 4$ cases, it is possible to compute analytical expressions for the norms of the projected states. First, we are concerned with particle-number projected states, which have the form

$$|A\rangle = \frac{(\hat{Z}^+)^{A/2}}{(A/2)!}|0\rangle, \tag{G.30}$$

where $\hat{Z}^+ = Z^{01}\hat{P}_0^+ + Z^{10}\hat{D}_0^+$, with $Z^{01} = \cos(\alpha/2)e^{i\varphi}$ and $Z^{10} = \sin(\alpha/2)e^{-i\varphi}$, is the Thouless pair, for $A = 2, 4$ we obtain

$$\begin{aligned} |2\rangle &= \hat{Z}^+|0\rangle, \\ |4\rangle &= \frac{1}{2}(\hat{Z}^+)^2|0\rangle. \end{aligned} \tag{G.31}$$

To obtain projected states on spin and isospin, we need to apply the convenient projection operators. For the state $|AST\rangle = |A = 2, S = 1, T = 0\rangle$ we will have then

$$|A = 2, S = 1, T = 0\rangle = \hat{P}^1\hat{P}^0|2\rangle = \frac{3}{8\pi^2}\frac{1}{8\pi^2}\int d\Omega_T d\Omega_S \hat{D}^{0*}_{00}(\Omega_T)\hat{D}^{1*}_{00}(\Omega_S)\hat{R}_S(\Omega_S)\hat{R}_T(\Omega_T)|2\rangle, \tag{G.32}$$

where, to rotate the state $|A = 2\rangle$, it is equivalent to rotate the Thouless pair

$$\hat{R}_S(\Omega_S)\hat{R}_T(\Omega_T)|2\rangle = \left(Z^{01}\sum_N \hat{D}^{1*}_{N0}(\Omega_T)\hat{P}^+_N + Z^{10}\sum_M \hat{D}^{1*}_{M0}(\Omega_S)\hat{D}^+_M\right)|0\rangle, \tag{G.33}$$

now, using the well-known integration properties of the Wigner functions

$$\begin{aligned} &\int d\Omega D^{0*}_{00}(\Omega) = 8\pi^2, \\ &\int d\Omega_T D^{0*}_{00}(\Omega_T)D^{1*}_{N0}(\Omega_T) = 0, \\ &\int d\Omega_S D^{1*}_{00}(\Omega_S)D^{1*}_{M0}(\Omega_S) = (-1)^M\frac{8\pi^2}{3}\delta_{M0}, \end{aligned} \tag{G.34}$$

we have for the projected $|A = 2, S = 1, T = 0\rangle$ state

$$|A = 2, S = 1, T = 0\rangle = Z^{10}\hat{D}^+_0|0\rangle, \tag{G.35}$$

whose norm is

$$\langle A=2,S=1,T=0|A=2,S=1,T=0\rangle = |Z^{10}|^2\langle 0|\hat{D}_0\hat{D}_0^+|0\rangle = |Z^{10}|^2\Omega. \tag{G.36}$$

For the projected state $|A=4,S=0,T=0\rangle$ we analogously proceed

$$|A=4,S=0,T=0\rangle = \hat{P}^0\hat{P}^0|4\rangle = \frac{1}{8\pi^2}\frac{1}{8\pi^2}\int d\Omega_T d\Omega_S \hat{D}^{0*}_{00}(\Omega_T)D^{0*}_{00}(\Omega_S)\hat{R}_S(\Omega_S)\hat{R}_T(\Omega_T)|4\rangle, \tag{G.37}$$

with

$$\begin{aligned}\hat{R}_S(\Omega_S)\hat{R}_T(\Omega_T)|4\rangle = \frac{1}{2}\Bigg(&\sum_{NN'} D^{1*}_{N0}(\Omega_T)D^{1*}_{N'0}(\Omega_T)Z^{10^2}\hat{P}^+_N\hat{P}^+_{N'} \\ &+ \sum_{MM'} D^{1*}_{M0}(\Omega_S)D^{1*}_{M'0}(\Omega_S)Z^{01^2}\hat{D}^+_M\hat{D}^+_{M'} \\ &+ 2\sum_{MN} D^{1*}_{N0}(\Omega_T)D^{1*}_{M0}(\Omega_S)Z^{10}Z^{01}\hat{P}^+_N\hat{D}^+_M\Bigg)|0\rangle.\end{aligned} \tag{G.38}$$

Using yet another integration property of the Wigner functions

$$\int d\Omega D^{0*}_{00}(\Omega)D^{1*}_{N0}(\Omega)D^{1*}_{N'0}(\Omega) = 8\pi^2 C^{00}_{1N1N'}C^{00}_{1010}, \tag{G.39}$$

we finally have

$$\begin{aligned}|A=4,S=0,T=0\rangle &= \frac{1}{2}\Bigg(Z^{01^2}\sum_{NN'}C^{00}_{1N1N'}C^{00}_{1010}\hat{P}^+_N\hat{P}^+_{N'} + Z^{10^2}\sum_{MM'}C^{00}_{1M1M'}C^{00}_{1010}\hat{D}^+_M\hat{D}^+_{M'}\Bigg)|0\rangle \\ &= -\frac{1}{2\sqrt{3}}\Big[Z^{01^2}(\hat{P}^+\hat{P}^+)^{00} + Z^{10^2}(\hat{D}^+\hat{D}^+)^{00}\Big]|0\rangle,\end{aligned} \tag{G.40}$$

and the norm of this state is

$$\begin{aligned}\langle A=4,S=0,T=0|A=4,S=0,T=0\rangle = \frac{1}{12}\Bigg(&|Z^{01}|^4\langle 0|(PP)^{00}(\hat{P}^+\hat{P}^+)^{00}|0\rangle \\ &+ |Z^{10}|^4\langle 0|(DD)^{00}(\hat{D}^+\hat{D}^+)^{00}|0\rangle + (Z^{10*}Z^{01})^2\langle 0|(DD)^{00}(\hat{P}^+\hat{P}^+)^{00}|0\rangle \\ &+ (Z^{10}Z^{01*})^2\langle 0|(PP)^{00}(\hat{D}^+\hat{D}^+)^{00}|0\rangle\Bigg) \\ = \frac{\Omega}{12}\Big[&(|Z^{01}|^4+|Z^{10}|^4)(2\Omega+1) - 3(Z^{10*}Z^{01})^2 - 3(Z^{10}Z^{01*})^2\Big].\end{aligned} \tag{G.41}$$

We now compare if the exact and projected results are equivalent. Indeed, the exact state (G.2) and the projected state (G.35) for $|AST\rangle = |A = 2, S = 1, T = 0\rangle$ are the same if $|Z^{10}|^2 = 1$, which has to be if the system is just an isoscalar pair. We see that in that case then the norms (G.25) and (G.36) are also equivalent and constant. For $|AST\rangle = |A = 4, S = 0, T = 0\rangle$, the comparison of the exact state (G.3) and the projected state (G.40) yields

$$\alpha = -\frac{Z^{01^2}}{2\sqrt{3}}, \qquad \beta = -\frac{Z^{10^2}}{2\sqrt{3}}, \tag{G.42}$$

and by the substitution of these coefficients in the exact norm (G.28), we see that we obtain the projected norm (G.41). We now have everything in order to compute the deuteron transfer using projected states (G.35) and (G.40)

$$\begin{aligned}\langle A = 4, S = 0, T = 0|\hat{D}_0^+|A = 2, S = 1, T = 0\rangle = -\frac{Z_R^{10}}{2\sqrt{3}}\Big(& Z_L^{01*^2}\langle 0|(PP)^{00}\hat{D}_0^+\hat{D}_0^+|0\rangle \\ & + Z_L^{10*^2}\langle 0|(DD)^{00}\hat{D}_0^+\hat{D}_0^+|0\rangle\Big)\end{aligned} \tag{G.43}$$

where we have introduced subindices L, R to differentiate between right and left states, respectively. Explicitly,

$$\begin{aligned}\langle 0|(PP)^{00}\hat{D}_0^+\hat{D}_0^+|0\rangle &= \frac{3}{\sqrt{3}}\Omega, \\ \langle 0|(DD)^{00}\hat{D}_0^+\hat{D}_0^+|0\rangle &= -\frac{\Omega}{\sqrt{3}}(2\Omega + 1),\end{aligned} \tag{G.44}$$

thus

$$\langle A = 4, S = 0, T = 0|\hat{D}_0^+|A = 2, S = 1, T = 0\rangle = -\frac{\Omega}{6}Z_R^{10}\Big(3Z_L^{01*^2} - (2\Omega + 1)Z_L^{10*^2}\Big), \tag{G.45}$$

and we see that this expression is exactly (G.24) when $Z_R^{10} = 1$ and

$$\alpha = -\frac{Z_L^{01^2}}{2\sqrt{3}}, \qquad \beta = -\frac{Z_L^{10^2}}{2\sqrt{3}}. \tag{G.46}$$

We conclude from these calculations that, while in general a HFB plus VAP symmetry restoration calculation will yield a result which is an upper bound of the exact one, under certain circumstances this method can obtain the proper exact result. This could be achieved because the exact states in these cases, for two and four particles, can be built from purely isoscalar and isovector pairs, with no other possible combinations. These isoscalar and isovector pairs

are also the only ones that build our intrinsic state that we use for the mean-field calculation, neglecting other particle correlations that now are obvious to play a role, since they do not match the exact results for $A > 6$ particles, as seen in the Results section.

Appendix H

Matrix elements of the $SO(8)$ interaction

In this Appendix we address the problem of dealing with time-reversed single-particle creation and annihilation operators and how they are related to the usual ones by a phase. The single-particle creation operator reads

$$\hat{a}^{+}_{\ell m;\frac{1}{2}\sigma;\frac{1}{2}\tau}, \tag{H.1}$$

where $\{\ell, m; \frac{1}{2}, \sigma; \frac{1}{2}, \tau\}$ are the orbital angular momentum and its projection, spin and its projection and isospin and its projection; quantum numbers, respectively.

For the single-particle annihilation operator we have two choices. The *time-reversed* will be denoted by $\hat{\tilde{a}}$

$$\hat{\tilde{a}}_{\ell m;\frac{1}{2}\sigma;\frac{1}{2}\tau}, \tag{H.2}$$

and the usual one will be denoted by a

$$\hat{a}_{\ell m;\frac{1}{2}\sigma;\frac{1}{2}\tau}. \tag{H.3}$$

The reason is that only $\hat{\tilde{a}}$ is a spherical tensor of rank ℓ. $\hat{a}$ is not but we like to work with this one instead of $\tilde{a}$.

According to Kota [KA06], $\hat{\tilde{a}}$ and $\hat{a}$ are related by

$$\hat{a}_{\ell m;\frac{1}{2}\sigma;\frac{1}{2}\tau} = (-1)^{\ell+1+m-\sigma-\tau}\tilde{a}_{\ell -m;\frac{1}{2}-\sigma;\frac{1}{2}-\tau} \tag{H.4}$$

according to Evans [Eva81], $\tilde{a}$ and a are related by

$$\tilde{a}_{\ell m;\frac{1}{2}\sigma;\frac{1}{2}\tau} = (-1)^{\ell+1+m+\sigma+\tau}\hat{a}_{\ell -m;\frac{1}{2}-\sigma;\frac{1}{2}-\tau}. \tag{H.5}$$

It is easily seen that both relations are equivalent. However, there are more ways to define $\hat{a}$ from $\hat{\tilde{a}}$, as in for example

$$\hat{\tilde{a}}_{\ell m;\frac{1}{2}\sigma;\frac{1}{2}\tau} = (-1)^{\ell+1-m-\sigma-\tau}\hat{a}_{\ell -m;\frac{1}{2}-\sigma;\frac{1}{2}-\tau}, \tag{H.6}$$

being equivalent to the relation (H.4) and concluding that the phase that relates $\hat{a}$ and $\hat{\tilde{a}}$ is entirely up to convention.

Following Kota's convention, defining the isovector pair creation operator as

$$\hat{P}^{+}_{\mu\ell} = \sqrt{\frac{2\ell+1}{2}}\left(\hat{a}^{+}_{\ell m_1^+;\frac{1}{2}\sigma_1^+;\frac{1}{2}\tau_1^+}\hat{a}^{+}_{\ell m_2^+;\frac{1}{2}\sigma_2^+;\frac{1}{2}\tau_2^+}\right)^{0,0,1}_{0,0,\mu}, \tag{H.7}$$

and the isovector pair annihilation operator

$$\hat{P}_{\mu\ell} = (-1)^{\mu}\sqrt{\frac{2\ell+1}{2}}\left(\hat{\tilde{a}}_{\ell m_1;\frac{1}{2}\sigma_1;\frac{1}{2}\tau_1}\hat{\tilde{a}}_{\ell m_2;\frac{1}{2}\sigma_2;\frac{1}{2}\tau_2}\right)^{0,0,1}_{0,0,-\mu}, \tag{H.8}$$

with similar relations hold up for the isoscalar pair creation and annihilation operators, it is explicitly used time-reversed single-particle operators. As we see for the number, spin and isospin operators

$$\begin{aligned}
\hat{A} &= 2\sqrt{2\ell+1}\left(\hat{a}^{+}_{\ell m_1^+;\frac{1}{2}\sigma_1^+;\frac{1}{2}\tau_1^+}\hat{\tilde{a}}_{\ell m_2;\frac{1}{2}\sigma_2;\frac{1}{2}\tau_2}\right)^{0,0,0}_{0,0,0},\\
\hat{S} &= \sqrt{2\ell+1}\left(\hat{a}^{+}_{\ell m_1^+;\frac{1}{2}\sigma_1^+;\frac{1}{2}\tau_1^+}\hat{\tilde{a}}_{\ell m_2;\frac{1}{2}\sigma_2;\frac{1}{2}\tau_2}\right)^{0,\mu,0}_{0,1,0},\\
\hat{T} &= \sqrt{2\ell+1}\left(\hat{a}^{+}_{\ell m_1^+;\frac{1}{2}\sigma_1^+;\frac{1}{2}\tau_1^+}\hat{\tilde{a}}_{\ell m_2;\frac{1}{2}\sigma_2;\frac{1}{2}\tau_2}\right)^{0,0,\mu}_{0,0,1},
\end{aligned} \tag{H.9}$$

which are of course computed using a density matrix of the form $\rho_{ij} = \langle\Phi|\hat{a}^{+}_{j}\hat{\tilde{a}}_{i}|\Phi\rangle$.

Therefore, if we use Kota's phase convention for the construction of the matrix elements of the interaction, we must also include this phase in the density matrix (and subsequent operators as they depend on the density matrix) as it includes $\hat{\tilde{a}}$. Otherwise, we are not consistent and the solver will retrieve wrong solutions.

However, if we are not enforcing any symmetry in our system, the usual convention has to be used with $\hat{a}^{+}$ and $\hat{a}$ single-particle creation and annihilation operators. Defining now our density matrix (and subsequent operators) in the usual way $\rho_{ij} = \langle\Phi|\hat{a}^{+}_{j}\hat{a}_{i}|\Phi\rangle$. In the following, we will stick to this convention, rewriting all $\hat{\tilde{a}}$ operators in terms of $\hat{a}$.

We expand the pair creation and annihilation operators as

$$\hat{P}^{+}_{\mu\ell} = \sum_{q^+} C^{00}_{\ell m_1^+;\ell m_2^+} C^{00}_{\frac{1}{2}\sigma_1^+;\frac{1}{2}\sigma_2^+} C^{1,\mu}_{\frac{1}{2}\tau_1^+;\frac{1}{2}\tau_2^+} \sqrt{\frac{2\ell+1}{2}} \hat{a}^{+}_{\ell m_1^+;\frac{1}{2}\sigma_1^+;\frac{1}{2}\tau_1^+} \hat{a}^{+}_{\ell m_2^+;\frac{1}{2}\sigma_2^+;\frac{1}{2}\tau_2^+}, \tag{H.10}$$

$$\begin{aligned}\hat{P}_{\mu\ell} = (-1)^{\mu} \sum_{q} (-1)^{2\ell+m_1+m_2+\sigma_1+\sigma_2+\tau_1+\tau_2} C^{00}_{\ell-m_1;\ell-m_2} C^{00}_{\frac{1}{2}-\sigma_1;\frac{1}{2}-\sigma_2} C^{1,-\mu}_{\frac{1}{2}-\tau_1;\frac{1}{2}-\tau_2} \\ \times \sqrt{\frac{2\ell+1}{2}} \hat{a}_{\ell-m_1;-\frac{1}{2}-\sigma_1;\frac{1}{2}-\tau_1} \hat{a}_{\ell-m_2;\frac{1}{2}-\sigma_2;\frac{1}{2}-\tau_2},\end{aligned} \tag{H.11}$$

where q^+ spans over the quantum numbers of both particles: $q^+ = \{m_1^+, \sigma_1^+, \tau_1^+; m_2^+, \sigma_2^+, \tau_2^+\}$ and q is: $q = \{m_1, \sigma_1, \tau_1; m_2, \sigma_2, \tau_2\}$.

We change the signs of the projections of angular momentum, spin and isospin (m, σ, τ), taking into account that the Clebsch-Gordan coefficients transform under this sign changing as

$$C^{c-\gamma}_{a-\alpha b-\beta} = (-1)^{a+b-c} C^{c\gamma}_{a\alpha b\beta}, \tag{H.12}$$

obtaining

$$\begin{aligned}\hat{P}_{\mu\ell} = (-1)^{\mu} \sum_{q} (-1)^{4\ell-m_1-m_2-\sigma_1-\sigma_2-\tau_1-\tau_2+1} C^{00}_{\ell m_1;\ell m_2} C^{00}_{\frac{1}{2}\sigma_1;\frac{1}{2}\sigma_2} C^{1,\mu}_{\frac{1}{2}\tau_1;\frac{1}{2}\tau_2} \\ \times \sqrt{\frac{2l+1}{2}} \hat{a}_{\ell m_1;\frac{1}{2}\sigma_1;\frac{1}{2}\tau_1} \hat{a}_{\ell m_2;\frac{1}{2}\sigma_2;\frac{1}{2}\tau_2}.\end{aligned} \tag{H.13}$$

Using the following identities

$$\begin{aligned}C^{00}_{\ell m_1;\ell m_2} C^{00}_{\ell m_1^+;\ell m_2^+} &= \frac{1}{2\ell+1} (-1)^{2\ell-m_1-m_1^+} \delta_{m_1-m_2} \delta_{m_1^+-m_2^+}, \\ C^{00}_{\frac{1}{2}\sigma_1;\frac{1}{2}\sigma_2} C^{00}_{\frac{1}{2}\sigma_1^+;\frac{1}{2}\sigma_2^+} &= \frac{1}{2} (-1)^{1+-\sigma_1-\sigma_1^+} \delta_{\sigma_1-\sigma_2} \delta_{\sigma_1^+-\sigma_2^+},\end{aligned} \tag{H.14}$$

we are ready to obtain the matrix elements of the interaction. The product $\hat{P}^{+}_{\mu} \hat{P}_{\mu}$ gives

$$\begin{aligned}\hat{P}^{+}_{\mu\ell} \hat{P}_{\mu\ell} = \frac{1}{4} (-1)^{\mu} \sum_{q,q^+} (-1)^{2\ell-m_1-m_1^+} (-1)^{1-\sigma_1-\sigma_1^+} (-1)^{4\ell-m_1-m_2-\sigma_1-\sigma_2-\tau_1-\tau_2+1} \delta_{m_1-m_2} \\ \times \delta_{m_1^+-m_2^+} \delta_{\sigma_1^+-\sigma_2^+} \delta_{\sigma_1-\sigma_2} C^{1,\mu}_{\frac{1}{2}\tau_1^+;\frac{1}{2}\tau_2^+} C^{1,\mu}_{\frac{1}{2}\tau_1;\frac{1}{2}\tau_2} \hat{a}^{+}_{\ell m_1^+;\frac{1}{2}\sigma_1^+;\frac{1}{2}\tau_1^+} \hat{a}^{+}_{\ell m_2^+;\frac{1}{2}\sigma_2^+;\frac{1}{2}\tau_2^+} \hat{a}_{\ell m_1;\frac{1}{2}\sigma_1;\frac{1}{2}\tau_1} \hat{a}_{\ell m_2;\frac{1}{2}\sigma_2;\frac{1}{2}\tau_2},\end{aligned} \tag{H.15}$$

and, equivalently, for the product of isoscalar pair creation and annihilation operators $\hat{D}^+_\mu \hat{D}_\mu$

$$\hat{D}^+_{\mu\ell}\hat{D}_{\mu\ell} = \frac{1}{4}(-1)^\mu \sum_{q,q^+}(-1)^{2\ell-m_1-m_1^+}(-1)^{1-\tau_1-\tau_1^+}(-1)^{4\ell-m_1-m_2-\sigma_1-\sigma_2-\tau_1-\tau_2+1}\delta_{m_1-m_2} \\ \times \delta_{m_1^+-m_2^+}\delta_{\tau_1^+-\tau_2^+}\delta_{\tau_1-\tau_2} C^{1,\mu}_{\frac{1}{2}\sigma_1^+;\frac{1}{2}\sigma_2^+} C^{1,\mu}_{\frac{1}{2}\sigma_1;\frac{1}{2}\sigma_2}\hat{a}^+_{\ell m_1^+;\frac{1}{2}\sigma_1^+;\frac{1}{2}\tau_1^+}\hat{a}^+_{\ell m_2^+;\frac{1}{2}\sigma_2^+;\frac{1}{2}\tau_2^+}\hat{a}_{\ell m_1;\frac{1}{2}\sigma_1;\frac{1}{2}\tau_1}\hat{a}_{\ell m_2;\frac{1}{2}\sigma_2;\frac{1}{2}\tau_2}, \tag{H.16}$$

where we have expanded the Clebsch-Gordan coefficients. Rearranging the phases we obtain

$$\hat{P}^+_{\mu\ell}\hat{P}_{\mu\ell} = \frac{1}{4}(-1)^\mu \sum_{q,q^+}(-1)^{2l-2m_1-m_2-m_1^+-\sigma_1^+-\sigma_2-\tau_1-\tau_2+1}\delta_{m_1-m_2}\delta_{m_1^+-m_2^+}\delta_{\sigma_1^+-\sigma_2^+}\delta_{\sigma_1-\sigma_2} \\ \times C^{1,\mu}_{\frac{1}{2}\tau_1^+;\frac{1}{2}\tau_2^+} C^{1,\mu}_{\frac{1}{2}\tau_1;\frac{1}{2}\tau_2}\hat{a}^+_{\ell m_1^+;\frac{1}{2}\sigma_1^+;\frac{1}{2}\tau_1^+}\hat{a}^+_{\ell m_2^+;\frac{1}{2}\sigma_2^+;\frac{1}{2}\tau_2^+}\hat{a}_{\ell m_1;\frac{1}{2}\sigma_1;\frac{1}{2}\tau_1}\hat{a}_{\ell m_2;\frac{1}{2}\sigma_2;\frac{1}{2}\tau_2}, \tag{H.17}$$

$$\hat{D}^+_{\mu\ell}\hat{D}_{\mu\ell} = \frac{1}{4}(-1)^\mu \sum_{q,q^+}(-1)^{2\ell-2m_1-m_2-m_1^+-\tau_1^+-\tau_2-\sigma_1-\sigma_2+1}\delta_{m_1-m_2}\delta_{m_1^+-m_2^+}\delta_{\tau_1^+-\tau_2^+}\delta_{\tau_1-\tau_2} \\ \times C^{1,\mu}_{\frac{1}{2}\sigma_1^+;\frac{1}{2}\sigma_2^+} C^{1,\mu}_{\frac{1}{2}\sigma_1;\frac{1}{2}\sigma_2}\hat{a}^+_{\ell m_1^+;\frac{1}{2}\sigma_1^+;\frac{1}{2}\tau_1^+}\hat{a}^+_{\ell m_2^+;\frac{1}{2}\sigma_2^+;\frac{1}{2}\tau_2^+}\hat{a}_{\ell m_1;\frac{1}{2}\sigma_1;\frac{1}{2}\tau_1}\hat{a}_{\ell m_2;\frac{1}{2}\sigma_2;\frac{1}{2}\tau_2}. \tag{H.18}$$

The pairing Hamiltonian is of the form (2.17), so we obtain

$$-\frac{1}{4}\sum_{q,q^+}\sum_{\mu}(-1)^\mu(-1)^{2\ell-2m_1-m_2-m_1^+-\sigma_2-\tau_2+1}\delta_{m_1-m_2}\delta_{m_1^+-m_2^+}[(1-x)(-1)^{-\sigma_1^+-\tau_1}\delta_{\sigma_1^+-\sigma_2^+}\delta_{\sigma_1-\sigma_2} \\ \times C^{1,\mu}_{\frac{1}{2}\tau_1^+;\frac{1}{2}\tau_2^+} C^{1,\mu}_{\frac{1}{2}\tau_1;\frac{1}{2}\tau_2} + (1+x)(-1)^{-\tau_1^+-\sigma_1}\delta_{\tau_1^+-\tau_2^+}\delta_{\tau_1-\tau_2} C^{1,\mu}_{\frac{1}{2}\sigma_1^+;\frac{1}{2}\sigma_2^+} C^{1,\mu}_{\frac{1}{2}\sigma_1;\frac{1}{2}\sigma_2}] \\ \times \hat{a}^+_{\ell m_1^+;\frac{1}{2}\sigma_1^+;\frac{1}{2}\tau_1^+}\hat{a}^+_{\ell m_2^+;\frac{1}{2}\sigma_2^+;\frac{1}{2}\tau_2^+}\hat{a}_{\ell m_1;\frac{1}{2}\sigma_1;\frac{1}{2}\tau_1}\hat{a}_{\ell m_2;\frac{1}{2}\sigma_2;\frac{1}{2}\tau_2}. \tag{H.19}$$

Therefore, the general matrix elements, comparing the former formula with the usual form of the pairing Hamiltonian [RS80]

$$\frac{1}{4}\sum_{l_1 l_2 l_3 l_4}\overline{v}_{l_1 l_2 l_3 l_4}\hat{a}^+_{l_1}\hat{a}^+_{l_2}\hat{a}_{l_4}\hat{a}_{l_3}, \tag{H.20}$$

are

$$\overline{v}_{l_1l_2l_3l_4} = -\sum_{\mu}(-1)^{\mu}(-1)^{-m_2-m_1^+-\sigma_2-\tau_2+1}\delta_{m_1-m_2}\delta_{m_1^+-m_2^+}\Big[(1-x)(-1)^{-\sigma_1^+-\tau_1}\delta_{\sigma_1^+-\sigma_2^+}\delta_{\sigma_1-\sigma_2} \\ \times C^{1,\mu}_{\frac{1}{2}\tau_1^+;\frac{1}{2}\tau_2^+}C^{1,\mu}_{\frac{1}{2}\tau_1;\frac{1}{2}\tau_2} + (1+x)(-1)^{-\tau_1^+-\sigma_1}\delta_{\tau_1^+-\tau_2^+}\delta_{\tau_1-\tau_2}C^{1,\mu}_{\frac{1}{2}\sigma_1^+;\frac{1}{2}\sigma_2^+}C^{1,\mu}_{\frac{1}{2}\sigma_1;\frac{1}{2}\sigma_2}\Big], \tag{H.21}$$

where in this case

$$\begin{aligned} l_1 &= \{m_1^+;\sigma_1^+;\tau_1^+\}, \\ l_2 &= \{m_2^+;\sigma_2^+;\tau_2^+\}, \\ l_3 &= \{m_2;\sigma_2;\tau_2\}, \\ l_4 &= \{m_1;\sigma_1;\tau_1\}. \end{aligned} \tag{H.22}$$

H.1 Multi-orbit case

In this case, we define the multi-orbit pair creation and annihilation operators as a sum of the single-orbit pair operators

$$\begin{aligned} \hat{P}^+_{\mu} &= \sum_{\ell}\beta_{\ell}\hat{P}^+_{\mu\ell}, \\ \hat{D}^+_{\mu} &= \sum_{\ell}\beta_{\ell}\hat{D}^+_{\mu\ell}, \end{aligned} \tag{H.23}$$

where for convenience we will take the phase factors $\beta_\ell = 1$. The product becomes

$$\begin{aligned} \hat{P}^+_{\mu}\hat{P}_{\mu} &= \sum_{\ell^+\ell}\hat{P}^+_{\mu\ell^+}\hat{P}_{\mu\ell}, \\ \hat{D}^+_{\mu}\hat{D}_{\mu} &= \sum_{\ell^+\ell}\hat{D}^+_{\mu\ell^+}\hat{D}_{\mu\ell}. \end{aligned} \tag{H.24}$$

We compute now $\hat{P}^+_{\mu\ell^+}\hat{P}_{\mu\ell}$, evaluating the pair operators

$$\hat{P}^+_{\mu\ell^+} = \sum_{q^+}C^{00}_{\ell^+m_1^+;\ell^+m_2^+}C^{00}_{\frac{1}{2}\sigma_1^+;\frac{1}{2}\sigma_2^+}C^{1,\mu}_{\frac{1}{2}\tau_1^+;\frac{1}{2}\tau_2^+}\sqrt{\frac{2\ell^+ + 1}{2}}\hat{a}^+_{\ell^+m_1^+;\frac{1}{2}\sigma_1^+;\frac{1}{2}\tau_1^+}\hat{a}^+_{\ell^+m_2^+;\frac{1}{2}\sigma_2^+;\frac{1}{2}\tau_2^+}, \tag{H.25}$$

$$\hat{P}_{\mu\ell} = (-1)^{\mu} \sum_{q} (-1)^{4\ell - m_1 - m_2 - \sigma_1 - \sigma_2 - \tau_1 - \tau_2 + 1} C^{00}_{\ell m_1; \ell m_2} C^{00}_{\frac{1}{2}\sigma_1; \frac{1}{2}\sigma_2} C^{1,\mu}_{\frac{1}{2}\tau_1; \frac{1}{2}\tau_2} \sqrt{\frac{2\ell+1}{2}} \times \hat{a}_{\ell m_1; \frac{1}{2}\sigma_1; \frac{1}{2}\tau_1} \hat{a}_{\ell m_2; \frac{1}{2}\sigma_2; \frac{1}{2}\tau_2}, \tag{H.26}$$

and using the identity

$$C^{00}_{\ell^+ m_1^+; \ell^+ m_2^+} C^{00}_{\ell m_1; \ell m_2} = \frac{1}{\sqrt{(2\ell+1)(2\ell^+ + 1)}} (-1)^{\ell^+ + \ell - m_1 - m_1^+} \delta_{m_1 - m_2} \delta_{m_1^+ - m_2^+}. \tag{H.27}$$

Thus

$$\hat{P}^+_{\mu\ell^+} \hat{P}_{\mu\ell} = \frac{1}{4} (-1)^{\mu} \sum_{qq^+} (-1)^{4\ell - m_1 - m_2 - \sigma_1 - \sigma_2 - \tau_1 - \tau_2 + 1} (-1)^{\ell^+ + \ell - m_1^+ - m_1} (-1)^{1 - \sigma_1^+ - \sigma_1} C^{1,\mu}_{\frac{1}{2}\tau_1; \frac{1}{2}\tau_2} C^{1,\mu}_{\frac{1}{2}\tau_1^+; \frac{1}{2}\tau_2^+} \times \delta_{m_1 - m_2} \delta_{m_1^+ - m_2^+} \delta_{\sigma_1 - \sigma_2} \delta_{\sigma_1^+ - \sigma_2^+} \hat{a}^+_{\ell^+ m_1^+; \frac{1}{2}\sigma_1^+; \frac{1}{2}\tau_1^+} \hat{a}^+_{\ell^+ m_2^+; \frac{1}{2}\sigma_2^+; \frac{1}{2}\tau_2^+} \hat{a}_{\ell m_1; \frac{1}{2}\sigma_1; \frac{1}{2}\tau_1} \hat{a}_{\ell m_2; \frac{1}{2}\sigma_2; \frac{1}{2}\tau_2}, \tag{H.28}$$

and, rearranging the phases

$$\hat{P}^+_{\mu\ell^+} \hat{P}_{\mu\ell} = \frac{1}{4} (-1)^{\mu} \sum_{qq^+} (-1)^{\ell^+ + \ell - m_1^+ - m_2 - \sigma_1^+ - \sigma_2 - \tau_1 - \tau_2 + 1} C^{1,\mu}_{\frac{1}{2}\tau_1; \frac{1}{2}\tau_2} C^{1,\mu}_{\frac{1}{2}\tau_1^+; \frac{1}{2}\tau_2^+} \times \delta_{m_1 - m_2} \delta_{m_1^+ - m_2^+} \delta_{\sigma_1 - \sigma_2} \delta_{\sigma_1^+ - \sigma_2^+} \hat{a}^+_{\ell^+ m_1^+; \frac{1}{2}\sigma_1^+; \frac{1}{2}\tau_1^+} \hat{a}^+_{\ell^+ m_2^+; \frac{1}{2}\sigma_2^+; \frac{1}{2}\tau_2^+} \hat{a}_{\ell m_1; \frac{1}{2}\sigma_1; \frac{1}{2}\tau_1} \hat{a}_{\ell m_2; \frac{1}{2}\sigma_2; \frac{1}{2}\tau_2}. \tag{H.29}$$

Equivalently for $\hat{D}^+_{\mu\ell^+} \hat{D}_{\mu\ell}$ we obtain

$$\hat{D}^+_{\mu\ell^+} \hat{D}_{\mu\ell} = \frac{1}{4} (-1)^{\mu} \sum_{qq^+} (-1)^{\ell^+ + \ell - m_1^+ - m_2 - \tau_1^+ - \tau_2 - \sigma_1 - \sigma_2 + 1} C^{1,\mu}_{\frac{1}{2}\sigma_1; \frac{1}{2}\sigma_2} C^{1,\mu}_{\frac{1}{2}\sigma_1^+; \frac{1}{2}\sigma_2^+} \times \delta_{m_1 - m_2} \delta_{m_1^+ - m_2^+} \delta_{\tau_1 - \tau_2} \delta_{\tau_1^+ - \tau_2^+} \hat{a}^+_{\ell^+ m_1^+; \frac{1}{2}\sigma_1^+; \frac{1}{2}\tau_1^+} \hat{a}^+_{\ell^+ m_2^+; \frac{1}{2}\sigma_2^+; \frac{1}{2}\tau_2^+} \hat{a}_{\ell m_1; \frac{1}{2}\sigma_1; \frac{1}{2}\tau_1} \hat{a}_{\ell m_2; \frac{1}{2}\sigma_2; \frac{1}{2}\tau_2}. \tag{H.30}$$

We observe that these expressions correspond to the single orbit case when $\ell = \ell^+$.

Now we are able to construct the matrix elements of the interaction. The Hamiltonian is

again given by expression (2.17), so we obtain

$$
\begin{aligned}
-\frac{1}{4}\sum_{q,q^+}\sum_{\mu}(-1)^{\mu}(-1)^{\ell^+ +\ell-m_2-m_1^+-\sigma_2-\tau_2+1}\delta_{m_1-m_2}\delta_{m_1^+-m_2^+}\Big[(1-x)(-1)^{-\sigma_1^+-\tau_1}\delta_{\sigma_1^+-\sigma_2^+}\delta_{\sigma_1-\sigma_2} \\
\times C^{1,\mu}_{\frac{1}{2}\tau_1^+;\frac{1}{2}\tau_2^+}C^{1,\mu}_{\frac{1}{2}\tau_1;\frac{1}{2}\tau_2}+(1+x)(-1)^{-\tau_1^+-\sigma_1}\delta_{\tau_1^+-\tau_2^+}\delta_{\tau_1-\tau_2}C^{1,\mu}_{\frac{1}{2}\sigma_1^+;\frac{1}{2}\sigma_2^+}C^{1,\mu}_{\frac{1}{2}\sigma_1;\frac{1}{2}\sigma_2}\Big] \\
\times \hat{a}^+_{\ell^+ m_1^+;\frac{1}{2}\sigma_1^+;\frac{1}{2}\tau_1^+}\hat{a}^+_{\ell^+ m_2^+;\frac{1}{2}\sigma_2^+;\frac{1}{2}\tau_2^+}\hat{a}_{\ell m_1;\frac{1}{2}\sigma_1;\frac{1}{2}\tau_1}\hat{a}_{\ell m_2;\frac{1}{2}\sigma_2;\frac{1}{2}\tau_2},
\end{aligned}
\tag{H.31}
$$

where we have to keep in mind that we are also summing over the shells l, l^+ in q, q^+, respectively. Comparing the former formula with the pairing Hamiltonian (H.20) the matrix elements are

$$
\begin{aligned}
\overline{v}_{l_1l_2l_3l_4} = -\sum_{\mu}(-1)^{\mu}(-1)^{\ell^+ +\ell-m_2-m_1^+-\sigma_2-\tau_2+1}\delta_{m_1-m_2}\delta_{m_1^+-m_2^+}\Big[(1-x)(-1)^{-\sigma_1^+-\tau_1}\delta_{\sigma_1^+-\sigma_2^+}\delta_{\sigma_1-\sigma_2} \\
\times C^{1,\mu}_{\frac{1}{2}\tau_1^+;\frac{1}{2}\tau_2^+}C^{1,\mu}_{\frac{1}{2}\tau_1;\frac{1}{2}\tau_2}+(1+x)(-1)^{-\tau_1^+-\sigma_1}\delta_{\tau_1^+-\tau_2^+}\delta_{\tau_1-\tau_2}C^{1,\mu}_{\frac{1}{2}\sigma_1^+;\frac{1}{2}\sigma_2^+}C^{1,\mu}_{\frac{1}{2}\sigma_1;\frac{1}{2}\sigma_2}\Big],
\end{aligned}
\tag{H.32}
$$

where in this case

$$
\begin{aligned}
l_1 &= \{\ell^+; m_1^+; \sigma_1^+; \tau_1^+\}, \\
l_2 &= \{\ell^+; m_2^+; \sigma_2^+; \tau_2^+\}, \\
l_3 &= \{\ell; m_2; \sigma_2; \tau_2\}, \\
l_4 &= \{\ell; m_1; \sigma_1; \tau_1\}.
\end{aligned}
\tag{H.33}
$$

Instead of dealing with several single $\ell-$shell, we will deal with the total degeneracy $\Omega = \sum_\ell (2\ell+1)$.

The size of the wavefunction, densities and fields matrices is $N = 4\Omega$ and the size of the matrix elements is N^2. For the case of interest, namely a pair of $l = 2, 3$ shells, $N = 48$ and $N^2 = 2304$.

Appendix I

Alternative derivation of the matrix elements of the separable interaction

An alternative derivation of the separable matrix elements computed in Section 6.1.1 can be performed noticing that the Moshinsky transformation (6.19) can be rewritten as

$$\phi_{n_1}(x_1,b)\phi_{n_2}(x_2,b) = \sum_{nN} M^{nN}_{n_1n_2}\phi_n(x,b_r)\phi_N(X,b_R), \tag{I.1}$$

where $b_r = b/\sqrt{2}$ and $b_R = \sqrt{2}b$. Using this expression instead, we perform the following integration

$$\begin{aligned} I_x(n_1n_2;n_1'n_2') = &\sum_{n,n',N,N'} M^{nN}_{n_1n_2}M^{n'N'}_{n_1'n_2'} \\ &\times \int dxdx'dXdX'\delta(X-X')P(x)P(x')\phi_n(x,b_r)\phi_{n'}(x',b_r)\phi_N(X,b_R)\phi_{N'}(X',b_R), \end{aligned} \tag{I.2}$$

again, integrating over the variables X, X',

$$\begin{aligned} &\int dXdX'\delta(X-X')\phi_N(X,b_R)\phi_{N'}(X',b_R) = \int dX\phi_N(X,b_R)\phi_{N'}(X,b_R) = \\ &= \int d(b_RX)H^{(0)}_N(b_RX)H^{(0)}_{N'}(b_RX)e^{-b_R^2X^2} = \delta_{NN'}, \end{aligned} \tag{I.3}$$

we find the matrix elements can be written as

$$I_x(n_1n_2;n_1'n_2') = \frac{1}{\sqrt{2}}\sum_{n,n',N} M^{nN}_{n_1n_2}M^{n'N}_{n_1'n_2'}W(n)W(n'), \tag{I.4}$$

with

$$W(n) = \int dx P(x)\phi_n(x, b_r), \tag{I.5}$$

and integrating now over x

$$W(n) = \frac{b_r^{1/2}}{\sqrt{\pi a^2}} \int dx e^{-x^2/a^2} H_n^{(0)}(b_r x) e^{-\frac{b_r^2 x^2}{2}} = \frac{b_r^{1/2}}{\sqrt{\pi a^2}} \int dx H_n^{(0)}(b_r x) e^{-c^2 x^2}, \tag{I.6}$$

with $c = \sqrt{\frac{2+a^2 b_r^2}{2a^2}}$. Making the change $t = cx$ we obtain

$$W(n) = \frac{b_r^{1/2}}{\sqrt{\pi a^2}} \frac{1}{c} \int dt H_n^{(0)}(b_r t/c) e^{-t^2}, \tag{I.7}$$

and making use of identity (6.28)

$$\begin{aligned} W(n) &= \frac{b_r^{1/2}}{\sqrt{\pi a^2}} \frac{1}{c} \pi^{1/4} \frac{\sqrt{n!}}{(n/2)!} \left(\frac{b_r^2/c^2 - 1}{2} \right)^{n/2} \\ &= b_r^{1/2} \pi^{-1/4} \sqrt{\frac{2}{2 + a^2 b_r^2}} \frac{\sqrt{n!}}{(n/2)!} \left(\frac{a^2 b_r^2 - 2}{2a^2 b_r^2 + 4} \right)^{n/2}, \end{aligned} \tag{I.8}$$

disentangling the scaling $b_r = b/\sqrt{2}$, we finally obtain

$$W(n) = \left(\frac{8}{\pi} \right)^{1/4} \sqrt{\frac{b}{4 + a^2 b^2}} \frac{\sqrt{n!}}{(n/2)!} \left(\frac{a^2 b^2 - 4}{2a^2 b^2 + 8} \right)^{n/2}. \tag{I.9}$$

Therefore, defining the auxiliary functions

$$G(N, n_1, n_2) = M_{n_1 n_2}^{n_1 + n_2 - N, N} W(n_1 + n_2 - N), \tag{I.10}$$

we have for the total matrix element

$$I_x(n_1 n_2; n_1' n_2') = \sum_{N=0}^{n_1+n_2} G(N, n_1, n_2) G(N, n_1', n_2'), \tag{I.11}$$

which is the same expression as (6.30), where the factor of $\sqrt{2}$ was taken into the expression of the matrix elements (I.8).

List of abbreviations

BCS	Bardeen-Cooper-Schrieffer
HF	Hartree-Fock
HFB	Hartree-Fock-Bogoliubov
ALM	Augmented Lagrangian Method
VAP	Variation After Projection
PAV	Projection After Variation
PNP	Particle-Number Projection
AMP	Angular Momentum (Spin) Projection
ISOP	Isospin Projection
np	neutron-proton
ph	particle-hole
pp	particle-particle
rhs	right-hand side
lhs	left-hand side

Bibliography

[AEE08] Frank T Avignone III, Steven R Elliott, and Jonathan Engel. "Double beta decay, Majorana neutrinos, and neutrino mass". In: *Reviews of Modern Physics* 80.2 (2008), p. 481.

[AI75] A Arima and F Iachello. "Collective nuclear states as representations of a SU (6) group". In: *Physical Review Letters* 35.16 (1975), p. 1069.

[AS48] Milton Abramowitz and Irene A Stegun. *Handbook of mathematical functions with formulas, graphs, and mathematical tables*. Vol. 55. US Government printing office, 1948.

[Bac19] Pawel Baczyk. "Naruszenie symetrii izospinowej przez oddzialywanie silne w podejsciu opartym na teorii funkcjonalu gestosci". In: (2019).

[Bal98] Marcello Baldo et al. "$3P^2$- $3F^2$ pairing in neutron matter with modern nucleon-nucleon potentials". In: *Physical Review C* 58.4 (1998), p. 1921.

[Bar99] F Barranco et al. "Surface vibrations and the pairing interaction in nuclei". In: *Physical review letters* 83.11 (1999), p. 2147.

[BCS57] John Bardeen, Leon N Cooper, and John Robert Schrieffer. "Theory of superconductivity". In: *Physical Review* 108.5 (1957), p. 1175.

[Ben16] K. Bennaceur. *Private communication*. 2016.

[Bes00] DR Bes et al. "Structure of the vacuum states in the presence of isovector and isoscalar pairing correlations". In: *Physical Review C* 61.2 (2000), p. 024315.

[BG16] Brendan Bulthuis and Alexandros Gezerlis. "Probing mixed-spin pairing in heavy nuclei". In: *Physical Review C* 93.1 (2016), p. 014312.

[BGG91] JF Berger, M Girod, and D Gogny. "Time-dependent quantum collective dynamics applied to nuclear fission". In: *Computer Physics Communications* 63.1-3 (1991), pp. 365–374.

[BHM67] Z Bochnacki, IM Holban, and IN Mikhailov. "Residual interaction in nuclei". In: *Nuclear Physics A* 97.1 (1967), pp. 33–51.

[BHR03] Michael Bender, Paul-Henri Heenen, and Paul-Gerhard Reinhard. "Self-consistent mean-field models for nuclear structure". In: *Reviews of Modern Physics* 75.1 (2003), p. 121.

[BM98] Aage Bohr and Ben R Mottelson. *Nuclear structure*. Vol. 1. World Scientific, 1998.

[BMP58] A. Bohr, B. R. Mottelson, and D. Pines. "Possible Analogy between the Excitation Spectra of Nuclei and Those of the Superconducting Metallic State". In: *Phys. Rev.* 110 (4 1958), pp. 936–938.

[BMS10] Simone Baroni, Augusto O Macchiavelli, and Achim Schwenk. "Partial-wave contributions to pairing in nuclei". In: *Physical Review C* 81.6 (2010), p. 064308.

[BR86] Jean-Paul Blaizot and Georges Ripka. *Quantum theory of finite systems, Vol. 3*. 1986.

[Bro73] RA Broglia. "The pairing model". In: *Annals of Physics* 80.1 (1973), pp. 60–85.

[BRT96] CT Black, DC Ralph, and M Tinkham. "Spectroscopy of the superconducting gap in individual nanometer-scale aluminum particles". In: *Physical review letters* 76.4 (1996), p. 688.

[BW88] B Alex Brown and BH Wildenthal. "Status of the nuclear shell model". In: *Annual Review of Nuclear and Particle Science* 38.1 (1988), pp. 29–66.

[Car10] BG Carlsson et al. "Solution of self-consistent equations for the N3LO nuclear energy density functional in spherical symmetry. the program hosphe (v1.02)". In: *Computer Physics Communications* 181.9 (2010), pp. 1641–1657.

[Car15] J Carlson et al. "Quantum Monte Carlo methods for nuclear physics". In: *Reviews of Modern Physics* 87.3 (2015), p. 1067.

[Cau05] E Caurier et al. "The shell model as a unified view of nuclear structure". In: *Reviews of Modern Physics* 77.2 (2005), p. 427.

[Ced11] B. Cederwall et al. "Evidence for a spin-aligned neutron-proton paired phase from the level structure of ^{92}Pd". In: *Nature* 469 (2011), p. 68.

[Cha76] RR Chasman. "Density-dependent delta interactions and actinide pairing matrix elements". In: *Physical Review C* 14.5 (1976), p. 1935.

[Cha97] E Chabanat et al. "A Skyrme parametrization from subnuclear to neutron star densities". In: *Nuclear Physics A* 627.4 (1997), pp. 710–746.

[Che95] MK Cheoun et al. "Total Gamow-Teller strength, ground-state correlations and sum rules in QRPA with neutron-proton pairing". In: *Nuclear Physics A* 587.2 (1995), pp. 301–317.

[Cla76] JW Clark et al. "Effect of polarization on superfluidity in low density neutron matter". In: *Physics Letters B* 61.4 (1976), pp. 331–334.

[Dav19] PJ Davies et al. "Toward the limit of nuclear binding on the N= Z line: Spectroscopy of Cd 96". In: *Physical Review C* 99.2 (2019), p. 021302.

[DB04] WH Dickhoff and C Barbieri. "Self-consistent Green's function method for nuclei and nuclear matter". In: *Progress in Particle and Nuclear Physics* 52.2 (2004), pp. 377–496.

[DD97] J Dobaczewski and J Dudek. "Solution of the Skyrme—Hartree—Fock equations in the Cartesian deformed harmonic oscillator basis II. The program HFODD". In: *Computer physics communications* 102.1-3 (1997), pp. 183–209.

[De 93] Walt A De Heer. "The physics of simple metal clusters: experimental aspects and simple models". In: *Reviews of Modern Physics* 65.3 (1993), p. 611.

[DE05] J Dobaczewski and J Engel. "Nuclear Time-Reversal Violation and the Schiff Moment of Ra 225". In: *Physical review letters* 94.23 (2005), p. 232502.

[DG80] J Dechargé and D Gogny. "Hartree-Fock-Bogolyubov calculations with the D1 effective interaction on spherical nuclei". In: *Physical Review C* 21.4 (1980), p. 1568.

[DM92] WH Dickhoff and H Muther. "Nucleon properties in the nuclear medium". In: *Reports on progress in physics* 55.11 (1992), p. 1947.

[DNS03] J Dobaczewski, W Nazarewicz, and MV Stoitsov. "Nuclear ground-state properties from mean-field calculations". In: *Exotic Nuclei and Atomic Masses*. Springer, 2003, pp. 55–60.

[Dob01] J Dobaczewski et al. "Odd-even staggering of binding energies as a consequence of pairing and mean-field effects". In: *Physical Review C* 63.2 (2001), p. 024308.

[Dob07] J Dobaczewski et al. "Particle-number projection and the density functional theory". In: *Physical Review C* 76.5 (2007), p. 054315.

[Dob09] Jacek Dobaczewski et al. "Solution of the Skyrme–Hartree–Fock–Bogolyubov equations in the Cartesian deformed harmonic-oscillator basis.:(VI) hfodd (v2.40h): A new version of the program". In: *Computer Physics Communications* 180.11 (2009), pp. 2361–2391.

[Dob97] J Dobeš. “How to count nucleon pairs?” In: *Physics Letters B* 413.3-4 (1997), pp. 239–245.

[Dug14] T Duguet. “Symmetry broken and restored coupled-cluster theory: I. Rotational symmetry and angular momentum”. In: *Journal of Physics G: Nuclear and Particle Physics* 42.2 (2014), p. 025107.

[Egi95] JL Egido et al. “On the solution of the Hartree-Fock-Bogoliubov equations by the conjugate gradient method”. In: *Nuclear Physics A* 594.1 (1995), pp. 70–86.

[Ell58a] JP Elliott. “Collective motion in the nuclear shell model II. The introduction of intrinsic wave-functions”. In: *Proceedings of the Royal Society of London. Series A. Mathematical and Physical Sciences* 245.1243 (1958), pp. 562–581.

[Ell58b] JP Elliott. “Collective motion in the nuclear shell model. I. Classification schemes for states of mixed configurations”. In: *Proceedings of the Royal Society of London. Series A. Mathematical and Physical Sciences* 245.1240 (1958), pp. 128–145.

[ELV96] J Engel, K Langanke, and P Vogel. “Pairing and isospin symmetry in proton-rich nuclei”. In: *Physics Letters B* 389.2 (1996), pp. 211–216.

[Eng97] J. Engel et al. “Neutron-proton correlations in an exactly solvable model”. In: *Phys. Rev. C* 55 (4 1997), pp. 1781–1788.

[Eng99] Jonathan Engel et al. “β decay rates of r-process waiting-point nuclei in a self-consistent approach”. In: *Physical Review C* 60.1 (1999), p. 014302.

[Erl12] Jochen Erler et al. “The limits of the nuclear landscape”. In: *Nature* 486.7404 (2012), p. 509.

[Eva81] J.A. Evans et al. “Isovector and isoscalar pairing correlations in a solvable model”. In: *Nuclear Physics A* 367.1 (1981), pp. 77–94.

[FGG13] T Faestermann, M Górska, and H Grawe. “The structure of 100Sn and neighbouring nuclei”. In: *Progress in Particle and Nuclear Physics* 69 (2013), pp. 85–130.

[FM14] S. Frauendorf and A.O. Macchiavelli. “Overview of neutron-proton pairing”. In: *Prog. Part. Nucl. Phys.* 78 (2014), pp. 24–90.

[FS64] B H Flowers and S Szpikowski. “Quasi-spin in LS coupling”. In: *Proceedings of the Physical Society* 84.5 (1964), p. 673.

[Fu16] GJ Fu et al. “Shell model study of T= 0 states for Cd 96 by the nucleon-pair approximation”. In: *Physical Review C* 94.2 (2016), p. 024336.

[GBL11] Alexandros Gezerlis, GF Bertsch, and YL Luo. "Mixed-spin pairing condensates in heavy nuclei". In: *Physical review letters* 106.25 (2011), p. 252502.

[GK65] A Goswami and LS Kisslinger. "Particle Correlation Arising from Isospin Pairing in Light Nuclei". In: *Physical Review* 140.1B (1965), B26.

[GM96] Walter Greiner and Joachim A Maruhn. *Nuclear models*. Springer, 1996.

[GMY63] IM Gel'fand, RA Milnos, and Z Ya. *Shapiro, Representations of the Rotation and Lorentz Groups*. 1963.

[Goo01] Alan L Goodman. "T= 0 and T= 1 pairing in rotational states of the N= Z nucleus 80 Zr". In: *Physical Review C* 63.4 (2001), p. 044325.

[Goo72] AL Goodman. "Generalized gap equations and the coherence of the α-α pair field". In: *Nuclear Physics A* 186.3 (1972), pp. 475–492.

[Goo99] Alan L. Goodman. "Proton-neutron pairing in $Z = N$ nuclei with $A = 76 - 96$". In: *Phys. Rev. C* 60 (1999), p. 014311.

[GR14] Izrail Solomonovich Gradshteyn and Iosif Moiseevich Ryzhik. *Table of integrals, series, and products*. Academic press, 2014.

[GRB11] C González-Ballestero, LM Robledo, and George F Bertsch. "Numeric and symbolic evaluation of the pfaffian of general skew-symmetric matrices". In: *Computer Physics Communications* 182.10 (2011), pp. 2213–2218.

[Ham12] Morton Hamermesh. *Group theory and its application to physical problems*. Courier Corporation, 2012.

[HE14] Nobuo Hinohara and Jonathan Engel. "Proton-neutron pairing amplitude as a generator coordinate for double-β decay". In: *Physical Review C* 90.3 (2014), p. 031301.

[Hin12] CB Hinke et al. "Superallowed Gamow–Teller decay of the doubly magic nucleus 100 Sn". In: *Nature* 486.7403 (2012), p. 341.

[HP69] KT Hecht and Sing Chin Pang. "On the Wigner supermultiplet scheme". In: *Journal of Mathematical Physics* 10.9 (1969), pp. 1571–1616.

[Ing54] DR Inglis. "Particle derivation of nuclear rotation properties associated with a surface wave". In: *Physical Review* 96.4 (1954), p. 1059.

[Ing56] DR Inglis. "Nuclear moments of inertia due to nucleon motion in a rotating well". In: *Physical Review* 103.6 (1956), p. 1786.

[KA06] VKB Kota and JA Castilho Alcarás. “Classification of states in SO(8) proton-neutron pairing model”. In: *Nucl. Phys. A* 764 (2006), pp. 181–204.

[Ker61] AK Kerman. “Pairing forces and nuclear collective motion”. In: *Annals of Physics* 12.2 (1961), pp. 300–329.

[Kim18] YH Kim et al. “Generic features of the neutron-proton interaction”. In: *Physical Review C* 97.4 (2018), p. 041302.

[KLM61] AK Kerman, RD Lawson, and MH Macfarlane. “Accuracy of the superconductivity approximation for pairing forces in nuclei”. In: *Physical Review* 124.1 (1961), p. 162.

[KLZ78] Hermann Kümmel, Karl Heinz Lührmann, and John G Zabolitzky. “Many-fermion theory in exp(S)-(or coupled cluster) form”. In: *Physics Reports* 36.1 (1978), pp. 1–63.

[KSA17] K Kaneko, Y Sun, and G de Angelis. “Enhancement of high-spin collectivity in N= Z nuclei by the isoscalar neutron–proton pairing”. In: *Nuclear Physics A* 957 (2017), pp. 144–153.

[Kuc89] H Kucharek et al. “Pairing properties of nuclear matter from the Gogny force”. In: *Physics Letters B* 216.3-4 (1989), pp. 249–251.

[Mac00] AO Macchiavelli et al. “Is there np pairing in N= Z nuclei?” In: *Physical Review C* 61.4 (2000), p. 041303.

[MDP17] A Márquez Romero, J Dobaczewski, and A Pastore. “Neutron-proton pairing correlations in a single $l-$ shell model”. In: *Acta Phys. Polon.* 49.arXiv: 1710.09151 (2017), pp. 347–352.

[Mes66] A. Messiah. *Quantum Mechanics*. Vol. II. John Wiley & Sons, Inc, 1966.

[Mio19] ME Miora et al. “Exact isovector pairing in a shell-model framework: Role of proton-neutron correlations in isobaric analog states”. In: *Physical Review C* 100.6 (2019), p. 064310.

[Mos59] Marcos Moshinsky. “Transformation brackets for harmonic oscillator functions”. In: *Nuclear Physics* 13.1 (1959), pp. 104–116.

[Nam12] H Nam et al. “UNEDF: Advanced scientific computing collaboration transforms the low-energy nuclear many-body problem”. In: *Journal of Physics: Conference Series*. Vol. 402. 1. IOP Publishing. 2012, p. 012033.

[Neg18] D Negrea et al. “Isovector and isoscalar proton-neutron pairing in N>Z nuclei”. In: *Physical Review C* 98.6 (2018), p. 064319.

[Nik10] Tamara Nikšić et al. "3D relativistic Hartree-Bogoliubov model with a separable pairing interaction: Triaxial ground-state shapes". In: *Physical Review C* 81.5 (2010), p. 054318.

[OY66] Naoki Onishi and Shiro Yoshida. "Generator coordinate method applied to nuclei in the transition region". In: *Nuclear Physics* 80.2 (1966), pp. 367–376.

[Paa05] Nils Paar et al. "Isotopic dependence of the pygmy dipole resonance". In: *Physics Letters B* 606.3-4 (2005), pp. 288–294.

[Pan69] Sing Chin Pang. "Exact solution of the pairing problem in the LST scheme". In: *Nuclear Physics A* 128.2 (1969), pp. 497–526.

[Pan96] G Pantis et al. "Neutrinoless double beta decay within the quasiparticle random-phase approximation with proton-neutron pairing". In: *Physical Review C* 53.2 (1996), p. 695.

[Pas08] Alessandro Pastore et al. "Microscopic calculation and local approximation of the spatial dependence of the pairing field with bare and induced interactions". In: *Physical Review C* 78.2 (2008), p. 024315.

[Per04] E Perlińska et al. "Local density approximation for proton-neutron pairing correlations: Formalism". In: *Physical Review C* 69.1 (2004), p. 014316.

[PH67] Sing Chin Pang and KT Hecht. "Lowering and Raising Operators for the Orthogonal Group in the Chain $O(n) \supset O(n-1) \supset \ldots$, and their Graphs". In: *Journal of Mathematical Physics* 8.6 (1967), pp. 1233–1251.

[Pre92] William H Press et al. "Numerical recipes in C++". In: *The art of scientific computing* 2 (1992), p. 1002.

[Qi11] Chong Qi et al. "Spin-aligned neutron-proton pair mode in atomic nuclei". In: *Physical Review C* 84.2 (2011), p. 021301.

[RB11] LM Robledo and GF Bertsch. "Application of the gradient method to Hartree-Fock-Bogoliubov theory". In: *Physical Review C* 84.1 (2011), p. 014312.

[RDP19a] AM Romero, J Dobaczewski, and A Pastore. "Finite-range separable pairing interaction in Cartesian coordinates". In: *arXiv preprint arXiv:1909.13041* (2019).

[RDP19b] AM Romero, J Dobaczewski, and Alessandro Pastore. "Symmetry restoration in the mean-field description of proton-neutron pairing". In: *Physics Letters B* (2019).

[RER05] Tomás R Rodríguez, JL Egido, and LM Robledo. "Restricted variation after projection and the Lipkin-Nogami methods". In: *Physical Review C* 72.6 (2005), p. 064303.

[Rob09] Luis M Robledo. “Sign of the overlap of Hartree-Fock-Bogoliubov wave functions”. In: *Physical Review C* 79.2 (2009), p. 021302.

[Rob10] Luis M Robledo. “Separable approximation to two-body matrix elements”. In: *Physical Review C* 81.4 (2010), p. 044312.

[Rod05] Tomás R Rodríguez et al. “Quality of the restricted variation after projection method with angular momentum projection”. In: *Physical Review C* 71.4 (2005), p. 044313.

[RS80] P. Ring and P. Schuck. *The Nuclear Many-Body Problem*. Springer-Verlag, Berlin, 1980.

[RW10] David J Rowe and John L Wood. *Fundamentals of nuclear models: foundational models*. World Scientific Publishing Company, 2010.

[San12] N Sandulescu et al. “Quartet condensation and isovector pairing correlations in N=Z nuclei”. In: *Physical Review C* 85.6 (2012), p. 061303.

[Sat13] K. Sato et al. “Energy-density-functional calculations including proton-neutron mixing”. In: *Phys. Rev. C* 88 (2013), p. 061301.

[Sch17] Nicolas Schunck et al. “Solution of the Skyrme-Hartree–Fock–Bogolyubov equations in the Cartesian deformed harmonic-oscillator basis.(VIII) hfodd (v2.73y): A new version of the program”. In: *Computer Physics Communications* 216 (2017), pp. 145–174.

[Sch96] H-J Schulze et al. “Medium polarization effects on neutron matter superfluidity”. In: *Physics Letters B* 375.1-4 (1996), pp. 1–8.

[SDN98] W Satuła, J Dobaczewski, and W Nazarewicz. “Odd-even staggering of nuclear masses: Pairing or shape effect?” In: *Physical review letters* 81.17 (1998), p. 3599.

[She03] Caiwan Shen et al. “Screening effects on 1 S 0 pairing in neutron matter”. In: *Physical Review C* 67.6 (2003), p. 061302.

[She14] JA Sheikh et al. “Isospin-invariant Skyrme energy-density-functional approach with axial symmetry”. In: *Physical Review C* 89.5 (2014), p. 054317.

[She19] JA Sheikh et al. “Symmetry restoration in mean-field approaches”. In: *arXiv preprint arXiv:1901.06992* (2019).

[Sin11] BS Nara Singh et al. “16+ Spin-Gap Isomer in Cd 96”. In: *Physical Review Letters* 107.17 (2011), p. 172502.

[Sky56] THR Skyrme. "CVII. The nuclear surface". In: *Philosophical Magazine* 1.11 (1956), pp. 1043–1054.

[Sky58] THR Skyrme. "The effective nuclear potential". In: *Nuclear Physics* 9.4 (1958), pp. 615–634.

[SS13] M Sambataro and N Sandulescu. "Isovector pairing in a formalism of quartets for N= Z nuclei". In: *Physical Review C* 88.6 (2013), p. 061303.

[SSJ15] M Sambataro, N Sandulescu, and CW Johnson. "Isoscalar and isovector pairing in a formalism of quartets". In: *Physics Letters B* 740 (2015), pp. 137–140.

[Sta10] A Staszczak et al. "Augmented Lagrangian method for constrained nuclear density functional theory". In: *The European Physical Journal A* 46.1 (2010), pp. 85–90.

[Suh07] Jouni Suhonen. *From Nucleons to Nucleus: Concepts of Microscopic Nuclear Theory*. Springer Science & Business Media, 2007.

[SW01a] Wojciech Satuła and Ramon Wyss. "Microscopic Structure of Fundamental Excitations in $N = Z$ Nuclei". In: *Phys. Rev. Lett.* 87 (5 2001), p. 052504.

[SW01b] Wojciech Satuła and Ramon Wyss. "Rotations in Isospace: A Doorway to the Understanding of Neutron-Proton Superfluidity in $N = Z$ Nuclei". In: *Phys. Rev. Lett.* 86 (20 2001), pp. 4488–4491.

[Tal03] Igal Talmi. "Fifty years of the shell model—the quest for the effective interaction". In: *Advances in Nuclear Physics, Volume 27*. Springer, 2003, pp. 1–275.

[Tho60] D.J. Thouless. "Stability conditions and nuclear rotations in the Hartree-Fock theory". In: *Nuclear Physics* 21 (1960), pp. 225–232.

[TMR09] Y Tian, ZY Ma, and P Ring. "A finite range pairing force for density functional theory in superfluid nuclei". In: *Physics Letters B* 676.1-3 (2009), pp. 44–50.

[Van11] P Van Isacker. "The scientific legacy of JP Elliott". In: *Nuclear Physics A* 850.1 (2011), pp. 157–166.

[Van16] P Van Isacker et al. "Properties of isoscalar-pair condensates". In: *Physical Review C* 94.2 (2016), p. 024324.

[VMK88] Dmitriĭ Aleksandrovich Varshalovich, Anatolï Nikolaevitch Moskalev, and Valerii Kel'manovich Khersonskii. *Quantum theory of angular momentum*. World Scientific, 1988.

[Wan17] Meng Wang et al. "The AME2016 atomic mass evaluation (II). Tables, graphs and references". In: *Chinese Physics C* 41.3 (2017), p. 030003.

[Wig37] Eugene Wigner. “On the Consequences of the Symmetry of the Nuclear Hamiltonian on the Spectroscopy of Nuclei”. In: *Physical Review* 51.2 (1937), p. 106.

[Wyb74] Brian G Wybourne. “Classical groups for physicists”. In: (1974).

[ZV11] S Zerguine and P Van Isacker. “Spin-aligned neutron-proton pairs in N= Z nuclei”. In: *Physical Review C* 83.6 (2011), p. 064314.